A Multi-Proxy Study of Holocene Atmospheric Circulation Dynamics Recorded in Lake Sediments in Fennoscandia

by

Natalie Ann St.Amour

A thesis
presented to the University of Waterloo
in fulfillment of the
thesis requirement for the degree of
Doctor of Philosophy
in
Earth Sciences

Waterloo, Ontario, Canada, 2009

Author's Declaration

I hereby declare that I am the sole author of this thesis. This is a true copy of the thesis, including any required final revisions, as accepted by my examiners.

I understand that my thesis may be made electronically available to the public.

Abstract

Cellulose-inferred lake water oxygen-isotope records were obtained from five throughflow lakes situated along a north-south transect across Fennoscandia to help develop a better picture of Holocene changes in atmospheric circulation in the region. This research addresses prior evidence for the existence of non-temperature-dependent shifts in $\delta^{18}O$ of precipitation in the early Holocene attributed to changes in atmospheric circulation. The validity of this hypothesis is tested through the development of oxygen-isotope records from lake sediments and their interpretation in the context of independent reconstructions of temperature and precipitation from pollen and chironomid head-capsules collected from the same or nearby sites, and well-documented changes in vegetation composition. Records of carbon and nitrogen elemental content and isotopic composition and magnetic susceptibility are included in this multi-proxy investigation. Extensive modern isotope hydrology datasets spanning several years at four of the five sites also help to inform interpretations of the cellulose $\delta^{18}O$ records.

Key results from this research are:

1) Elevated $\delta^{18}O$ in relation to prevailing temperature occurred during the early Holocene (*c*. 10,000-6000 cal. BP) for sites in northern Fennoscandia (Lake Tibetanus, Lake Spåime), in harmony with previous interpretations suggesting that strong zonal atmospheric circulation led to deepening of the precipitation and isotope shadows in the lee of the Scandes Mountains.

2) Evidence from a southern site (Arbovatten) reveals a previously unrecognized negative offset in the $\delta^{18}O$-temperature relation during the early Holocene, apparently transferred directly from the North Atlantic without the orographic effects associated with a topographic barrier.

3) The modern $\delta^{18}O$-temperature relation appears to have been established throughout Fennoscandia by *c.* 6000-4000 cal. BP, probably due to generally weaker circumpolar atmospheric circulation in response to lower summer insolation.

4) Comparison of two sites (Lake Spåime, Svartkälstjärn) in a west-east transect across central Fennoscandia reveals higher-frequency variability in atmospheric circulation at submillennial scales throughout the Holocene, which appears to be analogous to contemporary variability in the North Atlantic Oscillation (NAO) at seasonal-to-decadal time-scales. Evidence of such NAO-like variability also exists at two northern sites (Lake Keitjoru, Oikojärvi) during the Holocene, likely reflecting variations in summer and winter atmospheric circulation.

5) Complex lake-specific changes in productivity occurred in response to Holocene climate change, as revealed by carbon and nitrogen elemental and isotopic data in lake sediments. A major shift in atmospheric circulation pattern occurring at *c.* 4000 cal. BP probably led to a reduction in soil-derived ^{13}C-depleted nutrients in five lakes (Lake Keitjoru, Oikojärvi, Lake Spåime, Svartkälstjärn, Arbovatten) associated with changes in terrestrial vegetation. Changes in sediment nitrogen isotope composition also occurred in these lakes at *c.* 4000 cal. BP, possibly reflecting changing nutrient supply dynamics because of enhanced nitrogen losses during spring snowmelt.

Acknowledgements

I sincerely thank Tom Edwards for providing tremendous amount of support, patience, and a rewarding graduate research experience that included fieldwork in the Peace Athabasca Delta, NWT, and Sweden, and numerous opportunities to present my research at scientific conferences. I sincerely thank Dan Hammarlund for the considerable support he has provided during my program, through e-mailing and travelling to Canada a number of times. And, I greatly appreciated the hospitality I received by Dan and his family when I visited Sweden. I had an incredible experience doing fieldwork at Naimakka and Arbovatten. I sincerely thank Brent Wolfe for always providing suggestions for improvements and directions in my studies, and engaging me in stimulating teaching opportunities.

Special thanks goes to Kjell Erik Siikavuopio, Hans-Göran Nilsson, and Kjell-Evert Olsson for their dedication in collecting water samples at the Naimakka Lakes, Svartkälstjärn and Arbovatten, respectively. Thanks in particular to Ian Snowball for helping with the magnetic susceptibility measurements. Discussions with Matt Falcone on the analytical approach of cellulose analysis were gladly welcomed. Laboratory assistance was gratefully appreciated by Tracy Barkhouse and Tiffany Chiu. Thanks also go to the staff at the Environmental Isotope Laboratory and to Bill Mark and Lois Graham for getting my samples processed.

An incredible amount of gratitude goes to Elaine Garner at the Graduate Studies Office for providing financial assistance throughout my program and for unwavering confidence in my ability to complete my degree requirements.

Financial support was provided by the Swedish Research Council through a grant to Dan Hammarlund and the Natural Sciences and Engineering Research Council of Canada through grants to Tom Edwards. Additional funding was provided by the Northern Scientific Training Program of Indian and Northern Affairs Canada.

Sincere gratitude goes to family, especially my husband Mike for incredible patience.

Table of Contents

List of Figures

List of Tables

Chapter 1
Introduction

The effects of rising global surface temperatures are now observed to be having an impact on high-latitude hydrological and ecological systems (IPCC, 2007). Global average air temperature has increased for the past 50 years, and especially since 1970, possibly due to the increase in anthropogenic greenhouse gas emissions, such as carbon dioxide (CO_2) and methane (CH_4). Climate warming is amplified through the melting of snow and ice on land, as well as a reduction in sea ice extent, which lowers the surface albedo. This in turn allows incoming radiation from the sun to be absorbed at the surface, thus further heating the air above. At the same time, increased evaporation of oceans and greater evapotranspiration rates over land have increased the water vapour budget in the atmosphere, leading to increased precipitation, especially significant in northern Europe (Lindström and Alexandersson, 2004; IPCC, 2007). The recent trend towards mild and wet years has been linked to stronger westerlies associated with a persistently positive phase of the North Atlantic Oscillation (NAO) since the 1980s (Hurrell, 1995).

The NAO is a key mode of seasonal-to-decadal climate variability in the North Atlantic region, such that it can directly affect changes in temperature and precipitation distribution over different spatial scales, and in turn influence terrestrial and freshwater ecosystems (e.g., Mysterud *et al.*, 2003; Straile *et al.*, 2003). Hurrell *et al.* (2003) provided an example of how the NAO can have an economic impact in Norway and Sweden due to the spatial heterogeneity of available water supply. During a positive NAO index phase, increased precipitation in Norway fills reservoirs and generates plentiful hydroelectric power, while Sweden purchases hydropower from Norway. On the other hand, a negative phase in the NAO index leads to lower winter precipitation in Norway, thus reducing the availability of energy supply. In this case, Norway may need to buy nuclear power from Sweden. Understanding changes in climate modes would thus be very useful in assessing future water and energy management practices. Certainly, long records of the NAO are needed to investigate patterns of climate variability and to place recent trends in a better long-term context. For example, sea level pressure measurements in Fennoscandia provide a record of

variability in the NAO index as far back as to the 17th century (e.g., Jacobeit *et al.*, 2001). To investigate climate variability over centennial to millennial-scales, proxy-based reconstructions (e.g., temperature and precipitation) are necessary. Since the intensity of the NAO's influence on climate varies spatially within a region, the response of the proxies to the influences of the NAO will, in turn, depend on where the proxies originate (Cook, 2003).

Numerous proxy records from Fennoscandia have documented significant changes in atmospheric circulation throughout the Holocene Epoch (the last 11,600 years), generally reflecting variations in temperature and effective moisture, such as peat humification stratigraphy (e.g., Gunnarson *et al.*, 2003; Borgmark, 2005), tree-line dynamics (e.g., Seppä and Hammarlund, 2000; Barnekow, 2000; Barnekow and Sandgren, 2001; Bjune *et al.*, 2004; Kullman and Kjällgren, 2006), temperature and precipitation reconstructions inferred from pollen and chironomid head capsules (e.g., Seppä and Birks, 2001, 2002; Heikkilä and Seppä, 2003; Hammarlund *et al.*, 2004; Seppä *et al.*, 2005), lake-level fluctuations (e.g., Digerfeldt, 1988; 1997; Almquist-Jacobson, 1995; Yu and Harrison, 1995; Korhola *et al.*, 2005), glacier fluctuations and winter precipitation reconstructions (e.g., Dahl and Nesje, 1996; Nesje *et al.*, 2001), and an oxygen-isotope record of effective moisture from lacustrine carbonates (Hammarlund *et al.*, 2003). Indeed, these paleoclimatic reconstructions have added valuable information about the general development of climate, but have only yielded partial understanding of the complex dynamics involved between long-term solar forcing and circulation of the atmosphere and ocean in the North Atlantic, as well as the downwind response of ecological and hydrological systems on land.

A recent interval of significant atmospheric circulation change occurred during the transition from the Medieval Warm Period (MWP; *c.* AD 700-1300) to the Little Ice Age (LIA; *c.* AD 1450-1850). Particular attention has been focused on this climate fluctuation since it has occurred within human-documented history. Evidence suggests that the influence of climate variability on terrestrial and hydrological systems during the MWP and LIA was felt in other areas, such as North America (e.g., Watson and Luckman, 2004), and not only Europe and the North Atlantic region. This geographical variability in climate is likely reflecting changes in atmospheric circulation strength during the LIA, as reflected in ice-core records of high sea salt and dust concentrations from Greenland (O'Brien *et al.*,

1995). Meridional flow likely intensified and the northern polar vortex expanded in the winter, resulting in cold, moist conditions in the North Atlantic region (O'Brien *et al.*, 1995). Bond *et al.* (1997, 2001) suggested that the LIA is the most recent cold phase in a series of millennial-scale cycles in atmospheric circulation that may be influenced by variations in solar output.

The early Holocene was characterized by considerable change in climate since it was a time when large Northern Hemisphere ice sheets were still present. Summer solar insolation in the northern hemisphere also reached maximum values during the early Holocene, leading to increased sea surface temperatures and reduced sea-ice extent in the Iceland and Norwegian Seas (Koç *et al.*, 1993). An abrupt 200-year cooling episode amounting to 1-2 K occurred at around 8200 cal. BP, as recorded in various records in the North Atlantic region and Europe (e.g., von Grafenstein *et al.*, 1998; Johnsen *et al.*, 2001; Magny *et al.*, 2003; Hammarlund *et al.*, 2005; Seppä *et al.*, 2005). Terrestrial evidence of climate cooling coincides with increased ice-rafting in the North Atlantic (Bond *et al.*, 1997), which suggests possible ocean-terrestrial coupling through significant rearrangements of the atmospheric circulation pattern over the North Atlantic and across Europe (O'Brien *et al.*, 1995). The cold event may have been the result of enhanced discharge of freshwater from drainage of Lake Agassiz, which led to a freshening of the North Atlantic surface waters, a weakening of the thermohaline circulation and a reduction of heat transfer to the Nordic Seas (Alley *et al.*, 1997; Barber *et al.*, 1999). As summer solar insolation in the northern hemisphere declined after 8000 cal. BP, millennial-scale variability in atmospheric circulation over the North Atlantic and Europe (O'Brien *et al.*, 1995) may have been influenced by variations in solar irradiance during the rest of the Holocene (Denton and Karlén, 1973; Bond *et al.*, 2001; Mayewski *et al.*, 2004).

During the period between *c.* 8000 and 4000 cal. BP, commonly referred to as the Holocene Thermal Maximum (HTM), temperatures reached their Holocene maxima (Seppä and Birks, 2001; Seppä *et al.*, 2005; Velle *et al.*, 2005), lake water levels lowered (Digerfeldt, 1988; Barnekow, 2000; Korhola *et al.*, 2005) and there was widespread melting and even the complete disappearance of glaciers (Karlén, 1976; Nesje and Kvamme, 1991). In addition, warmer summer temperatures and longer growing seasons allowed the spread of *Pinus*

sylvestris to higher latitudes and altitudes (e.g., Kullman, 1988; 1995; Barnekow and Sandgren, 2001; Kullman and Kjällgren, 2006). Despite the warm climate conditions during the HTM, sea surface temperatures in the North Atlantic were gradually declining (Koç *et al.*, 1993; Snowball *et al.*, 2004). Between 4000 and 3500 cal. BP, a shift in atmospheric circulation in Fennoscandia is suggested from changes in climate parameters, temperature and precipitation (Seppä and Birks, 2001; Seppä *et al.*, 2005), glacier expansion (Nesje and Kvamme, 1991; Nesje *et al.*, 2001), and a general descent and retreat of *Pinus* tree-line from higher altitudes and latitudes (Barnekow and Sandgren, 2001; Hammarlund *et al.*, 2004; Kullman and Kjällgren, 2006). After 3500 cal. BP, the late Holocene climate was characterized as being more variable and moist (Korhola *et al.*, 2005; Seppä *et al.*, 2005; Barnekow *et al.*, 2008). The increase in moisture is consistent with the spread of peatlands, as indicated by increased frequencies of *Sphagnum* spores, as well as extensive paludification of soils and the establishment of *Picea abies* in central and northern Fennoscandia (Seppä and Weckström, 1999; Barnekow *et al.*, 2008). In addition, higher lake levels may also reflect decreased summer temperatures and higher effective moisture in southern Sweden at this time (Hammarlund *et al.*, 2003, Seppä *et al.*, 2005).

The isotopic composition of precipitation is a natural tracer of the global water cycle, and since it is strongly linked to variability in meteorological parameters and atmospheric circulation (e.g., Dansgaard, 1964; Rozanski *et al.*, 1993), it affords a valuable opportunity for paleohydrological and paleoclimatological investigations. Precipitation isotopes are commonly used as a "paleothermometer" (e.g., Sundqvist *et al.*, 2007), yet water isotopes in precipitation can provide additional information about changes in moisture source, rain-out history, and seasonality of precipitation, brought on as a result of changing atmospheric circulation independent of temperature (McKenzie and Hollander, 1993; Charles *et al.*, 1994; Amundson *et al.*, 1996; Edwards *et al.*, 1996, 2008; Teranes and McKenzie, 2001; Hammarlund *et al.*, 2002; Rosqvist *et al.*, 2007). In addition, the isotopic composition of precipitation is increasingly being used as a diagnostic test for the performance of atmospheric general and regional circulation models (Jouzel *et al.*, 1996; Hoffmann *et al.*, 2000; Edwards *et al.*, 2002; Sturm *et al.*, 2005).

As part of the multidisciplinary research programme HYDRO-ISO-CLIM (Hydrological and Meteorological Analysis of Precipitation Isotopic Composition as a Key to Present and Past Climates), the goal of this research is to use the systematic labeling of isotopic composition of precipitation for characterizing past changes in circulation and moisture transport during the Holocene. In this dissertation, lake water $\delta^{18}O$ values[1] inferred from aquatic plant cellulose preserved in sediment cores obtained at several sites in Fennoscandia have recorded sub-millennial variability in atmospheric circulation during the past 10,000 years. Following a multi-proxy approach, qualitative and quantitative characterization of past changes in the seasonality of precipitation, isotope-temperature relations and distillation of moisture help to contribute better understanding of atmospheric circulation dynamics across Fennoscandia during the Holocene.

1.1 Research Objectives

Atmospheric circulation changes during the Holocene have been interpreted from a carbonate-inferred precipitation $\delta^{18}O$ record from Lake Tibetanus, northern Sweden, manifested as apparent offsets from the modern Dansgaard (1964) $\delta^{18}O$-temperature relation (Hammarlund *et al.*, 2002). The precipitation $\delta^{18}O$ record at Lake Tibetanus showed a gradual decrease in $\delta^{18}O$ and a gradual decline in the offset from the modern $\delta^{18}O$-temperature relation from the early Holocene to about 6000 cal. BP. Anomalously high $\delta^{18}O$ during the early Holocene was attributed to the effects of reduced distillation of moisture traversing the Scandes Mountains under the influence of intense westerly circulation (i.e., strong zonal index; Hammarlund *et al.*, 2002). Other oxygen-isotope archives, such as calcite $\delta^{18}O$ from a speleothem in Søylegrotta, northern Norway (Lauritzen and Lundberg, 1999) and biogenic silica $\delta^{18}O$ from lake sediments near Abisko, northern Sweden (Shemesh *et al.*, 2001) have suggested a similar decline in $\delta^{18}O$ during the Holocene. However, these sites are located in northern Fennoscandia and in the Scandes Mountains. The extent of circulation-dependent effects on precipitation $\delta^{18}O$ elsewhere in Fennoscandia and the

[1] The δ-value is defined as $\delta\text{‰} = (R_{sample}/R_{standard} - 1) \times 10^3$, where R represents the isotopic ratio ($^{18}O/^{16}O$ or $^{2}H/^{1}H$). A positive δ-value indicates an enrichment of the heavy isotopic species relative to the standard VSMOW (Vienna standard mean ocean water), whereas negative values signify depletion.

variability at sub-millennial scales for the Holocene are unknown. In order to investigate changes in atmospheric circulation over different time and spatial scales, cellulose-inferred $\delta^{18}O$ records have been developed at five sites situated along a north-south transect in Sweden and Finland (Figure 1-1). The objectives of this research are as follows:

1) To evaluate past changes in atmospheric circulation by deconvoluting the records of cellulose-inferred lake water $\delta^{18}O$ into components of paleoprecipitation and paleohydrology at different sites (i.e., lakes Keitjoru, Oikojärvi, Spåime, Svartkälstjärn, and Arbovatten; Figure 1-1). The variability recorded in the cellulose $\delta^{18}O$ archives reflects different sensitivities to changing precipitation $\delta^{18}O$ (due to changes in distillation and moisture source), seasonal distribution of precipitation, and water balance. The amalgamation of these signals provides an opportunity to examine different aspects of climate (e.g., summer versus winter, oceanic versus continental) over millennial and spatial scales.

2) To investigate temporal oxygen-isotope-temperature relations during the Holocene by comparing records of $\delta^{18}O$ from three sites (i.e., lakes Tibetanus, Spåime, and Arbovatten; Figure 1-1) that cover a range of latitudes in combination with independent estimates of temperature. Independent temperature reconstructions are derived from pollen (e.g., Hammarlund *et al.*, 2002; Seppä *et al.*, 2005) and chironomids (Hammarlund *et al.*, 2004). This investigation presents an opportunity to explore changes in precipitation $\delta^{18}O$ and $\delta^{18}O$-temperature relations in response to changes in atmospheric circulation over centennial to millennial scales. The evolution of precipitation $\delta^{18}O$ and $\delta^{18}O$-temperature relations during the Holocene may reflect varying precipitation distillation because of changes in the efficiency of moisture transport across a topographic barrier. Clues to this effect are probed by comparing changes in the offsets from the $\delta^{18}O$-temperature relation between two lakes situated in the lee of the Scandes Mountains and a lake located in southern Sweden.

3) To explore nutrient cycling within lake catchments using records of carbon and nitrogen elemental content and isotopic composition from five sites (i.e., lakes Keitjoru, Oikojärvi, Spåime, Svartkälstjärn, and Arbovatten; Figure 1-1). The carbon and nitrogen records are compared with records of cellulose-inferred lake water $\delta^{18}O$ and magnetic susceptibility in order to separate factors (i.e., rates of lake productivity and changes in precipitation runoff

and water balance) that may be controlling the nutrient balance within the lakes and their catchments. A comparison with independent pollen-based records of vegetational dynamics at each lake also helps to provide information about carbon and nitrogen sources developed in forest soils during the Holocene. Thus, changes in nutrient cycling in response to changes in hydrology and climate are investigated.

The North Atlantic, and its prevailing westerlies carrying heat and moisture, has a direct influence on the climate of Fennoscandia. The Scandes Mountains act as a topographic barrier to the transport of oceanic air masses, causing well-defined east-west and north-south gradients in temperature and moisture, which is manifested in vegetation zonations. Present-day vegetation zonations exist over different latitudes and altitudes, including climatically sensitive ecotones in mountain areas, and numerous studies on the climatic development and tree-limit dynamics during the Holocene in the Fennoscandian Peninsula have been undertaken (Kullman, 1989, 1992; Barnekow, 2000; Barnekow and Sandgren, 2001). Both pollen and macrofossil evidence suggest that fluctuations of these zonation patterns reflect post-glacial variability in climate. A comparison between changes in vegetation zonations and the $\delta^{18}O$ archives provide supporting evidence that variation in precipitation $\delta^{18}O$ also occurred in response to major changes in atmospheric circulation patterns. Key vegetational changes during the Holocene include shifts in birch and pine altitudinal and latitudinal limits along the Scandes and northern Fennoscandia during the mid-Holocene (Kullman, 1995; Barnekow, 2000; Hammarlund *et al.*, 2004), spruce and peatland expansions during the late Holocene (Seppä and Weckström, 1999; Giesecke, 2005; Barnekow *et al.*, 2008), and changes in the distributional limits of thermophilous trees in southern Sweden during the Holocene Thermal Maximum (Giesecke, 2005; Barnekow *et al.*, 2008). These vegetational changes have been noted to occur in response to changes in oceanicity and continentality (Seppä and Hammarlund, 2000; Bjune *et al.*, 2004; Giesecke *et al.*, 2008).

The selection criteria for the study lakes are based on the modern hydrological settings of the catchments. Generally, lakes are open-drainage (i.e., high ratio of total inflow to evaporation), have short residence times and low evaporative isotope enrichment, so that modern lake water $\delta^{18}O$ values closely resemble $\delta^{18}O$ of groundwater and mean annual precipitation. In addition, a thorough assessment of modern catchment hydrology of the

study sites and the availability of an isotope database consisting of modern precipitation (IAEA/WMO-GNIP) and river samples in Sweden help establish constraints for interpreting past $\delta^{18}O$ records from lake sediment cellulose. The coupling of oxygen isotopes with temperature records was key to detecting a circulation-dependent signal in Lake Tibetanus precipitation $\delta^{18}O$ record. Thus, a multi-proxy approach in comparing $\delta^{18}O$ cellulose records with independent proxy records provides new insight into Holocene variations in effective moisture, air mass circulation, rain-out effects, seasonality, and oxygen isotope-temperature relations over a regional scale. The results from this research may also provide a useful $\delta^{18}O$ database to test and refine atmospheric circulation models.

1.2 Research Approach

A multi-proxy approach is undertaken in this thesis to better evaluate past hydrologic and climatic conditions. The interpretation of cellulose $\delta^{18}O$ records is facilitated by accompanying records of elemental and isotopic composition of carbon and nitrogen in lake sediment organic matter and magnetic susceptibility. Since each proxy can reflect and respond to different components of the hydrologic and climate systems, this approach affords insightful information about the paleoenvironment. An assessment of the modern isotope hydrology also helps to constrain qualitative and quantitative paleoenvironmental interpretations of $\delta^{18}O$ data obtained on lake sediment cellulose. The details below describe some of the fundamental processes and factors that control the behaviour of water isotopes in the hydrological cycle, as well as those that influence oxygen isotope labeling of aquatic cellulose, and carbon and nitrogen content and isotopic composition in organic matter. Together, these processes are summarized as part of the research approach used in this thesis.

1.2.1 Modern isotope hydrology

1.2.1.1 Isotopic labeling in the water cycle

The water molecule exhibits various combinations of naturally occurring stable isotopes of hydrogen (^{1}H, ^{2}H) and oxygen (^{18}O, ^{17}O, ^{18}O). Partitioning (fractionation) of isotopic species occurs during phase transitions (equilibrium) and diffusive transport (kinetic) because of slight differences in vapour pressures and molecular behaviour of the rare, heavy isotopic

species compared to the light isotopic species (Gat, 1981). This results in a systematic distribution of water isotopes in specific parts of the hydrological cycle (i.e., atmospheric moisture, precipitation, surface water, groundwater, etc.) to occur along two linear trends in δ^2H-$\delta^{18}O$ space at a given location (Figure 1-2). One linear relation is the Global Meteoric Water Line (GMWL), expressed as $\delta^2H = 8\delta^{18}O + 10$ (Craig, 1961), representing the variation of isotopic composition of precipitation at a global scale. The slope of the GMWL reflects temperature-dependent equilibrium fractionation of the heavy isotopes between the atmospheric moisture and the condensing precipitation. Local meteoric water lines (LMWL) are similar to the GMWL, but represent a regression line through isotopic data obtained on monthly weighted precipitation for specific regions of study. These lines usually have a slightly lower slope due to the re-evaporation of summer rain and kinetic effects during snow formation (Rozanski *et al.*, 1993). The other linear relation results from waters that have undergone heavy-isotope evaporative enrichment, which typically plot along a local evaporation line (LEL) in $\delta^{18}O$-δ^2H space (Figure 1-2). The slope of the LEL typically ranges between 4 and 6 due to additional mass-dependent kinetic fractionation, which is primarily controlled by local atmospheric parameters, such as relative humidity, temperature, and the isotopic composition of atmospheric moisture (δ_A) prevailing during the open-water season. In general, the systematic isotopic labeling of water makes oxygen and hydrogen isotope data extremely valuable as tracers within the hydrological cycle, and allows for a conceptual isotopic framework to be established for a particular region (Figure 1-2). This is especially important in differentiating meteoric waters from surface waters that have undergone evaporative enrichment.

1.2.1.2 Evaporation and water balance

The water- and isotope-mass balances of lakes are governed by the relative amounts of inputs (precipitation and runoff) versus outputs (outflow and evaporation), and respective isotopic signatures. In the $\delta^{18}O$-δ^2H space of the conceptual isotopic framework (Figure 1-2), the isotopic composition of input waters (δ_P) in a catchment is commonly the intersection of the LMWL and the LEL. The displacement of the lake water (δ_L) isotope composition from δ_P along the LEL is an index of water balance that is described in terms of evaporation/inflow

(E/I). In high-latitude lakes, negative shifts of δ_L are caused by the dilution of lake water with isotopically-depleted input waters (groundwater, annual precipitation, or snowmelt), followed by positive shifts of δ_L along the LEL due to the evaporative enrichment of heavy isotopes during the summer. A closed-basin lake exhibiting equal balances of both input and outflows (E/I=1) has an isotopic composition approaching δ_{SSL} (Figure 1-2). The limiting isotopic composition δ^* is another important parameter to consider in the conceptual isotopic framework (Figure 1-2) since it is the theoretical maximum isotopic enrichment that water attains as it approaches complete desiccation. The determination of δ^* requires estimates of climate data (humidity and temperature) and the isotopic composition of evaporation-flux-weighted atmospheric moisture (δ_A), which is commonly approximated by assuming isotopic equilibrium with amount-weighted summer precipitation δ_{Ps} such that $\delta_A = (\delta_{Ps} - \varepsilon^*)/\alpha^*$ (Gibson and Edwards, 2002), where ε^* and α^* are the liquid-vapour equilibrium separation and equilibrium fractionation factor, respectively.

1.2.1.3 Global distribution of isotopes in precipitation

The modern spatial distribution of the oxygen-isotope composition of monthly precipitation has been well-documented using data from the IAEA/WMO GNIP network (Dansgaard, 1964; Rozanski *et al.*, 1993; Fricke and O'Neil, 1999). The isotopic composition of precipitation is determined by the progressive rain-out (i.e., Rayleigh distillation) and depletion of the heavy isotopes of a moist air mass as it is transported over some distance from the source, such as across long stretches of land (i.e., continental effect), from the tropics to polar latitudes (i.e., latitude effect), and to higher elevations, especially over large mountain ranges (i.e., altitude effect; Rozanski *et al.*, 1993). At high latitudes, the expression of seasonality in precipitation is enhanced, with snow being more depleted in the heavy isotopes than rain. In addition, the seasonal amplitude of precipitation $\delta^{18}O$ at coastal stations tends to be subdued compared to larger $\delta^{18}O$ fluctuations observed for continental stations.

1.2.1.4 Oxygen isotope-temperature relations

A good correlation between mean annual temperature and weighted mean annual $\delta^{18}O$ of precipitation exists at mid- to high-latitudes (Fricke and O'Neil, 1999). This relationship is

consistent with the fact that temperature and precipitation $\delta^{18}O$ tend to co-vary during transport and distillation of moisture-laden air masses. Spatial $\delta^{18}O$-temperature relations represent conditions of a characteristic climate mode over a geographical area. On the other hand, temporal $\delta^{18}O$-temperature relations compare data from different climate modes for a specific site. Temporal $\delta^{18}O$-temperature relations incorporate a number of factors that reflect a change in temperature, a change in the relative influence of non-temperature factors, or a combination of effects (Fricke and O'Neil, 1999). The strength of the correlation of temporal $\delta^{18}O$-temperature relations provides a basis for a meaningful first-order approximation of non-temperature-dependent factors influencing $\delta^{18}O$.

There are separate spatial $\delta^{18}O$-temperature relations for different geographic areas and times. The slope of the $\delta^{18}O$-temperature relation generally increases polewards, from almost zero at the equator, to 0.58 ‰/K at mid-latitude (25°-60°) stations (Fricke and O'Neil, 1999), and to 0.67 ‰/K at high-latitudes, such as in Greenland (Johnsen *et al.*, 1989) and 0.90 ‰/K for the Antarctic Peninsula (Rozanski *et al.*, 1993). For coastal stations in the North Atlantic, Dansgaard (1964) determined the relation $\delta^{18}O = 0.69T - 13.6$ (where T = mean annual temperature in °C), which has been used frequently in the literature for paleoclimate reconstructions. The change in slope is likely attributable to variability in the seasonal distribution of precipitation $\delta^{18}O$ for a given temperature and location. For a given region, the $\delta^{18}O$-temperature slope is relatively invariant over time, regardless of a change in climate mode, although the $\delta^{18}O$-temperature relations may be offset for different seasons, as demonstrated by Fricke and O'Neil (1999).

Offsets between $\delta^{18}O$-temperature relations of equal slope occur between sites because of factors influencing $\delta^{18}O$ and/or temperature that are unique to a given climate condition. For instance, an increase in altitude due to rapid glacio-isostatic uplift during the early Holocene can result in a change in $\delta^{18}O$ (–0.5 ‰/100 m) and temperature (–0.6 K/100m; Ingraham, 1998). In the same way, the degree of continentality also influences $\delta^{18}O$-temperature relations as depicted by the Rayleigh model (Edwards *et al.*, 1996). A change in the amount of water vapour in the air can result in a modification of $\delta^{18}O$, independent of changes in surface temperature, through factors associated with changes in the seasonal distribution of

precipitation and air mass rain-out (Fricke and O'Neil, 1999). These processes are likely to be sensitive to changes in atmospheric circulation patterns and the position of air mass boundaries. A change in $\delta^{18}O$ of the initial moisture source (e.g., ocean) may also cause an offset in the $\delta^{18}O$-temperature relation, which would change the initial composition of water vapour formed from that source. The melting of ice sheets in the Northern Hemisphere, for example, caused an increase in $\delta^{18}O$ of the global ocean by *c.* 0.8‰ (Shrag *et al.*, 1996), which was transferred into atmospheric vapour.

Importantly, the strength of the correlation between $\delta^{18}O$ and temperature can indicate factors other than temperature that influence $\delta^{18}O$ to varying degrees depending on the climate condition. For example, a weak correlation can result if significant moisture is recycled back to the atmosphere through local evaporation of lakes and transpiration of plants (Krabbenhoft *et al.*, 1990; Brunel *et al.*, 1992; Gat *et al.*, 1994). As a result, local precipitation tends to be less depleted in the heavy isotopes as predicted by a partially-closed system rather than an open Rayleigh distillation model. In addition, changes in the seasonal distribution of precipitation can result in positive shifts in $\delta^{18}O$ if there is an increase in the rain component, or negative shifts if there is an increase in the snow component, resulting in weak correlation coefficients. Thirdly, the evaporation of precipitation as it falls through dry air can shift the condensing water to higher $\delta^{18}O$ values, also leading to a weak correlation with temperature. At low-latitude tropical marine locations, there is no correlation between precipitation $\delta^{18}O$ and temperature due to the amount effect, in which there is a strong inverse relationship between precipitation $\delta^{18}O$ and precipitation amount (Rozanski et al., 1993).

1.2.2 Oxygen isotopes in cellulose

A key tool in investigations of lake paleohydrology and paleoclimatology is the use of oxygen isotope records of lake sediment cellulose. This approach has been used increasingly over the past 15 years, as sample preparation and analytical techniques have improved (Wolfe *et al.*, 2007). An attractive quality of cellulose is that it is abundant in nature and often preserves well in diverse geologic environments, thus increasing the number of suitable lakes available for study, including carbonate-poor lakes. Cellulose is a structural component

found in the cell walls of terrestrial and aquatic vascular plants, as well as in most algae, comprising up to 10% dry weight (Wolfe *et al.*, 2001a). Cellulose is also contained within zooplankton fecal pellets through grazing of phytoplankton (Edwards, 1993).

The fundamental bases for analysis of $\delta^{18}O$ in lake-sediment cellulose are that (1) the aquatic cellulose instantaneously records the $\delta^{18}O$ of the lake water from which it forms, (2) the isotopic fractionation is independent of water temperature, plant species, the oxygen isotopic composition of CO_2, and the photosynthetic mode (e.g., C_3, C_4, CAM) of the organism (DeNiro and Epstein, 1981; Sternberg and DeNiro, 1983; Yakir 1992; Wolfe *et al.*, 2001a), and (3) the oxygen isotope fractionation between cellulose and water is constant through time. Through field and laboratory experiments, the isotopic fractionation factor between cellulose and water has been well-constrained within the range of 1.025-1.030 (Epstein, 1977; DeNiro and Epstein, 1981; Yakir and DeNiro 1990; Wolfe *et al.*, 2001a; Sauer *et al.*, 2001; Yi, 2008). These assumptions allow cellulose $\delta^{18}O$ to be directly converted to lake water $\delta^{18}O$ using an $\alpha_{cell\text{-}water}$ value of 1.028 based on the following expression in decimal notation (Edwards *et al.*, 1985; Edwards and McAndrews, 1989; Wolfe *et al.*, 2001a, 2007):

$$\delta^{18}O_{water} = \frac{1 + \delta^{18}O_{cell} - \alpha_{cell-water}}{\alpha_{cell-water}}$$

With this expression, a record of paleohydrology can be directly inferred from the cellulose oxygen isotope composition ($\delta^{18}O_{cell}$), as long as the sediment cellulose is aquatic in origin and information on lake hydrology is available. Surface sediment cellulose-inferred water $\delta^{18}O$ have shown to be in good agreement with measured lake water $\delta^{18}O$ using $\alpha_{cell\text{-}water}$ value of 1.028 in field studies and substantiated by the availability of multiple water samples spanning over different seasons over several years (Wolfe *et al.*, 2005, 2007, 2008).

In order to successfully deconvolute $\delta^{18}O$ history and provide quantitative paleoenvironmental reconstructions, interpretations depend on the ability to resolve isotopic shifts along the LMWL and LEL in $\delta^{2}H$-$\delta^{18}O$ space (Figure 1-2). In hydrologically open lakes that experience little evaporation, changes in $\delta^{18}O$ over time are controlled by variations in the oxygen isotope composition of the source water (i.e., precipitation and

inflow), and are reflected as shifts along the LMWL. Such records of cellulose $\delta^{18}O$ provide a measure of precipitation $\delta^{18}O$, which can provide evidence of circulation changes and variations in the seasonal distribution of precipitation and/or temperature (Edwards *et al.*, 1996). On the other hand, lakes that are influenced by secondary isotopic effects, such as evaporative enrichment, exhibit shifts along the LEL (e.g., Wolfe *et al.*, 2001b, 2005). Cellulose-inferred lake water $\delta^{18}O$ records may also reflect co-varying changes along both MWL and LEL through effects of snowmelt bypass, as shown for Weslemkoon Lake, Ontario (Edwards and McAndrews, 1989). The cellulose $\delta^{18}O$ archives may be used to quantitatively reconstruct changes in paleohydrology in terms of evaporation/inflow ratio and relative humidity, provided that appropriate constraints on the interpretations can be made (e.g., Wolfe *et al.*, 2001b, 2005; Edwards *et al.*, 2004). In some cases where past changes in atmospheric parameters (e.g., relative humidity) are not available, the water balance of a lake may be determined based on the separation between δ_L from δ_P as a first approximation of the apparent isotopic enrichment by evaporation (e.g., Edwards and McAndrews, 1989).

1.2.3 Carbon and nitrogen content of lake-sediment organic matter

The interpretation of cellulose $\delta^{18}O$ records in terms of processes related to hydrology, is often better constrained when combined with records of carbon and nitrogen content and isotopic composition of lake-sediment organic matter. Carbon and nitrogen records provide evidence of biogeochemical processes that occur in a lake and its catchment, as well as ancillary information about the origin of the organic matter. Thus, variations observed in these records commonly reflect changes in lake productivity, which depend on the availability of nutrients. In turn, the availability of nutrients depends on climate and hydrology, since runoff from precipitation is the main mechanism of delivery of organic matter to the lake. In general, parallel variations in total organic carbon (TOC) and total nitrogen (TN) concentrations are indicators of changing lake productivity. Both TOC and TN concentrations are expressed as weight percentages, and thus, are influenced by other sediment components (Meyers and Lallier-Vergès, 1999).

The carbon/nitrogen (C/N) ratio is traditionally used as a means of identifying the source of organic matter due to differences in the biochemical components between non-vascular

and vascular plants. Non-vascular plants, such as algae, contain abundant proteins and lipids, which are rich in nitrogen. On the other hand, vascular plants (both aquatic and terrestrial) are rich in cellulose and lignin, which contain proportionally less nitrogen. As a result, C/N values of algae generally range between 4 and 10, whereas, terrestrial C/N ratios are generally higher than 20 (Meyers and Lallier-Vergès, 1999). Values between these ranges may be due to a mixture of aquatic and terrestrial sources. However, organic matter may also be composed of other material, such as zooplankton fecal material, that may account for an array of C/N values (Brahney *et al.*, 2006). For instance, high C/N ratios (C/N > 20) can occur in lakes dominated by green algae (*Botryococcus*, C/N=36; Street-Perrott *et al.*, 1997). In addition, C/N ratios may be high in lake waters that are nitrogen-deficient (Talbot and Lærdal, 2000; Brahney *et al.*, 2006), or result from diagenetic effects on organic matter that selectively degrades nitrogen compounds (Talbot, 2001). The sensitivity to terrestrial inputs into the lake is, however, greater if the algal production is low (Sauer *et al.*, 2001). As a precautionary measure for obtaining records of organic matter that are predominantly aquatic in origin, cores are commonly retrieved from the deepest part of the lake, where the likelihood of terrestrial inputs is minimized. Additionally, terrestrial material is generally coarser than the fine-grained cellulose fraction. Thus, terrestrial material can be successfully separated and removed by sieving before subsequent elemental and isotopic analyses.

1.2.4 Carbon isotopes in lake sediments

The carbon-isotope composition of lake–sediment organic matter is influenced by various factors that are mediated through in-lake biological processes, which importantly depend on the source isotopic composition of the dissolved inorganic carbon (DIC) pool and the availability of nutrients. A chief determinant that defines the variability observed in $\delta^{13}C$ values is the rate of carbon uptake during algal productivity. During photosynthesis, algae preferentially utilize ^{12}C to produce organic matter that averages ~20‰ lighter than the $^{13}C/^{12}C$ ratio of their DIC source (Meyers and Teranes, 2001). The discrimination against ^{13}C may decrease at times of high productivity or when DIC is limited, causing $\delta^{13}C$ of lake sediments to approach values close to that of the DIC pool (Hollander and McKenzie, 1991). Hence, the availability of the DIC supply becomes very important in characterizing the amount of ^{13}C-enrichment that occurs in the sediments over time. If DIC is limited, perhaps

due to long periods of low precipitation, the $\delta^{13}C$ values of the remaining DIC increases and produces a subsequent increase in the $\delta^{13}C$ value of the substrate, as the DIC supply is consumed. During strong productivity-driven ^{13}C-enrichment, such as in cases of lake eutrophication, atmospheric CO_2 uptake becomes an important mechanism for obtaining a DIC source. In cases where the utilization of $CO_{2(aq)}$, is limited, the source of the DIC consumed during high algal productivity may switch to other dissolved carbon species (e.g., HCO_3^- or CO_3^{2-}) depending on the lake pH, which greatly enhances ^{13}C-enrichment of the lake sediments. In contrast, a continuous supply of DIC can suppress ^{13}C-enrichment, or result in no change in the $\delta^{13}C$ of lake sediments. The decay of organic matter at the lake bottom releases ^{13}C-depleted CO_2 and CH_4 through respiration and methanogenesis, respectively to the water column. This process introduces ^{13}C-depleted DIC to the overall DIC pool, thus making it readily available for subsequent assimilation during algal productivity, and may result in a decrease in the $\delta^{13}C$ of lake-sediment organic matter.

In some settings the supply of catchment-derived DIC (e.g., $CO_{2(aq)}$ and HCO_3^-) from groundwater and runoff may override the primary effects of photosynthesis and respiration on $\delta^{13}C$ of lake-water DIC. In such cases, changes in $\delta^{13}C$ of lake sediments can greatly reflect the variability in hydrologic conditions of the catchment (e.g., Wolfe *et al.*, 1999; Lee *et al.*, 2005). For instance, an increase in the influx of ^{13}C-depleted DIC produced from soil respiration in non-carbonate catchments results in a decrease in the $\delta^{13}C$ of the DIC pool in the lake. Consequently, DIC sources derived from soil decomposition also depend on the availability of plant debris that is derived from vegetation surrounding the lake. Furthermore, the supply of $CO_{2(aq)}$ may be controlled by large changes in temperature, but for the Holocene these changes are commonly too small to be detected in $\delta^{13}C$ records of lake sediments (Håkansson, 1985). Atmospheric CO_2 exchange with lake-water DIC may become an important process in lakes with long residence times and large surface areas, and especially if catchment-derived DIC sources become limiting. Moreover, $\delta^{13}C$ of atmospheric CO_2 has decreased by 1.5‰ in the past 200 years due to anthropogenic increases of CO_2 from burning of fossil fuels and deforestation, a process known as the Suess effect (Verburg, 2006). This change in $\delta^{13}C$ may be detected in recent sediment records from lakes

where atmospheric CO_2 is in equilibrium with lake water, or where DIC is mainly derived from soil respiration via catchment runoff (Verburg, 2006).

1.2.5 Nitrogen isotopes in lake sediments

The use of nitrogen isotopes in paleolimnological studies has received less consideration because the biochemical behaviour of nitrogen in nature is highly complex, and thus, difficult to interpret in terms of environmental change. However, similar to carbon-isotope systematics in lakes, $\delta^{15}N$ variability in lake–sediment organic matter occurs through in-lake processes governed by algal productivity and water column mixing. If the dissolved inorganic nitrogen (DIN) pool is in ample supply, the uptake of ^{14}N during algal productivity leads to a progressive ^{15}N-enrichment of the remaining DIN pool (mainly NH_4^+ and NO_3^-). Water column mixing in seasonally stratified lakes can also return ^{15}N-enriched DIN to the epilimnion where it is subsequently utilized by algae during growth. Microbial reworking of organic matter, such as processes of denitrification and ammonification, takes place in anoxic conditions and leads to considerable ^{15}N-enrichment in lake sediments (Meyers and Teranes, 2001; Talbot, 2001). On the other hand, subsequent nitrification in the epilimnion may act to suppress the ^{15}N-enrichment of the residual DIN pool. In addition, under moist conditions, high rates of soil organic matter decomposition, and subsequent leaching of ^{15}N-enriched DIN from forested catchments may influence the DIN pool of lakes (Wolfe *et al.*, 1999). Moreover, nitrogen fixation is accomplished by specialized bacteria in soils and diazotrophs, such as blue-green algae (cyanobacteria), which are capable of utilizing dissolved molecular nitrogen with almost no fractionation. In lakes this process occurs under highly eutrophic conditions, resulting in ^{15}N-depletion of the residual DIN pool. Overall, the biochemical nitrogen-isotope fractionations that occur in lakes are generally small, which may be attributable to the buffering effect of the atmospheric N_2 reservoir ($\delta^{15}N = 0‰$). In general, $\delta^{15}N$ values of lake-sediment organic matter range from –2 to +20‰, depending on the main source of DIN (Talbot, 2001).

In some lake systems nitrogen may be a limiting nutrient for organic productivity (Talbot, 2001), which leads to reduced discrimination of ^{15}N values of algal matter approaching those of the total DIN pool. However, non-linear relationships between sediment $\delta^{15}N$ and the $\delta^{15}N$

of DIN through losses of nitrogen from the DIN pool (e.g., Brahney *et al.*, 2006) may develop through a number of processes. (1) Denitrification in the anoxic hypolimnion can lead to significant losses of molecular nitrogen from the DIN pool to the atmosphere, a process which in turn, depends on the overall rate of return of atmospheric nitrogen through dissolution (Talbot, 2001). Denitrification can result in elevated $\delta^{15}N$ values and C/N ratios of lake sediments. (2) The loss of nitrogen via ammonia degassing is a special case where the pH of lake water exceeds 8.5. The fractionation factor is very high, leaving the residual DIN pool ~34‰ heavier than the ammonium (Talbot, 2001). (3) A decreased supply of catchment-derived DIN via runoff and groundwater, generally in response to reduced precipitation, limits the availability of ^{15}N-enriched DIN. The loss of nitrogen may be further enhanced in high-latitude lakes due to the early release of nitrogen from soils in spring and subsequent loss during spring snowmelt (Grogan and Jonasson, 2003). In this case, atmospheric-derived DIN becomes important for algal productivity, resulting in a decrease in $\delta^{15}N$ of the lake sediments (Wolfe *et al.*, 1999). (4) Rapid flushing of DIN through the lake system may occur, especially in hydrologically open lakes with short residence times. This process may suppress $\delta^{15}N$ of residual DIN to lower values, particularly if the DIN pool is continuously replenished by sources that are depleted in ^{15}N. Brahney *et al.* (2006) observed that nitrogen limitation in salmon nursery lakes resulted in a negative correlation between C/N ratios and $\delta^{15}N$, which may be also true for processes in (3) and (4).

1.3 Thesis Organization

The remainder of this dissertation is organized into four main chapters followed by a concluding chapter. The main chapters are designed as drafts of individual manuscripts to be modified for later publication. Each chapter is intended to sequentially follow each other geographically, starting with reconstructions of atmospheric circulation dynamics in northern Fennoscandia to regional scale assessments.

CHAPTER 2: HOLOCENE ATMOSPHERIC CIRCULATION CHANGES RECORDED IN OXYGEN-ISOTOPE RECORDS OF LAKE SEDIMENT CELLULOSE FROM TWO LAKES IN NORTHERN FENNOSCANDIA

This chapter compares $\delta^{18}O$ records of lake sediment cellulose from two throughflow lakes (Lakes Oikojärvi and Keitjoru) with differing water residence times within the same climatic setting. Reconstructions of changes in the seasonal distribution of precipitation and effective moisture are presented and Holocene changes in atmospheric circulation are inferred.

CHAPTER 3: HOLOCENE CHANGES IN CONTINENTALITY ACROSS CENTRAL SWEDEN INFERRED FROM OXYGEN-ISOTOPE RECORDS OF LAKE SEDIMENT CELLULOSE

This chapter compares $\delta^{18}O$ records of lake sediment cellulose from two throughflow lakes (Lakes Spåime and Svartkälstjärn) situated in different climatic settings (oceanic versus continental). Holocene dynamics of atmospheric circulation across central Sweden are highlighted.

CHAPTER 4: HOLOCENE CIRCULATION-DEPENDENT SHIFTS IN THE PRECIPITATION $\delta^{18}O$-TEMPERATURE RELATION IN SWEDEN

This chapter introduces an additional lake sediment cellulose $\delta^{18}O$ record from a throughflow lake (Lake Arbovatten) in southwestern Sweden. This record is compared with other studies in the region to assess changes in effective moisture during the Holocene. The discussions addresses effects of the "8.2 kyr cold event", as well as inferred offsets from the modern precipitation $\delta^{18}O$-temperature relation based on comparison with data from two other lakes in a north-south transect across Sweden as presented in chapter 2 and 3.

CHAPTER 5: HOLOCENE CHANGES IN HYDROLOGY AND NUTRIENT CYCLING INFERRED FROM CARBON- AND NITROGEN–ISOTOPE RECORDS OF ORGANIC LAKE SEDIMENTS FROM FENNOSCANDIA

This chapter compares records of carbon and nitrogen elemental and isotopic data, cellulose $\delta^{18}O$, and magnetic susceptibility from five lakes as presented in chapters 2-4. The

response of nutrient cycling to changes in hydrology and vegetation dynamics is examined in light of climate variability during the Holocene.

CHAPTER 6: SUMMARY AND SYNTHESIS

This chapter summarizes important conclusions presented in chapters 2-5. A synthesis is provided in the context of regional and northern circumpolar scales of atmospheric circulation dynamics and changes in the oxygen-isotope composition of precipitation.

Figure 1-1. Map of Fennoscandia showing the location of lakes studied in thesis.

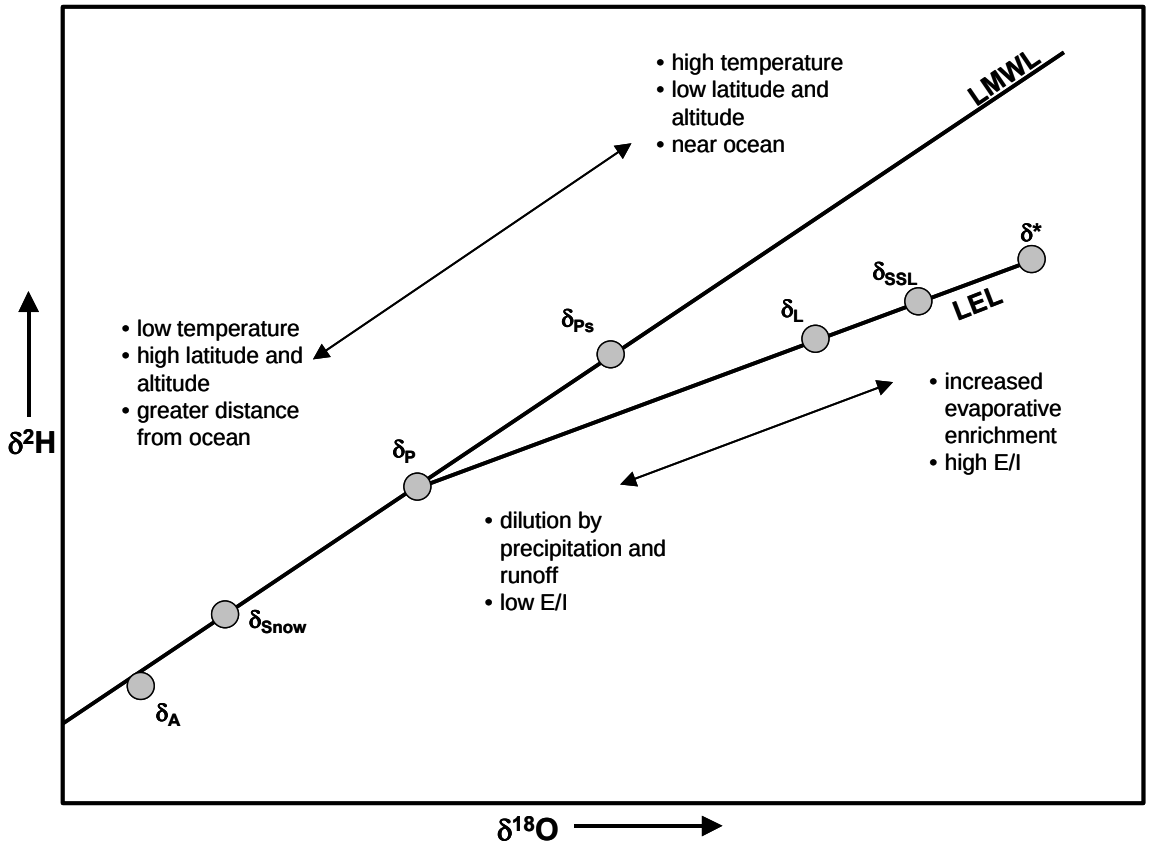

Figure 1-2. Conceptual isotopic framework of the water isotopic compositions that define two linear trends in δ^2H-$\delta^{18}O$ space for a particular geographical area. Key parameters along the Local Meteoric Water Line (LMWL) are the isotopic compositions of weighted mean annual precipitation (δ_P), summer rain (δ_{Ps}) and snow (δ_{Snow}). Key parameters along the Local Evaporation Line (LEL) are the isotopic compositions of lake water (δ_L), steady-state terminal lake (δ_{SSL}) and the limiting isotopic composition (δ^*). Also shown is the isotopic composition of evaporation-flux-weighted atmospheric moisture (δ_A).

Chapter 2
Holocene Atmospheric Circulation Changes Recorded in Oxygen-Isotope Records of Lake Sediment Cellulose from Two Lakes in Northern Fennoscandia

2.1 Introduction

Many studies have documented aspects of Holocene circulation change in northern Fennoscandia, generally as a long-term trend in climate conditions from oceanic during the early Holocene to continental in the mid-Holocene (e.g., Seppä and Hammarlund, 2000; Hammarlund *et al.*, 2002; Giesecke *et al.*, 2008). Supporting evidence for this change in climate in northern Fennoscandia derives from pollen-based studies of vegetation dynamics (e.g., Seppä and Hammarlund, 2000; Bjune, 2004) and reconstructions of summer temperature and annual precipitation (Seppä and Birks, 2001, 2002) and lake-level change based on cladocera (e.g., Korhola *et al.*, 2005). In addition, a carbonate-inferred precipitation $\delta^{18}O$ record from Lake Tibetanus, northern Sweden, also reveals a gradual shift in atmospheric circulation during the Holocene as illustrated by declining precipitation $\delta^{18}O$ and diminishing magnitude of the offset from the Dansgaard (1964) $\delta^{18}O$-temperature relation (Hammarlund *et al.*, 2002). Other records of $\delta^{18}O$ in northern Norway (Lauritzen and Lundberg, 1999; Hammarlund and Edwards, 2008) and near Abisko, northern Sweden (Shemesh *et al.*, 2001) also illustrate decreasing $\delta^{18}O$ over time that may reflect a gradual increase in continentality. These trends observed in the proxy archives are probably reflecting a gradual shift between two types of large-scale circulation patterns, i.e., a strong zonal or westerly flow during the early Holocene transitioning to more meridional or north-south flow by the mid-Holocene (Hammarlund *et al.*, 2002). Superimposed on the gradual trend in atmospheric circulation is considerable variability in climate across continental areas in Fennoscandia, especially during the late Holocene (Seppä and Birks, 2001; Snowball *et al.*, 2004; Seppä *et al.*, 2005).

Climate variability in the North Atlantic is often related to variations in the North Atlantic Oscillation (NAO). The NAO index is represented as the sea-level pressure difference

between the Icelandic Low and the Azores High (Hurrell, 1995). A positive NAO index is associated with zonal circulation and increased intensity of cyclones, leading to mild, moist winters and cool, moist summers in northern Europe. In contrast, a negative NAO index is characterized by meridional circulation resulting in cold, dry winters and warm, dry summers. However, the impact of the NAO on climate differs regionally, which is important to consider when interpreting proxy records. For instance, during positive index winters, precipitation amount is greatest southwest of the Scandes Mountains and considerably reduced on the lee side (Wallén, 1970; Johannessen, 1970; Uvo, 2003). Instead, precipitation inland is mainly related to northwesterly flow of air masses, carrying moisture into northern Fennoscandia (Alexandersson and Andersson, 1995).

For this study, two lakes were selected near a meteorological station at Naimakka, northern Fennoscandia, to obtain sediment cellulose records of $\delta^{18}O$ for the Holocene. The purpose of this paper is to shed some understanding on specific aspects of climate variability, namely as summer and winter atmospheric circulation patterns for the Holocene, based on changes in the seasonal distribution of precipitation and hydrology as recorded in lake water $\delta^{18}O$. In particular, insight on the Holocene variability of the winter NAO index is provided from changes in reconstructed winter precipitation, whereas the variability of the summer NAO index is inferred from evaporative enrichment. The two lakes in this study are hydrologically open, but the difference in the residence time and catchment morphology provides contrasting hydrological responses under the same climatic conditions. This difference is manifested in the isotope composition of the modern lake water, and subsequently imprinted in the oxygen isotope record derived from lake sediment cellulose. A multi-proxy approach is undertaken to aid in the interpretation of the sediment cellulose $\delta^{18}O$ archive. The interpretation of the cellulose $\delta^{18}O$ records is supported by an extensive modern isotope hydrology dataset from 2002-2006 and precipitation isotopes collected at Naimakka (IAEA/WMO GNIP dataset), which helps to set firmer constraints on reconstructing the paleoclimate in the region. One of the lakes has previously been included in a study of $\delta^{2}H$ in surface sediment n-alkanes (Sachse *et al.*, 2004), which also help to assess the water signal recorded in the cellulose $\delta^{18}O$. Results are compared to independent records of pollen-inferred reconstructions of mean July temperature and annual precipitation from Lake

Tsuolbmajavri, northwest Finland (Seppä and Birks, 2001) and the carbonate-inferred precipitation $\delta^{18}O$ from Lake Tibetanus (Hammarlund *et al.*, 2002).

2.2 Site Description

Lake Keitjoru (informal name; 68º40'N, 21º30'E; 418 m a.s.l.) is located 1 km southwest of the Naimakka meteorological station and the river Könkämäälven, in the Lapland province of Sweden, near the Swedish-Finland border (Figure 2-1). It is a small (0.02 km^2) throughflow and shallow lake (1.8 m) that drains a catchment area of 1.9 km^2 through two inlets located southeast and southwest and one wide outlet at the north end. Mount Keitjoru (*c*. 700 m a.s.l.), *c.* 1.6 km from the lake, is the highest elevation in the catchment and forms a steep north-facing slope. In spite of the shallowness of the lake, it does not freeze completely to the bottom during winter, possibly because relatively warm groundwater discharges continuously to the lake. Abundant groundwater discharge and surface runoff were evident during field observations in May 2003. Based on the water balance (precipitation = evaporation + outflow) and catchment characteristics (volume and area), the average residence time of water is approximately 15 days (Table 2-1).

Oikojärvi (68°50'N, 21°10'E; 463 m a.s.l.) is located approximately 23.5 km north of Lake Keitjoru and east of Könkämäälven in Finland (Figure 2-1). It is a large, oligotrophic, open-drainage lake (1.3 km^2) having two elongated, connected basins in an east-west orientation, and has a water depth of 8.0 m at the sampling point. There are two inlets from the north entering into the larger eastern basin, and one main outlet exiting at the west side of the lake, where it drains into Könkämäälven. Oikojärvi has a much longer average water residence time of about 1.5 years, assuming a uniform water depth in both basins (Table 2-1). The topographic gradient to the east is relatively gentle, whereas the north and south sides of the lake are surrounded by elevations ranging from 520 to 585 m a.s.l.

Both lakes lie within an area of Precambrian granite gneiss blanketed by hummocky till of Quaternary age (Lundqvist, 1998). Extensive deposits of poorly sorted outwash gravels from the last deglaciation are also present in the Oikojärvi catchment. The vegetation at both lakes is characterized by communities consisting of *Betula pubescens*, *B. nana*, *Juniperus communis*, *Empetrum nigrum*, *Vaccinium vitis-idaea*, *V. uliginosum*, *Salix* sp., *Populus*

tremula, *Carex* sp., *Sphagnum*, lichens and herbs. The Lake Keitjoru catchment also contains sporadic occurrences of *Picea abies* and *Pinus sylvestris*. Both lakes are located within the mountain birch subalpine zone, with Lake Keitjoru being closer to the coniferous-mountain birch tree-line located *c.* 16 km southeast. Oikojärvi is located closer to the tundra zone boundary situated west of the Sweden-Finland border, *c.* 19 km north (Seppä *et al.*, 2002).

The climate in northern Fennoscandia is generally continental due to the strong moisture gradient on the lee side of the Scandes Mountains. The mean July and January temperature at Naimakka meteorological station (403 m a.s.l.; 68º41'N, 22º21'E) are 12.6°C and –12.9°C, respectively, mean annual precipitation is 456 mm, and the average June-September relative humidity is 74% (SMHI 1990-2006). Evapotranspiration is relatively low, amounting to 100-200 mm per year (Bringfelt and Forsman, 1995; Alexandersson *et al.*, 1991). Lakes in this area are generally ice-free between late May and mid-October, providing a growing season of *c.* 120 days. About 60% of the total annual precipitation falls during this time.

2.3 Methods

2.3.1 Fieldwork and subsectioning

A series of overlapping sediment cores was retrieved near the northeast part of Lake Keitjoru at a water depth of 1.84 m, and from the north-central end of the westernmost basin of Oikojärvi at a water depth of 8.0 m, through lake-ice in May 2003 using a 1 m long Russian peat sampler. Segments from the deep cores were correlated in the laboratory using surface-scanned measurements of magnetic susceptibility, and observable changes in lithostratigraphy (Table 2-2). The 1.53 m sediment sequence from Lake Keitjoru was divided into 55 sections at 2-3 cm thick intervals. The 3.2 m sediment sequence from Oikojärvi was divided into 120 sections, also at 2-3 cm thick intervals. In addition, surface sediment profiles, 0.22 and 0.29 m thick, from Lake Keitjoru and Oikojärvi, respectively, were retrieved using a gravity corer, and divided into 19 and 27 contiguous sections, respectively, at 1-2 cm intervals in the field.

2.3.2 Water sampling and isotope analyses

Water samples from Oikojärvi and Lake Keitjoru were collected monthly (except February and December) between August 2002 and August 2005, and several times in July-August 2006, yielding a total of 86 samples. In addition, 33 river samples were collected from Könkämäälven over the same period. The determinations of oxygen and hydrogen isotope compositions were performed at the University of Copenhagen, the University of Aarhus, the University of Waterloo and the NERC Isotope Geosciences Laboratory, Nottingham, using the CO_2-equilibration and Zn- or Cr-reduction methods. All stable isotope results are expressed as δ-values, representing deviations in per mil (‰) from the VSMOW (Vienna Standard Mean Ocean Water) standard such that $\delta_{sample}=1000[(R_{sample}/R_{VSMOW}) -1]$, where R is the $^{18}O/^{16}O$ or $^{2}H/^{1}H$ ratio in sample and standard. $\delta^{18}O$ and $\delta^{2}H$ values are normalized to SLAP having values of –55.5‰ and –428‰, respectively (see Coplen, 1996). Analytical uncertainties are ±0.2‰ for $\delta^{18}O$ and ±2‰ for $\delta^{2}H$.

Lake sediment samples were prepared for oxygen isotope analysis following the techniques developed and refined at the University of Waterloo Environmental Isotope Laboratory (UW-EIL) and described in detail by Wolfe *et al.* (2001a, 2007). Briefly, sediment samples are initially acid-washed to eliminate biogenic and mineral carbonates and subsequently dry-sieved using a 500-μm mesh. The fine-grained fraction is then processed through four additional steps: 1) solvent extraction to remove lipids, resins, and tannins, 2) bleaching to remove lignins, 3) alkaline hydrolysis to remove polysaccharides, and 4) leaching to remove iron and manganese oxyhydroxides. A final step involves the separation of cellulose from minerogenic constituents in the sediment sample by using a heavy-liquid (sodium polytungstate) density separation technique (Wolfe *et al.*, 2007). Cellulose $\delta^{18}O$ was determined by CO generated from high-temperature (1300°C) pyrolysis using an on-line continuous-flow isotope-ratio mass spectrometer at the UW-EIL (see Wolfe *et al.*, 2007). Sufficient sample amount enabled duplicates of $\delta^{18}O$ analysis to be performed on a total of 51 out of 55 Lake Keitjoru cellulose samples, and a total of 117 out of 119 Oikojärvi cellulose samples. The uncertainty (one standard deviation) based on the analytical reproducibility estimated from repeated measurements conducted on the same cellulose

samples resulted in an average of ±0.7‰ and ±0.5‰ for Lake Keitjoru and Oikojärvi, respectively.

2.4 Results and Interpretations

2.4.1 Modern isotope hydrology

In the Naimakka region, precipitation and surface waters plot along trajectories defined by the Local Meteoric Water Line (LMWL) and the Local Evaporation Line (LEL), respectively, as shown in Figure 2-2a. The LMWL is formed by the regression through oxygen- and hydrogen-isotope data of weighted monthly average precipitation collected from the Naimakka meteorological station (403 m a.s.l) during the period 1990-1995 (IAEA/WHO GNIP data). Significant points along the LMWL are the amount-weighted means for annual precipitation (δ_P; $\delta^{18}O$=–16.1‰, δ^2H=–119‰), rain (δ_{Ps}; $\delta^{18}O$=–12.9‰, δ^2H=–94‰), and snow (δ_{snow}; $\delta^{18}O$=–20.3‰, δ^2H=–152‰). The predicted LEL is based on the Craig and Gordon (1965) model that describes the isotopic enrichment of an evaporating water body with an initial input water isotopic composition starting at δ_P. The predicted LEL slope is defined in decimal notation as (Gibson *et al.*, 2008):

$$S_{LEL} = \frac{\left[\dfrac{h(\delta_A - \delta_P) + (1+\delta_P)(\varepsilon_K + \varepsilon^*/\alpha^*)}{h - \varepsilon_K - \varepsilon^*/\alpha^*}\right]_2}{\left[\dfrac{h(\delta_A - \delta_P) + (1+\delta_P)(\varepsilon_K + \varepsilon^*/\alpha^*)}{h - \varepsilon_K - \varepsilon^*/\alpha^*}\right]_{18}}$$

where ε^* and ε_K are the equilibrium and kinetic separations, respectively, α^* is the liquid-vapour equilibrium fractionation factor, in which $\alpha^* > 1$, and the subscripts refer to deuterium and oxygen-18. The ε^* term is defined as α^*-1 (in decimal notation) and α^* is dependent on temperature (Horita and Wesolowski, 1994) and the ε_K term is dependent on relative humidity (h) normalized to the water surface temperature, expressed as ε_K (^{18}O) = 14.2(1–h) and ε_K (^2H) = 12.5(1–h) (Gonfiantini, 1986). The evaporation-flux-weighted isotopic composition of atmospheric moisture (δ_A; $\delta^{18}O$=–22.4‰, δ^2H=–165‰) is estimated by assuming isotopic equilibrium with δ_{Ps} such that $\delta_A=(\delta_{Ps} - \varepsilon^*)/\alpha^*$ (Zuber, 1983; Gibson and Edwards, 2002). The climate data used are the June-September average estimates of

temperature (9.3°C) and relative humidity (74%; SMHI 1999-2006). Shown along the predicted LEL in Figure 2-2a are two points, which are the isotopic composition of a steady-state terminal lake (δ_{SSL}; $\delta^{18}O$=–6.6‰, $\delta^{2}H$=–70‰) and the limiting isotopic composition (δ^*; $\delta^{18}O$=–3.2‰, $\delta^{2}H$=–52‰). The limiting isotopic composition δ^* is theoretically the maximum isotopic enrichment that water attains as it approaches complete desiccation. The δ^* value is the end-point on the LEL and it is dependent on local atmospheric conditions (h, T, and δ_A) as expressed in decimal notation by:

$$\delta^* = \frac{h\delta_A + \varepsilon_K + \varepsilon^*/\alpha^*}{h - (\varepsilon_K + \varepsilon^*/\alpha^*)}$$

Superimposed on this isotopic framework are results obtained on lake water samples collected from Lake Keitjoru and Oikojärvi during August 2002-2005 and August-September 2006 (Figure 2-2b). In general, both lakes show values that cluster close to δ_{Ps}, reflecting a greater importance of summer precipitation to the overall lake balances. Therefore, evaporative enrichment of water from these lakes may follow a lake-specific LEL, which is taken as a line between the average isotopic composition of Oikojärvi lake water (δ_L; $\delta^{18}O$=–12.9‰, $\delta^{2}H$=–97‰) and δ^*. The intersection of the lake-specific LEL with the LMWL characterizes the isotopic composition of the input water (δ_{input}) recharging Oikojärvi. As confirmation, the isotope signature of a closed-basin lake (δ_{lake}), sampled in August 2002, 600 m southwest of Naimakka, plots very close to the lake-specific LEL indicating isotopic enrichment of water that evolved from an initial isotopic composition similar to δ_{input} (Figure 2-2b). The offset between δ_P and δ_{input} may reflect a difference in the amount of snow in the overall total precipitation over two separate time periods. For instance, during precipitation monitoring (IAEA/WMO GNIP; 1990-1995), the amount of snow ranged between 31 and 49% of the total annual precipitation. In contrast, during the lake sampling period (2002-2006), the snow amount was slightly lower, totalling 21-31%. Indeed, there has been a significant increase in precipitation and summer rainfall-induced floods in Sweden during the last two decades as compared to the long observational records of the past century (Lindström and Alexandersson, 2004).

Upon closer inspection, the isotopic compositions of Lake Keitjoru water samples vary along and above the LMWL having values ranging from –16.2 to –12.3‰, similar to the range of the weighted precipitation means, δ_P and δ_{Ps} (Figure 2-3a). The influx of isotopically depleted snowmelt results in lake water isotopic signatures that plot closer to δ_P in spring, and then shift towards δ_{Ps} by September (Figure 2-3b). Snowmelt contributions in Lake Keitjoru and its corresponding imprint on the isotopic composition of the lake water is likely attributable to late-melting snow on the north-facing slope of Mount Keitjoru and the rapid hydrological response of the lake system. The trend in the isotopic composition of Lake Keitjoru in δ^2H-$\delta^{18}O$ space confirms that lake water is effectively recording seasonal variations in the isotopic composition of precipitation in the area. Likewise, water isotope data from Könkämäälven ($\delta^{18}O$ ranges from –15.6 to –12.6‰) are also observed to have a nearly identical isotopic pattern as Lake Keitjoru lake water signatures, indicating similar source waters (i.e., groundwater and precipitation), but integrated over a larger area. As further evidence of precipitation control, the isotopic composition of groundwater in the Lake Keitjoru catchment is likely to reflect the source water composition that enters the lake, which should closely mirror the isotopic composition of precipitation. A sample of groundwater collected in August 2002 has a $\delta^{18}O$ value of –13.9‰ and plots close to the intersection between the Oikojärvi lake-specific LEL and the LMWL (δ_{input}; $\delta^{18}O$=–13.6‰; Figure 2-3a). In the following spring of May 2003, the isotopic composition of groundwater, having a $\delta^{18}O$ value of –15.8‰, lies very close to δ_P. Although the number of groundwater samples is limited, this does provide an indication that groundwater feeding the lake is very sensitive to seasonal changes in $\delta^{18}O$ of precipitation, and is reflected in the $\delta^{18}O$ composition of Lake Keitjoru.

The isotopic composition of Oikojärvi water samples plot along the lake-specific LEL having values ranging from –14.3 to –11.8‰ (Figure 2-3a). The evolution of lake water δ_L along the LEL is a measure of the water loss due to evaporation and can be expressed as the evaporation/inflow ratio (E/I). Based on an isotope-mass balance approach, E/I is defined in decimal notation as (Gonfiantini, 1986):

$$\frac{E}{I} = \left[\frac{1 - h + \varepsilon_K}{h - \varepsilon_K - \varepsilon^* / \alpha^*} \right] \times \left[\frac{\delta_L - \delta_{input}}{\delta^* - \delta_L} \right]$$

where δ_{input} ($\delta^{18}O$=–13.6‰) and the average and maximum isotopic composition of Oikojärvi water δ_L ($\delta^{18}O$=–12.9‰ and –11.8‰) results in an E/I ratio of 0.03 and 0.08, respectively. This very small degree of evaporative enrichment reflects the fact that δ_L is very close to the lake-specific δ_{input}, since Oikojärvi is receives a significant proportion of rainfall-dominated precipitation. On the other hand, if Oikojärvi received input waters with an isotopic composition closer to δ_P, then the average and maximum E/I ratios are 0.12 and 0.18, respectively. The isotopic composition of lake water is, thus, sensitive to the dilution by precipitation. For instance, during the open water season, evaporative enrichment of lake water is generally suppressed by input of summer rainfall (Figure 2-3b), which is likely efficiently captured by Oikojärvi's large surface area. In May and June, Oikojärvi's larger lake volume and longer residence time than Lake Keitjoru likely damps the isotopic signal of snowmelt, such that the monthly average isotopic composition of lake water maintains a signature close to that of δ_{input} (Figure 2-3b). Sampling of input waters by Sachse *et al.* (2004) concluded that the headwater lakes in the Oikojärvi catchment do not contribute significant amounts of evaporatively-enriched waters to Oikojärvi, indicating that this lake is heavily dependent on recharge by local precipitation and runoff.

The time-series shown in Figure 2-4 exemplifies the sensitivity of the isotopic composition of lake water to changes in the monthly precipitation amount measured concurrently during the period of water sample collection. In the 2002 and 2003 open water seasons, the precipitation (average 169 mm) that fell in the region was less than the long-term June-September mean (231 mm; SMHI 1990-2006). In fact, the summer of 2003 was a time of record dryness in Fennoscandia (Kauppinen, 2003), resulting in evaporative enrichment of Oikojärvi lake water along the LEL, while the isotopic compositions of Lake Keitjoru water and Könkämäälven were generally maintained between δ_P and δ_{Ps} (Figure 2-4 and 2-5a). By contrast, the 2004 open-water season was considerably wet, with the total June-September precipitation (453 mm) much greater than the long-term average. Correspondingly, the summer relative humidity also increased from an average of 72% in

2003 to 77% in 2004. Hence, no evaporative enrichment was detected in Oikojärvi lake water, which instead varied along the LMWL, similar to the isotopic signature of Lake Keitjoru (Figure 2-5b). In response to greater amounts of summer precipitation, the isotopic compositions of both Lake Keitjoru and Oikojärvi plot slightly above δ_{Ps} (Figure 2-4 and 2-5b). The offset between δ_{input} from δ_P, as shown in Figure 2-2a, may reflect snowmelt bypass effects as observed in Weslemkoon Lake, Canada (Edwards and McAndrews, 1989). However, snowmelt bypass occurs as a consequence of greater precipitation and efficient throughflow of meltwater, potentially resulting in the appearance of more evaporation during the summer. This trend is not observed in the time-series of Oikojärvi lake water $\delta^{18}O$ and precipitation amounts. In general, the offset between the isotopic signatures of Lake Keitjoru and Oikojärvi waters is greatest during dry years (2002, 2003), and most similar during wet years (2004).

The response of lake water to the input of isotopically depleted snowmelt appears to also reflect changes in the water balance in the catchment. For instance, isotopic depletion of Lake Keitjoru water due to spring snowmelt in 2004 was much more pronounced than in 2003 and less so than in 2005 (Figure 2-4). The water table in the lake catchment was likely drawn down significantly during the dry years, so that subsequent snowmelt contributions replenished the groundwater storage in spring 2004. In comparison, spring snowmelt in 2005 is likely to have flushed rapidly through the lake catchment if it was saturated from the previous wet year (2004), thus resulting in a subdued response to the input of isotopically depleted snowmelt in Lake Keitjoru water.

2.4.2 Sediment description and chronology

2.4.2.1 Lake Keitjoru

The sediment sequence from the Lake Keitjoru (1.46 m) long core was classified into ten lithostratigraphic units based on appearance and lithology of the sediments (Table 2-2). Lake Keitjoru shows considerable variation, starting at the bottom of the sequence with 0.7 m of grey silty clay (unit 1) that grades rapidly to a 0.05 m-thick interval of brown to dark brown silty gyttja (unit 2; Figure 2-6). This is followed by 0.18 m of dark brown silty gyttja (unit 3) that is rich in moss and coincides with increasing, but variable TOC content. The next 0.33

m (unit 4) contains lighter brown algal-rich gyttja that is consistently high in TOC content, followed by a significant drop in TOC content in unit 5 (0.15 m). The subsequent 0.12 m thick sequence (unit 6) consists of dark brown banded gyttja and coincides with very high, but variable TOC content. This unit is followed by a much thicker unit (0.42 m) of light brown moss-rich gyttja with low and variable TOC content (unit 7). The uppermost 0.21 m of the sediment core consists of watery brown gyttja (units 8–10), with the lower 0.09 m part of this sequence (units 8-9) being slightly lighter brown and have consistently low TOC content. The upper 0.12 m part of this sequence (unit 10) consists of very watery brown gyttja and very high TOC content, similar to that of unit 6.

The chronology for the Lake Keitjoru sediment core is based on combining seven calibrated AMS radiocarbon dates of aquatic and terrestrial macrofossil remains obtained from the long core (Table 2-3) and the Constant Rate of Supply (CRS) model ^{210}Pb dates (Oldfield and Appleby, 1984) from the gravity core. Two terrestrial macrofossils (see Table 2-3), located at a mid-depth of 2.445 m and 2.605 m below the water surface, have ages that are likely too old and were excluded from the age-depth model, since these may have been reworked in the catchment soils prior to burial into the lake sediments. The aquatic moss is likely to reflect a more accurate time of burial. For instance, aquatic moss at 2.445 m (Table 2-3) was dated younger than a terrestrial macrofossil from the same depth (Figure 2-6).

Radiometric isotopes ^{210}Pb, ^{214}Bi, and ^{137}Cs were measured by gamma spectrometry on 11 contiguous samples from the gravity core (Figure 2-7). Total ^{210}Pb activity declines exponentially with depth, reaching supported ^{210}Pb levels (0.001 Bq/g) at 1.93-1.95 m below water depth. Errors in ±1 SD units of the CRS model ^{210}Pb dates range from ±0.2 to ±3.3 years (average ±1.0 years). Unfortunately, there was no detection of a ^{137}Cs peak in the profile (Figure 2-7), possibly because of the high mobility of this radioisotope in organic-rich, clay-poor sediments. After matching organic carbon and nitrogen elemental and stable isotope composition profiles between the long and gravity cores, the depth of the top of the long core was shifted down by 5 cm (Figure 2-8). By design, the gravity corer effectively captures the water-sediment interface. The collection of sediments using a Russian peat corer is less effective in collecting the uppermost sediment with high water content.

The resulting age-depth model is based on a polynomial fit through the five accepted radiocarbon dates and near-surface ^{210}Pb dates (Figure 2-6). The apparent sediment accumulation rate decreased from 0.18 mm/year below *c.* 3.12 m (unit 1-3) to 0.09 mm/year at *c.* 2.79–3.12 m (unit 4), and then increased again to 0.16 mm/yr between *c.* 2.52–2.79 m (unit 5-6), followed by rapid accumulation at a rate of 0.67 mm/year above *c.* 2.5 m (unit 7-10). The onset of gyttja development corresponds to a basal date of 9430 cal. BP at the bottom of unit 2.

2.4.2.2 Oikojärvi

The Oikojärvi (3.20 m) sediment core was classified into three lithostratigraphic units (Table 2-2). The lowermost sequence (unit 1) is composed of grey clay, grading into a 0.24 m brown detritus gyttja (unit 2) with low TOC content. The following unit is a substantial 2.96 m sequence of homogeneous, brown, fine detritus gyttja (unit 3) with higher TOC content (Figure 2-9).

The chronology for Oikojärvi long core sediments was developed by combining two AMS radiocarbon dates obtained near the bottom of the sequence, CRS model ^{210}Pb dates from the gravity core, and the identification of lead pollution chronological markers. Nine AMS radiocarbon dates were obtained from the Oikojärvi long core sediments, two of which are based on remains of terrestrial vegetation and seven based on bulk sediment (Table 2-3). The calibrated age of the lowermost bulk sediment sample is 11,500 cal. BP, which is *c.* 1500 years older than the lowermost macrofossil sample positioned only 4 cm above the bulk sample. Since deglaciation and subsequent infilling of the lake likely commenced around 10,200 cal. BP (Lundqvist, 1998), the bulk sediment sample is believed to be too old. Indeed, all seven bulk sediment samples appear to be consistently too old and were thus excluded from the age-depth model (Figure 2-9).

Similar to Lake Keitjoru, the gravity core sediments obtained from Oikojärvi were also dated based on the CRS model of ^{210}Pb, combined with measurements of ^{214}Bi and ^{137}Cs activities (Figure 2-7). Errors (±1 SD unit) of the CRS model ^{210}Pb dates range from ±0.2 to ±0.8 years (average = ±0.5 years). In particular, the resulting CRS age model is in excellent agreement with the 1986 ^{137}Cs date pertaining to the Chernobyl fall-out, which occurs at *c.*

8.03 cm. Additionally, peak sediment accumulation rates reaching *c.* 0.150 cm/yr at around 8.08 m (1943 year AD) and 8.06 m (1957 year AD), also coincide with the timing of maximum activity at a gravel pit located adjacent to the lake, which became active in the early 1940s. Stratigraphic agreement exists on the organic carbon and nitrogen elemental and stable isotope composition between the long and gravity cores (Figure 2-10). The CRS model ^{210}Pb model was applied to the uppermost samples of the long core, assuming that the sediment surface represents approximately modern-day conditions (Figure 2-9).

The age-depth model was additionally constrained through the identification of lead pollution chronological markers using a method according to Renberg *et al.* (2001). This method is successfully applied if there is a well-defined contrast between the ^{206}Pb/^{207}Pb ratios of natural lead and pollution lead in the sediments and corresponding source concentrations are characterized for the area. In this case, a two-point mixing ratio can be used to detect the influx of pollution lead. In Sweden, the natural ^{206}Pb/^{207}Pb ratio is higher than the anthropogenic airborne pollution lead ratio (Renberg *et al.*, 2001). Therefore, increasing lead concentrations and decreasing ^{206}Pb/^{207}Pb ratios, identified at 8.66 and 9.29 m, reflect peak lead productivity during the Roman Empire and the Medieval period at 100 BC - AD 200 and AD 1000-1200, respectively (Figure 2-9). Notably, the sediments show an increase in lead pollution starting at *c.* 8.18 m, which likely represents increased industrial activity in the early 20th century (Renberg *et al.*, 2001; Figure 2-9). However, the lead pollution marker at AD 1970, representing peak industrial emissions and usage of lead in gasoline, followed by a decline to the present, is missing from the profile, and this may indicate some sample loss of the uppermost surface sediments during Russian core extraction. Therefore, the uppermost age of the long core is likely to be older than the assigned age of AD 2003 (–53 cal. BP), but rather closer to the 1970s. The complete age-depth model results in a tentative basal date of *c.* 10,200 cal. BP, which is consistent with the timing of deglaciation (Lundqvist, 1998). The apparent sediment accumulation rate of 0.23 mm/year below 11.0 m (*c.* 9200 cal. BP) declined to an average of 0.12 mm/year from 11.0-10.6 m (*c.* 9200-6000 cal. BP), then gradually increased until present with an average rate of 1.4 mm/year during the last 200 years.

2.4.3 Cellulose-inferred oxygen-isotope records

The lake water $\delta^{18}O$ records for Lake Keitjoru and Oikojärvi were reconstructed from cellulose $\delta^{18}O$ values using a cellulose-water isotopic fractionation factor of 1.028 (Edwards *et al.*, 1985; Edwards and McAndrews, 1989; Wolfe *et al.*, 2001a, 2007). The cellulose-inferred lake water $\delta^{18}O$ values from Lake Keitjoru and Oikojärvi in northern Fennoscandia show different trends (Figure 2-11). At the base of the Lake Keitjoru record, $\delta^{18}O$ values are low (–19.3 ‰) before *c.* 8800 cal. BP, followed by a steep rise to –14.7‰ by *c.* 7600 cal. BP. Between *c.* 7600 and 6600 cal. BP, $\delta^{18}O$ values decrease to an average of –17.1‰ before increasing to –15.2‰ by *c.* 6400 cal. BP. From *c.* 6400 to 4400 cal. BP, Lake Keitjoru $\delta^{18}O$ remains fairly consistent within the range of –15.9 to –14.0‰, followed by a substantial decline to –18.6‰ by *c.* 3800 cal. BP. Low $\delta^{18}O$ values (–18.3‰) persist until *c.* 2000 cal. BP and then rise significantly to a maximum of –13.7‰ by *c.* 1200 cal. BP. There is a sharp decrease to $\delta^{18}O$ values of –20.2‰ by *c.* 500 cal. BP, followed by an increase to –17.4‰ at the top of the core. Three cellulose samples from Lake Keitjoru at *c.* 1520, 2519, and 2692 cal. BP were identified as possible outliers (Figure 2-11) due to contamination of terrestrial input. This conclusion is based on a combination of increased cellulose $\delta^{18}O$, increased TOC (15-19%), and high C/N ratios >17 (see detailed discussion in Chapter 5).

Inferred Oikojärvi $\delta^{18}O$ values decline from –14.7 to –17.5‰ by *c.* 8000 cal. BP, followed by a substantial increase to an average of –12.8‰ at *c.* 7800-7200 cal. BP (Figure 2-11). From *c.* 7200 to 5500 cal. BP, $\delta^{18}O$ values decrease considerably to –18.6‰, followed by an abrupt rise to –14.3 ‰ by *c.* 5300 cal. BP. Between *c.* 5300 and 4200 cal. BP, $\delta^{18}O$ values fluctuate in the range of –16.5 to –13.4‰, and then decrease to an average value of –16.7‰ by *c.* 3200-2900 cal. BP. At *c.* 2900-1400 cal. BP, $\delta^{18}O$ values fluctuate, but gradually increase to a maximum value of –13.2‰. From *c.* 1400 cal. BP to the present, large swings in $\delta^{18}O$ values occur with negative excursions at *c.* 1100 (–17.7‰) and 45 cal. BP (–17.9‰) and positive excursions at *c.* 1000 (–13.9‰) and 400 cal. BP (–13.7‰).

An aquatic origin is assumed for the lake sediments from Lake Keitjoru and Oikojärvi. However, the cellulose-inferred lake water $\delta^{18}O$ values for the topmost sediment samples from both Lake Keitjoru and Oikojärvi are negatively offset from that of the lake water

obtained at the time of water sampling and core collection (Figure 2-11). For instance, the topmost sediment sample from Oikojärvi spans *c.* 26 years (with a mid-age of AD 1971) and is offset by *c.* 2.5‰ from the measured average lake water $\delta^{18}O$. The inferred $\delta^{18}O$ from the topmost sediment sample from Lake Keitjoru, spanning a longer period of time (33 years, with a mid-age of AD 1976) gives a larger offset by 4.0‰ from $\delta^{18}O$ of average lake water. This difference may be attributed to the mismatch between the lake water sampling period and the time represented by the surface sediment. The cellulose-inferred lake water $\delta^{18}O$ in Oikojärvi and Lake Keitjoru suggests that cellulose may be recording isotopically-depleted melt waters early in the spring. This is suggested by the overlap between the cellulose $\delta^{18}O$ record and minimum measured lake water $\delta^{18}O$ (Figure 2-11). However, the modern isotope hydrology at Oikojärvi does not indicate a strong snowmelt signal in the lake water $\delta^{18}O$ time-series. The topmost cellulose $\delta^{18}O$ value (15.5‰) at Oikojärvi does correspond more closely with the weighted annual precipitation δ_P ($\delta^{18}O$=–16.1‰), which represents an age (AD 1990-1995) that is closer to the age represented by the Oikojärvi cellulose $\delta^{18}O$ (AD 1971). Hydrogen-isotope ratios were measured on n-alkanes obtained from surface sediments of several lakes, including Oikojärvi, by Sachse *et al.* (2004). The resulting analysis of $\delta^{2}H$ from algae n-alkane (n-C_{17}) gives a value *c.* –114‰, which lies between the $\delta^{2}H$ value of weighted annual precipitation at Naimakka, ($\delta^{2}H$=–119‰) and the intersection between the lake-specific LEL and LMWL ($\delta^{2}H$=–101‰), consistent with the fact that precipitation and runoff are the dominant sources of water to Oikojärvi.

2.5 Discussion

2.5.1 Reconstruction of Holocene paleohydrology

The analysis of the modern lake water isotopic composition of Oikojärvi illustrated trends in $\delta^{2}H$-$\delta^{18}O$ space that followed the LEL during dry periods (e.g., AD 2003) and the LMWL during wet periods (e.g., AD 2004). In spite of its long residence time and small evaporative enrichment, the range of $\delta^{18}O$ values in the cellulose record shows variations of up to 8‰ (Figure 2-11), which surpasses the range observed in modern precipitation $\delta^{18}O$ (7.4‰) only slightly, and modern lake water $\delta^{18}O$ (2.5‰) considerably. This implies that Oikojärvi

cellulose-inferred water $\delta^{18}O$ is tracking both variability in the seasonal distribution of precipitation, mainly between the mean annual precipitation $\delta^{18}O_P$ and the present-day lake-specific LEL-LMWL intersect $\delta^{18}O_{input}$, and changes in the degree of evaporative enrichment. Thus, the greatest evaporative enrichment of Oikojärvi lake water is likely to occur when $\delta^{18}O_P$ characterizes the input water composition, such as the case if winters are snow-rich and summers are dry. In order to reconstruct past changes in evaporative enrichment in Oikojärvi, a precipitation $\delta^{18}O_P$ record is needed.

A carbonate-inferred precipitation $\delta^{18}O_P$ record at Lake Tibetanus (Figure 2-11; 560 m a.s.l.; Hammarlund *et al.*, 2002), which is *c.* 100 km southwest of Naimakka (Figure 2-1), is used to deconvolute lake water $\delta^{18}O$ of Oikojärvi, and thus obtain a record of evaporative enrichment. Lake Tibetanus is fed predominantly by groundwater that recharges the lake at a high flushing rate, and thus, the oxygen isotope composition of the lake water is believed to represent the long-term average precipitation $\delta^{18}O_P$ in the Abisko region (Hammarlund *et al.*, 2002). Lake Tibetanus $\delta^{18}O_P$ was about 2‰ higher in the early Holocene than present, likely as a result of stronger westerlies that penetrated into the continent. A similar pattern of circulation-dependent variations in $\delta^{18}O_P$ is also evident in other oxygen-isotope archives, such as calcite $\delta^{18}O$ from a speleothem in Søylegrotta, northern Norway (Lauritzen and Lundberg, 1999) and biogenic silica $\delta^{18}O$ from lake sediments near Abisko, northern Sweden (Shemesh *et al.*, 2001). The systematic trends emerging at a regional scale in northern Fennoscandia provides support for using Lake Tibetanus $\delta^{18}O_P$ as a record of mean annual precipitation at Naimakka, and thus as the input water $\delta^{18}O$ composition needed to reconstruct the paleohydrology at Oikojärvi. Shown in Figure 2-11, Lake Tibetanus $\delta^{18}O_P$ corresponds closely with low values of Oikojärvi cellulose-inferred lake water $\delta^{18}O$ at *c.* 9800-8000, 6000-5500, and 3100 cal. BP. However, during other periods, Oikojärvi $\delta^{18}O$ values show considerable offset of up to *c.* 4.5‰ from $\delta^{18}O_P$, probably due to moderate evaporative enrichment. The magnitude is very similar to the difference between the modern $\delta^{18}O_P$ and the measured closed-basin lake isotopic composition (Figure 2-2).

To reconstruct an approximation of changing evaporative enrichment during the Holocene, the difference between Lake Tibetanus $\delta^{18}O_P$ and Oikojärvi 5-point running average lake

water $\delta^{18}O$ is obtained. Lake Tibetanus $\delta^{18}O_P$ is shifted by –3.6‰ to match the lowest value of Oikojärvi $\delta^{18}O$ occurring at *c.* 5750 cal. BP, suggesting that Oikojärvi lake water $\delta^{18}O$ may be closest to $\delta^{18}O_P$ at this time (Figure 2-11). The difference between Oikojärvi and Lake Tibetanus $\delta^{18}O$ records likely reflects the distribution of precipitation $\delta^{18}O$ over the region, such as the difference observed in the modern annual precipitation $\delta^{18}O$ between Naimakka and Abisko (~2.7‰). Only the general trend in evaporative enrichment is considered as a comparison with other records in the interpretations, so z-scores are calculated with respect to the Holocene average amount (2.3‰) and the results are shown in Figure 2-12. The results of the Tibetanus-Oikojärvi $\delta^{18}O$ separation show that very low or no evaporative enrichment took place during the periods of *c.* 9500-8000, 6500-5200, 3800-2700, and 1300-600 cal. BP, corresponding to wet summers. Conversely, significantly drier summer conditions occurred at *c.* 8000-6500 cal. BP, and conditions of variable moisture are suggested at 5200-3800, 2700-1300, 1000-800, and 600-100 cal. BP.

2.5.2 Reconstruction of Holocene seasonal distribution of precipitation

The cellulose-inferred $\delta^{18}O$ record from Lake Keitjoru likely reflects variations that fall along the LMWL, as assessed from the contemporary isotope hydrology. However, unlike the Lake Tibetanus $\delta^{18}O_P$ reconstruction, which is believed to reflect variations in the long-term annual mean precipitation $\delta^{18}O$ because of the long catchment water residence time, the Lake Keitjoru $\delta^{18}O$ reconstruction probably reflects variations in the seasonality of precipitation. The maximum variability in the isotopic composition of cellulose-inferred water $\delta^{18}O$ in Lake Keitjoru amounts to 7.2‰ (Figure 2-11), which is similar to the modern difference of 7.4‰ between the amount-weighted mean precipitation of rain (δ_{Ps}) and snow (Figure 2-2). The range in $\delta^{18}O$ values is also considerably more than could be accounted for by temperature alone, given the small magnitude of temperature change of about 2°C shown in the pollen-inferred temperature reconstruction from Lake Tsuolbmajavri, Finland (Seppä and Birks, 2001; Figure 2-11).

Variations in the Lake Keitjoru $\delta^{18}O$ record are thus believed to represent variations in the relative amount of snow and rain contributed to the lake's catchment during the Holocene (Figure 2-11). Low $\delta^{18}O$ values, suggesting increased snow, occur at *c.* 9400-8400, 7600-

6600, 4300-3800, 3300-2100, and 600-100 cal. BP. In contrast, high $\delta^{18}O$ values occurring at *c.* 8400-7600, 6600-4300, 3800-3300, 2100-600 cal. BP indicates a greater contribution of rainfall. Based on the range in variability of $\delta^{18}O$ in the cellulose record, the amount of snow contributing into Lake Keitjoru can be semi-quantitatively reconstructed for the Holocene. To reconstruct past changes in winter precipitation amount, as shown in Figure 2-12, the total snow contribution, P_{snow}, entering into Lake Keitjoru is determined using a two-point mixing model, as follows:

$$\frac{P_{snow}}{P_{total}} = \frac{\delta_{cell} - \delta_{rain}}{\delta_{snow} - \delta_{rain}}$$

where δ_{cell} corresponds to cellulose-inferred water $\delta^{18}O$. δ_{rain} represents the maximum isotopic composition of modern rain (–8.7‰) that was attained July-August 1994, and δ_{snow} is the minimum $\delta^{18}O$ value (–24.0‰) attained December 1993-January 1994. The full isotopic range of precipitation $\delta^{18}O$ used in the reconstruction provides a conservative record of winter precipitation for the Holocene. P_{total} represents the total annual precipitation as reconstructed by pollen stratigraphy obtained from Lake Tsuolbmajavri (Seppä and Birks, 2001; Figure 2-11), which provides an independent data source. For example, the modern average Lake Keitjoru water $\delta^{18}O$ corresponds to 31% snow contribution. This compares well with the average estimate of winter precipitation (35%) using meteorological data at Naimakka (1990-2006; SMHI), assuming that precipitation falls as snow between November and April.

For the Holocene winter precipitation reconstruction, several assumptions are made. (1) Lake Keitjoru $\delta^{18}O$ record is shifted by +4.0‰ because of the offset between the cellulose-inferred lake water $\delta^{18}O$ and the measured average lake water $\delta^{18}O$. This step is needed so that the range of $\delta^{18}O$ values in the Lake Keitjoru record is centered within the modern range of lake water $\delta^{18}O$. (2) The end-member precipitation isotopic compositions, δ_{snow} and δ_{rain} are assumed constant. However, these values are likely to have shifted very slightly during the Holocene, as observed in Lake Tibetanus $\delta^{18}O_P$. As a result, estimates of snow contributions may be underestimated. (3) There are uncertainties associated with the pollen-based reconstruction of annual precipitation is about ±350-370 mm (Seppä and Birks, 2001),

as well as errors based on chronology for both records. Although there is the combined uncertainty inherited in the cellulose $\delta^{18}O$ and the pollen-based reconstructions, the general trends in the winter precipitation reconstruction are considered meaningful.

In Figure 2-12, the reconstruction of winter precipitation at Lake Keitjoru shows maximum snow contributions (*c*. 400 mm, or *c.* 50% of the annual precipitation inferred from the pollen reconstruction) occurring at the base of the record, and then decreasing to *c.* 175 mm (23%), which is close to the modern winter precipitation amount, by *c.* 8000 cal. BP. After this period, snow-rich winters occurring at *c.* 7600-6600, 4300-3800 and 3300-2100 cal. BP reach a maximum value of 224 mm (*c*. 40%). At *c.* 600-100 cal. BP, snow contributions increase considerably, reaching a maximum value of 276 mm, but the percentage of 40% of the pollen-inferred annual precipitation does not change from previous snow-rich intervals since 7600 cal. BP. In comparison, strongly reduced snow contributions to the lake occur during the periods of *c.* 6600-4300 cal. BP and 2000-600 cal. BP, with an average amount estimated at *c.* 104 mm (*c*. 21%).

2.5.3 Holocene paleoenvironmental history

Based on the pollen-inferred mean July temperature and annual precipitation reconstructions at Lake Tsuolbmajavri (Seppä and Birks, 2001), cool and moist summers characterized the early Holocene period before *c.* 8000 cal. BP (Figure 2-11), as suggested by the dominance of *Betula pubescens* at Lake Keitjoru (Olsson, unpublished work) and in northwestern Finland (Seppä and Weckström, 1999; Seppä and Birks, 2001; Seppä *et al.*, 2002; Bjune et al, 2004). Interestingly, the smoothed Oikojärvi cellulose-inferred water $\delta^{18}O$ follows closely with the trend observed in the carbonate-inferred precipitation $\delta^{18}O$ at Lake Tibetanus between *c.* 10,000-8000 cal. BP. This correspondence may suggest that there was sufficient moisture in the region, allowing lake water $\delta^{18}O$ at Oikojärvi to track variations in the long-term precipitation $\delta^{18}O$. Thus, the separation between Oikojärvi and Lake Tibetanus $\delta^{18}O$ at *c.* 9500-8000 cal. BP indicates very little evaporative enrichment in Oikojärvi (Figure 2-12). High lake levels have also been inferred from *cladocera*, diatoms, and chironomids in lakes of northern Finnish Lapland before *c.* 8000 cal. BP (Hyvärinen and Alhonen, 1994; Eronen *et al.*, 1999; Sarmaja-Korjonen and Hyvärinen, 1999; Korhola *et al.*, 2005). Low $\delta^{18}O$ values at

Lake Keitjoru at *c.* 9400-8400 cal. BP may indicate greater winter precipitation, as suggested by increased glacial activity in western Norway (Karlén, 1976, 1988; Dahl and Nesje, 1996; Nesje *et al.*, 2001).

Between *c.* 8000 and 6500 cal. BP, the pollen-inferred mean July temperature record at Lake Tsuolbmajavri indicates very warm summers, during the so-called Holocene Thermal Maximum (HTM; Figure 2-12). Accordingly, the Oikojärvi-Tibetanus $\delta^{18}O$ separation is considerably higher than the Holocene average suggesting that the warm temperatures likely enhanced evaporation rates. Dry summers during this interval are supported by documented lake-level lowerings by as much as 4-6 m in kettle-hole basins in northwest Finland culminating around *c.* 6000 cal. BP (Korhola *et al.*, 2005), and a hiatus at *c.* 8000-5000 cal. BP in Lake Njargajavri record (Sarmaja-Korjonen *et al.*, 2006). Other studies also indicate minimum lake levels at *c.* 9000-5000 cal. BP in northern Fennoscandia (Hyvärinen and Alhonen, 1994; Almquist-Jacobson, 1995; Eronen *et al.*, 1999; Sarmaja-Korjonen and Hyvärinen, 1999; Barnekow, 2000). The change to warm and dry summers may have also contributed to the establishment of *Pinus sylvestris* forests at Lake Keitjoru (P. Olsson, Lund University, Sweden, unpublished data) beginning around 8000 cal. BP and in northwestern Finland between *c.* 8300-4300 cal. BP (Barnekow, 1999: Seppä and Weckström, 1999; Korhola *et al.*, 2000; Seppä and Birks, 2001; Seppä *et al.*, 2002; Bjune et al, 2004). Low Lake Keitjoru $\delta^{18}O$ values suggest that the pollen-inferred annual precipitation was still predominantly in the form of snow between *c.* 7600-6600 cal. BP. Low Lake Keitjoru $\delta^{18}O$ values are in agreement with reconstructed high winter precipitation at *c.* 8000-6500 in Lyngen, northern Norway (Bakke *et al.*, 2005). Significantly, small glacier advances were also noted to occur at *c.* 7200-6500 cal. BP, even though summer temperatures were notably higher, reflecting increased dependence on winter precipitation (Dahl and Nesje, 1996; Nesje *et al.*, 2001).

During the period following the HTM (*c.* 6500-5200 cal. BP), considerable depletion in ^{18}O of the Oikojärvi cellulose record may be strongly associated with an increase in summer moisture conditions (Figure 2-12). This observation coincides with a dramatic decrease in pollen-inferred July temperatures by *c.* 5200 cal. BP, which may have contributed to an increase in effective moisture, and thus lowered the extent of evaporative enrichment. In

addition, the increase in $\delta^{18}O$ of Lake Keitjoru water suggests that a significant component of summer rainfall comprised the total pollen-inferred annual precipitation at Lake Tsuolbmajavri (Figure 2-12). In support, water levels in Lake Jierstivaara at a site in Finnish Lapland had begun to increase just before 6000 cal. BP (Hyvärinen and Alhonen, 1994, Korhola *et al.*, 2005). The low cellulose-inferred water $\delta^{18}O$ values in Oikojärvi at *c.* 6000-5500 cal. BP converge with Lake Tibetanus $\delta^{18}O$ (Figure 2-11) suggesting that Oikojärvi lake waters continue to track $\delta^{18}O_P$ after the HTM, possibly due to a higher groundwater table.

By *c.* 5200, the Oikojärvi-Tibetanus $\delta^{18}O$ separation increased to positive values, which coincides with high pollen-inferred annual precipitation and high Lake Keitjoru $\delta^{18}O$ values, likely reflecting a greater contribution of summer rainfall to Oikojärvi, rather than evaporative enrichment (Figure 2-12). This suggests that high Oikojärvi $\delta^{18}O$ values at *c.* 5200-4300 cal. BP are following a LMWL trend similar to the 2004 season (Figure 2-5b). The increase in annual precipitation at Tsuolbmajavri is observed to coincide with an increase of *Betula pubescens* at the expense of *Pinus sylvestris* starting at *c.* 5500 cal. BP at Lake Keitjoru (P. Olsson, Lund University, Sweden, unpublished data), which has been observed elsewhere in northern Fennoscandia (Seppä and Weckström, 1999; Seppä and Birks, 2001; Seppä *et al.*, 2002; Bjune *et al.*, 2004). The combined onset of cool and moist summers by *c.* 5200 cal. BP has also likely contributed to the activation of paludification processes and subsequent expansion of peatlands (Seppä and Weckström, 1999; Seppä and Birks, 2001).

At *c.* 4300-2100 cal. BP, Lake Keitjoru $\delta^{18}O$ shows a pronounced shift towards more depleted $\delta^{18}O$ values likely in response to an increase in snow contributions (Figure 2-12). There is a striking resemblance between Lake Keitjoru $\delta^{18}O$ and the low frequency pattern of Oikojärvi $\delta^{18}O$ profile, but offset from each other. In addition the Oikojärvi-Tibetanus $\delta^{18}O$ separation is tightly constrained to the Holocene average, suggesting very little evaporative enrichment. This correspondence indicates that input waters entering Oikojärvi are similar to the mean annual precipitation, as represented by Lake Tibetanus $\delta^{18}O_P$. The annual precipitation inferred from pollen reconstruction at Lake Tsuolbmajavri is certainly less than

it was during the early Holocene. However, cooler summers and increased variability between wet and dry episodes have helped maintain higher effective moisture (Seppä and Weckström, 1999; Bjune *et al.*, 2004). A brief shift to positive $\delta^{18}O$ in the Lake Keitjoru record at around *c.* 3800-3300 cal. BP may reflect a small reduction in winter precipitation, which coincides with a short period of warm and slightly moist summers (Figure 2-12). Therefore, an earlier spring snowmelt may have provided favourable conditions for a slight rise of *Pinus sylvestris* to occur in Lake Keitjoru catchment and at Lake Tsuolbmajavri (Seppä and Weckström, 1999). The timing of snow-rich winters inferred at Lake Keitjoru at *c.* 4300-3800 and 3300-2100 cal. BP matches well with the advance of mountain glaciers at *c.* 3200-2500 cal. BP in northern Sweden (Karlén, 1976) and after *c.* 3800 cal. BP at Strupskardet in Lyngen, northern Norway (Bakke *et al.*, 2005).

Oikojärvi-Tibetanus $\delta^{18}O$ separation gradually becomes more positive during the period at *c.* 2700-1300 cal. BP, indicating moderate dryness and coincides with low mean annual precipitation, as inferred by the pollen reconstructions. In support, there is also an indication of lowered lake levels at *c.* 1500 cal. BP for kettle lakes in Finnish Lapland, based on cladoceran-inferred lake depth reconstructions (Korhola *et al.*, 2005).

From *c.* 1300-600 cal. BP a strong cooling trend is observed in the pollen-inferred mean July temperature record from Lake Tsuolbmajavri (Figure 2-12). There is a noteworthy increase in $\delta^{18}O$ of Lake Keitjoru water during this interval, likely signifying an increase in summer rain contributions, similar in magnitude to that which occurred at *c.* 4500 cal. BP. In addition, the peak in Lake Keitjoru $\delta^{18}O$ corresponds to a trough in Oikojärvi-Tibetanus $\delta^{18}O$ separation, which translates to very wet summer conditions, coinciding with the historical duration of the Dark Ages (Lamb, 1977). The short period between *c.* 800-600 cal. BP, known as the Medieval Warm Period (MWP), is characterized by a slight shift to below-modern average winter precipitation and moderately wet summer conditions.

From 600-100 cal. BP, encompassing the period of the Little Ice Age (LIA), significant depletion in Keitjoru $\delta^{18}O$ values suggests substantial contributions of winter precipitation, along with significant summer cooling and greater annual precipitation, as indicated by the pollen-based reconstructions (Figure 2-12). This period of cooling is also evidenced by tree-

ring summer temperature reconstructions in northern Fennoscandia (Grudd, 2008), aggradation of permafrost in Finnish Lapland (Oksanen, 2006), widespread glacial activity (Karlén, 1976; Nesje and Dahl, 1991; Dahl and Nesje, 1996; Bakke *et al.*, 2005) and an accompanying increase in winter precipitation (Nesje *et al.*, 2001; Dahl and Nesje, 1996; Nesje and Dahl, 2003; Bakke *et al.*, 2005). A substantial increase in the magnetic susceptibility is observed in the Lake Keitjoru record (Chapter 5), consistent with data from Lake Sarsjön, east-central Sweden (Snowball *et al.*, 1999), possibly indicating intense periods of catchment erosion and mineral deposition in response to greater snowmelt runoff. Significant cooling and greater annual precipitation also maintained moist, acidic soil conditions, as indicated by increased peatland development, a dominance of *Betula pubescens*, and the appearance of *Picea abies*, *Empetrum*, *Salix* sp. and *Sphagnum* in the area (P. Olsson, Lund University, Sweden, unpublished data; Seppä and Weckström, 1999). In spite of the substantial rise in pollen-inferred annual precipitation, which comprises a greater snow component, the Oikojärvi-Tibetanus $\delta^{18}O$ separation indicates that summers were considerably drier than the Holocene average.

2.5.4 Links between atmospheric circulation dynamics and changes in precipitation $\delta^{18}O$

Comparisons between Lake Keitjoru and Oikojärvi cellulose-inferred water $\delta^{18}O$ with the carbonate-inferred precipitation $\delta^{18}O_P$ at Lake Tibetanus offers insightful information about changing atmospheric circulation patterns over sub-millennial scales during the Holocene (Figure 2-11; 2-12). Independent reconstructions of mean July temperature and annual precipitation from pollen records at Lake Tsuolbmajavri (Seppä and Birks, 2001) also provide additional support for these interpretations. The Oikojärvi-Tibetanus $\delta^{18}O$ separation provides a semi-quantitative record, expressed as z-scores, of evaporative enrichment during the Holocene (Figure 2-12). Thus, negative z-scores suggest little or no evaporative enrichment of Oikojärvi $\delta^{18}O$ lake water, and it is interpreted as a period of moist summers in which lake water is fed predominantly by mean annual precipitation. Summer atmospheric circulation patterns for negative z-scores are interpreted as zonal or westerly flow. In this setting, the Icelandic Low is west of northern Fennoscandia, creating cool and moderately

moist conditions (Jacobeit *et al.*, 2003). Intervals characterized by zonal flow (or positive summer NAO) occur at *c.* 9500-8000, 6500-5200, 3800-2700, and 1300-600 cal. BP. These intervals coincide with occurrences of continental glacier advances and pine tree-limit descent, normally associated with cooler summer temperatures (Karlén, 1976). In contrast, positive z-scores suggest a change in summer atmospheric circulation to dominantly meridional flow. For instance, a positive Oikojärvi-Tibetanus $\delta^{18}O$ separation may represent greater evaporative enrichment during dry conditions characterized by an anticyclone-blocking pressure cell situated over northern Fennoscandia. However positive z-scores can also occur when summer rainfall comprises a large component of the total annual precipitation, which is high as well, such as during *c.* 5200-4300 cal. BP. In this case, a major cyclonic centre may be situated over Fennoscandia and the Baltic Sea, which has been associated with intense rainfall and cool conditions (Jacobeit *et al.*, 2003). Intervals characterized by meridional flow occur at *c.* 8000-6500, 5200-3800, 2700-1300, and 600-100 cal. BP (Figure 2-12).

Interpretation of the winter atmospheric circulation patterns is based on variability of Lake Keitjoru $\delta^{18}O$ and the Holocene decline of Lake Tibetanus $\delta^{18}O_P$ (and shifting $\delta^{18}O$-temperature relation), which suggest a gradual change from oceanic to continental conditions, as described in detail below. Low $\delta^{18}O$ values are interpreted as high winter precipitation, whereas high $\delta^{18}O$ represents low winter precipitation, as modeled using the pollen-inferred total annual precipitation at Tsuolbmajavri and the present-day range of precipitation $\delta^{18}O$ at Naimakka (Figure 2-12). Therefore, the low $\delta^{18}O$ values during the early Holocene (before *c.* 6000 cal. BP) represent winter precipitation originating from oceanic air masses transported by a strong westerly (zonal) flow pattern. In contrast, high $\delta^{18}O$ values are interpreted to occur during meridional flow conditions, characterizing cold and dry winters. After *c.* 6000 cal. BP, the winter atmospheric circulation signal in Lake Keitjoru $\delta^{18}O$ switches in concert with maximum continentality across Fennoscandia (Seppä and Hammarlund, 2000; Hammarlund *et al.*, 2001; Giesecke *et al.*, 2008). Thus, low $\delta^{18}O$ values suggest that winter precipitation originates from southeasterly flow circulating east of the Siberian High in a meridional atmospheric circulation pattern, whereas high $\delta^{18}O$ suggests low winter precipitation contributions in a westerly (zonal) flow setting. In a

modern westerly flow pattern in winter, precipitation is generally confined to the west coast, leaving the leeward side of the Scandes Mountains somewhat drier (Wallén, 1970; Johannessen, 1970; Uvo, 2003).

The seasonal distribution of precipitation recorded in the Lake Keitjoru $\delta^{18}O$ record may be sensitive to millennial-scale fluctuations in the strength of zonal atmospheric circulation, similar to the documented decadal-scale variability of the winter North Atlantic Oscillation (NAO; Hurrell, 1995). As a modern analogue, a positive NAO index has persisted since the 1980s, resulting in mild and wet winters in northern Europe, specifically in western Norway (Nesje and Dahl, 2003). The increasing trend of Keitjoru $\delta^{18}O$ since *c.* 600 cal. BP to the modern lake water $\delta^{18}O$ value (Figure 2-11), thus reflecting a decline in winter precipitation contribution, is consistent with a change from a negative NAO index (meridional) during the LIA to a more positive NAO index (zonal) during the late 20th century. Since Lake Keitjoru $\delta^{18}O$ may be reflecting variation in winter precipitation, it may be a good proxy for changes in the winter NAO during the Holocene. In this case, a predominantly positive NAO index may be inferred at *c.* 9400-8400 and 7600-6600 cal. BP when winter precipitation was high before *c.* 6000 cal. BP, and at *c.* 4800-4300, 3800-3300 and 2100-600 cal. BP when winter precipitation was low after *c.* 6000 cal. BP (Figure 2-12). These intervals of a positive NAO phase correspond roughly with higher winter precipitation estimated from a maritime glacier in western Norway (Dahl and Nesje, 1996; Nesje *et al.*, 2001). Conversely, a negative NAO index may have prevailed at *c.* 8400-7600, 6600-4800, 4300-3800, 3300-2100, and 600-100 cal. BP. These intervals correspond strongly with high sea-salt and dust concentrations in the GISP2 ice core record, which is believed to be a reflection of enhanced winter meridional circulation (O'Brien *et al.*, 1995; Mayewski *et al.*, 1997; Meeker and Mayewski, 2002). In addition, the inferred phases of negative NAO-like circulation, with the exception of the last interval, are consistent with increased ice-rafting in the North Atlantic (Bond *et al.*, 1997).

Hammarlund *et al.* (2002) proposed that higher cyclonic frequencies brought on by the vigorous flow of westerlies and reduced rain-out of moist Atlantic air masses across the Scandes Mountains was the cause of the relatively high $\delta^{18}O$ and positive offset from the Dansgaard (1964) $\delta^{18}O$-temperature relation, evident at Lake Tibetanus during the early Holocene (*c.* 10,000-6000 cal. BP). In addition, pollen-inferred climatic reconstructions at

Lake Tsuolbmajavri (Seppä and Birks, 2001) exhibited considerably higher annual precipitation and cooler conditions occurring in the region during this time. A higher winter component is suggested to comprise the total annual precipitation at *c.* 9400-8000 cal. BP, as indicated by low Lake Keitjoru $\delta^{18}O$ values (Figure 2-12). This is supported by the fact that westerly flow (zonal circulation) is strongest during the winter months because of the greater temperature contrast between the warm North Atlantic sea surface and the cold continental landmass (Johannessen, 1970). Furthermore, strong zonal atmospheric circulation (positive NAO index) during the early Holocene is also perhaps enhanced by the high summer insolation at this stage, allowing for the northward penetration of warm Atlantic surface waters to flow into the Norwegian Sea (Koç *et al.*, 1993) and a northward shift of the polar front, providing a westerly transport of heat and moisture to areas of northern Fennoscandia. Oceanic-like summers are exemplified by the negative Oikojärvi-Tibetanus $\delta^{18}O$ separation during the period at *c.* 9500-8000 cal. BP (Figure 2-12). Widespread distribution of greater winter precipitation is also evident, suggesting a strong penetration of westerly flow at *c.* 9400-8400 and 7600-6600 cal. BP.

The gradual decline in Lake Tibetanus $\delta^{18}O_P$ and the decrease in the offset from the Dansgaard (1964) $\delta^{18}O$-temperature relation by *c.* 6000 cal. BP is suggested to be associated with the weakening of westerly flow of air masses, increased rain-out of precipitation across landmasses, and greater continentality on the leeside of the Scandes Mountains (Hammarlund *et al.*, 2002). The change in atmospheric circulation may be in response to the lowering of summer insolation, which likely resulted in a southward shift of the atmospheric polar front and decreasing sea surface temperatures (Koç *et al.*, 1993). Summer atmospheric circulation likely changed from westerly flow to a more meridional pattern. The formation of a persistent high-pressure cell situated over northern Fennoscandia (Yu and Harrison, 1995; Seppä and Birks 2001, 2002) during the summer likely fostered warmer and drier conditions, as suggested by the ^{18}O-enrichment in Oikojärvi lake water during *c.* 8000-6500 cal. BP (Figure 2-12) and lake-level lowering in the region (Korhola *et al.* 2005, Sarmaja-Korjonen *et al.*, 2006).

The variability in the summer atmospheric circulation pattern may have switched from meridional to zonal flow at *c.* 6500-5200 cal. BP as suggested from the very negative Oikojärvi-Tibetanus $\delta^{18}O$ separation (Figure 2-12). The lowest estimate of evaporative enrichment based on the Oikojärvi-Tibetanus $\delta^{18}O$ separation occurs at *c.* 5500 cal. BP, in concert with lower annual precipitation and cooler mean July temperature inferred from the pollen record. This correspondence suggests reduced transport of moisture across the Scandes, possibly due to weaker westerlies. Notably, there is a slight increase in the smoothed Lake Tibetanus $\delta^{18}O$ record at *c.* 6000-5000 cal. BP, which also corresponds to a small positive offset from the Dansgaard (1964) $\delta^{18}O$-temperature relation (Hammarlund *et al.*, 2002), suggesting a return to a somewhat stronger westerly flow pattern.

At *c.* 5200-4300 cal. BP, the Oikojärvi-Tibetanus $\delta^{18}O$ separation increases in concert with an increase in the total annual precipitation as inferred from pollen reconstructions, while Lake Keitjoru $\delta^{18}O$ values remain high. These trends suggest that the summer atmospheric circulation pattern switched back to meridional flow conditions, but with a mode that is likely characterized by a major cyclonic centre over eastern Fennoscandia bringing in intense rainfall (*cf.* Jacobeit *et al.*, 2003). Meridional flow patterns are suggested to also occur at *c.* 4300-3800 and 2700-1300 cal. BP, but with slightly positive Oikojärvi-Tibetanus $\delta^{18}O$ separation corresponding with cool and dry conditions, based on pollen-inferred reconstructions (Figure 2-12). Evaporative enrichment is likely suppressed because of the high effective moisture maintained by lower summer temperatures.

Two periods of zonal atmospheric circulation flow characterizes summer conditions at *c.* 3800-2700 cal. BP and more strongly at *c.* 1300-600 cal. BP, based on the negative Oikojärvi-Tibetanus $\delta^{18}O$ separation (Figure 2-12). Wet summers are consistent with high Lake Keitjoru $\delta^{18}O$ values at *c.* 1300-600 cal. BP, indicating that summer rainfall is likely the main component of the total annual precipitation. Zonal atmospheric flow seems to coincide with the approximate timing of the Dark Ages between *c.* 1300 and 1000 cal. BP (AD 650-950), characterized by cool, moist summers and dry winters. Moist conditions during the Dark Ages are consistent with rapid peat accumulation in Scotland (Blundell and Barber, 2005) and high lake levels in Finnish Lapland (Eronen *et al.*, 1999). Following the Dark

Ages, the MWP at *c.* 1000-600 cal. BP (AD 950-1350) is characterized by an increase in evaporative enrichment in summer and a slight increase in winter precipitation (Figure 2-12).

From *c.* 600 to 100 cal. BP (AD 1350-1850), the LIA was characterized by snow-rich winters, as indicated by the Lake Keitjoru $\delta^{18}O$ record, and lower temperatures, as indicated by the pollen-inferred July temperature record (Seppä and Birks, 2001). The Oikojärvi-Tibetanus $\delta^{18}O$ separation indicates that summers during the LIA were dry. Hence, a meridional (negative NAO) circulation pattern likely occurred during both summer and winter (Kreutz *et al.*, 1997). A strong similarity between low Lake Keitjoru $\delta^{18}O$ values and low $\delta^{18}O$ in lakes of the Taimyr Peninsula, Russia (Wolfe *et al.*, 2000) after 600 cal. BP suggests that cyclonic activity occurring north of the high-pressure blocking cell is likely producing winter precipitation in this meridional circulation regime. The reconstructed winter precipitation and the Oikojärvi-Tibetanus $\delta^{18}O$ separation during the MWP appear as a transitional phase between the Dark Ages and the LIA (Figure 2-12). This transition likely reflects a centennial-scale change from zonal to meridional circulation pattern in both summer and winter. The change in circulation pattern may have also been associated with a southward displacement of the atmospheric polar front (Dansgaard *et al.*, 1975).

2.6 Summary

The reconstruction of the Holocene paleohydrology and seasonal distribution of precipitation from two open-drainage lakes, with contrasting residence times, has provided significant information on the millennial-scale variations of winter and summer atmospheric circulation patterns in northern Fennoscandia. Interpretation of sediment cellulose $\delta^{18}O$ records was facilitated by a robust modern isotope hydrology dataset spanning the period AD 2002-2006. Lake Keitjoru cellulose-inferred lake water $\delta^{18}O$ records changing seasonal distribution of precipitation during the Holocene. Together with a pollen-reconstructed annual precipitation record from Lake Tsuolbmajavri (Seppä and Birks, 2001), a record of winter precipitation amount was inferred. In particular, Lake Keitjoru record may be reflecting stronger zonal circulation at *c.* 9400-8400, 7600-6600, 4800-4300, 3800-3300, and 2100-600 cal. BP, and meridional flow during the intervening periods. The Oikojärvi cellulose-inferred lake water $\delta^{18}O$ was combined with a carbonate-inferred precipitation $\delta^{18}O$ record from Lake Tibetanus

(Hammarlund *et al.*, 2002) to provide an approximate record of evaporative enrichment in the area during the Holocene. The results of the Tibetanus-Oikojärvi $\delta^{18}O$ separation show that wet summers (zonal circulation) occurred at *c.* 9500-8000, 6500-5200, 3800-2700, and 1300-600 cal. BP, and significantly drier summers (meridional circulation) are suggested at *c.* 8000-6500, 2700-1300, and 600-100 cal. BP. The results of this study reveal submillennial-scale variations in the dominant circulation modes for both winter and summer during the Holocene that may be analogous to the variability of the North Atlantic Oscillation. Importantly, this study demonstrates the usefulness and significance of applying a multi-proxy approach to reconstructing or constraining past climate, especially in combining proxies that reflect varying aspects of the climate system, such as winter precipitation and summer evaporation.

Table 2-1. Summary of lake characteristics and determination of average residence time of water in Lake Keitjoru and Oikojärvi. Total annual precipitation obtained from SMHI 1990-2006 database (Alexandersson *et al.*, 1991) and annual evaporation interpolated from Bringfelt and Forsman (1995). Annual precipitation (P) and annual evaporation (E) are integrated over catchment area and lake area, respectively, to obtain volume estimates. Residence time is converted to days.

	Lake Keitjoru	Oikojärvi
water depth (m)	1.8	8.0
annual precipitation (mm)	456	456
annual evaporation (mm)	170	160
lake area (km^2)	0.02	1.30
catchment area (km^2)	1.9	15.6
lake volume, V (mm^3)	$3.6x10^{13}$	$1.0x10^{16}$
discharge, Q=P-E (mm^3/year)	$8.6x10^{14}$	$6.9x10^{15}$
residence time, t=V/Q (days)	15	550

Table 2-2. Lithostratigraphic description of Lake Keitjoru and Oikojärvi sediment profiles and total organic content (TOC). Depths are relative to the water surface. The water depth measured at the coring site is 1.8 m at Lake Keitjoru and 8.0 m at Oikojärvi.

Lake	Unit	Depth (m)	Description	TOC content (%)	Average TOC (%)
Keitjoru	10	1.89-2.01	Brown, very loose gyttja.	11.93–19.13	15.57
	9	2.01-2.07	Slightly lighter brown, loose gyttja.	11.79–12.36	12.07
	8	2.07-2.10	Brown, loose gyttja.	11.25–11.25	11.25
	7	2.10-2.52	Brown to light brown moss-rich gyttja.	9.83–15.10	12.02
	6	2.52-2.64	Brown/dark brown banded gyttja.	11.53–18.92	14.96
	5	2.64-2.79	Light brown algal-rich gyttja.	10.71–12.25	11.49
	4	2.79-3.12	Light brown, slightly silty algal-rich gyttja. Light layer at 2.93 m.	12.68–16.80	15.14
	3	3.12-3.30	Brown/dark brown silty, moss-rich gyttja.	10.84–14.45	13.00
	2	3.30-3.35	Brown to dark brown silty gyttja grading into silt.	9.16–10.65	9.91
	1	3.35-3.42	Grey silty clay and clay.	n.d.	n.d.
Oikojärvi	3	8.00–10.96	Brown fine detritus gyttja, lower boundary gradual.	7.43–12.15	9.76
	2	10.96–11.20	Grey clay grading into brown fine detritus gyttja.	1.94–7.86	3.70
	1	Below 11.20	Grey clay	n.d.	n.d.

Table 2-3. Radiocarbon dates.

Lake	Depth (m)	Lab no.	Material analyzed	Weight (mg)	Reported age (^{14}C years BP)	Calibrated age (2σ interval)	Calibrated age (mid intercept) (cal. BP)
Keitjoru	2.15–2.16	LuA-5677	Water mosses	20	925 ± 35	760-930	845
	2.44–2.45	LuS-5758	Water mosses	7	2065 ± 50	1890-2160	2035
	2.44–2.45	LuS-5757	*Pinus*, *Betula*, unid. leaves and twigs	3	2705 ± 50	2740-2930	2805*
	2.60–2.61	LuA-5678	*Salix*, *Betula*, *Pinus*	7	5220 ± 40	5900-6170	5965*
	2.97–2.98	LuA-5679	*Pinus*	11	5060 ± 40	5710-5920	5815
	3.14–3.15	LuS-5756	Water mosses	14	7510 ± 50	8190-8400	8290
	3.34–2.35	LuA-5680	*Betula*, *Alnus*	20	8430 ± 80	9260-9550	9405
Oikojärvi	8.30–8.31	LuA-5670	Bulk	>100	1165 ± 35	970-1180	1075*
	8.96–8.97	LuA-5671	Bulk	>100	2055 ± 35	1920-2120	2020*
	9.60–9.61	LuA-5672	Bulk	>100	2890 ± 35	2880-3170	3025*
	10.08–10.09	LuA-5673	Bulk	>100	3780 ± 40	3980-4290	4135*
	10.58–10.59	LuA-5674	Bulk	>100	5680 ± 50	6310-6630	6470*
	10.79–10.80	LuS-5754	*Empetrum*	12	6565 ± 100	7270-7620	7445
	10.97–10.98	LuA-5675	Bulk	>100	8620 ± 50	9490-9740	9580*
	11,12–11,14	LuS-5755	*Betula*, unid. leaves, water mosses	4	8905 ± 60	9770-10220	9995
	11.16–11.18	LuA-5676	Bulk	>100	10060 ± 60	11250-12100	11500*

*not included in age-depth calibration model
unid. = unidentified

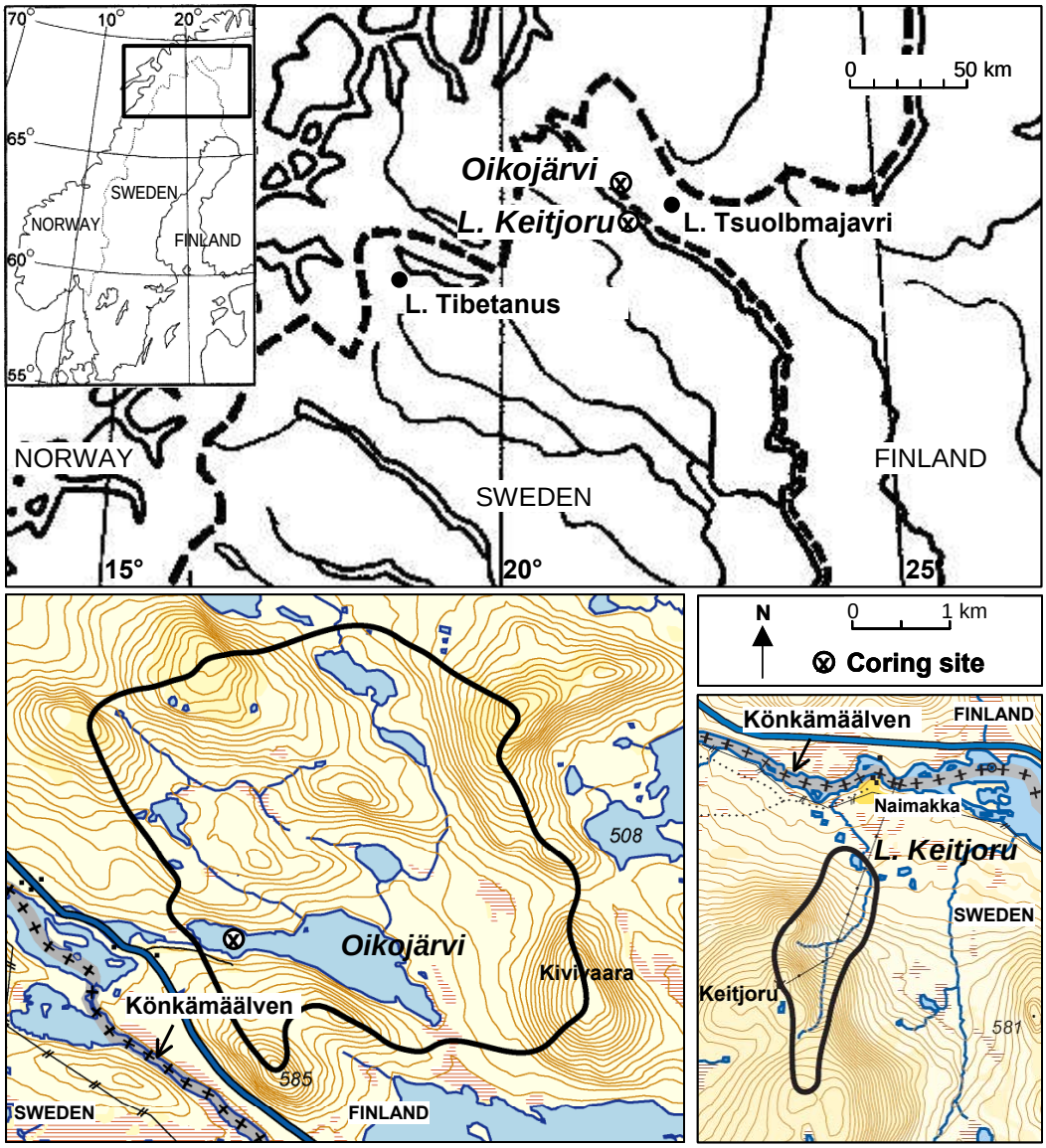

Figure 2-1. Map showing the location, catchment boundary and sampling site of Oikojärvi and Lake Keitjoru in Northern Fennoscandia. Other locations mentioned in text are shown. Contour intervals at 10 m. Note that the symbol denoted as coring site is not displayed for Lake Keitjoru, since it would encompass the entire lake.

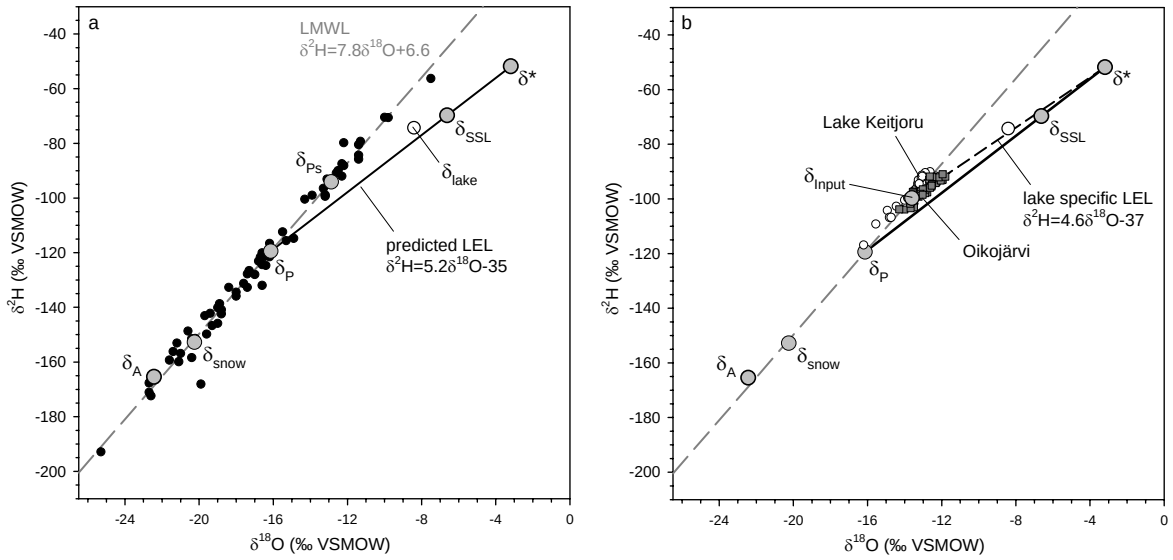

Figure 2-2. a) Calculated water isotopic framework for the Naimakka region. Isotopic composition of monthly average precipitation obtained from the Naimakka meteorological station (403 m a.s.l) during the period of 1990-1995 (IAEA/WHO GNIP-data) are shown as small black circles, and plot along the LMWL ($\delta^2H = 7.8\delta^{18}O + 6.6$). The amount-weighted means for annual precipitation (δ_P), rain (δ_{Ps}), and snow (δ_{snow}) are key points on the LMWL. The LEL is predicted by the Craig and Gordon (1965) model that describes isotopic enrichment during evaporation, and using climate normals and estimates of δ_P, and the isotopic composition of atmospheric moisture (δ_A), which is assumed to be in equilibrium with δ_{Ps}. The isotopic signature of a closed-basin lake (δ_{lake}) sampled in August 2002, 600 m southwest of Naimakka, plots slightly above the LEL and approaches δ_{SSL}. b) Using the same scale as in a), the isotopic composition of lake waters from Lake Keitjoru and Oikojärvi are plotted against the isotopic framework. The isotopic composition of input water, δ_{input}, is the intersection of the lake-specific LEL with the LMWL.

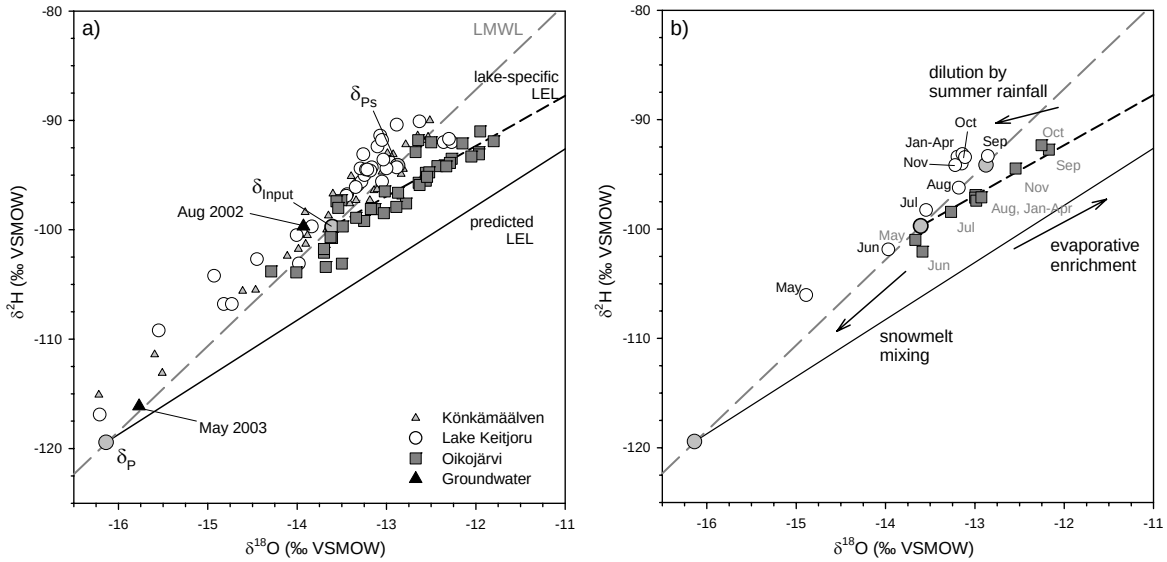

Figure 2-3. a) Stable isotope results for Lake Keitjoru, Könkämäälven and Oikojärvi samples collected during August 2002-2005, and August 2006, shown in relation to the isotope framework parameters, plotted as grey-filled circles. Groundwater samples collected in the Lake Keitjoru catchment during August 2002 and May 2003 are shown as black-filled triangles. b) The monthly average isotopic composition of Lake Keitjoru and Oikojärvi samples, illustrating isotopic evolution of waters along the LMWL and LEL trends, respectively.

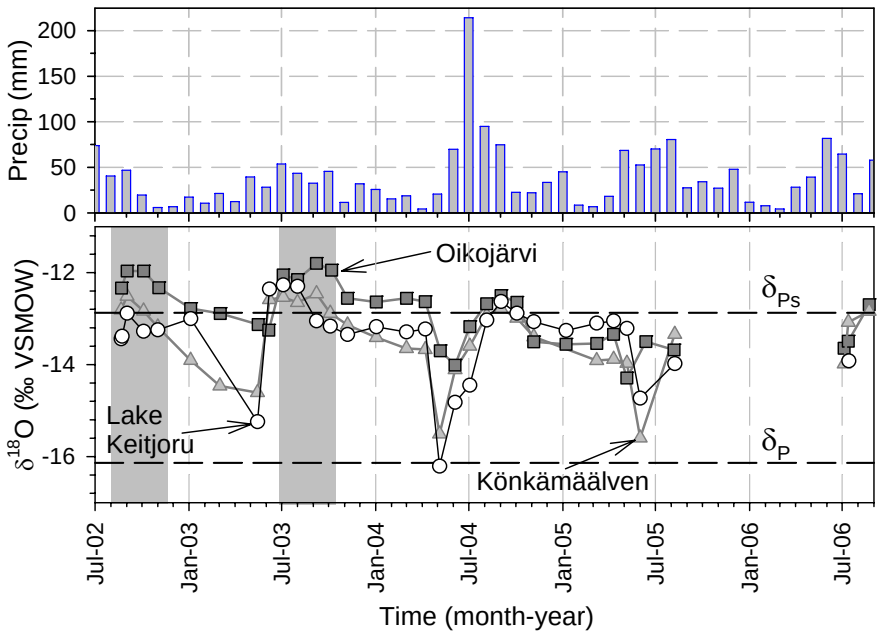

Figure 2-4. Time-series of monthly average measurements of precipitation obtained at Naimakka meteorological station for the period between July 2002 and September 2006 (SMHI database). The isotopic composition of water from Lake Keitjoru, Könkämäälven and Oikojärvi are shown in the bottom panel in relation to the average isotope compositions of δ_{Ps} and δ_{P}. Grey shading highlights periods during which the isotopic evolution of lake water at Oikojärvi follows a trend along the LEL.

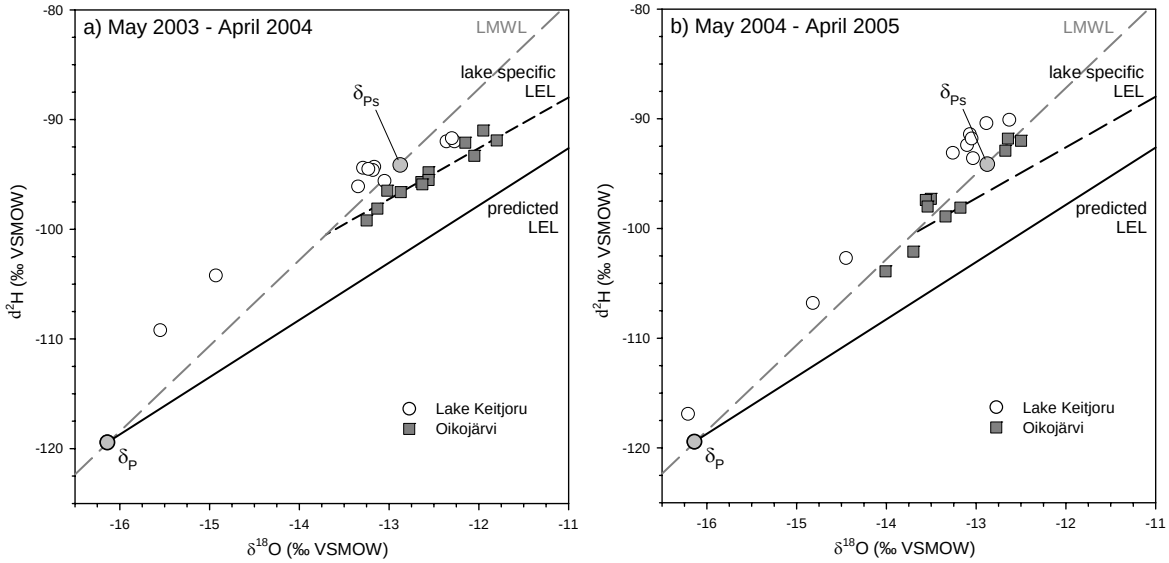

Figure 2-5. Evolution of the isotopic composition of waters from Lake Keitjoru and Oikojärvi, superimposed on the isotopic framework for a) a dry season (May 2003 – April 2004, and b) a wet season (May 2004 – April 2005).

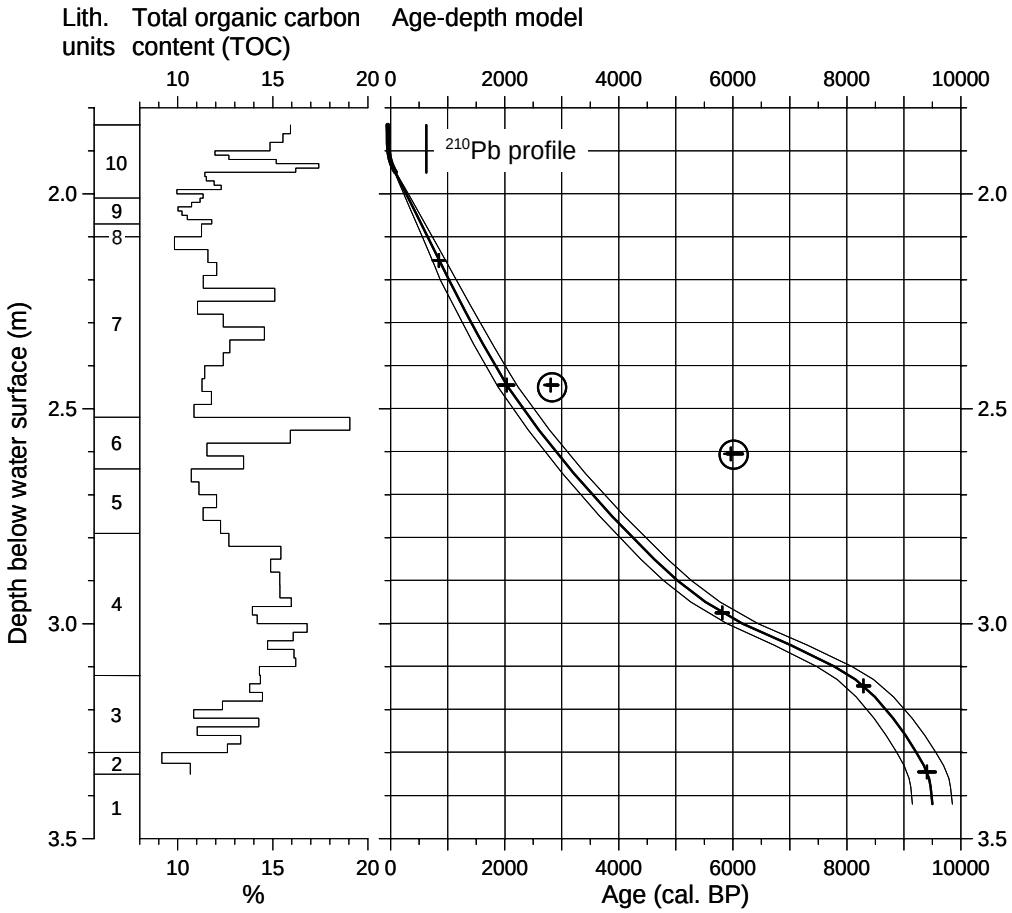

Figure 2-6. Age-depth model for Lake Keitjoru based on radiocarbon dates of five macrofossils (see Table 2-3) and ^{210}Pb model of surface sediments, are plotted together with lithological units (see Table 2-2) and total organic carbon content (TOC), expressed as weight percentages, versus depth below water surface. The encircled radiocarbon dates are terrestrial macrofossils that are suspected to have been reworked, and were thus excluded from the age model.

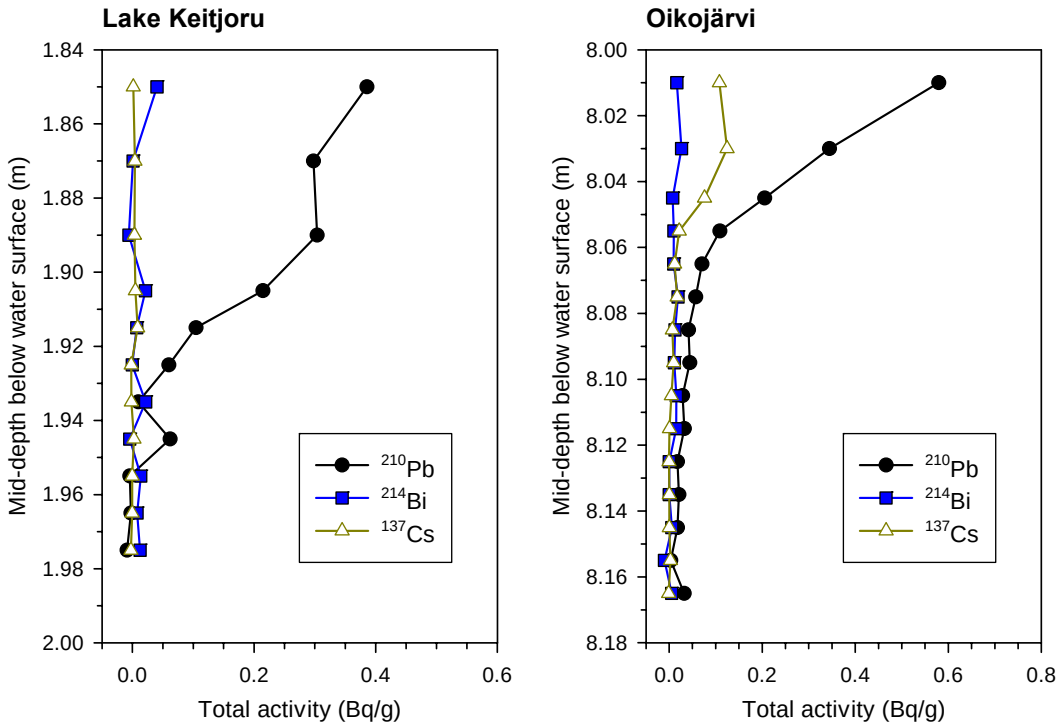

Figure 2-7. Total ^{210}Pb, ^{137}Cs, and ^{214}Bi activity versus mid-depth below the water surface from gravity cores collected at Lake Keitjoru and Oikojärvi.

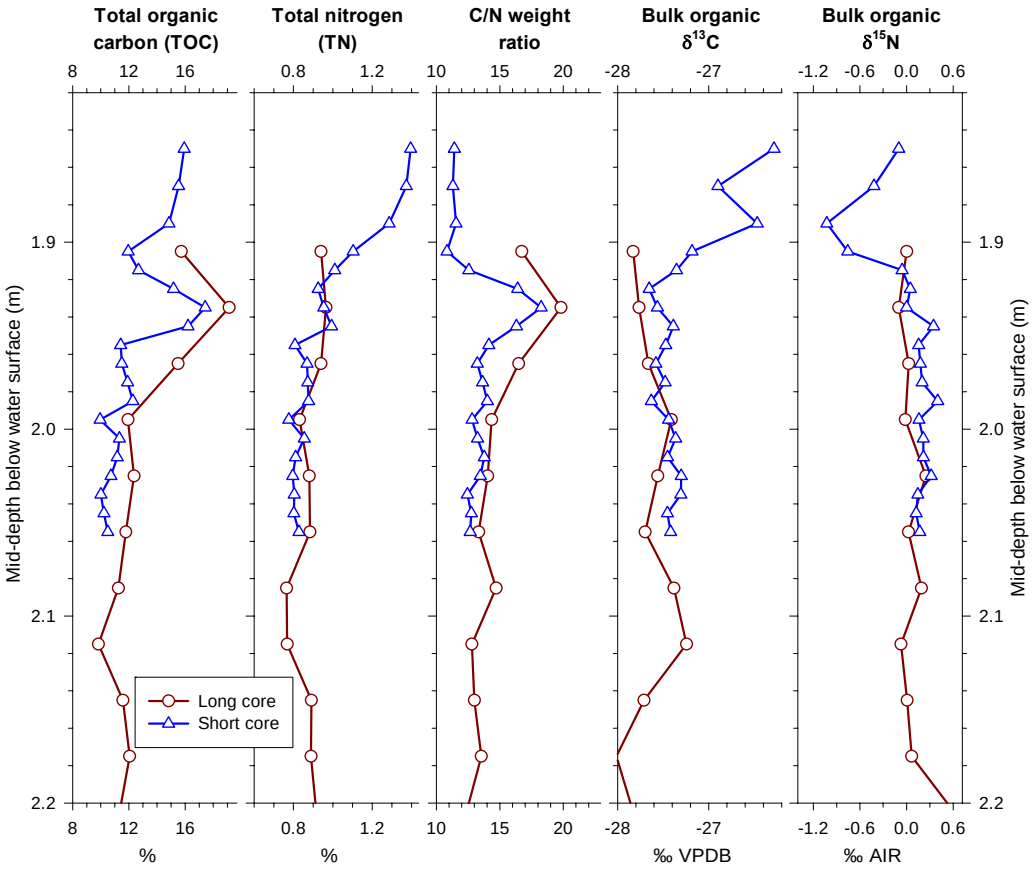

Figure 2-8. Matching of carbon and nitrogen elemental and isotopic composition of Lake Keitjoru between the long and short cores by depth to develop the age chronology for Lake Keitjoru long core.

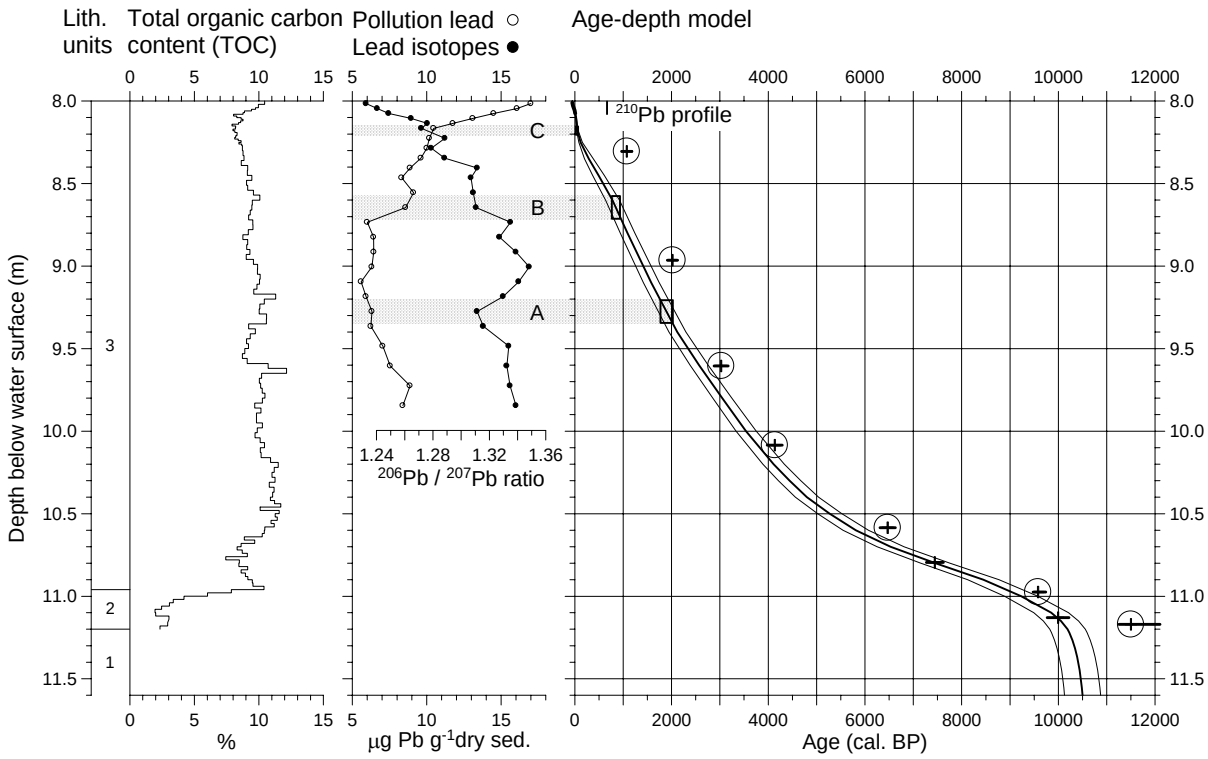

Figure 2-9. Age-depth model for Oikojärvi based on radiocarbon dates of two terrestrial macrofossils (see Table 2-3), ^{210}Pb model of surface sediments, and pollution lead isotopes, plotted collectively with lithological units (see Table 2-2) and total organic carbon content (TOC), lead pollution and flux profiles, versus depth below the water surface. The horizontal shading, indicated as A, B, and C, refer to stratigraphic horizons highlighting lead chronological markers of peak lead pollution during the Roman Empire, Medieval period, and the start of Industrial Revolution, respectively (Renberg *et al.*, 2001). Note that the post-1970 decline is not depicted, likely due to the loss of the uppermost sample of the long core. The encircled radiocarbon dates are all bulk samples that are excluded from the model.

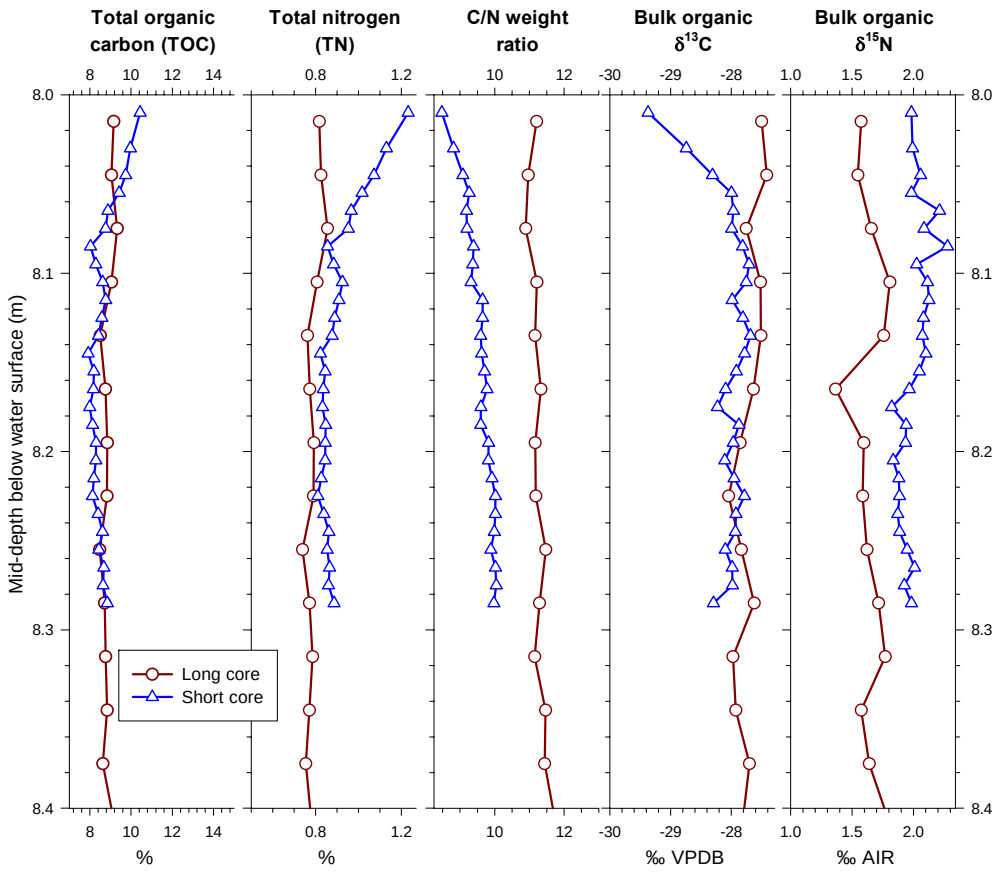

Figure 2-10. Matching of carbon and nitrogen elemental and isotopic composition of Oikojärvi between the long and short cores by depth. Both cores show stratigraphic agreement in trends, and thus, no adjustment of depth is needed in developing the chronology.

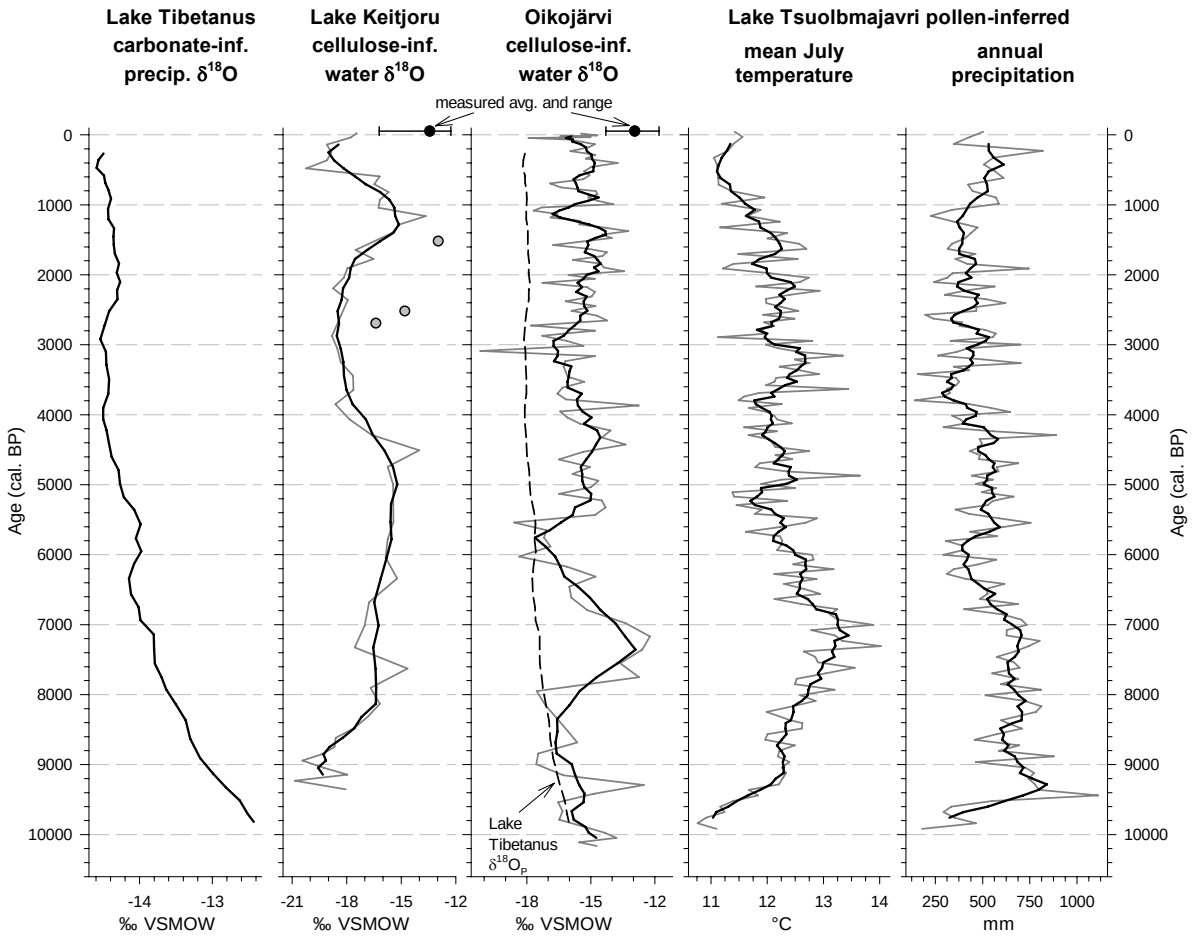

Figure 2-11. Profiles of cellulose-inferred water $\delta^{18}O$ from Lake Keitjoru and Oikojärvi. Grey-filled circles in the Lake Keitjoru profile are $\delta^{18}O$ values that may have been contaminated with terrestrial input. Also displayed are the measured average and range of $\delta^{18}O$ values for lake water sampled on a monthly basis during August 2002-2005, and August 2006. Presented in the first panel is the carbonate-inferred precipitation $\delta^{18}O$ from Lake Tibetanus adjusted to the VSMOW scale (Hammarlund *et al.*, 2002). For comparison, the Tibetanus $\delta^{18}O_P$ record is shown as a dashed line adjacent to the Oikojärvi $\delta^{18}O$ record by shifting the former to match the lowest $\delta^{18}O$ values of the latter (refer to text for detail explanation). The two rightmost panels are profiles of pollen-inferred reconstructions of July temperature and total annual precipitation for Lake Tsuolbmajavri (Seppä and Birks, 2001), located *c.* 30 km southeast from Oikojärvi (Figure 1). Black heavy lines represent the 5-point running average.

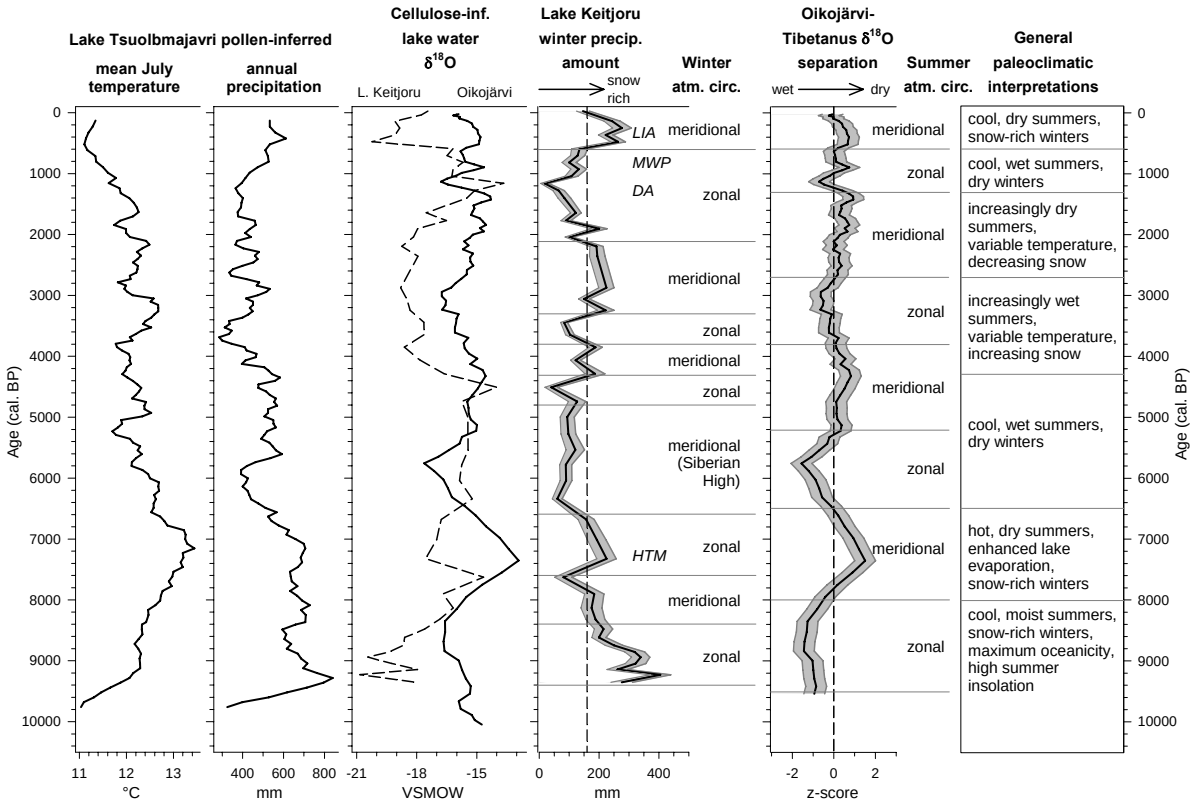

Figure 2-12. Reconstruction of winter precipitation amount from Lake Keitjoru cellulose-inferred water $\delta^{18}O$, with the vertical dashed line representing the modern estimate of winter (November-April) precipitation amount (160 mm; 1990-2006; SMHI). The lake $\delta^{18}O$ separation is an estimate of the evaporative enrichment in Oikojärvi, based on the $\delta^{18}O$ difference between Oikojärvi and Tibetanus $\delta^{18}O$, and is presented as normalized z-scores with respect to the Holocene average lake $\delta^{18}O$ separation. Uncertainty envelopes shown with the winter precipitation amount is estimated based on the analytical uncertainty (±0.7‰) in Lake Keitjoru cellulose $\delta^{18}O$. Uncertainty envelopes used in the lake $\delta^{18}O$ separation represents the analytical uncertainty in cellulose $\delta^{18}O$ of Oikojärvi (±0.5‰). Pollen stratigraphic reconstructions of mean July temperature and annual precipitation from Lake Tsuolbmajavri (Seppä and Birks, 2001) are shown in the first two panels. Inferred winter atmospheric circulation is shown beside Lake Keitjoru winter precipitation reconstruction, and inferred summer atmospheric circulation is displayed next to the Oikojärvi-Tibetanus $\delta^{18}O$ separation. General paleoclimatic interpretations are summarized in the rightmost panel. The Holocene Thermal Maximum (HTM) in northern Fennoscandia occurs at *c.* 8000-6500 cal. BP. The approximate peak timing of human history and climate change are indicated as DA (Dark Ages), MWP (Medieval Warm Period), and LIA (Little Ice Age).

Chapter 3

Holocene Changes in Continentality Across Central Sweden Inferred from Oxygen-Isotope Records of Lake Sediment Cellulose

3.1 Introduction

Shifting atmospheric circulation has been suggested from oxygen isotope records in Fennoscandia. Evidence for this includes inferred precipitation $\delta^{18}O$ that was anomalously high in relation to prevailing temperatures during the early Holocene in the Abisko region, northern Sweden (Hammarlund *et al.*, 2002). The elevated precipitation $\delta^{18}O$ was attributed to a reduction in precipitation distillation in response to intense penetration of westerly airflow across the Scandes Mountains during the early Holocene (Hammarlund *et al.*, 2002). This was followed by a gradual depletion in precipitation $\delta^{18}O$ reflecting the attenuation of westerly airflow after 6000 cal. BP. This change in precipitation $\delta^{18}O$ is suggested to coincide with a shift from an oceanic climate, characterized by a zonal atmospheric circulation pattern during the early Holocene, to a predominantly continental climate regime characterized by a meridional circulation pattern during the later half of the Holocene (Yu and Harrison, 1995; Seppä and Birks, 2001; Hammarlund *et al.*, 2002). A transition from relatively moist, oceanic conditions in the early Holocene to a continental climate after 6000 cal. BP is also reflected by major changes in vegetation extent and composition, as recorded in pollen records (Seppä and Hammarlund, 2000; Hammarlund *et al.*, 2004; Giesecke *et al.*, 2008).

Other precipitation $\delta^{18}O$ records, such as the SG93 speleothem calcite $\delta^{18}O$ record obtained in Søylegrotta, northern Norway (Lauritzen and Lundberg, 1999) and the Lake 850 biogenic silica $\delta^{18}O$ record retrieved from the Abisko region (Shemesh *et al.*, 2001) also suggest high $\delta^{18}O$ values during the early Holocene. Lauritzen and Lundberg (1999) interpreted the speleothem calcite $\delta^{18}O$ as an inverted temperature record, assuming the cave drip waters reflected the recharge of seasonally-modified groundwater. In contrast, the depletion of 3.5‰ in diatom $\delta^{18}O$ record presented by Shemesh *et al.* (2001) was attributed to an increased persistence of a polar Arctic continental air mass since the early Holocene.

Although these studies suggest alternative explanations for the $\delta^{18}O$ signals observed, similarities among the different records are thought to reflect variations in the mean annual $\delta^{18}O$ of precipitation as suggested for the SG93 record by Hammarlund and Edwards (2008). In this study, the addition of two new Holocene $\delta^{18}O$ records provides an opportunity to further evaluate the variations observed in the signals recorded in the $\delta^{18}O$ archives discussed above.

Records of $\delta^{18}O$ were obtained from cellulose at Lake Spåime and Svartkälstjärn, which are small, hydrologically-open, groundwater-fed basins situated at approximately the same latitude in the west-central Scandes Mountains and east-central Sweden, respectively. The west-east location of these lakes are key for assessing the strength, and thus, the extent of prevailing oceanic air masses across the continent, which may have varied and significantly affected the climatic and vegetational development during the Holocene (Hammarlund *et al.*, 2004). Lake Spåime, located close to the Atlantic coast, is likely to provide a characteristic record of the isotopic composition of precipitation reflecting the prevailing influence of North Atlantic air masses. In comparison, Svartkälstjärn is a more continental site whose precipitation isotopic signature may be governed by an additional moisture source, such as the Baltic Sea (Busuioc *et al.*, 2001; Uvo, 2003). In particular, this study provides an opportunity to: (1) test the hypothesis that an increase in the distillation of moisture transported across the Scandes Mountains took place from early to mid-Holocene in response to changes in atmospheric circulation, as postulated from the ^{18}O-enrichment observed in other archives of precipitation $\delta^{18}O$ (Hammarlund *et al.*, 2002; Hammarlund and Edwards, 2008); and (2) relate the variability in precipitation $\delta^{18}O$ to changes in climate that ultimately led to corresponding changes in vegetation dynamics at the study lakes during the Holocene (Hammarlund *et al.*, 2004; Barnekow *et al.*, 2008). An intriguing pattern emerges when comparing the variability between the two cellulose-inferred lake water $\delta^{18}O$ records, which suggests systematic fluctuations in the climate system of the North Atlantic. This study includes the assessment of the modern isotope hydrology and a spatial evaluation of the isotopic composition of modern precipitation across central Sweden, both of which set firmer constraints on reconstructions of the isotope paleoprecipitation records.

3.2 Site Description

Lake Spåime and Svartkälstjärn and their surrounding catchment characteristics were previously described by Hammarlund *et al.* (2004) and Barnekow *et al.* (2008), respectively. Briefly, Lake Spåime (63°07'N, 12°19'E; 887 m a.s.l.) is located in the central part of the Scandes Mountains in the province of Jämtland, west-central Sweden (Figure 3-1), and was formed as part of an ice-dammed lake during deglaciation, which occurred around 11,000-10,500 cal. BP (Lundqvist, 1998). The bedrock in the area consists of Precambrian gneiss, mica schist and amphibolite and is covered by Quaternary hummocky till. Lake Spåime is a small (*c*. 0.03 km^2), shallow (*c*. 3.4 m) throughflow lake that drains a catchment area of *c.* 3.5 km^2. The lake is part of a well-developed stream system, with a short average residence time of 12 days (Table 3-1). The catchment covers a gently sloping mountainside southwest of the lake with an altitude change of *c.* 200 m. Inflow of groundwater occurs on the western side of the basin. The entire catchment is vegetated by alpine tundra, dominated by heath communities with dwarf-shrubs, willows, grasses, sedges and herbs. The modern-day forest-limit of *Betula pubescens* occurs at *c.* 800 m a.s.l., and *Pinus sylvestris* is found up to *c.* 720 m a.s.l.

Svartkälstjärn (64°16′N; 19°33′E; 257 m a.s.l.) is situated in the province of Västerbotten, northeastern Sweden (Figure 3-1), and between two river valleys, including Vindelälven to the northeast. The bedrock in the area is composed of gneisses, mica schists, granites and pegmatites and is blanketed by discontinuous Quaternary till and peat deposits. Deglaciation took place around 10,200-10,000 cal. BP with ice receding towards the northwest. Svartkälstjärn subsequently formed just above the highest paleo-shoreline of the Yoldia Sea, which is estimated at *c.* 253 m a.s.l. in the area (Lundqvist, 1998). Svartkälstjärn is a small, elongated (*c*. 0.05 km^2), shallow (*c*. 3.1 m) and hydrologically open lake that is fed by two inlet streams receiving water from a catchment area of *c.* 2.5 km^2. There is one main outlet at the south side that drains into Vindelälven located 5 km to the east at *c.* 170 m a.s.l. Based on water balance, catchment area and lake volume, the average residence time of water in the lake is about 44 days (Table 3-1). The catchment slope rises to the north where Mount Brattåkersberget (*c*. 403 m a.s.l.), *c.* 2 km north of the lake, is the highest elevation in the area. Catchment vegetation is dominated by a dense coniferous forest consisting of Scots

pine (*Pinus sylvestris*), Norway spruce (*Picea abies*) and birch (*Betula pubescens*). Mire and fen vegetation, composed of shrubs, willows, alder, sedges, grasses and herbs surround the lake margin.

The climate across central Sweden, from west to east, is characterized by an oceanic-continental-oceanic gradient. The oceanic climate at Lake Spåime is moderated by the direct influence of the Atlantic Ocean through prevailing westerly winds, carrying precipitable moisture to the northwestern side of the Scandes Mountains, whereas Svartkälstjärn is situated within a continental climatic regime. The oceanic influence of the Baltic Sea to the east has only a marginal influence along the coast, but the penetration of southerly winds generally moderates climate conditions at Svartkälstjärn. As a result, temperature and precipitation gradients occur along a northwest-southeast trend across central Sweden. The mean annual air temperature at Spåime is –1°C (January –9°C; July 8°C) and at Svartkälstjärn is 2°C (January –12˚C, July 15˚C). The annual precipitation at Spåime is *c.* 900 mm, and at Svartkälstjärn it is *c.* 520 mm (1961-1990 climate normals; Alexandersson *et al.*, 1991). Average annual open-water evaporation at Spåime is *c.* 100 mm, and at Svartkälstjärn it is *c.* 380 mm (Bringfelt and Forsman, 1995). Generally, small lakes in the Lake Spåime region are ice-covered from mid-October to early June, whereas small lakes in the Svartkälstjärn region are ice-covered from late October to mid-May.

3.3 Methods

Sediment cores were retrieved through ice cover from the deepest, central part of Lake Spåime in April 1999 and Svartkälstjärn in February 2002 using a 1-m long Russian peat sampler. The multiple, overlapping 1-m sediment sequences were correlated in the laboratory using magnetic susceptibility measurements. The 3.13 m-long sequence at Lake Spåime was initially divided into 101 sections, 19-48 mm thick (average *c.* 30 mm; Hammarlund *et al.*, 2004), while in this study, each section in the lower part of the sequence (5.89-6.41) was further divided in half to increase sampling resolution, although the bottommost 0.12 m sequence was excluded from isotope analyses due to high clay and silt content. Subsamples of Lake Spåime sediment were separated for analyses of chironomids, mineral magnetics, pollen and plant macrofossils, and elemental and stable isotope

geochemistry (Hammarlund *et al.*, 2004). The 2.24 m long sequence from Svartkälstjärn was divided into 141 sections, 10-20 mm thick (average *c.* 16 mm). Svartkälstjärn sediments were subsampled for the analyses of mineral magnetics, pollen and plant macrofossils, charcoal, and elemental and stable isotope geochemistry (Barnekow *et al.*, 2008). The lowermost 0.09 m of silty clay was excluded from isotope analyses.

Water from Svartkälstjärn was sampled on a monthly basis during the period of February 2002 to October 2005. A total of 45 lake samples, 44 river samples from Vindelälven, five inflow and groundwater samples, and two snow samples were collected. However, the collection of water samples in the Lake Spåime region is relatively sparse due to logistical constraints. During the period of 1999 to 2003 and in 2006, intermittent sampling took place over different times of the year, providing a total of 11 lake samples, 8 samples from nearby rivers, 23 samples from nearby lakes, 5 groundwater and inflow waters, and 3 precipitation grab samples, all of which have been analyzed for both $\delta^{18}O$ and $\delta^{2}H$. The determinations of oxygen and hydrogen isotope composition were performed at the University of Copenhagen. All stable isotope results are expressed as δ-values, representing deviations in per mil (‰) from the VSMOW (Vienna Standard Mean Ocean Water) standard such that $\delta_{sample}=1000[(R_{sample}/R_{VSMOW}) -1]$, where R is the $^{18}O/^{16}O$ or $^{2}H/^{1}H$ ratio in sample and standard. $\delta^{18}O$ and $\delta^{2}H$ values are normalized to SLAP values of –55.5‰ and –428‰, respectively (see Coplen, 1996). Analytical uncertainties are ±0.2‰ for $\delta^{18}O$ and ±2‰ for $\delta^{2}H$.

Lake sediment cellulose was prepared for oxygen isotope analysis following the techniques described in detail by Wolfe *et al.* (2001, 2007). Sediments were washed in 10% HCl to eliminate biogenic and mineral carbonates, and subsequently dry-sieved using a 500-μm mesh. The fine-grained fraction was then processed through additional steps to remove non-cellulose organic components and minerogenic matter, which include solvent extraction, bleaching, alkaline hydrolysis, oxyhydroxide leaching, and sodium polytungstate density separation. Cellulose $\delta^{18}O$ was determined by high-temperature pyrolysis using an on-line continuous-flow isotope-ratio mass spectrometer at the University of Waterloo Environmental Isotope Laboratory. Lake Spåime oxygen-isotope analysis from sediment

cellulose comprises 41 out of 115 samples, 30 of which involved two or more (maximum of seven) repeated analyses. For Svartkälstjärn, 50 out of 137 samples were analyzed, 43 of which included duplicates. The uncertainty (one standard deviation) based on the analytical reproducibility estimated from the repeated measurements conducted on the same cellulose samples resulted in an average of ±0.9‰ and ±0.8‰ for Lake Spåime and Svartkälstjärn, respectively.

3.4 Results and Interpretations

3.4.1 Modern isotope hydrology

3.4.1.1 East-central Sweden

A framework for the distribution of isotopic composition of waters in east-central Sweden is shown in Figure 3-2a. In this isotopic framework, the Local Meteoric Water Line (LMWL) is based on monthly precipitation collected at Rickleå (Figure 3-1) during the period of 1984-1989 (IAEA/WHO GNIP data) when both $\delta^{18}O$ and $\delta^{2}H$ data are available. Accordingly, the amount-weighted means for annual precipitation (δ_P; $\delta^{18}O$=–12.9‰), rain (δ_{Ps}; $\delta^{18}O$=–10.6‰) and snow ($\delta^{18}O$=–16.1‰) are shown. The Local Evaporation Line (LEL), having a lower slope than the LMWL, defines a predicted relation of $\delta^{2}H=4.8\delta^{18}O-33$ based on the Craig and Gordon (1965) model describing isotopic enrichment of an evaporating water body. As described by Gibson *et al.* (2008), the determination of the LEL slope uses estimates of δ_P, the evaporation-flux-weighted isotopic composition of atmospheric moisture (δ_A), and climatic data using June-September average temperature of 12.6°C (Umeå 1962-1990; Alexandersson *et al.*, 1991) and relative humidity of 75%. The limiting isotopic composition (δ^*), which is dependent on δ_A and climatic data, is shown together with the isotopic composition of a terminal lake at hydrological and isotopic steady-state (δ_{SSL}) as points along the LEL (Figure 3-2a). The average isotopic composition of groundwater samples ($\delta^{18}O$=–12.7‰, $\delta^{2}H$=–91‰) collected in September 2003 appears to be capturing the mean annual precipitation isotopic composition, since it is very close to δ_P, and characterizes the input water composition that enters Svartkälstjärn. Figure 3-2b portrays the distribution of the isotopic composition of Svartkälstjärn collected during the period of 2002-

2005 superimposed on the isotopic framework. Lake water data are tightly constrained along the LMWL between the isotopic range of δ_P and δ_{Ps}, demonstrating that summer precipitation has a strong influence on the lake water isotopic composition. However, some lake water data are observed along the predicted LEL. The maximum isotopic composition of lake water at Svartkälstjärn ($\delta_{lakemax}$; $\delta^{18}O$=–8.5‰) is considerably less than δ_{SSL} ($\delta^{18}O$=–4.9‰), illustrating that evaporative enrichment of surface waters is likely minimal.

Measurements of precipitation $\delta^{18}O$ have been reported previously by Rodhe (1987) at Svartberget, *c.* 3 km southeast of Svartkälstjärn, during 1981-1982 and 1985-1989 (Figure 3-3). The monthly composite time series of precipitation $\delta^{18}O$ at Svartberget shows an average seasonal amplitude of 7.3‰, somewhat higher than 4.2‰ at Rickleå, reflecting continental and oceanic conditions, respectively. The difference is most noticeable in winter precipitation $\delta^{18}O$, with Rickleå precipitation being more enriched in ^{18}O than that of Svartberget by as much as +5.3‰ in December. In addition, Figure 3-3 illustrates that a greater component of rain comprises the total precipitation at Svartberget as compared to the more evenly distributed seasonal precipitation $\delta^{18}O$ at Rickleå. Consequently, the monthly average Svartkälstjärn $\delta^{18}O$ follows strikingly close to the Svartberget precipitation amounts; the average $\delta^{18}O$ in Svartkälstjärn lake water (–11.9‰) is very similar to the summer Svartberget precipitation $\delta^{18}O$ (–11.3‰).

The seasonal evolution of lake water isotopic composition at Svartkälstjärn is shown in Figure 3-4 for similar time frames over two different years (June 2002-April 2003 and June 2004-April 2005). Note that the isotopic data from 2002 season show the strongest evaporative evolution along the predicted LEL (Figure 3-4a). Based on isotope-mass balance equations and the Craig and Gordon (1965) model, the evaporation/inflow (E/I) ratio is expressed as (e.g., Wolfe *et al.*, 2005):

$$\frac{E}{I} = \left[\frac{1 - h + \varepsilon_K}{h - \varepsilon_K - \varepsilon^* / \alpha^*}\right] \times \left[\frac{\delta_L - \delta_P}{\delta^* - \delta_L}\right]$$

in decimal notation, where ε^* and ε_K are the equilibrium and kinetic separations, respectively, and α^* is the liquid-vapour equilibrium fractionation factor, in which $\alpha^* > 1$. The ε^* term is defined as α^*–1 (in decimal notation) and α^* is dependent on temperature

(Horita and Wesolowski, 1994) and the ε_K term is dependent on relative humidity (h) normalized to the water surface temperature, expressed as ε_K (^{18}O) = 14.2(1–h) and ε_K (^{2}H) = 12.5(1–h) (Gonfiantini, 1986). δ_A ($\delta^{18}O$=–20.8‰, $\delta^{2}H$=–153‰) is estimated by assuming isotopic equilibrium with δ_{Ps} such that $\delta_A=(\delta_{Ps} - \varepsilon^*)/\alpha^*$ (Zuber, 1983; Gibson and Edwards, 2002). For the August 2002 E/I estimate, $\delta^{18}O$ values of δ_L=–8.5‰, δ_P=–12.9‰, and δ^*=2.1‰ were used, resulting in a maximum E/I of 0.24. However, the average magnitude in E/I ratio at Svartkälstjärn is quite small (average E/I=0.03) and appears to be the typical case as observed during subsequent sampling in 2003-2005, where the lake water isotopic composition is strongly constrained between δ_P and δ_{Ps}, as shown in Figure 3-4b for the 2004 season. The time-series $\delta^{18}O$ data for Svartkälstjärn shown in (Figure 3-4c) also illustrate the seasonal variability between δ_P and δ_{Ps}. In comparison, $\delta^{18}O$ data from Vindelälven also reflect a similar seasonal cycle of precipitation distribution, but having subdued amplitude close to δ_P, which likely reflects a larger catchment size.

3.4.1.2 West-central Sweden

The isotopic distribution of waters in the Lake Spåime region is illustrated in two linear trends, LWML and LEL, which define the isotopic framework (Figure 3-5a). The LMWL is constructed using isotopic data from precipitation and input waters (i.e., sampled groundwater, river, rain, and snow). Similar to Svartkälstjärn, the slope of the LEL for the Lake Spåime region is predicted using the Craig and Gordon (1965) model for evaporative enrichment, the average isotopic composition of groundwater ($\delta^{18}O$=–11.6‰, $\delta^{2}H$=–83‰), the isotopic composition of atmospheric moisture (δ_A), assuming isotopic equilibrium with average summer isotopic composition of input waters, and climatic data. The estimates of meteorological parameters used are the June-September average temperature (6.6°C; Sylarna 1961-1990; Alexandersson *et al.*, 1991) and relative humidity (86%). Figure 3-5b illustrates the isotopic distribution of Lake Spåime water along the LMWL, which closely resembles the range of precipitation and input waters shown in Figure 3-5a. Likewise, the average isotopic composition of Lake Spåime water ($\delta^{18}O$=–11.7‰, $\delta^{2}H$=–83‰) is also indistinguishable from that of the measured groundwater. In comparison, lakes in the area undergoing evaporative enrichment plot along the predicted LEL towards the isotopic

composition of a hydrological and isotopic steady-state terminal lake (δ_{SSL}; Figure 3-5b). For reference, the limiting isotopic composition (δ^*), which is defined by δ_A and climate data, is also shown to plot at the positive extension of the LEL, theoretically reflecting the isotopic signal of a last drop of water before evaporating to dryness.

The collection of water samples for isotope analysis in the Lake Spåime region is relatively sparse due to logistical constraints. However, during 1999-2003, and in 2006, intermittent sampling took place over different times of the year, providing a reasonable picture of the seasonal variability of the isotopic composition of waters in the region (Figure 3-6). Snow samples collected at the site in April 1999 and February 2002 exhibited $\delta^{18}O$ values of –14.7 and –17.2‰, which provide some constraints on the low end of the precipitation isotopic spectrum. The Lake Spåime $\delta^{18}O$ value of –14.3‰ sampled in April 1999 may be representative of spring snowmelt. Overall, Lake Spåime $\delta^{18}O$ data show narrow fluctuations in the range of –13.0 to –10.5‰, which is similar to the range in $\delta^{18}O$ of Spåime input waters, owing to the short residence time of water in the lake, and minimal enrichment due to evaporation.

The average isotopic composition of monthly precipitation at Spåime was constructed by combining the isotopic data of collected precipitation, groundwater, inflow, and nearby river water and obtaining a monthly average (Figure 3-7). Only isotopic data for the months February, April and June-August are available from observations, so the remaining monthly values for precipitation are calculated using the temporal relations, $\delta^{18}O=0.11T_{month}-12.2$ and $\delta^{2}H=1.00T_{month}-86.6$, based on regression of the available data and corresponding monthly temperature values measured at Sylarna (1035 m a.s.l.; *c.* 8 km from Spåime; Alexandersson *et al.*, 1991). The resulting seasonal cycle of monthly precipitation $\delta^{18}O$ at Spåime, as shown in Figure 3-7, is especially subdued owing to the prevailing influence of the Atlantic Ocean. In comparison, precipitation $\delta^{18}O$ from Bredkälen (Figure 3-1), which is the nearest IAEA/WMO GNIP station with a complete monthly dataset, shows a greater seasonal amplitude as a result of greater continentality. This difference in continentality is also evident as a reduction in monthly precipitation amount and increased amplitude of monthly temperature (Figure 3-7).

3.4.1.3 West-east precipitation $\delta^{18}O$ transect

A regional perspective on the seasonal amplitude of precipitation $\delta^{18}O$ along a west-east transect in central Sweden is visualized in Figure 3-8. Notably, Spåime and Rickleå precipitation $\delta^{18}O$, on average, is more enriched than that at Bredkälen and Svartkälstjärn (i.e., represented as Svartberget precipitation $\delta^{18}O$), even though Spåime is located at much higher elevation. The trends observed appear to largely reflect oceanic climate conditions at Spåime and Rickleå owing to the prevailing influence of the Atlantic Ocean and Baltic Sea, respectively, as compared to more continental conditions at Bredkälen and Svartkälstjärn. Likewise, the seasonal spread in precipitation $\delta^{18}O$ increases from west to east, reflecting increasing continentality. On average, the difference in precipitation, $\Delta^{18}O_P$, between Spåime and Svartkälstjärn is +1.36‰. At a seasonal scale, the precipitation $\delta^{18}O$ at Svartkälstjärn can actually be more positive than that at Spåime during the summer, leading to a $\Delta^{18}O_P$ value of –1.84‰ in July. On the other hand, large positive $\Delta^{18}O_P$ values up to +7.75‰ occur during the winter months because precipitation distillation is more enhanced when temperatures are lower. Therefore, the seasonal pattern in the variability in $\Delta^{18}O_P$ is likely controlled to some degree by temperature in addition to the continental effect (Rozanski *et al.*, 1993).

3.4.2 Sediment description and chronology

3.4.2.1 Lake Spåime

The sediment sequence lithostratigraphy at Lake Spåime was divided into five units (Table 3-2). The bottom 0.02 m sequence (unit 1) from Lake Spåime is composed of greyish clayey silt with very low organic matter content (Figure 3-9), and is followed by 0.09 m (unit 2) of clay and sand. Unit 3 consists of 0.02 m of brown silty gyttja and increasing organic content. Unit 4 (1.38 m) is a prominent sequence rich in dark brown gyttja with elevated organic content. Moss remains found at 5.24-5.32 m in Lake Spåime sediments correlate with higher organic content. The upper 1.62 m sequence (unit 5) contains slightly clayey gyttja with low organic matter content. A slight rise in organic matter content at 3.56-3.59 m coincides with the presence of moss remains.

The chronology for Lake Spåime was developed and described in detail by Hammarlund *et al.* (2004). In brief, the chronology is based on eight calibrated AMS radiocarbon dates obtained on macroscopic remains of terrestrial plants (Table 3-3) and the age-model was derived by fitting a polynomial curve through the mid-intercept age values (Figure 3-9). The resulting lowermost age for the onset of gyttja sedimentation is estimated at *c.* 10,700 cal. BP (bottom of unit 2), which is consistent with the timing of deglaciation in the area (Lundqvist, 1998). The apparent sediment accumulation rate at Lake Spåime changed from 0.11 mm/year below *c.* 6.2 m to *c.* 0.40 mm/year in the upper part of unit 4 and the lower part of unit 5, followed by values exceeding 0.50 mm/year above *c.* 3.8 m.

3.4.2.2 Svartkälstjärn

The lithostratigraphy of the Svartkälstjärn sediment sequence was divided into eight units (Table 3-2). The bottom 0.09 m (unit 1) sequence contains greyish silty clay with low organic matter, grading into 0.13 m (unit 2) of brownish-grey silty clay-gyttja with low organic content (Figure 3-10). Unit 3 (0.10 m) consists of clay-gyttja grading into a slightly silty fine-detritus gyttja and increasing organic matter content. The following 1.04 m (unit 4) sequence comprises dark brown fine-detritus gyttja and high organic content, but with a layer of light brown silty gyttja and low organic content at 4.17 m. Unit 5 (0.16 m) consists of dark brown silty fine-detritus gyttja with low organic content, followed by a similar, but thicker unit (0.62 m; unit 6) of organic-rich gyttja. The upper two 0.10 m thick units (units 7-8) of fine-detritus gyttja consist of a shift from low organic matter content in unit 7 to high organic matter content in unit 8.

The Svartkälstjärn chronology was developed and described in detail by Barnekow *et al.* (2008). Briefly, seven calibrated AMS radiocarbon dates were obtained from terrestrial remains of macroscopic plants (Table 3-3). Three additional ^{14}C dates from Svartkälstjärn were also obtained from bulk organic sediment, but may have been influenced by reservoir effects and so were not included in the final age-model. An additional chronological tool, the radioisotope ^{137}Cs, was also applied to the recent sediments of Svartkälstjärn. As a result, an initial rise in ^{137}Cs activity, beginning at 3.175 m, is interpreted to reflect the start of nuclear

bomb testing in the 1950s. Accordingly, the final age-model was developed by fitting a polynomial curve through the mid-intercept ^{14}C dates and the ^{137}Cs date (Figure 3-10).

The resulting lowermost age for the onset of gyttja sedimentation is estimated at *c.* 10,000 cal. BP (bottom of unit 1) in Svartkälstjärn, which is consistent with the timing of deglaciation in the region (Lundqvist, 1998). The sediment accumulation rate varied within the range *c.* 0.16-0.41 mm/year in units 2-4. From unit 5 to the top of unit 6, the accumulation rate declined from 0.38 mm/year to a minimum of 0.11 mm/year due to the subsequent compaction of loose gyttja by the recent deposition of silty sediments, as reflected by a significant increase to 0.9 mm/year in the uppermost strata (units 7-8).

3.4.3 Cellulose-inferred oxygen-isotope records

The Lake Spåime and Svartkälstjärn $\delta^{18}O$ records were reconstructed from raw cellulose $\delta^{18}O$ values using a constant cellulose-water isotopic fractionation factor of 1.028 (Edwards and McAndrews, 1989; Wolfe *et al.*, 2001a, 2007). The Lake Spåime archive of sediment cellulose-inferred water $\delta^{18}O$ from west-central Sweden is shown in Figure 3-11. At the start of the Lake Spåime $\delta^{18}O$ record, the temporal resolution is rather coarse. $\delta^{18}O$ values increase from –17.9‰ at *c.* 9400 cal. BP to –15.2‰ at *c.* 7000 cal. BP, but with a slight decrease to –17.7‰ around 7400 cal. BP. From *c.* 7000 to 4000 cal. BP there is a gradual decrease in $\delta^{18}O$ with values fluctuating in the range of –19.7 to –17.3‰. A more distinctive depletion in ^{18}O in the cellulose record occurs at *c.* 4000-3500 cal. BP, leading to a minimum $\delta^{18}O$ value of –21.8‰ by 3500 cal. BP. Between *c.* 3500 and 2300 cal. BP, $\delta^{18}O$ increases to a maximum value of –18.1‰, followed by another pronounced decrease to –22.0‰ by *c.* 1700 cal. BP. Lake Spåime $\delta^{18}O$ increases to values of –19.1‰ by *c.* 950 cal. BP, and maintains similar $\delta^{18}O$ values until *c.* 600 cal. BP, with a dip to a low $\delta^{18}O$ value of –21.4‰ occurring at *c.* 750 cal. BP. From *c.* 600 to 165 cal. BP, $\delta^{18}O$ decreases to –22.1‰, followed by a slight increase to –20.0‰ at the top of the core. Overall, the Lake Spåime $\delta^{18}O$ profile shows a gradual decline amounting to 2.8‰ between the early Holocene (9400-8000 cal. BP average $\delta^{18}O$ = –17.5‰) and the late Holocene (4200-3200 cal. BP average $\delta^{18}O$ = –20.3‰), followed by a constant trend to the present (<1000 cal. BP average $\delta^{18}O$ = –20.4‰).

The oxygen isotope record inferred from lake sediment cellulose for Svartkälstjärn is shown in Figure 3-11. The early Holocene $\delta^{18}O$ record at Svartkälstjärn begins as a rise from –18.5‰ occurring at *c.* 9500 to a maximum value of –13.2‰ at *c.* 8300 cal. BP. Between *c.* 8300 and 7200 cal. BP, $\delta^{18}O$ decreases to a low of –18.7‰, followed by a rise to –15.0‰ by *c.* 7000 cal. BP. From *c.* 7000 to 6500 cal. BP, $\delta^{18}O$ maintains elevated values at an average of –15.7‰ before decreasing to low values (–21.6‰) by *c.* 5600 cal. BP. During the period of *c.* 5600-3900 cal. BP there is a gradual increase in $\delta^{18}O$ values, fluctuating within the range of –20.7 to –17.5‰. At *c.* 3900-3200 cal. BP, there is a more distinctive rise in $\delta^{18}O$ to a maximum value of –16.1‰, followed by a sharp decline to a minimum value of –23.0‰ occurring at *c.* 2500 cal. BP. After *c.* 2500 cal. BP, $\delta^{18}O$ increases to a value of –18.6‰ at *c.* 2300 cal. BP, and remains invariant until *c.* 1500 cal. BP. At *c.* 1500-500 cal. BP, Svartkälstjärn $\delta^{18}O$ record fluctuates between –19.5 and –16.4‰ with maxima occurring at *c.* 1200 and 500 cal. BP and a minimum at *c.* 700 cal. BP. The $\delta^{18}O$ value of –23.2‰ at the top of the core is considered to be an outlier, and is not considered further in the discussion. This anomalously negative $\delta^{18}O$ value coincides with a substantial rise in the magnetic susceptibility (Figure 3-11), reflecting increased minerogenic matter from the catchment due to intense logging activity around the lake since *c.* 200 cal. BP (Barnekow *et al.*, 2008). Overall, the Svartkälstjärn $\delta^{18}O$ profile displays a strong decrease amounting to 4.0‰ from the early Holocene (9600-8000 cal. BP average $\delta^{18}O$ = –15.8‰) to the mid-Holocene (6000-5000 cal. BP average $\delta^{18}O$ = –19.8‰). After the mid-Holocene, the trend in $\delta^{18}O$ shows a slight increase of about 1.8‰ to the late Holocene (average $\delta^{18}O$ = –18.0‰ during 1200-500 cal. BP).

The Lake Spåime and Svartkälstjärn sediments are aquatic based on evidence from elemental and isotopic composition of carbon and nitrogen, and magnetic susceptibility (Hammarlund *et al.*, 2004; Barnekow *et al.*, 2008; Chapter 5). However, the topmost cellulose-inferred lake water $\delta^{18}O$ in both lakes, excluding the outlier at Svartkälstjärn, are negatively offset from the measured samples of lake water $\delta^{18}O$ by –8.6‰ and –4.8‰ at Lake Spåime and Svartkälstjärn, respectively (Figure 3-11). As discussed previously (Chapter 2), this difference is likely attributable to the mismatch between the lake water

sampling period and the time represented by the surface sediment. For instance, the topmost sediment sample from Lake Spåime spans *c.* 65 years at a mid-age of AD 1903, whereas at Svartkälstjärn the sediment spans *c.* 171 years with a mid-age of *c.* 466 cal. BP. The large offset between modern lake water $\delta^{18}O$ and cellulose-inferred water $\delta^{18}O$ may also be attributed to seasonal isotopic variation, as reported in other studies (Edwards and McAndrews, 1989; Wolfe and Edwards, 1997; Wolfe *et al.*, 2001b). It is possible that the consistently lower offset of the cellulose $\delta^{18}O$ may be incorporating early thaw season melt waters, especially at Lake Spåime, having a shorter residence time than Svartkälstjärn. Although some uncertainties exist in the absolute $\delta^{18}O$ values, the trends are considered robust, particularly through multiple analyses of samples and by comparison with independent $\delta^{18}O$ data (see discussion). Notably, the difference between Lake Spåime and Svartkälstjärn topmost cellulose-inferred water $\delta^{18}O$ at the same interval (at AD 1903 after interpolating to the same age scale) is +1.56‰, which is very close to the modern day difference in precipitation $\delta^{18}O$ of +1.36‰.

3.5 Discussion

3.5.1 Lake Spåime oxygen-isotope record

The cellulose-inferred water $\delta^{18}O$ record from Lake Spåime likely portrays variations that fall along the LMWL, as assessed from the modern isotope hydrology. The overall spread in Lake Spåime cellulose $\delta^{18}O$ data is about 6.8‰ (Figure 3-11), which is within the maximum variability of 8.4‰ observed in the modern precipitation and input waters in the region (Figure 3-5). Since the residence time of water in Lake Spåime is considerably short, it is probable that the variability in Lake Spåime $\delta^{18}O$ during the Holocene reflects changes in the seasonal distribution of precipitation $\delta^{18}O$. The variability in Lake Spåime $\delta^{18}O$ has similarities with a record from Lake Keitjoru in northern Sweden, which is a lake that also has a short residence time and responds to changes in the seasonal precipitation $\delta^{18}O$, also having a maximum variability of 7.1‰ (Chapter 2). Both records show marked shifts to low $\delta^{18}O$ values at *c.* 4000 cal. BP and another at 500 cal. BP, which may be related to increased snow contributions occurring at a regional scale.

Low $\delta^{18}O$ values at Lake Spåime $\delta^{18}O$ show some correspondence with high winter precipitation in western Norway, based on equilibrium line altitude reconstructions (Nesje *et al.*, 2001). The shift to low $\delta^{18}O$ values at *c.* 9400-8600, 4000-3200, 2200-1400 cal. BP and 500 cal. BP agrees with the Nesje *et al.* (2001) winter precipitation reconstruction, although there may be slight differences in the timing in winter precipitation across regional distances during the Holocene (Almquist-Jacobson, 1995). In comparison, the high $\delta^{18}O$ values during *c.* 3200-2200 cal. BP likely indicate an increase in summer precipitation. This interpretation is consistent with high lake levels at Ljustjärnen, central Sweden over the same time frame (Almquist-Jacobson, 1995).

Lake Spåime cellulose-inferred water $\delta^{18}O$ may also reflect temperature-dependent changes in $\delta^{18}O$, considering the close relationship observed between the variability in the modern isotopic composition of Lake Spåime water and that of the input water isotopic data along the LMWL (Figure 3-5). For instance, there is some correspondence after *c.* 6000 cal. BP to the present between Lake Spåime $\delta^{18}O$ and the mean July temperature record inferred from chironomid head capsules analyzed from the same core (Figure 3-11; Hammarlund *et al.*, 2004; Velle *et al.*, 2005). Decreasing trends in $\delta^{18}O$ values at *c.* 5600-3500, 2000-1400, and 600-100 cal. BP generally follow weak cooling trends in the chironomid-inferred temperatures. By comparison, high $\delta^{18}O$ values correspond to slight warming at *c.* 3500-2000 and 1400-600 cal. BP. However, the magnitude of change observed in the $\delta^{18}O$ record is much greater than can be accounted for by temperature alone. For example, assuming a modern spatial $\delta^{18}O$-temperature relationship of 0.65 ‰/K, the maximum temperature change of –6 K is inferred at *c.* 4200 cal. BP over 148 years, which exceeds a cooling of *c.* 1.2 K inferred from the chironomid temperature record. As a result, increases in $\delta^{18}O$ of lake water is considered to reflect an increased importance of summer precipitation contributions and possibly warmer temperatures, while a decrease in $\delta^{18}O$ is presumed to indicate an increase in winter precipitation and perhaps cooler temperatures (Figure 3-11).

Variability in precipitation $\delta^{18}O$ in the Scandes Mountains is demonstrated by independent data of SG93 speleothem calcite $\delta^{18}O$ from Søylegrotta, northern Norway (Lauritzen and Lundberg, 1999) and lacustrine calcite $\delta^{18}O$ from Lake Tibetanus, northern Sweden

(Hammarlund *et al.*, 2002) as shown in Figure 3-11. A direct comparison with Lake Spåime $\delta^{18}O$ with the calcite $\delta^{18}O$ records show some similarities in both low- and high-frequency signals, specifically at *c.* 8000-500 cal. BP. In addition, Lake Spåime exhibits a gradual decline in $\delta^{18}O$ by 2.8‰ by *c.* 4200 cal. BP, followed by a near-constant trend to the present. This general trend is also seen in both calcite $\delta^{18}O$ records, but with a decline in $\delta^{18}O$ occurring until 6000 cal. BP, followed by a near-constant trend to the present. Similarly, the $\delta^{18}O$ record obtained from biogenic silica in lake sediments, near Abisko, also illustrates a long-term Holocene ^{18}O-depletion of about 3.5‰ (Shemesh *et al.*, 2001). Hammarlund and Edwards (2008) suggested that the calcite $\delta^{18}O$ records are capturing signals of the circulation-dependent variations in precipitation $\delta^{18}O$, and this may also be true for Lake Spåime $\delta^{18}O$ because of the similarities that exist between these records.

Interestingly, the Lake Spåime $\delta^{18}O$ Holocene record also shows close resemblance to a speleothem $\delta^{18}O$ record from southwest Ireland (McDermott *et al.*, 2001), generally reflecting a common forcing on $\delta^{18}O$ of precipitation. Specifically, there are striking similarities in the timing of peaks and troughs, as well as the magnitude of $\delta^{18}O$ shifts, for the period from *c.* 6600 cal. BP to the present. As noted by McDermott *et al.* (2001) in the speleothem $\delta^{18}O$ record, the variability in $\delta^{18}O$ values from the Lake Spåime record may also reflect the timing of historic climate variability, such as the $\delta^{18}O$ peaks at *c.* 2200 and 1000 cal. BP corresponding to the period of the Roman Empire and the Medieval Warm Period, respectively, whereas the $\delta^{18}O$ troughs at *c.* 1700 and 300 cal. BP respectively coincide with the Dark Ages and the Little Ice Age. As supporting evidence, Lake Spåime $\delta^{18}O$ also shows a close match with trends from planktic foraminifera $\delta^{18}O$ data between *c.* 6000 and 2000 cal. BP from a core obtained north of Iceland (B997-321; Smith *et al.*, 2005). Lake Spåime $\delta^{18}O$ profile after *c.* 2000 cal. BP also shows a remarkably good match with $\delta^{18}O$ data from a southern core site closer to Iceland (B997-328; Smith *et al.*, 2005).

At *c.* 9400-6000 cal. BP, there is very little correspondence in the trends observed between Spåime $\delta^{18}O$ and the mean July temperature record. Based on modern isotope hydrology, it is unlikely that the enrichment in $\delta^{18}O$ is due to evaporation. Hammarlund *et al.* (2002) evaluated past variations in the temporal precipitation $\delta^{18}O$-temperature relation in the

Abisko area. Deviations from the modern $\delta^{18}O$-temperature relation (Dansgaard, 1964) occurred during 10,000-6500 cal. BP at Lake Tibetanus, and together with high annual precipitation, as inferred from pollen reconstructions (Figure 3-11), indicate a highly oceanic climate. Increased efficiency of moisture transfer across the Scandes Mountains would have reduced the distillation of precipitation, thus resulting in elevated $\delta^{18}O$ values. A combination of both *Betula* and *Alnus* macrofossils found at higher elevations than Lake Spåime at *c.* 7500-5000 cal. BP suggests that oceanic (mild and wet) conditions prevailed (Hammarlund *et al.*, 2004). Later occurrences of pine, which favour warm and dry conditions, indicate increased seasonality during *c.* 6500-5500 cal. BP (Kullman, 1992; Hammarlund *et al.*, 2004). A decline in both Lake Spåime $\delta^{18}O$ and the calcite $\delta^{18}O$ records by 6500 cal. BP, in combination with decreasing annual precipitation inferred from pollen reconstructions at Lake Tibetanus, suggests a common response to shifting atmospheric circulation that resulted in the increased distillation of precipitation over the Scandes Mountains.

3.5.2 Svartkälstjärn oxygen-isotope records

Based on the assessment of the modern isotope hydrology at Svartkälstjärn, cellulose-inferred lake water $\delta^{18}O$ is likely to reflect variations along the LMWL in response to changes in the seasonal distribution of precipitation (Figure 3-11). However, under exceptionally warm and dry conditions, evaporative enrichment of Svartkälstjärn lake water, similar to the 2002 season, may potentially occur. Periods of greatest ^{18}O-enrichment, amounting to about 1-3‰ in the cellulose sediment record (looking at the 5-point running average), occur at *c.* 9400-8000, 7500-6800 and 4200-3200 cal. BP. In the modern setting, the maximum enrichment from δ_P to the maximum lake water $\delta^{18}O$ that occurred in 2002 amounted to 4.4‰ (Figure 3-4a), certainly greater than observed in the cellulose $\delta^{18}O$ record. On the other hand, the spread in modern lake water $\delta^{18}O$ during the 2004 season was 2.4‰, similar to the difference between modern δ_P and δ_{Ps} at Svartberget and Rickleå (Figure 3-4b), which falls short of the amount of enrichment observed in the cellulose $\delta^{18}O$ record. Extreme isotopic enrichment due to evaporation seems unlikely based on the nature of the

modern isotope hydrology, and especially since Svartkälstjärn water isotope data are tightly constrained to the LMWL for most of the sampling period.

In Figure 3-11, low magnetic susceptibility values at *c.* 8500-6500 cal. BP coincide with elevated Svartkälstjärn $\delta^{18}O$ values, suggesting evaporative enrichment in response to reduced precipitation. However, the low magnetic susceptibility values during this period reflect soil stability associated with a dense forest in the catchment during the Holocene Thermal Maximum (Heikkilä and Seppä, 2003; Barnekow *et al.*, 2008). Variation in magnetic susceptibility shows some correspondence with $\delta^{18}O$ variability at high frequency. For instance, high $\delta^{18}O$ values coincide with high magnetic susceptibility at *c.* 8500-8000 cal. BP, which may reflect a greater influx of minerogenic matter if summer rain contributions increased. Elevated $\delta^{18}O$ values in the Svartkälstjärn record before *c.* 8000 cal. BP because of increased rain contributions is also consistent with high lake levels at this time in southern Sweden (Digerfeldt, 1988; 1997; Hammarlund *et al.*, 2003). At 8000-7000 cal. BP, low $\delta^{18}O$ values suggest an increase in snow contributions at Svartkälstjärn. A period of dry summers is indicated by lowering of lake levels beginning at *c.* 8000 cal. BP in southern Sweden (Digerfeldt, 1988; 1997; Hammarlund *et al.*, 2003), and evaporative enrichment of cellulose-inferred lake water $\delta^{18}O$ at Oikojärvi, Finland, occurring at *c.* 8000-6500 cal. BP (Chapter 2). The only period during which evaporative enrichment may have taken place in Svartkälstjärn lake water may have been at *c.* 7000-6500 cal. BP. Generally high $\delta^{18}O$ coincides with low magnetic susceptibility, suggesting a combination of reduced winter precipitation and possibly evaporative enrichment in response to lower effective humidity. A small presence of charcoal particles in Svartkälstjärn sediments has been noted at *c.* 7000 cal. BP (Barnekow *et al.*, 2008), supporting dry summers occurring at this time.

The low $\delta^{18}O$ values at *c.* 6500-4200 cal. BP correspond with elevated magnetic susceptibility, which may reflect a lake water $\delta^{18}O$ composition that is close to that of mean annual precipitation (Figure 3-11). The subsequent increase in $\delta^{18}O$ at *c.* 4200-3200 cal. BP is likely due to an increase in summer rain contribution. A wetter climate after 4200 cal. BP is supported by high lake levels in southern and central Sweden (Digerfeldt, 1988; 1997;

Almquist-Jacobson, 1995; Hammarlund *et al.*, 2003) and northern Fennoscandia (Korhola *et al.*, 2005).

The variation in Svartkälstjärn $\delta^{18}O$ between *c.* 6500 cal. BP and the present shows similarities with a 3-point running average mean annual pollen-reconstructed temperature record from Laihalampi in southern Finland (Heikkilä and Seppä, 2003). For example, significant decreases in $\delta^{18}O$ at *c.* 6000 and 3000 cal. BP correspond with cooler climate conditions, whereas, peak $\delta^{18}O$ values centred at *c.* 3200, 1200 and 400 cal. BP relate to warmer climate conditions. This positive relationship with temperature variability provides additional support that Svartkälstjärn cellulose $\delta^{18}O$ is recording variations in regional atmospheric circulation. Differences between the Svartkälstjärn $\delta^{18}O$ and Spåime $\delta^{18}O$ records likely reflect a seasonality effect observed at each lake. However, both lakes show a general decline in $\delta^{18}O$ from early to mid-Holocene, possibly reflecting a gradual attenuation of westerly flow of precipitation (Figure 3-11).

3.5.3 Comparison of precipitation $\delta^{18}O$ variability and vegetation dynamics

The approximate timing of change in the vegetational composition from the mid- to late Holocene concurs with changes in the $\delta^{18}O$ profiles of Lake Spåime and Svartkälstjärn. For instance, the decreasing trends observed to occur at *c.* 4200 cal. BP in the precipitation $\delta^{18}O$ records from Lake Spåime and Svartkälstjärn in association with a deteriorating climate regime are accompanied by significant changes in the vegetation. For example, the complete disappearance of trees from the Lake Spåime area at *c.* 3700 cal. BP coincides with a minimum in precipitation $\delta^{18}O$. This is interpreted as a regional increase in winter snow contributions, which is consistent with equilibrium-line altitude fluctuations of maritime glaciers and inferred summer temperatures in western Norway by Nesje *et al.* (2001; Figure 11). This supports the suggestion made by Hammarlund *et al.* (2004) that the tree-limit retreat was likely caused by increasing moisture and shortening of the growing season by late-melting snow cover, rather than significant cooling. Similarly, in the Svartkälstjärn region, moister conditions at *c.* 3500 are indicated by the increased frequencies of *Sphagnum* spores and elevated pollen accumulation rates and pollen frequencies of *Calluna* and *Empetrum*, which signify the expansion of peat deposits and heath development, respectively

(Barnekow *et al.*, 2008). The high precipitation $\delta^{18}O$ values shown in the Svartkälstjärn record at *c.* 3500 cal. BP suggest a different precipitation source, which is likely from an air mass collecting moisture as it passes over the Baltic Sea. Therefore, more oceanic-like conditions in the Svartkälstjärn area may have been attributed to increased humidity during the summer. At around 3200 cal. BP, the substantial decrease in $\delta^{18}O$ of precipitation in the Svartkälstjärn region occurred simultaneously with a rapid increase in *Picea abies*, which is more adaptable to cold, snow-rich winters and acidic soils with relatively high water content (Kullman, 1988).

3.5.4 Changes in continentality during the Holocene

Significant variability in cellulose-inferred lake water $\delta^{18}O$ is evident between Svartkälstjärn and Lake Spåime, suggesting shifting atmospheric circulation during the Holocene. Figure 3-12 illustrates this variability between Svartkälstjärn $\delta^{18}O$ and Lake Spåime $\delta^{18}O$ in δ-δ space over time. The comparison shows generally higher $\delta^{18}O$ at both sites between *c.* 9100 and 6400 cal. BP, possibly reflecting a period of high oceanicity due to the influence of stronger westerlies. As suggested by Hammarlund *et al.* (2002), a reduction in precipitation distillation is likely influencing higher precipitation $\delta^{18}O$ without an associated increase in temperature (Figure 3-11). Peak summer insolation and generally high sea-surface temperatures occurred at around 10,000-6000 cal. BP and reduced sea ice extent allowed an extensive northward flow of warm Atlantic surface waters into the Nordic Seas (Koç et al, 1993; Birks and Koç, 2002; Calvo *et al.*, 2002; Smith *et al.*, 2005). A steep moisture gradient was suggested to have developed across northern Eurasia based on oxygen-isotope data from lake sediment cellulose (Wolfe *et al.*, 2000, 2003), illustrating strong penetration of westerlies during the early Holocene. Evidence of elevated moisture during the early Holocene is suggested by higher latitudinal and altitudinal tree-limits of *Pinus sylvestris* in northern Fennoscandia and in the Scandes Mountains (Kullman, 1988,1995; Barnekow, 2000; Seppä and Hammarlund, 2000; Hammarlund *et al.*, 2004).

Figure 3-12 shows a simultaneous shift to low $\delta^{18}O$ values at both Svartkälstjärn and Lake Spåime by *c.* 6000 cal. BP suggesting increased distillation of precipitation, consistent with increasing continentality (Seppä and Hammarlund, 2000; Hammarlund *et al.*, 2002, 2004;

Giesecke *et al.*, 2008). This long-term shift in atmospheric circulation suggested by the non-temperature-dependent decline in $\delta^{18}O$ coincides with a reduction in the strength of westerly flow and a decline in the pollen-inferred annual precipitation reconstruction from Lake Tibetanus (Figure 3-11; Hammarlund *et al.*, 2002). A decrease in $\delta^{18}O$ from early to mid-Holocene appears to be a common feature in precipitation $\delta^{18}O$ in northern Fennoscandia, as depicted by two calcite $\delta^{18}O$ records (Lauritzen and Lundberg, 1999; Hammarlund *et al.*, 2002; Hammarlund and Edwards, 2008) and biogenic silica $\delta^{18}O$ record (Shemesh *et al.*, 2001). This millennial scale evolution of $\delta^{18}O$ in precipitation may be reflecting a transition from strong zonal atmospheric circulation during the early Holocene to more meridional flow by mid-Holocene, possibly driven by decreasing summer insolation and declining sea-surface temperatures. This long-term shift from high to low $\delta^{18}O$ values in both lakes during the Holocene may reflect larger scale (hemispheric) climate mode variability analogous to the Northern Hemisphere annular mode (Thompson and Wallace, 2001).

A tight cluster between Svartkälstjärn $\delta^{18}O$ and Lake Spåime $\delta^{18}O$ values occur at *c.* 6000-5000 cal. BP, possibly reflecting high stability in atmospheric circulation. *Pinus sylvestris* fragments were found in Lake Spåime sediments between 6500 and 5500 cal. BP when chironomid-inferred mean July temperatures were high (Figure 3-11; Hammarlund *et al.*, 2004). This interval also coincides with the complete disappearance of glaciers (Snowball *et al.*, 2004). In addition, anomalously high concentrations of sea salt and dust is recorded in the Summit ice core from Greenland, indicating intense meridional circulation during winter (O'Brien *et al.*, 1995; Mayewski *et al.*, 1997). Antonsson *et al.* (2008) suggests that the development of dry and warm summers during 7000-5000 cal. BP is due to the persistent presence of an anticyclonic circulation pattern.

Considerable shifts occur inversely between Svartkälstjärn $\delta^{18}O$ and Lake Spåime $\delta^{18}O$ values after *c.* 5000 to 400 cal. BP (Figure 3-12). These variations are likely reflecting centennial to millennial scale changes in atmospheric circulation modes analogous to the variability of the North Atlantic Oscillation (NAO) index (Hurrell, 1995). The $\delta^{18}O$ trends observed in Figure 3-12 are perhaps due to regional variations in the influence of the NAO. For example, greater winter precipitation along the west coast of Norway and in the Scandes

Mountains have been linked to increased zonal atmospheric circulation in winter (i.e., positive NAO index) while a concurrent reduction in snow contributions occurs in the lee of the Scandes or eastern Sweden (Busuioc *et al.*, 2001; Nesje *et al.*, 2003; Uvo, 2003). Thus, a positive NAO index is suggested when Lake Spåime $\delta^{18}O$ values are low, suggesting increased snow contributions relative to rain, while Svartkälstjärn $\delta^{18}O$ values are high, indicating decreased snow relative to rain. A change to meridional flow (i.e., negative NAO index) implies dry winters in western Fennoscandia and dry summers in eastern Fennoscandia due to persistent blocking of anticyclones over these regions (Wallén, 1970; Johannessen, 1970; Uvo, 2003). Precipitation that falls at Svartkälstjärn is likely related to the transport of air masses capturing moisture from the Baltic Sea (Busuioc *et al.*, 2001; Uvo, 2003). From Figure 3-12, $\delta^{18}O$ trends toward a positive NAO phase may be inferred at *c.* 9000-8200, 7200-6600, 4600-3600, 2600-1400 cal. BP, and possibly 1000-600 cal. BP, whereas a negative NAO phase is suggested during the intervening periods. Positive NAO phases correspond with periods of high winter precipitation and glacier advances in the Jostedalsbreen region (Nesje *et al.*, 2001). Negative NAO phases coincide with ice-rafting in the North Atlantic (Bond *et al.*, 1997, 2001) and is consistent with chemical fluctuations of marine and terrestrial ion concentrations in GISP2 ice core, reflecting shifts in atmospheric circulation above Greenland (O'Brien *et al.*, 1995).

In particular, the major descent of tree-line occurring at Lake Spåime catchment at about 3700 cal. BP (Hammarlund *et al.*, 2004), described in the previous section, coincides with increased winter precipitation while chironomid-inferred mean July temperatures showed no significant cooling. This may be signifying mild, wet winters that are typically associated with a positive NAO phase. In contrast, the changes in vegetation composition at Svartkälstjärn, especially the rapid increase and eastward spread of *Picea abies* at *c.* 3200 cal. BP (Barnekow *et al.*, 2008), appears to have been triggered by cold, moist winters due to stronger meridional circulation.

3.6 Summary

The reconstruction of precipitation $\delta^{18}O$ from lake sediment cellulose provides additional insights into the atmospheric circulation dynamics across central Sweden during the

Holocene. Specifically, cellulose-inferred water $\delta^{18}O$ from Lake Spåime reflect variation in the seasonal distribution of precipitation, superimposed on the mean annual precipitation $\delta^{18}O$ variability in the Scandes Mountains of west-central Sweden, and thus, generally portray climate conditions that are governed predominantly by westerly flow from the North Atlantic. In contrast, the Svartkälstjärn $\delta^{18}O$ record depicts varying degrees of mixing between the North Atlantic and Eurasian air masses as continentality increases. Strong negative ^{18}O-excursions at Svartkälstjärn are reflective of snow-rich winters, whereas positive $\delta^{18}O$ values may be enhanced locally by ^{18}O-enriched precipitation from vapour originating from the Baltic Sea. In summary, four climatic stages can be identified from the cellulose $\delta^{18}O$ records, which also highlights major responses in the vegetation dynamics: 1) Elevated $\delta^{18}O$ values at Lake Spåime and Svartkälstjärn during the period between *c.* 9000 and 6400 cal. BP reflect high oceanicity due to the influence of stronger westerlies and reduced precipitation distillation across the continent, 2) Lower $\delta^{18}O$ values at Lake Spåime and Svartkälstjärn by *c.* 6000 cal. BP signal increased continentality and increased precipitation distillation due to reduced penetration of westerlies, 3) Stable $\delta^{18}O$ values at both lakes during *c.* 6000-5000 cal. BP indicate a persistent mode of atmospheric stability, 4) Contrasting $\delta^{18}O$ patterns between the two sites from 5000 cal. BP to the present suggest more systematically variable climate. Fluctuations in atmospheric circulation at both low (millennial) and high (centennial) frequencies are revealed from the $\delta^{18}O$ comparison. Long-term decreasing trends observed in $\delta^{18}O$ records may be analogous to large-scale variability in the Northern Hemisphere annular mode and higher frequency fluctuations in $\delta^{18}O$ may be expressing variability in climate modes specific to the North Atlantic region (North Atlantic Oscillation).

Table 3-1. Summary of lake characteristics and determination of average residence time of water in Lake Spåime and Svartkälstjärn. Total annual precipitation obtained from climate normals (SMHI 1961-1990; Alexandersson *et al.*, 1991) and annual evaporation extrapolated from Bringfelt and Forsman (1995). Annual precipitation (P) and annual evaporation (E) are integrated over catchment area and lake area, respectively, to obtain volume estimates. Residence time is converted to days. Note, the average residence time for Lake Spåime agrees with the estimate of 5-10 days determined by Hammarlund et al (2004).

	Lake Spåime	Svartkälstjärn
water depth (m)	3.4	3.1
annual precipitation (mm)	900	520
annual evaporation (mm)	100	380
lake area (km^2)	0.03	0.05
catchment area (km^2)	3.5	2.5
lake volume, V (mm^3)	$1.0x10^{14}$	$1.6x10^{14}$
discharge, Q=P-E (mm^3/year)	$3.2x10^{15}$	$1.3x10^{15}$
residence time, t=V/Q (days)	12	44

Table 3-2. Lithostratigraphic description of Lake Spåime and Svartkälstjärn sediment profiles. Depths are related to the water surface. The water depth measured at the coring site is 3.39 m at Lake Spåime and 3.13 m at Svartkälstjärn.

Lake	Unit	Depth (m)	Description
Spåime	5	3.39-5.01	Dark brown, slightly clayey gyttja. Lower boundary very gradual. Moss remains at 3.56-3.59 m.
	4	5.01-6.39	Dark brown, slightly clayey gyttja with occasional occurrences of coarse organic detritus. Abundant moss remains at 5.24-5.32 m. Lower boundary gradual.
	3	6.39-6.41	Dark brown silty gyttja. Lower boundary gradual.
	2	6.41-6.50	Grey slightly organic silt with layers of clay and sand. Lower boundary gradual.
	1	6.50-6.52	Grey clayey silt. Abrupt core stop at 6.52 m.
Svartkälstjärn	8	3.13-3.17	Brown slightly silty fine-detritus gyttja. Lower boundary gradual.
	7	3.17-3.23	Light brown silty fine-detritus gyttja. Lower boundary rather sharp.
	6	3.23-3.85	Dark brown fine-detritus gyttja. Slightly lighter layers at 3.31, 3.44 and 3.53 m. Lower boundary rather sharp.
	5	3.85-4.01	Dark brown slightly silty fine-detritus gyttja with faint laminations. Lower boundary gradual.
	4	4.01-5.05	Dark brown fine-detritus gyttja with a light brown layer at 4.17 m. Lower boundary gradual.
	3	5.05-5.15	Greyish brown clay-gyttja, grading upwards into slightly silty fine-detritus gyttja. Lower boundary gradual.
	2	5.15-5.28	Brownish grey silty clay-gyttja. Lower boundary gradual.
	1	5.28-5.37	Grey silty clay with low organic matter content. Abrupt core stop at 5.48 m (no recovery 5.37-5.48 m).

Table 3-3. Radiocarbon dates. Depths are relative to the water surface.

Lake	Depth (m)	Lab no.	Material analyzed	Reported age (^{14}C years BP)	Calibrated age (2σ interval)	Calibrated age (mid intercept) (cal. BP)
Spåime	3.90-3.96	Ua-16679	*Betula*, *Salix*	1295 ± 75	1010-1340	1175
	4.18-4.20	Ua-16678	*Betula*, *Salix*	1555 ± 65	1300-1570	1435
	4.51-4.54	Ua-16680	*Betula*, *Salix*	2420 ± 65	2340-2720	2530
	5.07-5.11	Ua-16392	*Betula*, *Empetrum*	3620 ± 80	3690-4150	3920
	5.65-5.68	Ua-16391	*Betula*, *Salix*	4580 ± 70	4950-5500	5290
	6.04-6.07	Ua-16390	*Betula*, *Empetrum*	6165 ± 75	6800-7250	7025
	6.22-6.25	Ua-16389	*Betula*, *Carex*	7395 ± 95	8010-8380	8195
	6.47-6.50	Ua-16388	*Salix*	9315 ± 160	10,150-11,000	10,470
Svartkälstjärn	3.53-3.55	LuS-6671	Plant macrofossils	2405 ± 50	2340-2705	2420
	3.71-3.73	LuS-6670	Plant macrofossils	2920 ± 50	2920-3245	3082
	3.67-3.69	LuA-5535	Gyttja	3080 ± 60	3070-3450	3260
	4.19-4.205	LuA-5532	*Pinus* (bark)	4280 ± 60	4610-5040	4825
	4.505-4.52	LuS-6669	Plant macrofossils	5845 ± 55	6495-6785	6640
	4.535-4.55	LuA-5534	Gyttja	5990 ± 50	6670-6950	6810
	4.94-4.97	LuA-5531	*Pinus*	7460 ± 95	8030-8410	8220
	5.10-5.11	LuA-5530	*Carex*	7555 ± 110	8050-8600	8325
	5.22-5.24	LuA-5533	Gyttja	8920 ± 70	9770-10,220	9995
	5.25-5.28	LuA-5385	*Pinus*, *Empetrum*	8910 ± 95	9650-10,250	9950

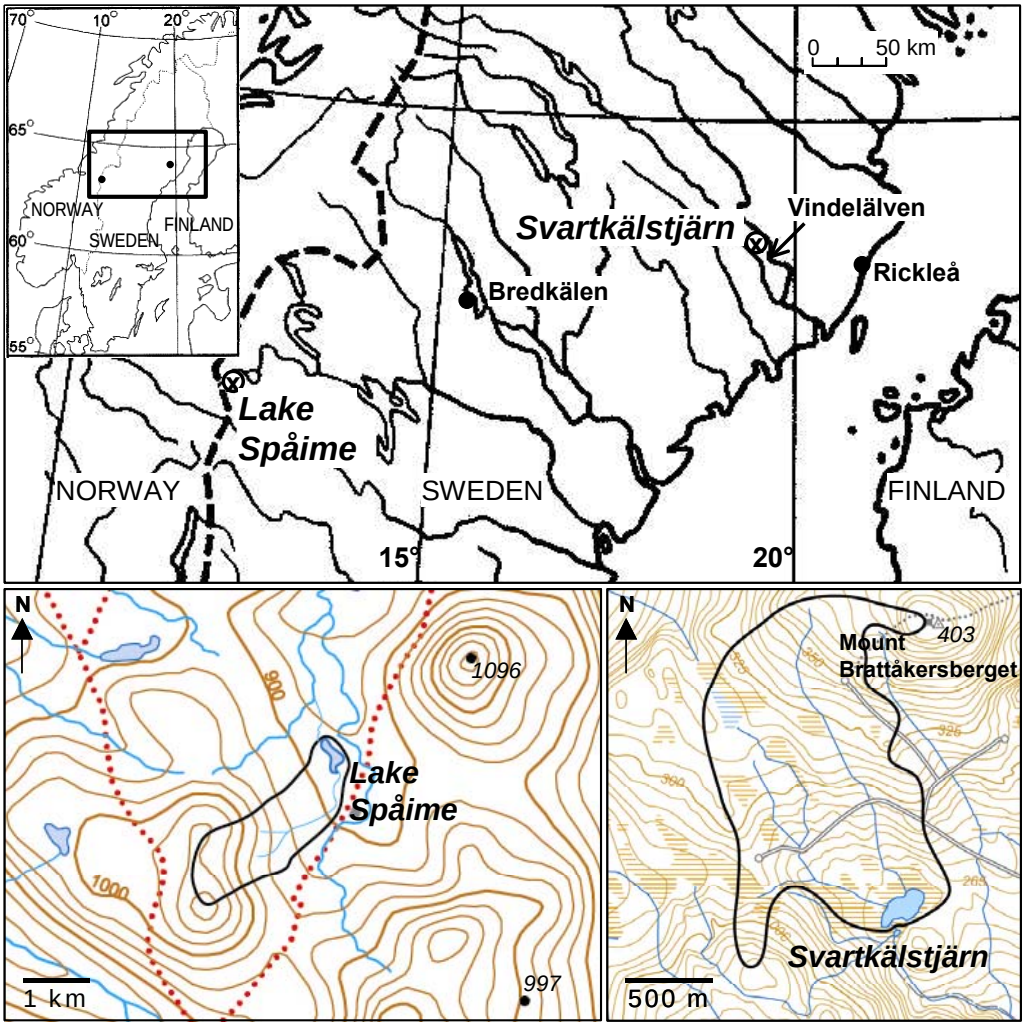

Figure 3-1. Map showing the location, catchment boundary and sampling site of Lake Spåime and Svartkälstjärn in central Sweden. Locations mentioned in text are also shown.

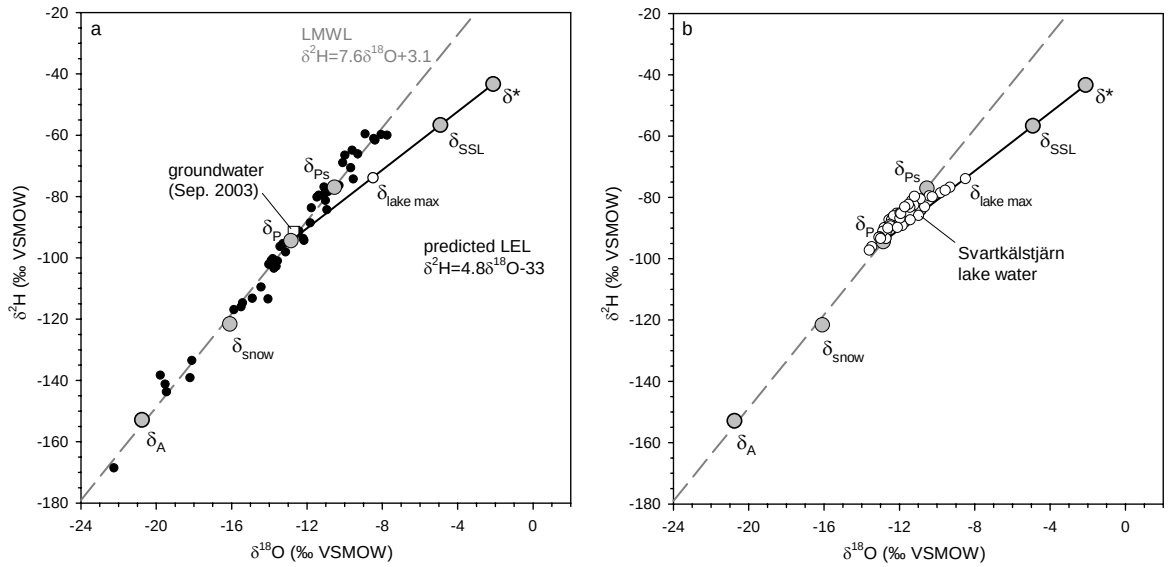

Figure 3-2. a) Calculated water isotopic framework for east-central Sweden. Isotopic data for monthly average precipitation obtained from Rickleå (10 m a.s.l) during the period of 1984-1989 (IAEA/WHO GNIP-data), shown as small black circles, plot along the LMWL ($\delta^2H=7.6\delta^{18}O+3.1$). The amount-weighted means for annual precipitation (δ_P), rain (δ_{Ps}), and snow (δ_{snow}) are key points on the LMWL. The slope of the LEL is predicted by the Craig and Gordon (1965) model that describes isotopic enrichment during evaporation, using climate normals and estimates of δ_P, and the isotopic composition of atmospheric moisture (δ_A), which is assumed to be in equilibrium with δ_{Ps}. Groundwater samples collected in September 2003 closely match δ_P. For reference, the maximum isotopic signature of Svartkälstjärn lake water plots on the LEL. b) The isotopic composition of Svartkälstjärn lake water is shown superimposed on the isotopic framework.

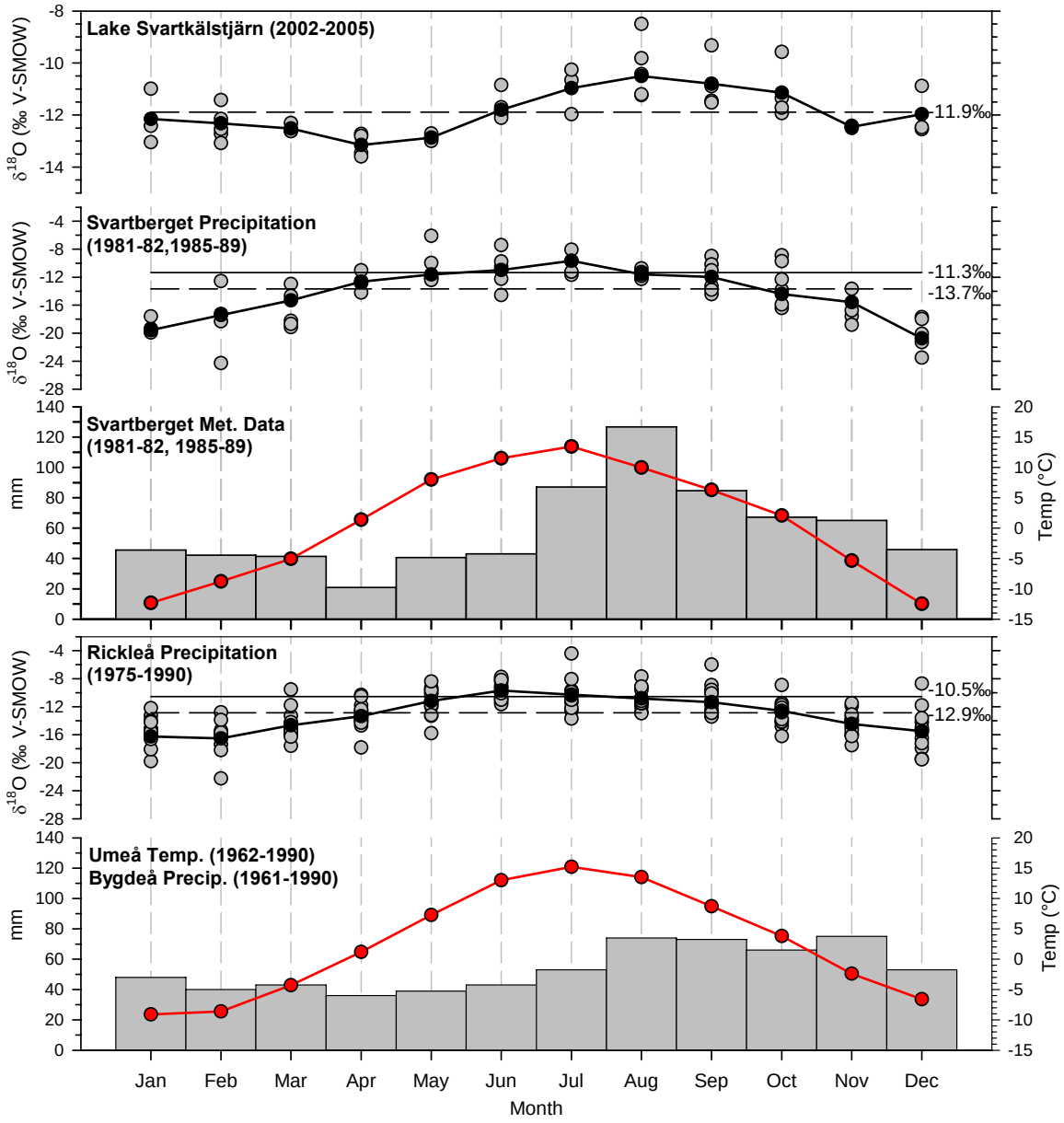

Figure 3-3. Monthly average of oxygen isotopic composition of waters (black-filled circles) and meteorological data from east-central Sweden. Water $\delta^{18}O$ data (grey-filled circles) from Svartkälstjärn are for samples obtained during February 2002 to October 2005. For data near Svartkälstjärn, precipitation $\delta^{18}O$, precipitation amount and temperature data were obtained at Svartberget (Rodhe, 1987). Precipitation $\delta^{18}O$ at Rickleå is from the GNIP-IAEA database, and compared to meteorological data at nearby stations (Alexandersson *et al.*, 1991). Dashed horizontal lines indicate mean annual average of $\delta^{18}O$ for lakewater and the weighted mean annual precipitation $\delta^{18}O$, and the solid horizontal line represents the weighted summer precipitation $\delta^{18}O$.

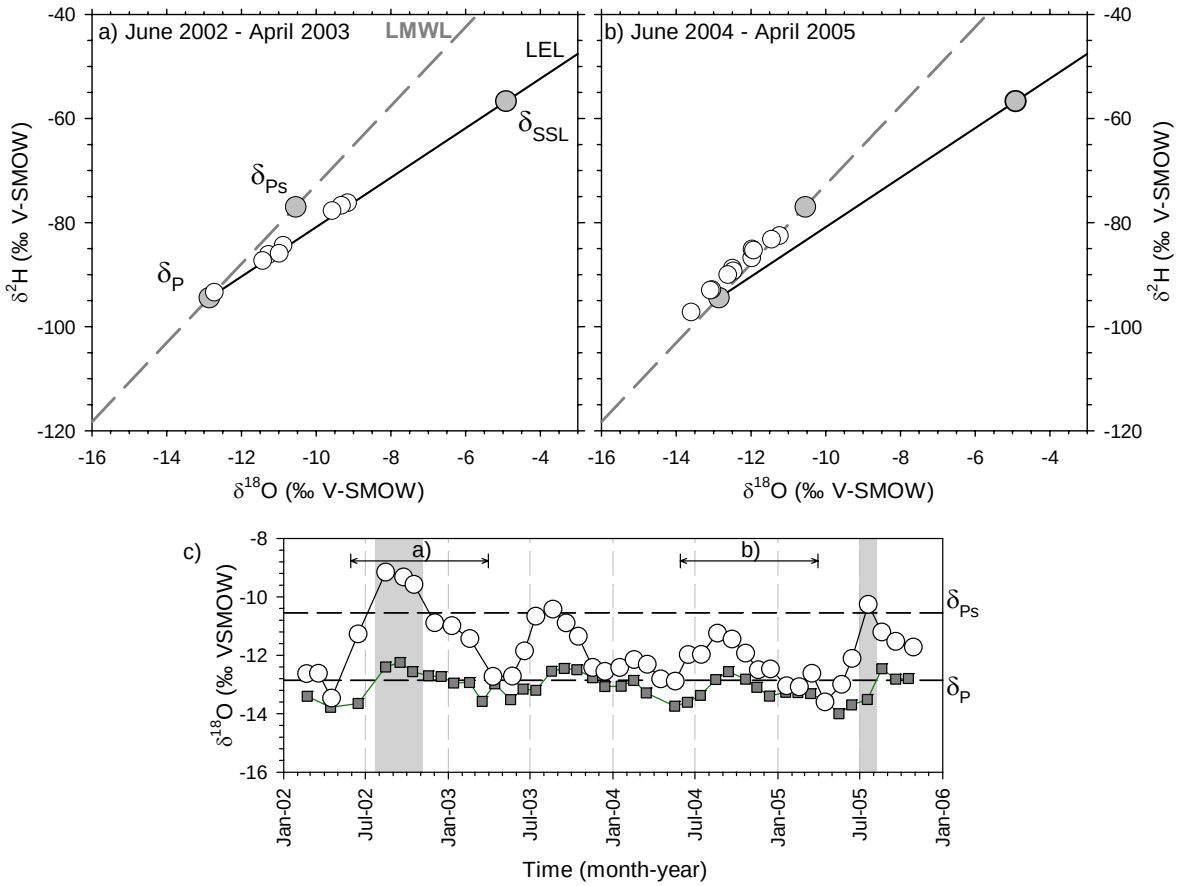

Figure 3-4. Evolution of the isotopic composition of water from Svartkälstjärn for similar time frames separated into different years showing a) minor evaporative enrichment along the LEL, and b) tightly constrained to the LMWL trend. Lake water samples are shown superimposed on the isotopic framework. c) Monthly average time-series for Svartkälstjärn (open circles) and Vindelälven (filled squares) $\delta^{18}O$ from February 2002 to October 2005. Grey shading highlights periods during which the isotopic evolution of lake water at Svartkälstjärn follows a trend along the LEL.

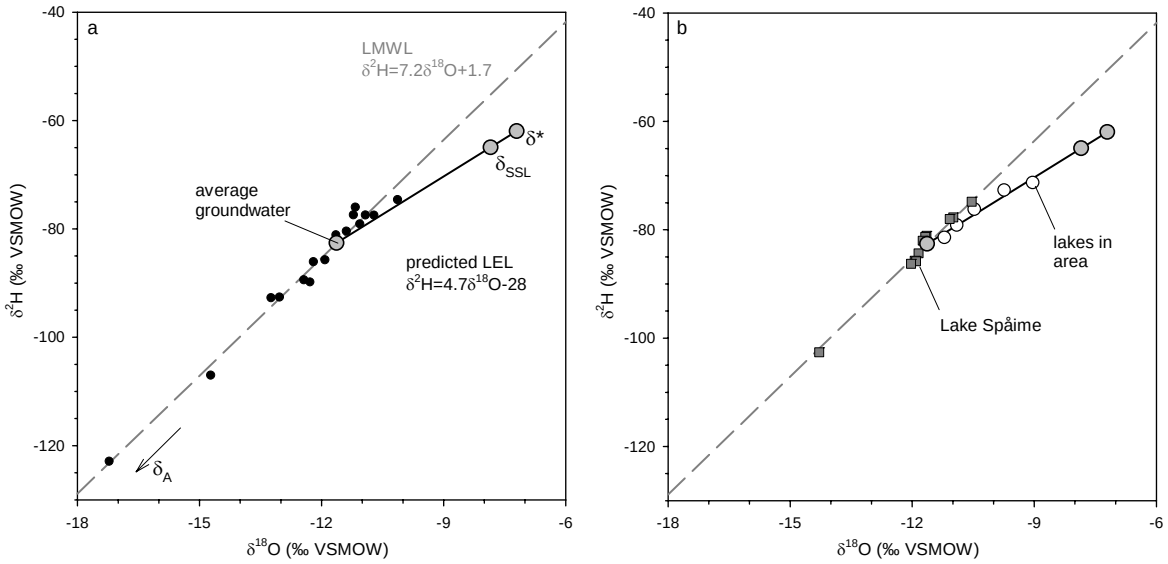

Figure 3-5. a) Calculated water isotopic framework for west-central Sweden. The isotopic compositions of input waters (groundwater, rain, snow, inlet streams, nearby rivers) are shown as black-filled circles, which plot along the LMWL ($\delta^2H=7.2\delta^{18}O+1.7$) in the Spåime region. The predicted LEL ($\delta^2H=4.7\delta^{18}O–28$) is based on the Craig and Gordon (1965) model that describes isotopic enrichment of an evaporating water body, and using atmospheric parameters (temperatures and relative humidity) and estimates of the isotopic compositions of average groundwater and inlet streams ($\delta^{18}O=–11.6‰$, $\delta^2H=–82.6‰$) and atmospheric moisture (δ_A; $\delta^{18}O=–22.1‰$, $\delta^2H=–160‰$), assuming equilibrium with the average isotopic composition of summer input waters. b) The isotopic composition of Lake Spåime water is shown superimposed on the isotopic framework. Isotopic data from local lakes that are undergoing evaporative enrichment plot along the predicted LEL.

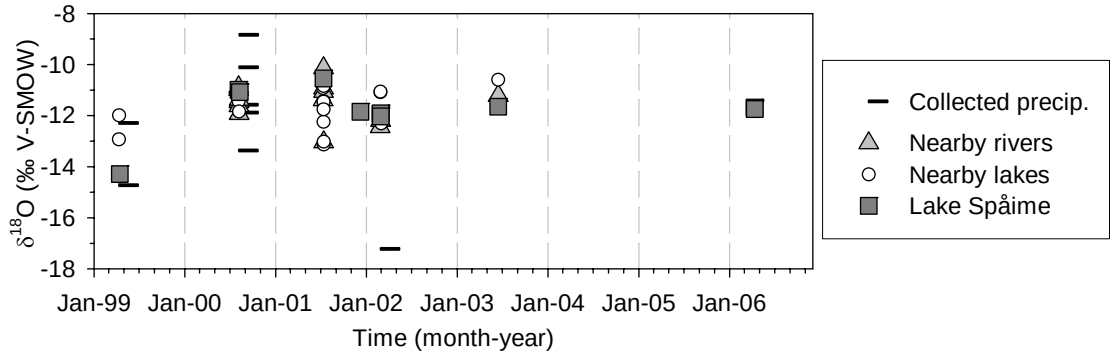

Figure 3-6. Sampling time-series of $\delta^{18}O$ for Lake Spåime in comparison with $\delta^{18}O$ of precipitation, river water, and non-evaporatively-enriched lakes.

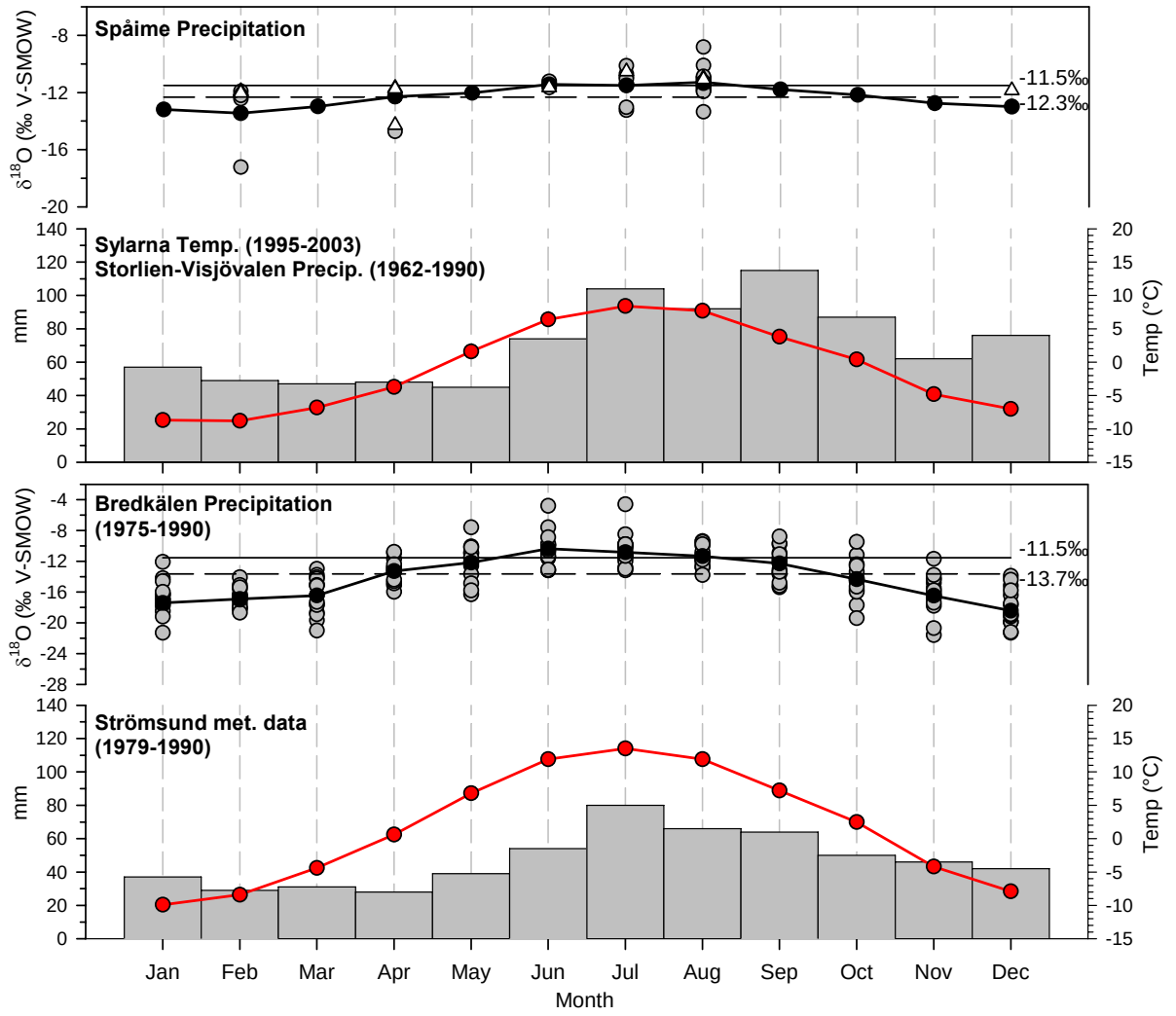

Figure 3-7. Monthly average of oxygen isotopic composition of waters (black-filled circles) and meteorological data from west-central Sweden. Measured water $\delta^{18}O$ from Lake Spåime are shown as open triangles. Measured precipitation and input water $\delta^{18}O$ data for the Lake Spåime region are presented as grey-filled circles, and monthly average precipitation $\delta^{18}O$ data are shown as black-filled circles, joined by solid line. Precipitation amount was recorded at Storlien-Visjövalen station (*c*. 642 m a.s.l.; Alexandersson *et al.*, 1991), *c.* 23 km from Spåime. Precipitation $\delta^{18}O$ data were obtained from Bredkälen (*c*. 400 m a.s.l.; IAEA/WMO GNIP database), located approximately 170 km northeast of Lake Spåime, and corresponding meteorological data from Strömsund (373 m a.s.l.; Alexandersson *et al.*, 1991). Dashed and solid horizontal lines indicate mean annual and summer average $\delta^{18}O$ for Spåime precipitation, and weighted annual and summer average $\delta^{18}O$ for Bredkälen precipitation, respectively. Note that precipitation $\delta^{18}O$ for Bredkälen and Spåime are shown at different permil scales.

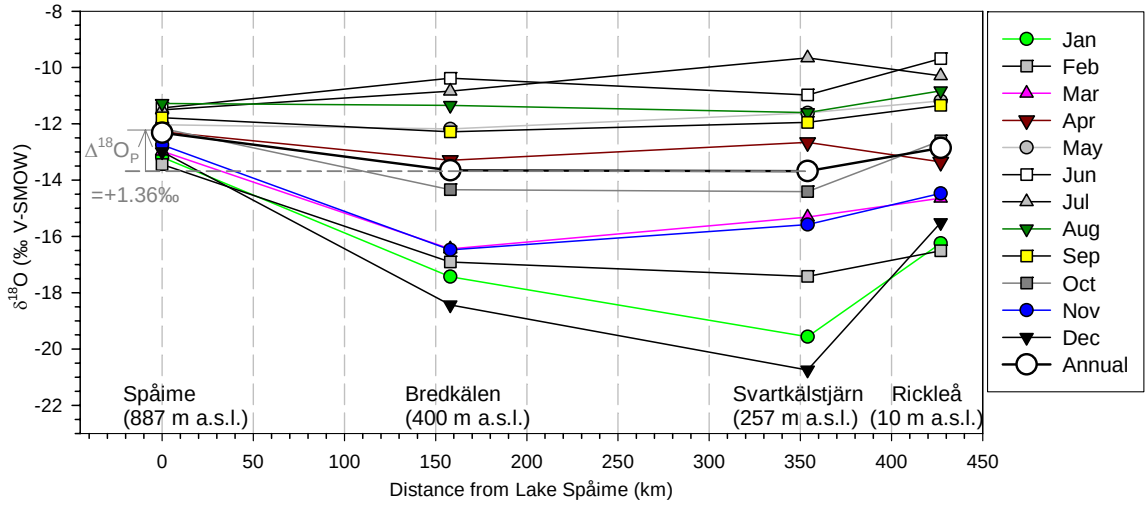

Figure 3-8. West-east transect of monthly and weighted mean annual precipitation $\delta^{18}O$ across central Sweden, with approximate distance relative to Lake Spåime. The difference in mean annual precipitation ($\Delta^{18}O_P$) between Spåime and Svartkälstjärn is +1.36‰.

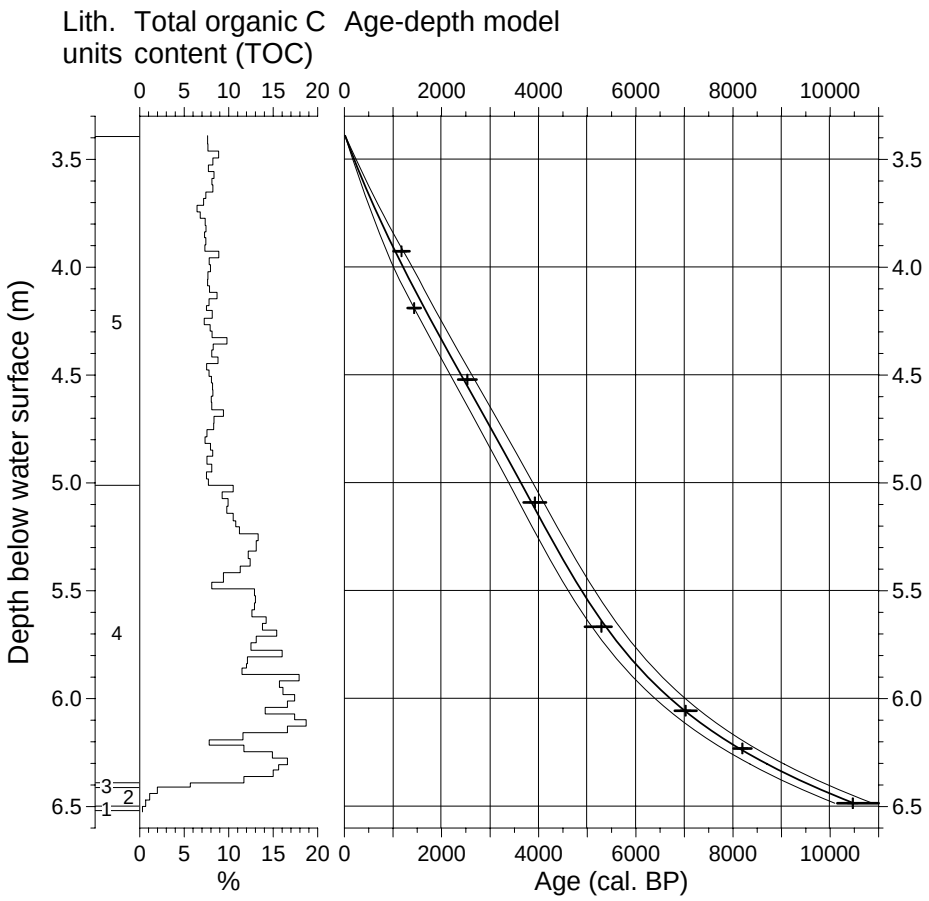

Figure 3-9. Age-depth model for Lake Spåime based on radiocarbon dates obtained on plant macrofossils (see Table 3-3). Lithostratigraphic units (see Table 3-2) and total organic carbon content (TOC) are plotted in the left-hand panel. Uncertainty envelopes represent two standard deviations from the age model curve.

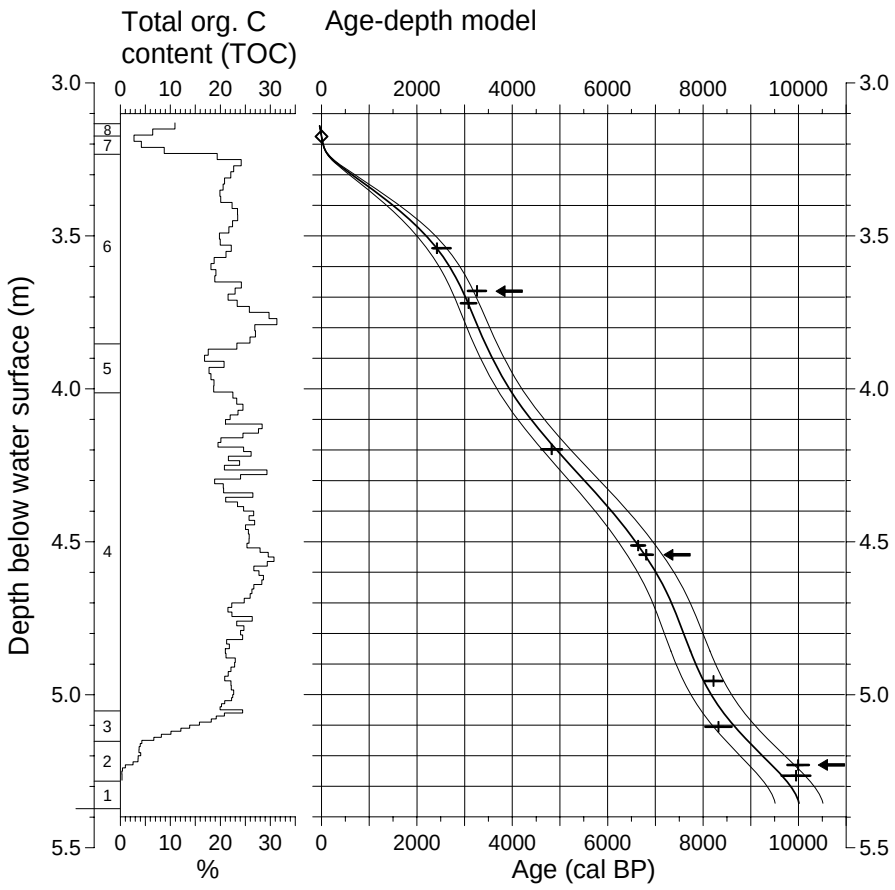

Figure 3-10. Age-depth model for Svartkälstjärn, based on radiocarbon dates obtained on plant macrofossils (see Table 3-3) and the first rise of ^{137}Cs in recent sediments (marked by open diamond at 3.175 m). Lithostratigraphic units (see Table 3-2) and total organic carbon content (TOC) are plotted in the left-hand panel. The arrows shown in the age model indicate three radiocarbon dates obtained on bulk organic matter that were excluded from the final chronology. Uncertainty envelopes represent two standard deviations from the age model curve.

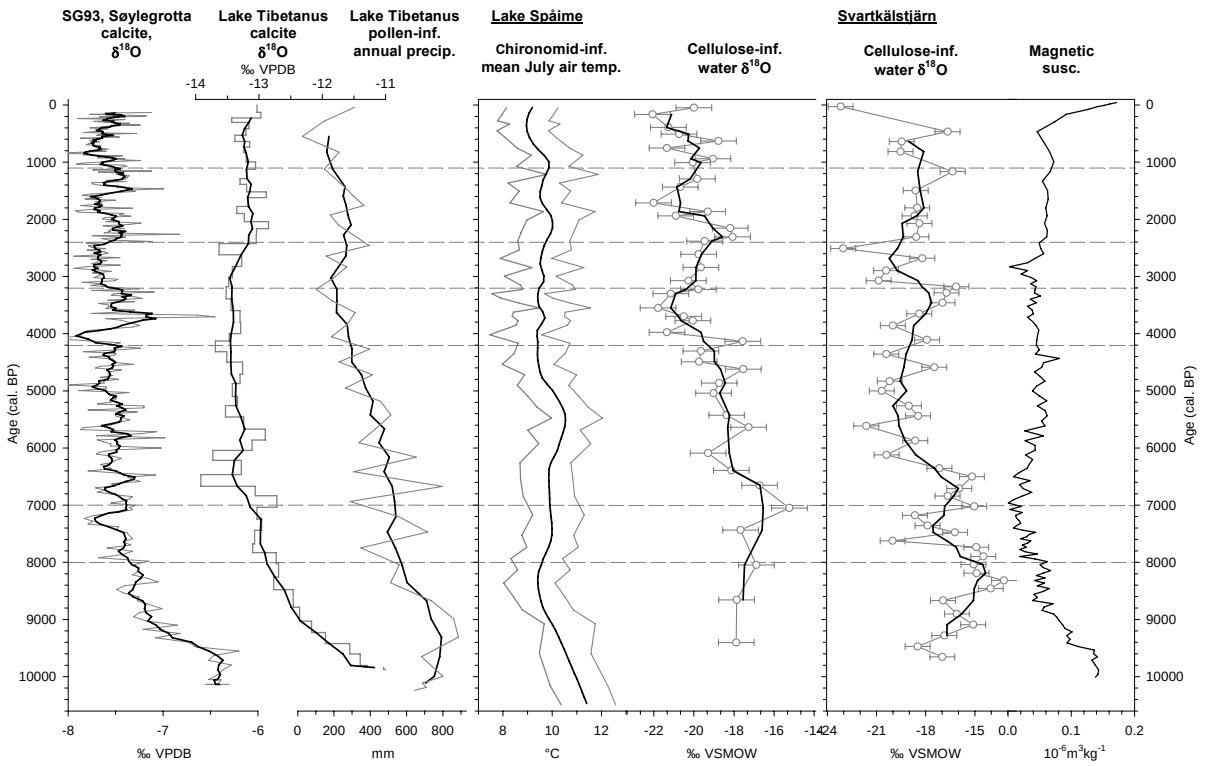

Figure 3-11. Profiles of cellulose-inferred water $\delta^{18}O$ from Lake Spåime and Svartkälstjärn. Black lines represent the 3-point and 5-point running averages for Lake Spåime $\delta^{18}O$ and Svartkälstjärn $\delta^{18}O$, respectively. Lake Spåime $\delta^{18}O$ record is compared with calcite $\delta^{18}O$ records of SG93 near Søylegrotta, Norway (Lauritzen and Lundberg, 1999) and Lake Tibetanus, northern Sweden (Hammarlund *et al.*, 2002), representing precipitation $\delta^{18}O$ variability in the Scandes Mountains. Also shown is the pollen reconstructed mean annual precipitation from Lake Tibetanus (Hammarlund *et al.*, 2002) and the chironomid-inferred mean July air temperature record from Lake Spåime, which is shown as a LOESS-smoothed curve (black line) with minimum and maximum temperature envelopes (grey line; Hammarlund *et al.*, 2004, Velle *et al.*, 2005). Magnetic susceptibility record for Svartkälstjärn is shown in the rightmost panel. Grey horizontal dashed lines highlight shifts in the Lake Spåime and Svartkälstjärn $\delta^{18}O$ profiles.

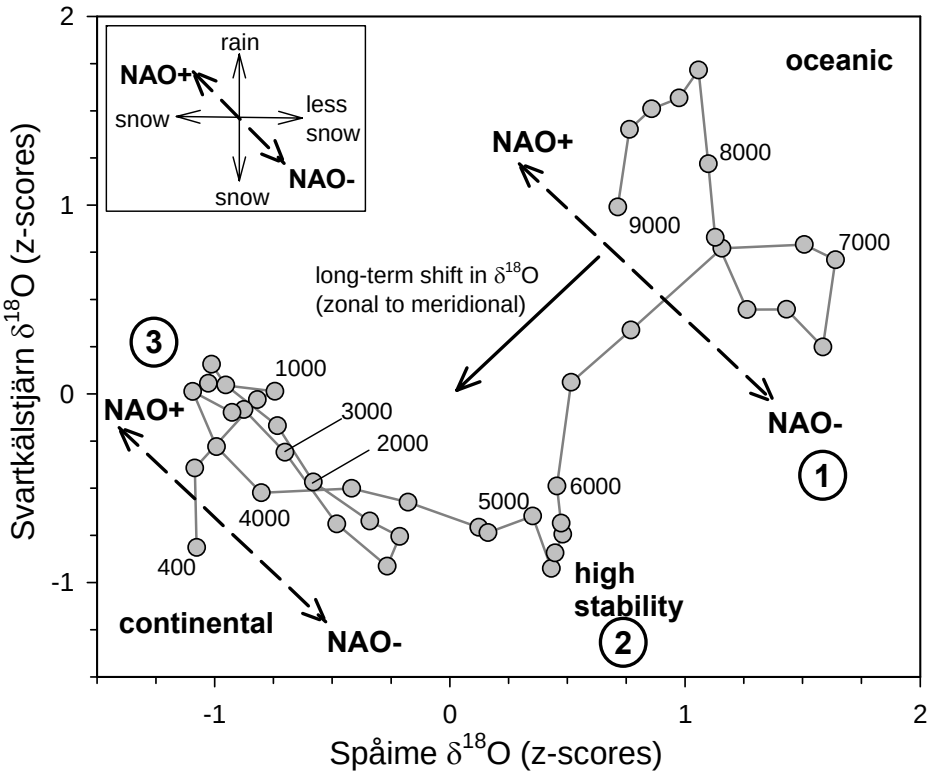

Figure 3-12. Cross-plot of Svartkälstjärn $\delta^{18}O$ versus Lake Spåime $\delta^{18}O$ variability during the Holocene (*c.* 400 and 9000 cal. BP) at 200-year intervals and dates are labeled every 1000 years. Cellulose-inferred lake water $\delta^{18}O$ data are expressed as 5-point running average z-scores, normalized to the Holocene average $\delta^{18}O$ of each lake (Svartkälstjärn $\delta^{18}O_{avg}$=–18.1‰, Spåime $\delta^{18}O_{avg}$=–19.0‰). The general trend towards lower $\delta^{18}O$ values at both lakes is believed to mark a shift in atmospheric circulation from high oceanicity during the early Holocene to increased continentality after *c.* 6000 cal. BP. Each distinct data cluster (1-3) shows an inverse trend reflecting different climate conditions concurring locally at each lake, as shown in the key in the upper left corner, with cluster 2 reflecting high stability and cluster 3 having the greatest variability. The centennial-to-millennial scale pattern at each cluster suggests a systematic mode of climate variability in the region, reflecting changes in the mean state of the NAO.

Chapter 4

Holocene Circulation-Dependent Shifts in the Precipitation $\delta^{18}O$-Temperature Relation in Sweden

4.1 Introduction

Oxygen isotopes in precipitation archives have commonly been used as a paleothermometer, assuming that modern oxygen-isotope-temperature relations as observed by Dansgaard (1964) also existed in the past (e.g., Lauritzen and Lundberg, 1999). This approach is based on the strong control that temperature has on the labeling of precipitation $\delta^{18}O$ at mid- to high latitudes through the process of Rayleigh distillation (Rozanski *et al.*, 1993). However, precipitation can also be influenced by non-temperature-dependent factors (e.g., changes in moisture source, rain-out history, air mass trajectories, and precipitation seasonality) that are related to air mass circulation (Edwards *et al.*, 1996; 2008; Jouzel *et al.*, 1998; Fricke and O'Neil, 1999). Variations in atmospheric circulation likely played a significant role in shifting precipitation $\delta^{18}O$, as portrayed by positive deviations from the modern $\delta^{18}O$-temperature relation during the early Holocene in central Canada (Edwards *et al.*, 1996) and northern Sweden (Hammarlund *et al.*, 2002). These effects were speculatively attributed to increased efficiency of moisture transport across mountain barriers caused by enhanced flow of westerlies, leading to reduced distillation of precipitation. The approach to the modern $\delta^{18}O$-temperature relation by *c.* 6000 cal. BP has been suggested to reflect a change from the dominance of westerlies to a more meridional flow pattern (Hammarlund *et al.*, 2002).

Changes in the $\delta^{18}O$-temperature relation have also been shown to shift over decadal time scales in response to changes in the intensity of atmospheric circulation, leading to variations in the amount of rain-out and distillation of Pacific air masses delivering moisture across the Cordillera into western Canada (Birks, 2003; Edwards *et al.*, 2008). During Medieval times, for example, pervasive westerly flow maintained deep precipitation and isotope shadows in the lee of the mountains and a precipitation isotope-temperature relation similar to the 20th century. In contrast, more meridional flow during the Little Ice Age led to reduced rain-out

and distillation, and a characteristic offset in the precipitation isotope-temperature relation (Edwards *et al.*, 2008).

In this chapter, oxygen isotope records at three different sites across Sweden, along a north-south transect (Figure 4-1), were combined with independent archives of temperature to reconstruct temporal $\delta^{18}O$-temperature relations. A record of $\delta^{18}O$ has been obtained from lake sediment cellulose at Arbovatten in southwest Sweden, which is situated in a region that is directly influenced by Atlantic air masses. The interpretation of the Arbovatten $\delta^{18}O$ record is constrained by modern isotope sampling of lake water during the period of 2004-2006 and a precipitation $\delta^{18}O$ dataset from Göteborg (1975-1989; IAEA/WMO-GNIP). Comparison between the Arbovatten cellulose $\delta^{18}O$ profile and the GRIP ice core $\delta^{18}O$ record from Greenland suggests that it is a good first-order proxy for temperature, but with systematic secondary signals related to shifts in atmospheric circulation. On the other hand, precipitation $\delta^{18}O$ records obtained at Lake Tibetanus, northern Sweden (Hammarlund *et al.*, 2002) and at Lake Spåime, central Sweden (Chapter 3), which are both located in the Scandes Mountains, seem to contain rather strong circulation-dependent signals. These shifts in the temporal $\delta^{18}O$-temperature relations can be probed to allow better characterization of atmospheric circulation change in Sweden during the Holocene.

The Arbovatten cellulose $\delta^{18}O$ record provides an additional opportunity to assess the paleohydrological changes that have taken place at Lake Igelsjön (Figure 4-1), where a carbonate $\delta^{18}O$ record has been presented previously by Hammarlund *et al.* (2003). Seppä *et al.* (2005) inferred moisture balance conditions at Lake Igelsjön by reconstructing precipitation $\delta^{18}O$ assuming a fixed $\delta^{18}O$-temperature relation using a pollen-inferred mean annual temperature record from Lake Flarken (Figure 4-1). Since relations between precipitation $\delta^{18}O$ and temperature is not constant over time, the separation of Lake Igelsjön carbonate $\delta^{18}O$ and Arbovatten cellulose $\delta^{18}O$ provides a better approximation of evaporative enrichment at Lake Igelsjön during the Holocene.

4.2 Site Description

Arbovatten (58º04'N, 12º04'E; 118 m a.s.l.) is located in the province of Bohuslän, 50 km north of Göteborg in southwest Sweden (Figure 4-1). The lake is situated in an area of Precambrian bedrock composed of granites, greywackes and mica gneiss, thinly covered with Quaternary clays and silt. Deglaciation took place in a shallow marine environment shortly before 14,000 cal. BP (Lundqvist and Wohlfarth, 2001), exposing numerous lake basins aligned to the bedrock topography followed by subsequent isolation from the sea due to glacio-isostatic rebound. Arbovatten is a small (0.02 km^2), humic throughflow lake that is 5.4 m deep at the south end and 3.0 m deep at the north end. The lake is fed by two relatively deep inlet streams, one of which is situated at the south end, as shown in Figure 4-1 inset. This wide inlet is flanked on the west side by a very steep slope reaching an elevation of *c.* 160 m a.s.l. The second, much smaller inlet (not visible in Figure 4-1 inset) enters Arbovatten from the southeast and drains from a very small headwater pond (*c.* 0.003 km^2), surrounded by marshes. Water flows through the lake system with an average residence time of 48 days based on water balance estimates and lake catchment characteristics (Table 4-1). The catchment consists of a dense mature forest containing mainly *Picea abies*, *Pinus sylvestris*, and *Betula pubescens*.

Arbovatten is one of the many lakes that are currently being limed to remediate acidification due to the effects of long-distance transport of acidifying air pollutants (Renberg and Hultberg, 1992). To raise pH levels in the lake, dumping of lime by aircraft was undertaken in 1987, 1989, 1991 and then yearly, with liming of the lake continuing to present (Environmental Protection Department, County Administrative Board of Västra Götaland, unpublished report). Lake Gårdsjön, located *c.* 2.8 km west of Arbovatten was the site of a covered catchment experiment to observe the reverse effects of acid deposition on chemistry and runoff in a forested catchment (Hultberg and Grennfelt, 1986; Molden *et al.*, 1995). As a comparison to the modern isotope hydrology at Arbovatten, water isotope samples have been collected at Gårdsjön. The lake has a surface area of *c.* 0.31 km^2, a maximum depth of 18.5 m and a mean depth of 4.9 m (Andersson and Olsson, 1985). The lake receives inflows from first-order headwater basins at the southeast end, as well as from a number of additional tributaries, and drains at the northwest end.

The climate in southwest Sweden is mainly oceanic. Arbovatten lies within the path of frequent cyclonic activity, with prevailing winds from the west and southwest. At Alvhem meteorological station (58º00'N, 12º08'E; 5 m a.s.l,), the mean annual air temperature is 6.5°C (January –2.6°C; July 15.8°C) and the annual precipitation is *c.* 804 mm, with *c.* 15% that falls as snow (1961-1990 climate normals; Alexandersson *et al.*, 1991). Average annual evaporation at Arbovatten is *c.* 480 mm (Bringfelt and Forsman, 1995). Small lakes are generally ice-covered from late December to late March.

The three lakes in this study form a north-south transect across Sweden (Figure 4-1). As noted above, the northernmost site, near Abisko, is Lake Tibetanus (68°20'N, 18º42'E; 560 m a.s.l.; Hammarlund *et al.*, 2002), and the other site is Lake Spåime (63°07'N, 12°19'E; 887 m a.s.l.; Chapter 3; Hammarlund *et al.*, 2004) in the west-central Scandes Mountains. Both of these lakes are small (*c.* 0.0046 and 0.03 km^2, respectively), shallow (3.9 and 3.5 m, respectively), open-drainage lakes with short residence times on the order of 12-25 days.

4.3 Methods

Overlapping sediment sequences were taken from the deepest, southeast part of Arbovatten in September 2004 using a 1-m Russian peat sampler. Surface sediment from Arbovatten (*c.* 23 cm) was extracted at the coring location using a gravity corer, and subsequently sectioned at 1-2 cm intervals in the field. Correlation of the core segments was conducted in the laboratory using a Bartington Instruments MS2E1 surface scanning sensor coupled to a Tamiscan-TS1 automatic logging conveyor. The 4.13 m-long sequence was divided into 110 sections that are 5 cm thick at the top (5.2-6.4 m), 4 cm at 6.4-7.8 m, and 3 cm thick at 7.8-9.3 m for higher resolution near the bottom of the core. An additional 0.42 m of sediment at the bottom of the core was not included in the analysis.

Water samples were collected from Arbovatten in September 2002 and on a monthly basis during the period of September 2004 to October 2006, totaling 33 lake and 3 inflow samples. In addition one lake sample near the outlet and two inflow samples were also obtained from Lake Gårdsjön. The oxygen and hydrogen isotope compositions of water samples were determined at the University of Copenhagen and the University of Waterloo. All stable isotope results are expressed as δ-values, representing deviations in per mil (‰) from the

VSMOW (Vienna Standard Mean Ocean Water) standard such that $\delta_{sample}=1000[(R_{sample}/R_{VSMOW}) -1]$, where R is the $^{18}O/^{16}O$ or $^{2}H/^{1}H$ ratio in sample and standard. $\delta^{18}O$ and $\delta^{2}H$ are normalized to values for SLAP of –55.5‰ and –428‰, respectively (see Coplen, 1996). Analytical uncertainties are ±0.2‰ for $\delta^{18}O$ and ±2‰ for $\delta^{2}H$.

Lake sediment cellulose was prepared for oxygen isotope analysis following the techniques described in detail by Wolfe *et al.* (2001a, 2007). After acid-washing to eliminate carbonates and dry-sieving, the fine-grained fraction (<500 μm) was processed through additional steps to remove non-cellulose components and minerogenic matter. These include solvent extraction, bleaching, alkaline hydrolysis, oxyhydroxide leaching, and sodium polytungstate density separation. Cellulose $\delta^{18}O$ was determined by high-temperature pyrolysis using an on-line continuous-flow isotope-ratio mass spectrometer at the University of Waterloo Environmental Isotope Laboratory. A total of 109 out of 110 cellulose samples from Arbovatten were analyzed, 108 of which were duplicated. The uncertainty (one standard deviation) based on estimates from the repeated measurements conducted on the same cellulose samples resulted in an average of ±0.3‰.

4.4 Results and Interpretations

4.4.1 Modern isotope hydrology

In Figure 4-2a, the distribution of oxygen and hydrogen isotopes in water plots along two trajectories that define the Local Meteoric Water Line (LMWL) and the Local Evaporation Line (LEL), which forms the isotopic framework for the Arbovatten region. The LMWL is based on the regression through monthly average precipitation data collected from Göteborg (15 m a.s.l.; Figure 4-1) during the period of 1976-1989 (IAEA/WHO GNIP data). Accordingly, the amount-weighted mean annual precipitation (δ_P; $\delta^{18}O$=–8.5‰, $\delta^{2}H$=–63‰), rain (δ_{Ps}; $\delta^{18}O$=–7.2‰, $\delta^{2}H$=–53‰) and snow (δ_{snow}; $\delta^{18}O$=–10.6‰; $\delta^{2}H$=–80‰) plot on the LMWL. The predicted Local Evaporation Line (LEL) is based on the Craig and Gordon (1965) model describing isotopic enrichment of an evaporating water body. As described by Gibson *et al.* (2008), the slope of the predicted LEL in decimal notation is defined as:

$$S_{LEL} = \frac{\left[\dfrac{h(\delta_A - \delta_P) + (1+\delta_P)(\varepsilon_K + \varepsilon^*/\alpha^*)}{h - \varepsilon_K - \varepsilon^*/\alpha^*}\right]_2}{\left[\dfrac{h(\delta_A - \delta_P) + (1+\delta_P)(\varepsilon_K + \varepsilon^*/\alpha^*)}{h - \varepsilon_K - \varepsilon^*/\alpha^*}\right]_{18}}$$

where ε^* and ε_K are the equilibrium and kinetic separations, respectively, α^* is the liquid-vapour equilibrium fractionation factor, in which $\alpha^* > 1$, and the subscripts refer to deuterium and oxygen-18. The ε^* term is defined as $\alpha^*–1$ (in decimal notation) and α^* is dependent on temperature (Horita and Wesolowski, 1994) and the ε_K term is dependent on relative humidity (h) normalized to the water surface temperature, expressed as ε_K (^{18}O) = 14.2(1–h) and ε_K (^{2}H) = 12.5(1–h) (Gonfiantini, 1986). The determination of the LEL slope uses estimates of δ_P, the isotopic composition of evaporation-flux-weighted atmospheric moisture (δ_A; $\delta^{18}O$=–17.0‰, $\delta^{2}H$=–124‰), assuming isotopic equilibrium with δ_{Ps}, and climatic data using June-September average temperature (14.2°C; Alvhem 1961-1990; Alexandersson *et al.*, 1991) and relative humidity (84%). The calculated limiting isotopic composition of a desiccating lake (δ^*; $\delta^{18}O$=–2.3‰, $\delta^{2}H$=–29‰) and the isotopic composition of a hydrological and isotopic steady-state terminal lake (δ_{SSL}; $\delta^{18}O$=–3.3‰, d1H=–34‰), which are both dependent on δ_A and atmospheric parameters, are shown on the LEL (Figure 4-2a). As expected, the isotopic composition of Gårdsjön lake water ($\delta^{18}O$=–6.0‰, $\delta^{2}H$=–48‰) plots along the predicted LEL in the isotopic framework. Likewise, the inflow tributaries that recharge Lake Gårdsjön plot close to δ_P.

Superimposed on the isotopic framework is the isotopic composition of Arbovatten lake water collected during September 2002 and September 2004-October 2006 (Figure 4-2b). The lake water isotopic distribution conforms closely to the LMWL, with an average lake water isotopic composition ($\delta^{18}O$=–8.0‰, $\delta^{2}H$=–55‰) that is similar to δ_P. In Figure 4-3, the monthly averages of lake water $\delta^{18}O$ fluctuate seasonally having a magnitude of 2.4‰, somewhat less than the seasonal amplitude of 3.4‰ for average composite monthly precipitation $\delta^{18}O$ at Göteborg. The damped seasonal variability in lake water isotopic composition and the lack of evaporative enrichment suggest that cellulose formed in

association with Arbovatten lake water is likely to be a good recorder of mean annual precipitation $\delta^{18}O$.

However, there are some samples of Arbovatten lake water that plot along the LEL and reach an isotopic composition equivalent to the Gårdsjön lake water isotopic data (Figure 4-2b). The evaporative enrichment observed in these samples may reflect lake water stratification during the summer and are not believed to be representative of well-mixed waters. For instance, there is a consistent offset between the surface lake water isotopic composition and that of the bottom lake waters during both periods of measurements in Sept. 2002 (Figure 4-4a) and in Sept. 2004 (Figure 4-4b). Furthermore, the lake water isotope data also demonstrate spatial variability, with samples measured near the outlet more isotopically enriched than samples measured at the coring site. Isotopic data plotting along the LEL may reflect sampling of evaporatively enriched epilimnetic waters. The time-series of Arbovatten lake water $\delta^{18}O$ in Figure 4-4c exhibits two positive $\delta^{18}O$ spikes at July 2005 and August 2006 that appear to be beyond the normal variation of the lake water isotopic composition, which is generally between values of δ_P and δ_{Ps}.

Figure 4-5a shows a linear regression through average yearly precipitation $\delta^{18}O$ and average yearly air temperature from eight IAEA/WMO GNIP stations across Sweden during periods having both $\delta^{18}O$ and temperature data, mainly between 1981 and 1988 (Calles and Westman, 1989). The resulting spatial relation is $\delta^{18}O=0.70MAT-14.8$ for Sweden and the slope agrees comparably well with the relation determined by Dansgaard (1964) for coastal stations in the North Atlantic, defined as $\delta^{18}O = 0.69MAT - 13.6$. In addition, Burgman *et al.* (1987) obtained a similar relation and slope ($\delta^{18}O = 0.64MAT - 14.3$) for seventeen precipitation stations in Sweden during the period 1978-1985, determined using the mean temperature weighted with respect to the amount of precipitation. For European stations (south of Sweden) the slope decreases slightly to 0.59 ‰/K, reflecting latitudinal gradients in the long-term precipitation $\delta^{18}O$ and air temperature (Rozanski *et al.*, 1992). These observations suggest that the average $\delta^{18}O$-temperature slope is consistently close to 0.69 ‰/K (Dansgaard, 1964) over time, and thus, it is suitable to assume a constant 0.69 ‰/K for interpreting the paleorecord.

In comparison, the distribution of the amount-weighted mean annual precipitation $\delta^{18}O$ and mean annual air temperature data for selected stations across Sweden are shown superimposed on the $\delta^{18}O$-temperature relations for Sweden and the North Atlantic (Figure 4-5b). Included in Figure 4-5b is the long-term average precipitation $\delta^{18}O$ and mean annual air temperature data at Lake Tibetanus (1975-1990; Hammarlund *et al.*, 2002), Lake Spåime (this study; Chapter 3), Arbovatten, and Lake Igelsjön (Hammarlund *et al.*, 2003). Interestingly, the sites (i.e., Tibetanus, Abisko, Spåime, Forshult, Arbovatten, Göteborg) that plot closer to the relation defined by Dansgaard (1964) are situated on the western side of Sweden, near the Atlantic Ocean (Figure 4-1). In contrast, the sites (i.e., Naimakka, Bredkälen, Svartberget, Rickleå, Hedesunda, Igelsjön, Arup) plotting closer to the Sweden $\delta^{18}O$-temperature relation (Figure 4-5b) are situated more inland (Figure 4-1).

The distribution of station points, illustrated in Figure 4-5b, reflects differing degrees of continentality. Changes in precipitation $\delta^{18}O$ can be simulated assuming a simple Rayleigh distillation process (Gat, 1996), described in decimal notation as:

$$\frac{R_{P_f}}{R_{P_0}} = f^{(\alpha-1)}$$

where R is the $^{18}O/^{16}O$ ratio in the initial precipitation (P_0) and subsequent (P_f) rain-out of precipitation after a fraction of moisture (f) is removed from an air mass during condensation, and α is the liquid-vapour equilibrium isotopic fractionation factor. Assuming that the initial precipitation $\delta^{18}O$ has an isotopic composition of about –3‰ (Gat, 1996) formed from a vapour originating from the Atlantic Ocean, the fraction of moisture remaining at Göteborg having a mean annual precipitation $\delta^{18}O$ of –8.5‰, is approximately 0.60. At a temperature of 7.4°C, Göteborg precipitation $\delta^{18}O$ lies on the modern Dansgaard (1964) $\delta^{18}O$-temperature relation. In Figure 4-6, at this given temperature, an increase in the moisture transport efficiency by Δf of +5% or +10% results in a positive offset of +0.9‰ or +1.7‰ relative to the modern Dansgaard (1964) $\delta^{18}O$-temperature relation. In contrast, at the same temperature, an increase in the precipitation distillation by Δf of –5% or –10% results in a negative offset of –0.9‰ or –2.0‰ from the modern Dansgaard (1964) $\delta^{18}O$-

temperature relation. Thus, the –1.2‰ difference between the Dansgaard (1964) and Sweden $\delta^{18}O$-temperature relations likely reflects an additional rain-out amount of 6% (f ~ 0.54).

4.4.2 Sediment description and chronology

The sediment sequence at Arbovatten was divided into 6 lithostratigraphic units (Table 4-2). The bottom 0.17 m (unit 1) is composed of grey silty clay and was not analyzed. Unit 2 (0.33 m) contains greyish brown, silty fine-detritus gyttja and increasing organic carbon content (TOC; Figure 4-8), followed by a gradual change to brown laminated gyttja (0.63 m; unit 3) with moderately stable TOC content. Unit 4 (0.06 m) begins sharply as a sequence of greyish brown, silty gyttja and low TOC content, similar to unit 2. Unit 5 (1.91 m) is a prominent dark brown gyttja having elevated TOC content, followed by unit 6 (0.95 m) of brown gyttja with lower TOC content. Unit 7 (0.22 m) consists of brown silty gyttja with a continuing decrease in TOC content, followed by a sharp change to greyish brown to brownish grey laminated gyttja with beige layers (0.03 m; unit 8). The laminations in the upper 0.03 m appear to correspond to yearly liming events beginning in AD 1987, 1989, and 1991-2004.

The chronology for Arbovatten sediments is based on combining AMS radiocarbon dates from the Russian core and measurements of ^{210}Pb, ^{214}Bi and ^{137}Cs isotopes by gamma spectrometry from the gravity core. A total of 29 dates were obtained from CRS (constant rate of supply; Oldfield and Appleby, 1984) model of ^{210}Pb activity. In Figure 4-7, the total ^{210}Pb activity declines exponentially with depth beginning at 5.263 m and reaching supported ^{210}Pb levels (0.02 Bq/g) by *c.* 5.40 m below water depth. From 5.263 m to the surface, the concentration of ^{210}Pb drops considerably and is highly variable. This decline in ^{210}Pb is accompanied by high, but variable ^{137}Cs activity and minimal ^{214}Bi values, and corresponds to the start of liming in AD 1987 (5.258 m). The introduction of lime, possibly older material, likely originates from a quarry far from the lake catchment, and hence explains the low and variable activity levels above 5.263 m. For the chronology of the upper sequence, liming events were identified and counted by observing beige layers in the sediment, with the top layer corresponding to AD 2004 and a total of 16 layers by AD 1987 (Figure 4-7). The ^{137}Cs data provide a validation test for the combined CRS model and liming events. The

peak in ^{137}Cs activity, occurring at 5.263 m, corresponds to AD 1986 date of the Chernobyl-fallout (Figure 4-7).

Eight calibrated AMS radiocarbon dates were obtained on terrestrial macroscopic plant remains in Arbovatten long core sediments (Table 4-3). The most recent date is anomalously young, possibly due to the incorporation of more recent terrestrial material (one leaf of *Myrica gale*) into the sediment and was, therefore, not included in the final chronology. The final age-model was derived by combining the radiocarbon dates with the CRS ^{210}Pb model dates and liming events from the gravity core. A polynomial curve was fitted through the data providing the final age-model for Arbovatten sediments (Figure 4-8). The resulting lowermost age for the onset of gyttja sedimentation is estimated at *c.* 10,500 cal. BP (bottom of unit 2), which is substantially later than the timing of deglaciation in the area (Lundqvist and Wohlfarth, 2001). This discrepancy is explained by the location of the lake below the marine limit (c. 130 m a.s.l.; Svedhage, 1985; Lundqvist and Wohlfarth, 2001), which led to deposition of marine clays before the isolation of the lake in response to glacio-isostatic rebound. In addition, the onset of gyttja sedimentation at c. 10,500 cal. BP may have been further delayed by redeposition of detrital material from initially unstable catchment soils. The apparent sediment accumulation rate at Arbovatten decreased from *c.* 0.85 mm/year at the bottom of unit 2 to *c.* 0.27 mm/year at *c.* 7.51 m in unit 5. The rest of unit 5 (*c.* 7.51-6.42 m) is characterized by low and relatively constant accumulation rates at around 0.22-0.27 mm/year. A considerable increase from 0.27 to 0.90 mm/year occurs in unit 6, followed by values exceeding 1.90 mm/year above *c.* 5.38 m.

4.4.3 Arbovatten oxygen-isotope record

The δ^{18}O record for Arbovatten was reconstructed from cellulose δ^{18}O values using a cellulose-water isotopic fractionation factor of 1.028 (Edwards and McAndrews, 1989; Wolfe *et al.*, 2001a, 2007). The cellulose-inferred water δ^{18}O values rise from a low value of –21.3‰ at the start of the record (*c.* 10,500 cal. BP) to –11.2‰ by *c.* 9600 cal. BP (Figure 4-9). Between *c.* 9600 and 9000 cal. BP, δ^{18}O declines to –13.8‰ and then values increase to –10.1‰ by *c.* 8500 cal. BP. At *c.* 8500-8200 cal. BP, δ^{18}O decreases to a value of –12.3‰, followed by a rise to –10.3‰ by *c.* 8000 cal. BP. From *c.* 8000 to 5500 cal. BP, δ^{18}O

narrowly fluctuates with values in the range of –11.2 to –9.9‰. At *c.* 5500-1800 cal. BP, fluctuations in $\delta^{18}O$ shift slightly more positive to values in the range of –10.8 to –9.4‰. During the period of *c.* 1800-200 cal. BP, $\delta^{18}O$ decreases slightly to a minimum of –12.0‰, followed by a pronounced decline to –14.7‰ at the top of the core.

The low $\delta^{18}O$ values at *c.* 10,500-10,200, 9200-9100 and after 200 cal. BP may have been subjected to minerogenic contaminants, and thus, are not considered further in the discussion (Figure 4-9). For instance, these intervals correspond to significant changes in carbon and nitrogen data from the same core, with low TOC, low TN, high C/N ratios and high magnetic susceptibility (see Chapter 5). For instance, the anomalously low $\delta^{18}O$ values after 200 cal. BP are likely attributable to the introduction of lime. Except for the above-mentioned intervals, lake sediments from Arbovatten are aquatic in origin based on two lines of evidence. First, there is a remarkable correspondence with the GRIP $\delta^{18}O$ ice core (as described in the following section). Second, consistently low magnetic susceptibility values suggests limited catchment disturbance, thus making it unlikely that Arbovatten $\delta^{18}O$ reflects a terrestrial origin (Chapter 5).

4.5 Discussion

4.5.1 Comparison with other proxy records

The small magnitude of variation in the cellulose-inferred water $\delta^{18}O$ profile from Arbovatten is likely reflecting hydrological stability and long-term variability in precipitation $\delta^{18}O$ in southern Sweden (Figure 4-9). The general pattern of variation observed in Arbovatten $\delta^{18}O$ matches remarkably well with the GRIP $\delta^{18}O$ ice core record from Greenland (Dansgaard *et al.*, 1993). Interestingly, low Arbovatten $\delta^{18}O$ values between *c.* 9600 and 8500 cal. BP corresponds with low values in a speleothem $\delta^{18}O$ record in southwestern Ireland (McDermott *et al.*, 2001) and low lake carbonate $\delta^{18}O$ values at Ammersee, Germany (von Grafenstein *et al.*, 1999). This interval also coincides with an episode of increased ice-rafting in the North Atlantic at 9400 cal. BP (Bond *et al.*, 1997). Cooler conditions are suggested to have occurred in Europe while Greenland was relatively warm, based on a negative difference between $\delta^{18}O$ of the Ammersee carbonate and the

GRIP ice core record (von Grafenstein *et al.*, 1999). This climate asymmetry between Europe and Greenland may also explain some of the minor differences in the patterns of variability observed in Arbovatten and GRIP $\delta^{18}O$ records. In addition, the low $\delta^{18}O$ values *c.* 9600-8500 cal. BP appear to correspond with anomalously high GISP2 potassium ion concentrations due to enhanced atmospheric loading of terrestrial dust over Greenland, possibly related to a stronger Siberian High in winter and spring (O'Brien *et al.*, 1995; Mayewski *et al.*, 1997; Meeker and Mayewski, 2002). These observations suggest that the low Arbovatten $\delta^{18}O$ values may reflect changes in atmospheric circulation, perhaps accompanied by ocean surface cooling.

In Figure 4-9, the cellulose-inferred water $\delta^{18}O$ record at Arbovatten and the GRIP $\delta^{18}O$ ice core record are compared with other records from southern Sweden, including a carbonate $\delta^{18}O$ record from Lake Igelsjön (Figure 4-1; Hammarlund *et al.*, 2003) and pollen-inferred mean annual temperatures from Lake Flarken (Figure 4-1; Seppä *et al.*, 2005). The most striking agreement between low Arbovatten $\delta^{18}O$ values and all four records shown in Figure 4-9 occurs at *c.* 8300-8000 cal. BP, which may correspond to the "8.2 kyr cold event" (Alley *et al.*, 1997). This is an episode of cold sea surface temperatures in the North Atlantic that may be associated with the final drainage of glacial Lake Agassiz, resulting in a weakening of the North Atlantic thermohaline circulation and a reduction of heat transport from lower latitudes (Barber *et al.*, 1999; Fisher *et al.*, 2002). The decrease in Arbovatten $\delta^{18}O$ by about 1.1‰ may be translated to a cooling of *c.* 2 K (assuming a modern spatial $\delta^{18}O$-temperature slope of 0.69 ‰/K), which is slightly more than the pollen-inferred cooling of about 1.5 K at Lake Flarken (Seppä *et al.*, 2005).

From *c.* 8000 to 2500 cal. BP, the magnitude of variation in Arbovatten $\delta^{18}O$ values amounts to *c.* 0.5-1.0‰, similar to the GRIP $\delta^{18}O$ record (Figure 4-9). After *c.* 2500 cal. BP, $\delta^{18}O$ values in the Arbovatten record show a gradual decline to *c.* 200 cal. BP by about 2.0‰. The GRIP ice $\delta^{18}O$ record also shows a similar decline of about 0.5‰ over the same period. Overall, Arbovatten shows a slightly wider range in $\delta^{18}O$ variability than the GRIP ice $\delta^{18}O$ record. Although very subtle, a slight positive shift in cellulose $\delta^{18}O$ between *c.* 5500 and 3600 cal. BP corresponds with elevated pollen-inferred temperatures. After 2500 cal. BP, the

general decrease in cellulose $\delta^{18}O$ by 2‰ corresponds to a cooling trend of *c.* 3 K (again, using the modern $\delta^{18}O$-temperature relation), which is slightly more than the cooling trend of 1.7 K observed in the Lake Flarken pollen-inferred temperature record.

4.5.2 Lake Igelsjön evaporative enrichment

The Lake Igelsjön carbonate $\delta^{18}O$ record shown in Figure 4-9 is believed to mainly reflect changes in the hydrological balance of the lake (Hammarlund *et al.*, 2003). Assuming the Arbovatten $\delta^{18}O$ profile is a record of changing precipitation $\delta^{18}O$ in the region, the separation between Lake Igelsjön carbonate $\delta^{18}O$ and Arbovatten cellulose $\delta^{18}O$ should reflect changes in lake water balance during the Holocene. First, the equilibrium fractionation effects on the carbonate $\delta^{18}O$ have been accounted for by applying –0.25 ‰/K related to changes in lake water temperature as inferred from Lake Flarken pollen reconstruction of mean annual temperature (Seppä *et al.*, 2005). The long-term changes in annual temperature and summer lake-water temperature are assumed to be approximately the same due to the small volume of the lake (Seppä *et al.*, 2005). Second, the inferred Lake Igelsjön water $\delta^{18}O$ was anchored to the VSMOW scale by relating the observed modern *Chara* $\delta^{18}O$ values (–9‰ VPDB) to corresponding measured $\delta^{18}O$ lake water (–9‰ VSMOW; Seppä *et al.*, 2005). Both the carbonate $\delta^{18}O$ and the inferred lake water $\delta^{18}O$ for Lake Igelsjön are shown together in Figure 4-9. The difference between inferred lake water $\delta^{18}O$ in Igelsjön and Arbovatten is considered to be a first-order approximation of changes in the evaporation enrichment of Lake Igelsjön. The interval *c.* 10,500-10,300, 9200-8900 and after 200 cal. BP is excluded from the Igelsjön-Arbovatten $\delta^{18}O$ separation due to uncertainties in the cellulose $\delta^{18}O$ values (Figure 4-9). Aside from the gaps in the Igelsjön-Arbovatten $\delta^{18}O$ separation, this reconstruction of evaporative enrichment should be superior to that of Seppä *et al.* (2005), since it is not constrained by the use of a fixed $\delta^{18}O$-temperature relation. In their analysis, they qualitatively compared Lake Igelsjön $\delta^{18}O$ with an inferred precipitation $\delta^{18}O$ based on the Flarken pollen-inferred temperature record and a fixed $\delta^{18}O$-temperature relation of $\delta^{18}O = 0.59MAT - 14.2$ (as reported for recent decades by Rozanski *et al.*, 1992). The separation between Lake Igelsjön lake water $\delta^{18}O$ and inferred $\delta^{18}O_P$ suggested by Seppä *et al.* (2005) is shown in Figure 4-9 in comparison to the Igelsjön-

Arbovatten $\delta^{18}O$ separation. As a result, the former underestimates the amount of evaporative enrichment before *c.* 4300 cal. BP, whereas the results of both somewhat overlap after *c.* 4300 cal. BP. This observation supports the notion that precipitation $\delta^{18}O$ has varied independently of the change in temperature during the early to mid-Holocene.

In Figure 4-9, the results of the Igelsjön-Arbovatten $\delta^{18}O$ separation reflect changes in evaporative enrichment during the Holocene. The trend from high $\delta^{18}O$ separation at 10,200 cal. BP to low values by 9600 cal. BP, indicating a shift from dry to moist conditions. This corresponds well to increasing lake levels, as inferred from sedimentology and fossil pollen analysis from kettle lakes at *c.* 10,500-8000 cal. BP at Bysjön, which is 300 km south (Digerfeldt, 1988), and at 10,300-9100 cal. BP at Ljustjärnen, which is 150 km north of Igelsjön (Almquist-Jacobson, 1995). A shift to slightly drier conditions, as indicated by a small increase in the Igelsjön-Arbovatten $\delta^{18}O$ separation, occurs during *c.* 9500-8300 cal. BP, followed by a return to moist conditions at *c.* 8300-8000 cal. BP. Although the dating control precludes more detailed analysis, the onset of the 8.2 kyr cold event does seem to exist as reduced Igelsjön-Arbovatten $\delta^{18}O$ separation, consistent with an increase in effective moisture and much cooler summer temperatures (Seppä *et al.*, 2005; Hammarlund *et al.*, 2005). Nesje *et al.* (2001) noted that glacier expansion during this interval was likely driven by lower summer temperatures (i.e., reduced ablation rates), which had compensated for the negative effects of decreased winter precipitation.

From *c.* 8000 to 4300 cal. BP, the Igelsjön-Arbovatten $\delta^{18}O$ separation increases to reflect persistently higher apparent evaporative enrichment, which is consistent with previous interpretations of drier conditions (Digerfeldt, 1988, 1997; Hammarlund *et al.*, 2003; Seppä *et al.*, 2005), and stable hydrology at Lake Igelsjön (Figure 4-9). For instance, lake levels were generally lower between *c.* 8000 and 4000 cal. BP at Bysjön (Digerfeldt, 1988) and between *c.* 9100 and 4500 cal. BP at Ljustjärnen (Almquist-Jacobson, 1995). This period also coincides with the major retreat of maritime glaciers in western Norway in response to higher summer temperatures (Dahl and Nesje, 1996; Nesje *et al.*, 2001). As suggested by elevated values in the pollen-inferred mean annual temperature record at Lake Flarken, warm

summers during *c.* 8000-4300 cal. BP likely enhanced evaporative enrichment of the surface waters in Lake Igelsjön (Hammarlund *et al.*, 2003).

After *c.* 4300 cal. BP to the present, there is an increase in effective humidity as reflected by a shift to lower apparent evaporative enrichment, but also an increase in the magnitude of fluctuations, suggesting increased hydrological variability. In comparison, lake levels at Bysjön (Digerfeldt, 1988) and Ljustjärnen (Almquist-Jacobson, 1995) also support moister conditions during the late Holocene. However, a short period of lower lake levels during *c.* 2000-1500 cal. BP at both Bysjön (Digerfeldt, 1988) and Ljustjärnen (Almquist-Jacobson, 1995) does not appear as an increase in the evaporative enrichment at Lake Igelsjön. This interval may be interpreted as an increase in human activity and soil erosion, rather than lower lake levels (Digerfeldt, 1988). Peat humification analysis in two bogs, *c.* 150 km northwest of Lake Igelsjön, indicated a wet phase occurring at *c.* 4300-4200, 3700-3500 and 2250 cal BP, likely in response to increased precipitation and lowered temperatures (Borgmark, 2005). On the other hand, a slight shift to higher Igelsjön-Arbovatten $\delta^{18}O$ separation values at *c.* 3200-2200 cal. BP appears to coincide with a dry phase at 3250-2250 cal. BP in the two bogs (Borgmark, 2005). Humidity fluctuations recorded in Undarsmosse bog, southwestern Sweden, suggest large shifts to wetter conditions at *c.* 4300-3700 and *c.* 1500-600 cal. BP (de Jong *et al.*, 2006), consistent with low Igelsjön-Arbovatten $\delta^{18}O$ separation values.

4.5.3 Reconstruction approach for $\delta^{18}O$-temperature relations

Past variations in $\delta^{18}O$-temperature relations are examined using cellulose records from Lake Spåime (Chapter 3), Arbovatten, and the carbonate $\delta^{18}O$ record from Lake Tibetanus (Hammarlund *et al.*, 2002), all of which are suggested to reflect past changes in precipitation $\delta^{18}O$ at the annual to seasonal scale. Independent temperature records at each respective site are used in the reconstruction of $\delta^{18}O$-temperature relations. Lake Tibetanus carbonate-inferred precipitation $\delta^{18}O$ data are used with the pollen-inferred mean July temperature derived from the same lake (Hammarlund *et al.*, 2002). At Lake Spåime, the mean July temperature records inferred from chironomid head capsules are available from the same lake (Hammarlund *et al.*, 2004). At Arbovatten, cellulose $\delta^{18}O$ data are combined with the

pollen-inferred mean annual temperature from Lake Flarken, *c.* 100 km northeast from Arbovatten (Seppä *et al.*, 2005).

Paleotemperature records, expressed as the mean July temperature (MJT), were first converted to the mean annual temperature (MAT) using a linear regression relationship derived from modern temperature data obtained from stations near the study sites. At Lake Tibetanus, the pollen-inferred MJT record was converted to MAT using the relation MAT = 0.23MJT – 3.8 (r^2=0.55; Hammarlund *et al.*, 2002). Likewise, Lake Spåime chironomid-inferred MJT record is converted to a MAT record using the relation MAT = 0.50MJT – 4.8 (r^2 = 0.85), based on three stations in the area (Alexandersson *et al.*, 1991). The conversion from MJT to MAT provides a conservative estimate of relative trends in temporal δ^{18}O-temperature relation with respect to the Dansgaard (1964) δ^{18}O-temperature relation. For the reconstruction of the δ^{18}O-temperature relation at Arbovatten, a shift of +0.6 K was applied to the pollen-inferred MAT record from Lake Flarken to reflect the temperature difference between the two sites.

In order to compare temporal trends in δ^{18}O with respect to the modern Dansgaard (1964) spatial δ^{18}O-temperature relation, the topmost cellulose δ^{18}O value, representing modern precipitation δ^{18}O, is normalized to a common δ^{18}O-temperature relation having a slope of 0.69 ‰/K (Dansgaard, 1964) by using the topmost value from the corresponding inferred MAT record. For Arbovatten, the trend in the temporal δ^{18}O-temperature relation is normalized to the 500-year average intercept value, due to uncertainty in the topmost cellulose δ^{18}O values. The results show temporal trends in δ^{18}O records expressed as 500-year averages relative to the modern δ^{18}O-temperature relation during the Holocene (Figure 4-10). In effect, changes in atmospheric circulation that lead to changes in climate as recorded by δ^{18}O and temperature at each site are manifested as offsets from the modern δ^{18}O-temperature relation (Figure 4-11). The offsets can thus be interpreted as varying degrees of distillation of precipitation as illustrated in Figure 4-6.

4.5.4 Past precipitation $\delta^{18}O$-temperature relations

Figure 4-10 illustrates variability in the 500-year average temporal $\delta^{18}O$-temperature relation at each site during the Holocene (*c.* 9500 cal. BP to the present), with respect to the modern local $\delta^{18}O$-temperature relation, assuming a slope coefficient of 0.69 ‰/K (Dansgaard, 1964). Important to note from this figure is the correlation between the $\delta^{18}O$ data and the corresponding temperature. For instance, Lake Spåime shows considerable non-temperature-dependent variability in $\delta^{18}O$ due to strong seasonality recorded in the cellulose $\delta^{18}O$. If a constant slope of 0.69 ‰/K is assumed, then this results in large shifts in the intercept. Lake Tibetanus $\delta^{18}O$, on the other hand, exhibits moderate variation in the intercept. In contrast, Arbovatten $\delta^{18}O$ shows a strong dependency with temperature, spanning *c.* 3°C, and two distinct shifts in the intercept that are perhaps related to changes in distillation (Figure 4-6). Overall, there is generally non-temperature-dependent variation at the northern sites (Tibetanus, Spåime), which are situated in the lee of the Scandes. Variation at Arbovatten, situated in southern Sweden, is predominantly temperature-dependent and is influenced by a persistent westerly flow of air masses directly from the North Atlantic.

Profiles showing the inferred offset from the modern local $\delta^{18}O$-temperature relation for Lake Tibetanus, Lake Spåime and Arbovatten at 500-year averages during the Holocene are illustrated in Figure 4-11. Beginning at *c.* 9500 cal. BP, both Lake Tibetanus and Lake Spåime illustrate a positive offset of about +2‰ from the modern $\delta^{18}O$-temperature relation. At Tibetanus, this is followed by a gradual reduction in the offset, reaching the modern $\delta^{18}O$-temperature relation by *c.* 6000 cal. BP. At Spåime the offset increases to +3 by *c.* 8000 cal. BP, followed by a variable reduction to modern values by *c.* 4000 cal. BP. Lake Spåime and Lake Tibetanus remain close to the modern $\delta^{18}O$-temperature relation to the present, but with Lake Spåime offset being much more variable than that of Lake Tibetanus. The much smaller variability in Lake Tibetanus offset likely reflects a longer residence time of water in the catchment, capturing a mean annual signal, whereas the noisier profile of Lake Spåime may be reflecting seasonality of precipitation because of the much shorter catchment residence time. In contrast to both of these lakes, Arbovatten shows a negative offset

between *c.* 9500 and 5000 cal. BP of up to 2‰ and then remains close to the modern $\delta^{18}O$-temperature relation until at least 500 cal. BP (and perhaps to present).

Hammarlund *et al.* (2002) proposed that the early Holocene offset in the $\delta^{18}O$-temperature relation at Lake Tibetanus is the result of strong zonal atmospheric circulation. High summer insolation during this period likely reduced sea ice cover and allowed more extensive northward flow of warm surface waters into the Iceland and Norwegian Seas (Koç *et al.*, 2003). Enhanced efficiency of moisture transport likely resulted in reduced precipitation distillation as air masses traversed the Scandes Mountains, driven by steep east-west temperature and pressure gradients between the ocean and landmass (Hammarlund *et al.*, 2002). The positive offset in the $\delta^{18}O$-temperature relation during the early Holocene at Lake Spåime is also consistent with this mechanism, perhaps enhanced by increased summer precipitation (Figure 4-11). Abundant moisture may have also penetrated further inland on the Kola Peninsula and in the lower Yenisey River region, north-central Russia at 8000 cal. BP as suggested in lake sediment cellulose $\delta^{18}O$ records (Wolfe *et al.*, 2000, 2003). However, the propagation of moisture was suggested to have strongly dissipated eastward from the lower Yenisey River to Lena River during the early Holocene (Wolfe *et al.*, 2000).

Convergence of the Lake Tibetanus and Lake Spåime offsets toward the modern $\delta^{18}O$-temperature relation during the late Holocene is attributed to weakening westerlies and a transition to more continental conditions (Hammarlund *et al.*, 2002). Increasing continentality in the Lake Tibetanus area is suggested from evidence of increased *Pinus sylvestris* pollen and macrofossils by 6300 cal. BP (Barnekow 2000; Seppä and Hammarlund, 2000). Drier conditions are also noted in the Kola Peninsula (Wolfe *et al.*, 2003) and lake-level lowering in kettle lakes from Finnish Lapland (Korhola *et al.*, 2005) at 7000 cal. BP, as well as increased evaporative enrichment shown in a cellulose $\delta^{18}O$ record from Oikojärvi, Finland at *c.* 8000-6500 cal. BP (Chapter 2).

The temporal $\delta^{18}O$-temperature relations at Lake Tibetanus and Lake Spåime, from *c.* 6000 cal. BP to the present, agree well with the modern Dansgaard (1964) $\delta^{18}O$-temperature relation (Figure 4-11). However, Lake Spåime shows greater variability in the offset at *c.* 6000 cal. BP to the present reflecting greater sensitivity to changes in the seasonal

distribution of precipitation (Figure 4-11). Thus, the precise time in which the offset of Lake Spåime δ^{18}O-temperature relation approaches the modern relation is uncertain, but may have occurred between *c.* 6000 and 4000 cal. BP. The retreat of *Pinus sylvestris* from high elevation after *c.* 5000 cal. BP in the Spåime region (Kullman, 1995) suggests that forests were no longer supported by abundant moisture supply (Hammarlund *et al.*, 2004). Thus, the intercept of the Lake Spåime δ^{18}O-temperature relation probably reached the modern intercept by *c.* 6000-5000 cal. BP, approximately at or shortly after Lake Tibetanus.

In contrast, the offset from modern δ^{18}O-temperature relation shown in the Arbovatten profile clearly shows an opposite trend compared to Lake Tibetanus and Lake Spåime (Figure 4-11). The negative offset of about 1-2‰ at the start of the Arbovatten record is comparable to a change in the intercept equivalent to the modern Sweden precipitation δ^{18}O-temperature relation (Figure 4-5), suggesting a slightly greater distillation of precipitation and a drop by 5-10% in the remaining moisture fraction (Figure 4-6). Given the postglacial change in sea surface isotopic composition (*c.* 0.8‰), this is a conservative estimate (Shrag *et al.*, 1996). The offset in Arbovatten gradually increases and reaches the modern δ^{18}O-temperature relation by *c.* 4000 cal. BP (Figure 4-11), possibly reflecting a persistent North Atlantic influence on climate in southern Sweden. This increase in the offset by 1-2‰ suggests an increase in the fraction of moisture being transported. The temporal offset at Arbovatten reaches the modern δ^{18}O-temperature relation at approximately the same period of increasing moisture in the area, as supported by the low Igelsjön-Arbovatten δ^{18}O separation, indicating decreased evaporative enrichment (Figure 4-9).

The changes in the temporal δ^{18}O-temperature relations for each site with respect to the modern Dansgaard (1964) relation during the Holocene may reflect shifts in the polar atmospheric front (i.e., mid-latitude jet stream), as suggested by Almquist-Jacobson (1995). The greatest difference in the offset, occurring during the early to mid-Holocene (before 6000 cal. BP) may reflect the northward extension of the polar atmospheric front induced by the higher summer insolation and warmer sea surface temperatures (Koç *et al.*, 1993) during that period. Reduced precipitation distillation across the Scandes Mountains at high latitudes, as inferred from the positive offset from the modern δ^{18}O-temperature relation at

Lake Tibetanus and Lake Spåime (Figure 4-11), perhaps indicates a higher frequency of cyclonic activity in connection with stronger westerlies. At the same time, a negative offset occurs at Arbovatten, suggesting a decrease in the transport of moisture to southern Sweden. During the later half of the Holocene, the polar atmospheric front may have shifted southward. The southward shift in the polar atmospheric circulation front appears to have been gradual, as suggested by the offset from $\delta^{18}O$-temperature reaching the modern relation earlier at Lake Tibetanus, followed by Lake Spåime, and then Arbovatten. Almquist-Jacobson (1995) suggested that the water balance of lakes had increased synchronously across Fennoscandia during the late Holocene, possibly due to a consistent source of moist air flowing into Fennoscandia. A consistent flow of moisture may indicate that the variability in the latitudinal position of the polar atmospheric front was similar to that of modern-day (i.e., between 65°N and 50°N; Wallén, 1970). This is consistent with the increasing trend in the offset of Arbovatten $\delta^{18}O$-temperature relation, reflecting an increase in the migration of cyclones across southern Sweden during the Late Holocene. In addition, the shift to more continental climate at Lake Tibetanus and Lake Spåime after *c.* 6000-5000 cal. BP suggests a long-term weakening of the westerly flow of air masses, and increased attenuation of moisture transport. Thus, the decreasing trend in the offset at these two northern sites reflects the importance of the Scandes Mountains as being an efficient barrier to the westerly transport of moisture since *c.* 6000-5000 cal. BP.

4.6 Summary

Changes in the water balance in terms of the apparent evaporative enrichment at Lake Igelsjön are shown as a separation between Lake Igelsjön carbonate $\delta^{18}O$ and Arbovatten cellulose $\delta^{18}O$ for the Holocene. Moist conditions are inferred at *c.* 10,000-8000 cal. BP and *c.* 4300-200 cal. BP, and predominantly dry conditions at *c.* 8000-4300 cal. BP. Variability in the Arbovatten cellulose-inferred lake water $\delta^{18}O$ record corresponds remarkably well with the GRIP ice core $\delta^{18}O$ record, including the 8.2 kyr cold event. This similarity illustrates that the Arbovatten $\delta^{18}O$ record from southern Sweden reflects variation in precipitation $\delta^{18}O$ originating from vapour derived directly from the North Atlantic. The Arbovatten $\delta^{18}O$ record is compared with Lake Spåime cellulose $\delta^{18}O$ and Lake Tibetanus carbonate $\delta^{18}O$, and

are used in combination with independent proxy-inferred temperature records to reconstruct past changes in the temporal $\delta^{18}O$-temperature relations. Changes in the intercept of the $\delta^{18}O$-temperature relation have been shown to vary during the Holocene and likely reflects changes in the distillation of precipitation. Lake Tibetanus and Lake Spåime showed a positive offset from the modern Dansgaard (1964) $\delta^{18}O$-temperature relation from *c.* 9500 to 6000-5000 cal. BP, suggesting enhanced westerlies, and increased transport efficiency of moisture transport across the Scandes Mountains and a reduction in precipitation distillation. In contrast, Arbovatten showed a negative offset beginning in the early Holocene and gradually increased to the modern $\delta^{18}O$-temperature relation by *c.* 4000 cal. BP, possibly reflecting an increased frequency of cyclones traversing across southern Sweden, and hence reflecting a decreasing trend in precipitation distillation. By *c.* 6000-4000 cal. BP, the trend in the offsets at all three sites converges to the modern $\delta^{18}O$-temperature relation. The difference in the trends observed in the temporal $\delta^{18}O$-temperature relations between Arbovatten, located in southern Sweden, and that at the more northern sites (Lake Spåime and Lake Tibetanus) may be reflecting a gradual reduction in the strength of westerlies as well as a southward shift in the polar atmospheric front during the Holocene, possibly in response to a decline in the summer insolation and cooling of sea surface temperatures to present-day values. In addition, the Scandes Mountains act as an efficient barrier to the westerly flow of moisture, thus increasing the precipitation distillation at the northern sites during the later half of the Holocene.

Table 4-1. Summary of lake characteristics and determination of average residence time of water in Arbovatten. Total annual precipitation obtained from climate normals (SMHI 1961-1990; Alexandersson *et al.*, 1991) and annual evaporation extrapolated from Bringfelt and Forsman (1995). Annual precipitation (P) and annual evaporation (E) are integrated over catchment area and lake area, respectively, to obtain volume estimates. Residence time is converted to days.

	Arbovatten
water depth (m)	5.2
annual precipitation (mm)	820
annual evaporation (mm)	480
lake area (km^2)	0.02
catchment area (km^2)	0.97
lake volume, V (mm^3)	$1.0x10^{14}$
discharge, Q=P-E (mm^3/year)	$7.9x10^{14}$
residence time, t=V/Q (days)	48

Table 4-2. Lithostratigraphic description of the Arbovatten sediment profile. Depths are related to the water surface. The water depth measured at the coring site is 5.2 m.

Unit	Depth (m)	Sediment characteristics
8	5.20-5.23	Greyish brown to brownish grey, distinctly laminated fine-detritus gyttja with light layers representing yearly liming events. Lower boundary sharp.
7	5.23-5.45	Brown, slightly silty fine-detritus gyttja. Lower boundary gradual.
6	5.45-6.40	Brown fine-detritus gyttja. Lower boundary gradual.
5	6.40-8.31	Dark brown fine-detritus gyttja. Lower boundary gradual.
4	8.31-8.37	Greyish brown, slightly silty fine-detritus gyttja. Lower boundary sharp.
3	8.37-9.00	Brown, faintly laminated fine-detritus gyttja. Lower boundary gradual.
2	9.00-9.33	Greyish brown, slightly silty fine-detritus gyttja. Lower boundary sharp.
1	9.33-9.50	Light grey silty clay (not investigated). Abrupt core stop at 9.61 m (no recovery 9.50-9.61 m).

Table 4-3. Radiocarbon dates. Depths are related to the water surface.

Depth (m)	Lab. no.	Material analysed*	Weight (mg)	Reported age (^{14}C years BP)	Calibrated age (2 σ Interval)	Calibrated age (mid intercept)**
5.55-5.60	LuS-6031	*Myr.*	6.8	110 ± 50	0-280	***
6.44-6.48	LuS-6030	*Pin., Bet.*	7.7	2560 ± 50	2470-3340	2620 cal. BP
7.04-7.08	LuS-6029	*Pin., Bet.*	6.1	4425 ± 50	4860-5290	4975 cal. BP
7.64-7.68	LuS-6028	*Pin., Bet.*	9.4	6675 ± 60	7430-7660	7545 cal. BP
8.10-8.13	LuS-6027	*Pin., Bet.*	4.7	8070 ± 65	8650-9250	9025 cal. BP
8.61-8.64	LuS-6026	*Bet.*	15.1	8565 ± 60	9460-9680	9520 cal. BP
9.03-9.06	LuS-6025	*Bet.*	3.7	8750 ± 60	9500-10,150	9725 cal. BP
9.21-9.24	LuS-6024	*Bet., Emp.*	6.8	9370 ± 60	10,410-10,750	10,580 cal. BP

* *Myr.* = Leaf of *Myrica gale*, *Pin.* = seeds and needles of *Pinus sylvestris*, *Bet.* = fruits, catkin scales, leaves and small twigs of *Betula pubescens*, *Emp.* = fruits of *Empetrum nigrum*.

** Mean values of the age ranges or mid intercepts with the calibration curve for dates with irregular probability distributions.

*** Not determined (date not included in age model).

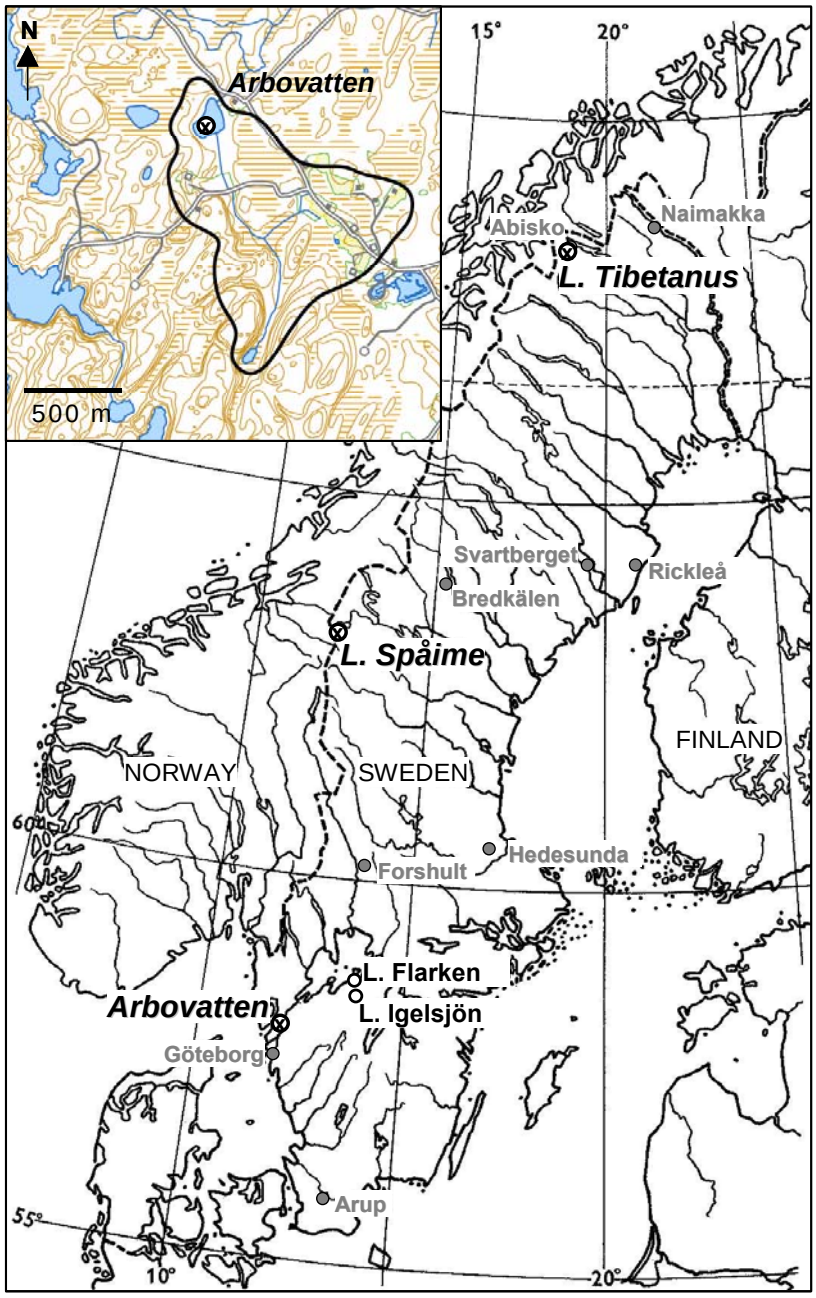

Figure 4-1. Map of Sweden showing the location of study lakes (large black text) and sites included in the interpretations (small black text). Location of precipitation $\delta^{18}O$ stations is shown in grey text. Inset displays a contour map and catchment boundary of Arbovatten. Contour intervals are 5 m and Arbovatten is at *c.* 118 m a.s.l.

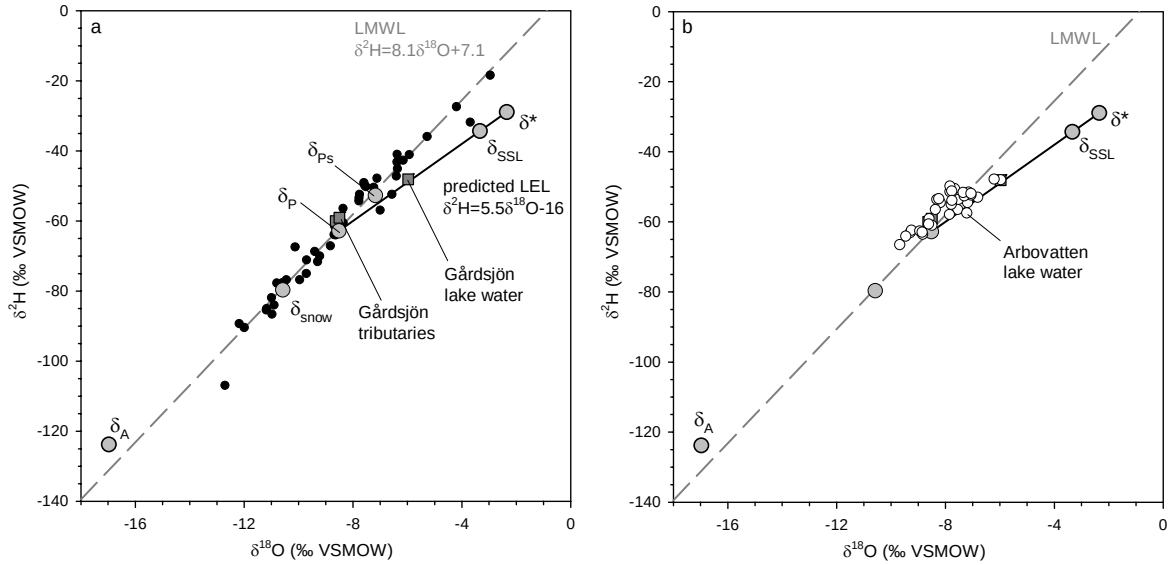

Figure 4-2. a) Isotopic framework for the distribution of waters in the Arbovatten area. Precipitation data collected at Göteborg (15 m a.s.l.) during the period of 1976-1989 (IAEA/WHO GNIP-data) are shown as small black circles, and defines the LMWL ($\delta^2H=8.1\delta^{18}O+7.1$). The main points on the LMWL are the amount-weighted means for annual precipitation (δ_P), rain (δ_{Ps}) and snow (δ_{snow}) isotopic compositions. The predicted LEL is based on the Craig and Gordon (1965) model that describes isotopic enrichment during evaporation, using δ_P and estimates of atmospheric parameters and the isotopic composition of atmospheric moisture (δ_A), which is assumed to be in equilibrium with δ_{Ps}. The isotopic steady-state lake (δ_{SSL}) and the limiting isotopic composition (δ^*) are shown as points on the predicted LEL. For reference, the isotopic composition of Gårdsjön lake water (1.4 km^2 west of Arbovatten) and its inflow tributaries plot on the LEL and near δ_P, respectively. b) The isotopic composition of Arbovatten lake water is shown with respect to the isotopic framework and Gårdsjön isotopic data.

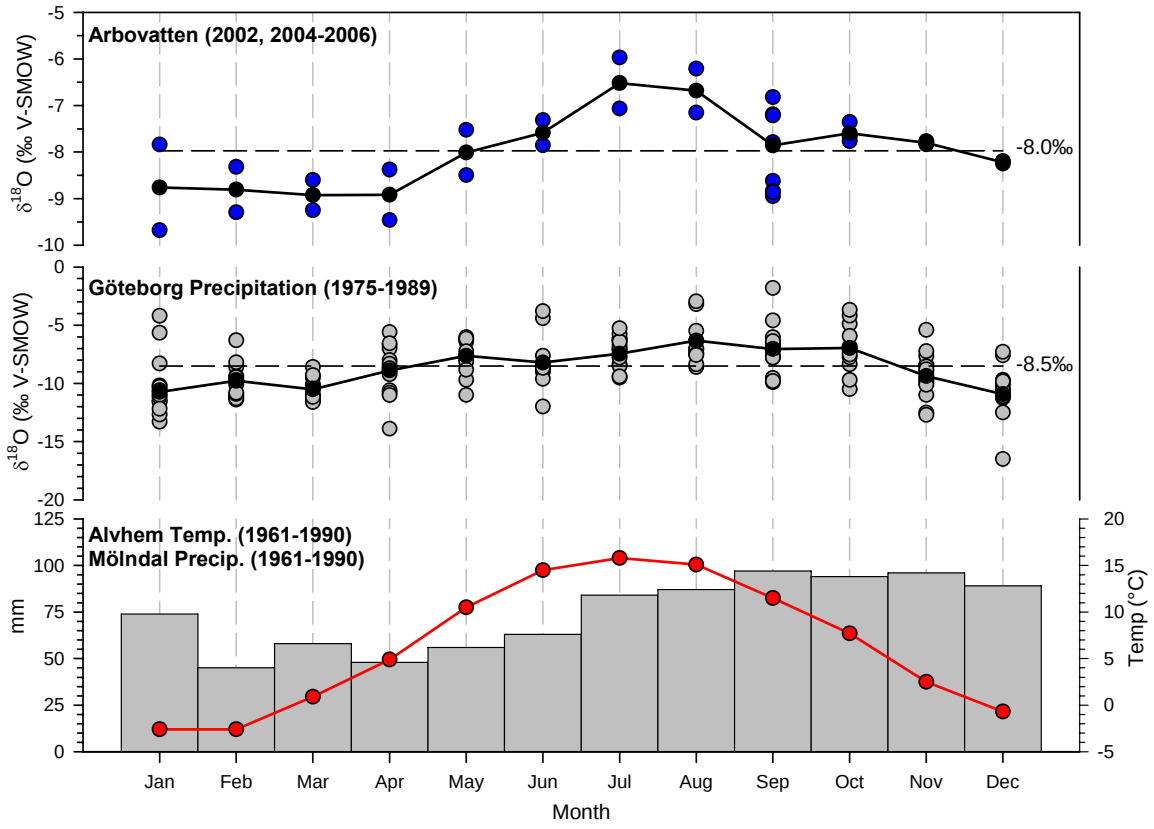

Figure 4-3. Monthly average of oxygen isotopic composition of lake water from Arbovatten collected during Sep. 2002, and Sep. 2004 to Oct 2006. Precipitation $\delta^{18}O$ and meteorological data collected at Göteborg for the period 1975-1989 (GNIP-IAEA database). Dashed horizontal lines indicate mean annual average of $\delta^{18}O$ for lake water, and the weighted annual average of $\delta^{18}O$ precipitation.

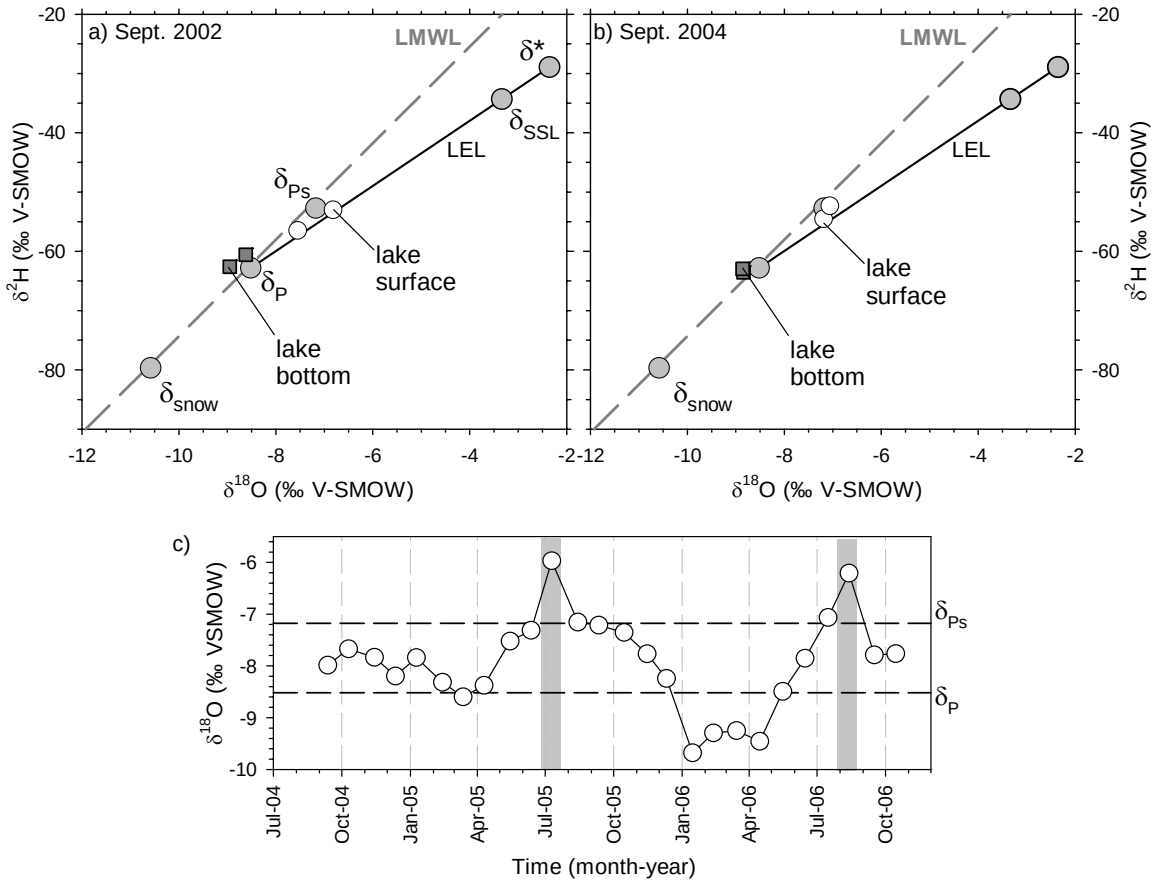

Figure 4-4. Comparison between surface and bottom lake waters during a) 2002 and b) 2004 sampling periods, showing a clear isotopic separation. c) Time-series of monthly average Arbovatten lake water $\delta^{18}O$ for sampling period of Sept. 2004 – Oct. 2006. Grey-shading highlights samples influenced by evaporative enrichment at the surface.

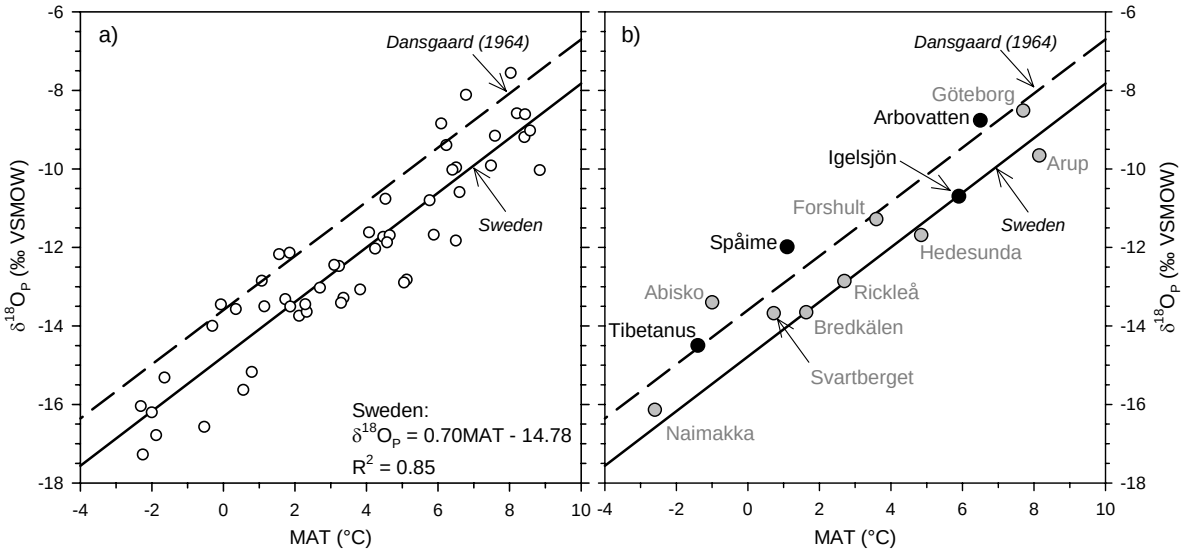

Figure 4-5. a) Regression through modern average yearly precipitation $\delta^{18}O$ and average yearly temperature values from eight stations across Sweden having both $\delta^{18}O$ and temperature data during 1981-1988 (except 1990-1995 for Naimakka data), yielding a modern spatial relation of $\delta^{18}O_P = 0.70MAT - 14.78$. b) Distribution of amount-weighted mean annual $\delta^{18}O$ and annual temperature data at selected precipitation stations (grey-filled circles) and average $\delta^{18}O$ (from precipitation and groundwater) and temperature data at Tibetanus, Spåime, Arbovatten and Igelsjön (black-filled circles). These points are shown in comparison to the $\delta^{18}O$-temperature relations derived for Sweden as displayed in a) and from Dansgaard (1964), defined as $\delta^{18}O_P = 0.69MAT - 13.6$.

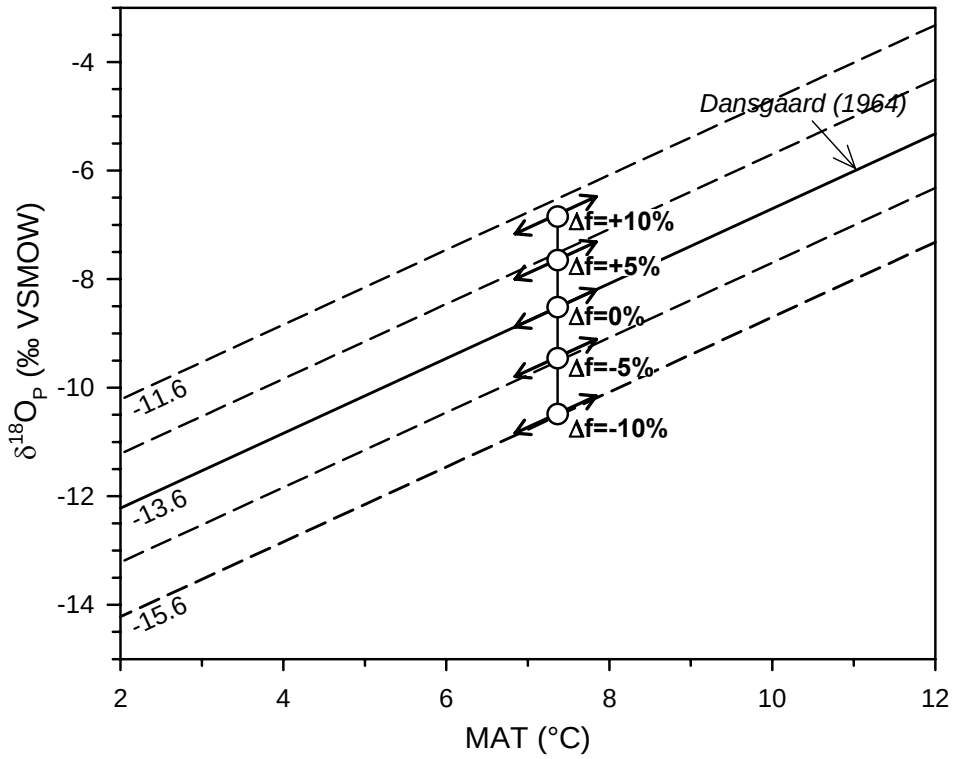

Figure 4-6. Schematic $\delta^{18}O$-temperature diagram illustrating changes in precipitation $\delta^{18}O$ with respect to the modern Dansgaard (1964) $\delta^{18}O$-temperature relation based on changes in the residual moisture fraction (Δf) due to Rayleigh distillation. The $\delta^{18}O$ value at $\Delta f = 0\%$ refers to Göteborg precipitation $\delta^{18}O$ that is formed from a vapour having about $f = 0.60$ remaining. Arrows at each relation refer to temperature-dependent variability over a period of time.

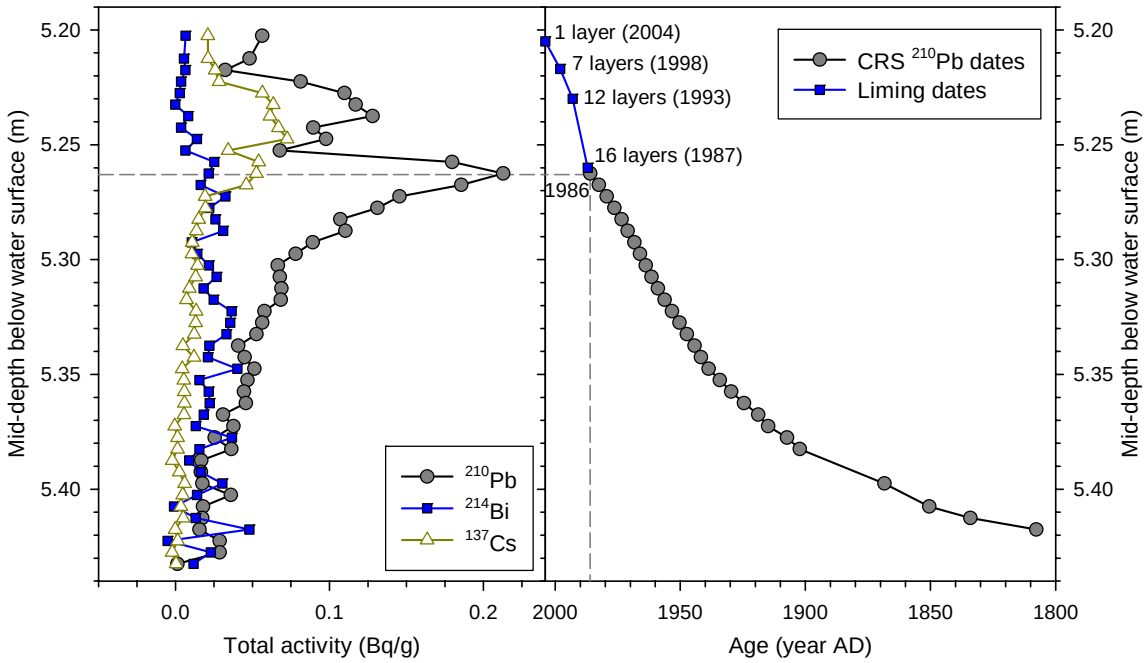

Figure 4-7. Total ^{210}Pb, ^{137}Cs, and ^{214}Bi activity versus mid-depth below the water surface shown in the left panel. The right panel refers to corresponding CRS ^{210}Pb dates and liming years. The 1987 ^{137}Cs date is indicated by the intersection of the vertical and horizontal dashed lines. The number of layers is the cumulative count starting at the top of the core.

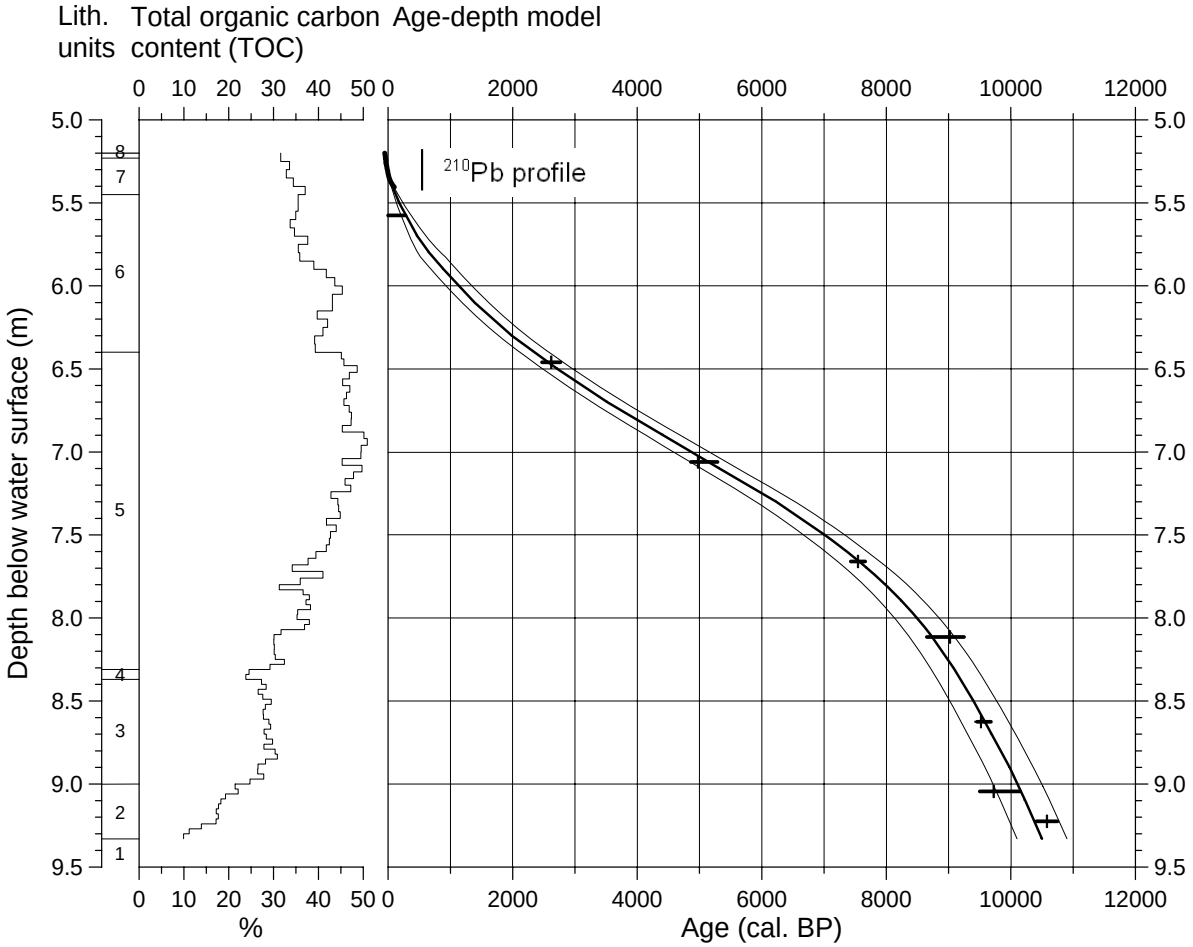

Figure 4-8. Age-depth model for Arbovatten based on seven radiocarbon dates obtained on plant macrofossils (see Table 4-3), ^{210}Pb model of surface sediments and liming events. The topmost radiocarbon date is shown as an age range, but was not included in the final age-model. This is shown together with lithological units (see Table 4-2) and total organic carbon content (TOC), expressed as weight percentages, and plotted against depth below water surface in the left-hand panel.

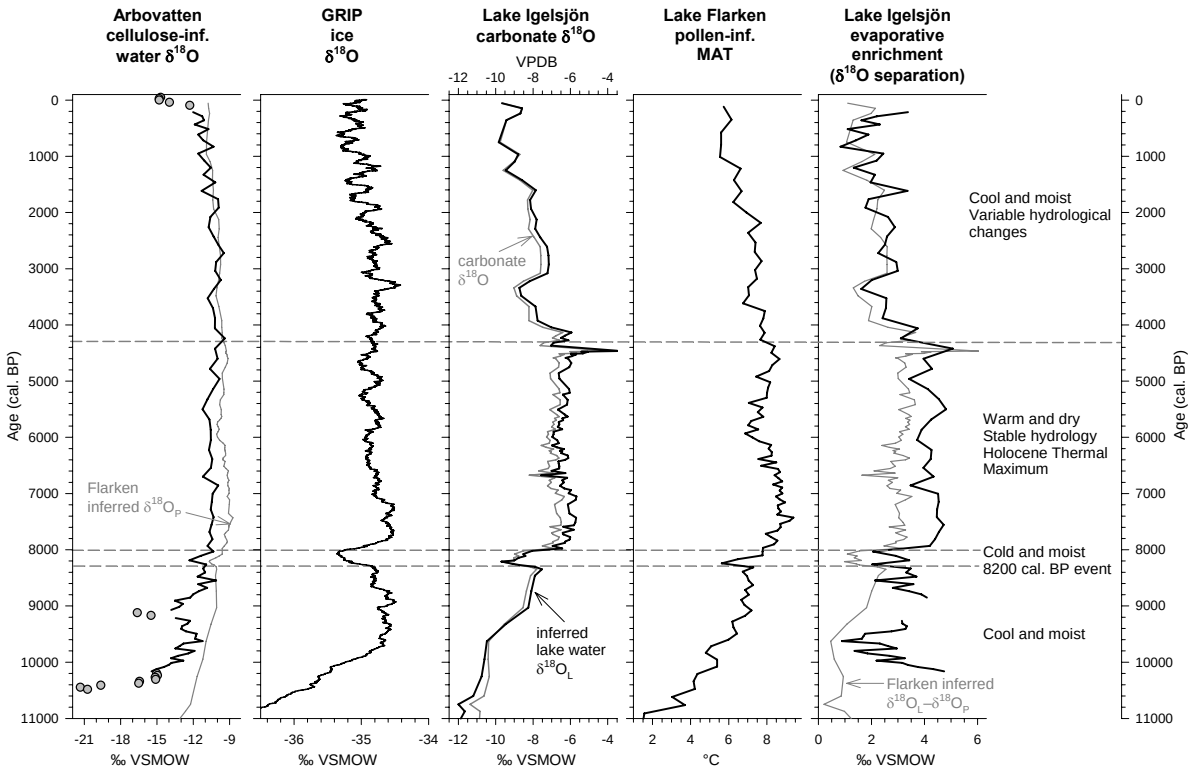

Figure 4-9. Profiles of cellulose-inferred water $\delta^{18}O$ from Arbovatten, 51-point running average of the GRIP ice core, Greenland (Dansgaard *et al.*, 1993), carbonate-inferred water $\delta^{18}O$ from Lake Igelsjön (Hammarlund *et al.*, 2003), and pollen-inferred reconstruction of mean annual temperature (MAT) from Lake Flarken (Seppä *et al.*, 2005). The carbonate $\delta^{18}O$ record has been corrected for temperature effects (Seppä *et al.*, 2005). Note that both VSMOW and VPDB for the carbonate $\delta^{18}O$ record are at the same scale. Also shown beside the Arbovatten cellulose $\delta^{18}O$ record is inferred precipitation $\delta^{18}O$ determined by Seppä *et al.* (2005) using the Lake Flarken MAT record and a fixed $\delta^{18}O$-temperature relation. The isotopic separation between Lake Igelsjön $\delta^{18}O_L$ and Arbovatten $\delta^{18}O$ reflects changes in evaporative enrichment, with positive $\delta^{18}O$ shifts suggesting drier climate conditions. The $\delta^{18}O$ separation between Igelsjön $\delta^{18}O_L$ and Flarken $\delta^{18}O_P$ is also shown for comparison. Grey-filled circles represent possible outliers in cellulose $\delta^{18}O$. The main paleoclimate interpretations are indicated on the right.

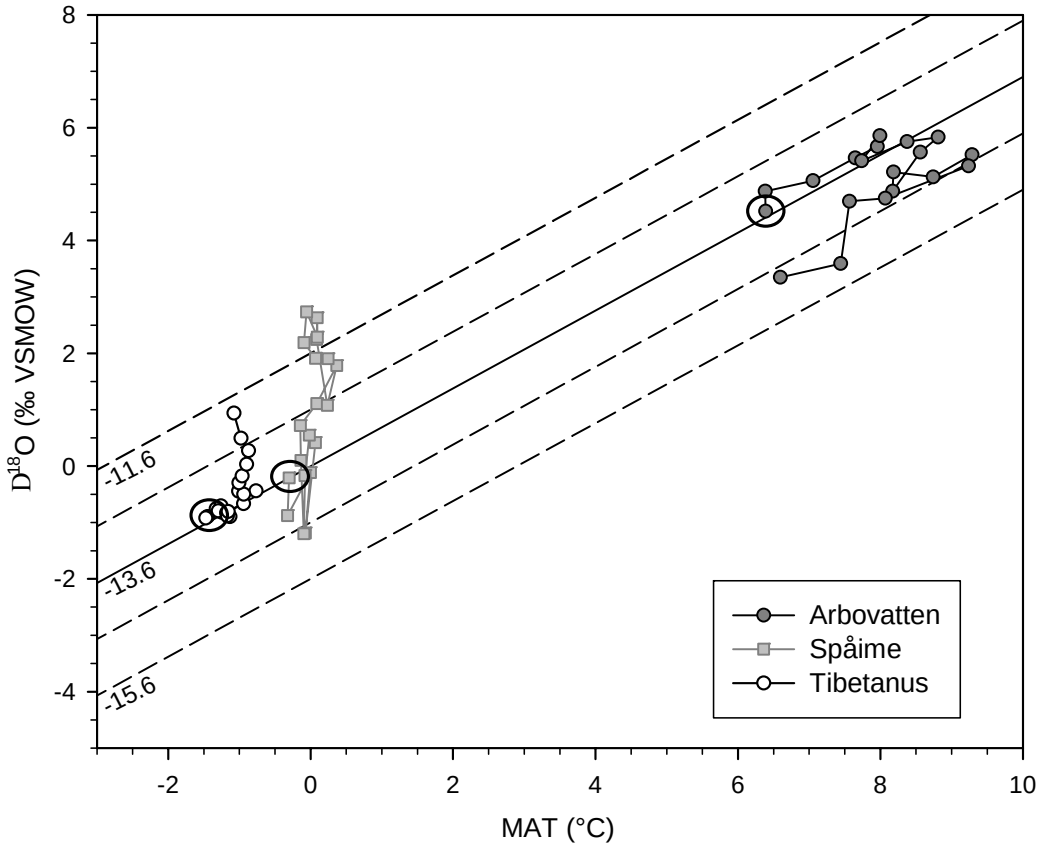

Figure 4-10. Temporal $\delta^{18}O$-temperature relations for each study site at 500-year intervals using cellulose $\delta^{18}O$ data from Lake Spåime and Arbovatten, and carbonate $\delta^{18}O$ data from Tibetanus (Hammarlund *et al.*, 2002), and independent reconstructed mean annual temperature (MAT) records (see text). Solid line denotes the isotope-temperature relation ($\delta^{18}O_P = 0.69MAT - 13.6$) reported by Dansgaard (1964). Dashed lines correspond to shifts in the intercept value of the $\delta^{18}O$-temperature relation. Open circles highlight the topmost value normalized to the modern $\delta^{18}O$-temperature line.

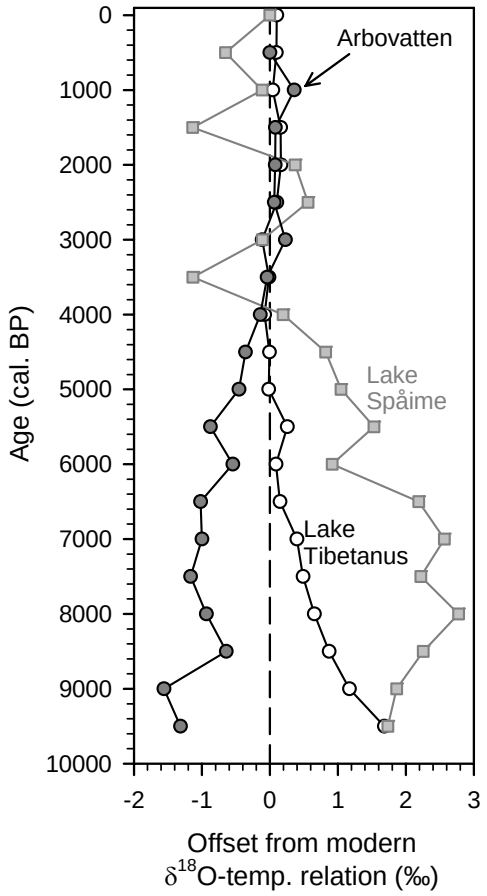

Figure 4-11. Profiles of the temporal offset from the local $\delta^{18}O$-temperature relation assuming a slope of 0.69 ‰/K (Dansgaard, 1964) at 500-year intervals for Arbovatten, Lake Spåime and Lake Tibetanus. Due to uncertainty in upper samples in Arbovatten, the profile is normalized to the average value at 500 cal. BP.

Chapter 5

Holocene Changes in Hydrology and Nutrient Cycling Inferred from Carbon– and Nitrogen–Isotope Records of Organic Lake Sediments from Fennoscandia

5.1 Introduction

The elemental and isotopic analyses of sediment organic matter provide important paleolimnological information about processes in the lake environment and surrounding catchment. There are numerous factors that influence the variability in the carbon and nitrogen elemental content and isotopic signatures in lake sediments (Meyers and Lallier-Vergès, 1999; Meyers and Teranes, 2001; Talbot, 2001). Commonly, the primary factor that affects lake productivity is the availability of nutrients, which depends on changes in the rates of delivery of dissolved byproducts from catchment soil decomposition and in-lake water column mixing (Wolfe *et al.*, 1996, 1999, 2003). Thus, changes in catchment vegetation and lake productivity are often tied closely to changes in climate and hydrology. For instance, moist conditions during the mid-Holocene forest interval on the Kola Peninsula likely enhanced the availability of nutrients via runoff, thereby favouring high aquatic productivity in the lake, and depletion of ^{13}C and enrichment of ^{15}N in the lake sediments (Wolfe *et al.*, 1999). In contrast, during the tundra interval of the late Holocene, the atmosphere played a more important role in the overall carbon and nitrogen balance in the lake, as the lake water residence time increased and soil organic matter decomposition rates declined (Wolfe *et al.*, 1999). This example implies that similar processes affect both carbon and nitrogen cycling and at similar rates. However, Wolfe *et al.* (1999) noted that the nitrogen cycling was slow to respond to changes in climate as compared to changes in lake productivity, water balance and terrestrial vegetation.

Variability in nitrogen cycling may be linked to hydrology, as well as the seasonal distribution of precipitation. For example, Sorensen *et al.* (2006) noted that in a drier environment, nitrogen fixation in the soils decreases, and thus limits the nitrogen availability to the surroundings. Wetter conditions increase nitrogen fixation, thereby accelerating the

nitrogen supply and promoting lake productivity. For example, the expansion of *Alnus*, which is capable of atmospheric N_2 fixation at the roots, coincided with enhanced nitrogen availability and increased productivity in an Alaskan lake during a mid-Holocene moist interval (Hu *et al.*, 2001). However, there is also a possibility for increased nitrogen loss due to rapid flushing of nitrogen through greater snowmelt runoff (Grogan and Jonasson, 2003).

For this study, five sediment cores were collected from small, open-drainage lakes situated in a north-south transect across Fennoscandia to reconstruct Holocene limnic carbon and nitrogen cycling in connection to long-term climate variability. The prominent influence of North Atlantic air masses and the Scandes Mountains have helped to develop a well-defined gradient in climate and vegetation zonations. The vegetation boundaries, specifically with altitudinal and latitudinal tree-limits of *Pinus sylvestris* and *Betula pubescens* and the distribution of *Picea abies* and thermophilous trees have substantially varied in the past in response to changes in climate (e.g., Kullman, 1999; Barnekow, 2000; Kullman and Kjällgren, 2006; Barnekow *et al.*, 2008; Giesecke *et al.*, 2008). The study lakes, thus, span an altitudinal and latitudinal range that encompasses a breadth of different vegetational characteristics within each lake catchment. This allows for comparisons to be made on the impact of carbon and nitrogen cycling in lakes in response to the changing catchment vegetation during the Holocene (e.g., Hammarlund *et al.*, 2004). In addition, a multiproxy approach is taken to aid in the interpretation of records of carbon and nitrogen elemental and isotopic composition by combining results from magnetic susceptibility and cellulose-inferred lake water $\delta^{18}O$ (Chapters 2-4) at each site. Each study lake also has a range of different water residence times, which can have significant implications on how quickly nutrients are attenuated within the lake system. This investigation aims to shed light on the nature of how lake productivity at a regional scale responds to changes in climate (temperature and precipitation) and the availability of nutrients.

5.2 Site Setting

All five lakes in this study are open-drainage lakes spanning across a range of altitudes and latitudes in Fennoscandia (Figure 5-1). The northernmost site, Oikojärvi (68°50'N, 21°10'E; 463 m a.s.l.), is a relatively deep (8.0 m) lake having an average residence time of 1.5 years,

and it is situated in Finland near the Swedish-Finland border. Approximately 23.5 km south of Oikojärvi is Lake Keitjoru (68º40'N, 21º30'E; 418 m a.s.l.), having a water depth of 1.8 m and a residence time of 15 days. A detailed description of these two lakes has been presented in Chapter 2. The next two lakes to the south are Lake Spåime (63°07'N, 12°19'E; 887 m a.s.l.) in the Scandes Mountains of west-central Sweden, and Svartkälstjärn (64°16′N; 19°33′E; 257 m a.s.l.) in east-central Sweden. Both of these lakes have been described in detail by Hammarlund *et al.* (2004) and Barnekow *et al.* (2008), respectively, and in Chapter 3. Lake Spåime is a small lake having a water depth of 3.5 m and an average water residence time of 12 days, whereas Svartkälstjärn has a water depth of 3.1 m and a residence time of 44 days. The southernmost site, Arbovatten (58º04'N, 12º04'E; 118 m a.s.l.), which has been described in Chapter 4, has a mean depth of 5.0 m and a water residence time of 48 days. The vegetation at Lake Spåime is characterized as alpine tundra. Both Lake Keitjoru and Oikojärvi are situated in the mountain birch subalpine zone. Svartkälstjärn catchment is within the boreal zone consisting of mainly conifers (pine and spruce), whereas the Arbovatten catchment is situated in the boreo-nemoral zone, comprising a mixture of spruce, pine and deciduous trees.

5.3 Methods

Long sediment cores were obtained from Lake Spåime, Svartkälstjärn, Lake Keitjoru, Oikojärvi, and Arbovatten (Figure 5-1) using a 1-m Russian peat sampler and surface sediments were extracted from the latter three lakes using a gravity corer. For each lake, overlapping core segments of the Russian cores were correlated in the laboratory using surface scanned measurements of magnetic susceptibility at 4 mm increments coupled to an automatic logging conveyor. Subsequent measurements of mass-dependent magnetic susceptibility were determined on wet subsamples using a Geofyzica Brno Kappa bridge at Lund University. The chronologies were developed using a combination of AMS radiocarbon dating of macrofossils obtained in the long cores and radioisotopes of lead and cesium in the short cores (see Chapters 2-4 for details). Lake Keitjoru, Oikojärvi and Arbovatten profiles of carbon and nitrogen elemental and isotopic composition and C/N ratios from the short cores are stratigraphically combined with the long cores in order to increase the resolution for the upper portion of the profiles.

Sediment samples were treated with 10% HCl to remove carbonate material, rinsed with de-ionized water, freeze-dried, and then sieved using a 500-μm mesh. The total organic carbon (TOC) and total nitrogen (TN) content and stable-isotope analyses were performed on the fine-grained fraction by an elemental analyzer interfaced with a continuous-flow isotope-ratio mass spectrometer (CF-IRMS) at the University of Waterloo Environmental Isotope Laboratory (UW-EIL). The results are expressed as 'δ' values, representing deviations in per mil (‰) from a standard, VPDB for carbon and AIR for nitrogen, such that $\delta_{sample}=1000[(R_{sample}/R_{standard})-1]$, where *R* is $^{13}C/^{12}C$ or $^{15}N/^{14}N$ ratio in sample and standard. The uncertainty, based on repeated analyses of all the lake samples combined, gives TOC results that are within ±2%, TN within ±0.1%, $\delta^{13}C$ within ±0.1‰ (with the exception of Svartkälstjärn, having ±0.8‰), and $\delta^{15}N$ within ±0.7‰.

Soil samples from each lake catchment (Spåime: n=6; Svartkälstjärn: n=2; Keitjoru: n=3; Oikojärvi: n=1; Arbovatten: n=1) and terrestrial vegetation from the Lake Spåime catchment (n=8) were analyzed for TOC, TN, $\delta^{13}C$ and $\delta^{15}N$ at the UW-EIL.

5.4 Results

5.4.1 Correction for inorganic nitrogen

The presence of inorganic nitrogen in the sediment records is tested through linear regression of the total nitrogen (TN) and total organic carbon (TOC) data (Talbot, 2001). Accordingly, a correction for minor amounts of inorganic nitrogen by 0.1 % was applied to the Oikojärvi sediments TN values (Figure 5-2a). For Svartkälstjärn sediments, a correction of *c.* 0.4 % was adjusted to the TN values between 4.71 and 5.15 m (7359-8903 cal. BP), and a correction of *c.* 0.3 % at 5.16-5.22 m (8964-9346 cal. BP) and 4.69-3.24 m (163-7316 cal. BP; Figure 5-2b). Likewise, a correction of *c.* 0.6 % was applied to the TN content in Arbovatten sediments (Figure 5-2c). The differences in the magnitude of the correction presumably reflect the amount of inorganic nitrogen bound to clays as a result of the release of ammonium during degradation of organic matter under moist climatic conditions (Talbot, 2001). As an example using elemental data from Middendorf Lake (Wolfe *et al.*, 1999),

Talbot (2001) demonstrated that the lake sediment deposited during the mild, humid forest interval contained some inorganically bound nitrogen as opposed to the tundra interval. The presence of dense forest and clays in the Arbovatten and Svartkälstjärn catchments may explain the higher correction needed for these sediments than that for Oikojärvi. The resulting nitrogen profiles for Oikojärvi, Svartkälstjärn and Arbovatten hereafter are expressed as the total organic nitrogen (TON). The measured C/N values for Oikojärvi, Svartkälstjärn and Arbovatten are also corrected such that only the organic fraction is represented in the sediments. A similar check for inorganic nitrogen was also performed for the Lake Spåime and Lake Keitjoru records and no inorganic nitrogen was evident in these sediments.

5.4.2 Lake Spåime

Previous work at Lake Spåime involved analysis of carbon and nitrogen elemental and isotopic composition from the same cores to reconstruct the impact of vegetational changes on aquatic productivity (Hammarlund *et al.*, 2004). In this study, the sampling resolution of the total nitrogen (TN) content, C/N ratio, and the isotopic components of the bulk organic matter ($\delta^{13}C$ and $\delta^{15}N$) was increased from 20 to 58 samples, spanning the length of the core. The resulting profiles are shown in Figure 5-3, revealing the same general trends and prominent features in TN, $\delta^{13}C$ and $\delta^{15}N$ profiles as observed before by Hammarlund *et al.* (2004). In Figure 5-3, both TOC and TN follow parallel trends. TOC content begins at a value of *c.* 2 % at the base of the record and rises to *c.* 15 % by 9000 cal. BP. From *c.* 9000-3700 cal. BP, TOC content remains elevated between values of 8 and 19 %, but with a significantly low value of 7.8 % at *c.* 7900 cal. BP. After *c.* 3700 cal. BP, the TOC content shows a considerable shift to low values in the range of 6-11 %. Similarly, elevated TN values of 0.7-1.8 % occur during *c.* 9000-3700 cal. BP, following a decline to values of 0.4–0.7 %. A general shift in the C/N ratio from values of 10-15 to higher C/N values (*c.* 14-18) is observed after 3200 cal. BP. The decline in the C/N ratio to a value of 16 near the top of the core is not as substantial as in the previous study (Hammarlund *et al.*, 2004).

As observed by Hammarlund *et al.* (2004), there is a gradual increase in $\delta^{13}C$ values ranging in –29 to –28‰ from the start of the record to *c.* 6200 cal. BP, and with a substantial

low value occurring at *c.* 7600 cal. BP (Figure 5-3). From *c.* 6200 cal BP to present, $\delta^{13}C$ values remain relatively consistent around –27 to –28‰, but with a slight depletion between *c.* 4000-3400 cal. BP. The $\delta^{15}N$ profile is quite variable, yet, superimposed on this variability is a subtle shift in $\delta^{15}N$ from an average value of 0.4‰ at *c.* 9000-3700 cal. BP to 0.7‰ after 3700 cal. BP to the present. In contrast, previous results by Hammarlund *et al.* (2004) showed $\delta^{15}N$ increasing at *c.* 1500 cal. BP, followed by a substantial decline to –0.3‰ at the top of the core. The higher resolution of the current $\delta^{15}N$ profile has revealed a much more consistent trend with variability ranging between 0.1-1.0‰ throughout the entire profile.

Magnetic susceptibility is generally high (*c.* 0.23-0.61 $\mu m^3 kg^{-1}$) and varies positively with high TOC content before *c.* 3700 cal. BP (Figure 5-3). After *c.* 3700 cal. BP, magnetic susceptibility decreases to values less than 0.20 $\mu m^3 kg^{-1}$, and coincides with a decrease in the variability in TOC content.

5.4.3 Svartkälstjärn

The carbon and nitrogen content and stable isotope composition in the Svartkälstjärn sediments show rather consistent trends during the Holocene (Figure 5-4). The TOC record begins with low values (0-5 %) and increases to 21 % by *c.* 8500 cal. BP. Slightly elevated TOC values ranging between 19 and 31 % occur at *c.* 8500-6000 cal. BP, followed by a small shift to lower TOC values that fluctuate between 17 and 29 % at *c.* 6000-2600 cal. BP. TOC reaches up to a maximum of 31 % at *c.* 3200 cal. BP, before returning to low TOC values (19 %). At *c.* 2600-200 cal. BP, TOC content increases slightly to a maximum of about 24 % by 200 cal. BP. After *c.* 200 cal. BP, there is a substantial decrease to 3 %, followed by a small increase to 11 % at the top of the core. The TON values are fairly low, but follow similar trends in the TOC content, with a rise in TON content to 1.0 % at *c.* 8500 cal. BP, followed by slightly higher values (1.0-1.6 %) at *c.* 8500-6000 cal. BP. From *c.* 6000 to 2600 cal. BP, TON fluctuates between 0.8 and 1.5 %, and then rises to 1.2 % by 200 cal. BP. Highly variable C/N ratios with values in the range of *c.* 7-26 occur before *c.* 9000 cal. BP with the maximum value occurring at *c.* 9400 cal. BP. At *c.* 9000-7000 cal. BP, C/N ratios decrease slightly to 19, followed by a gradual and steady increase to 22 by *c.* 3600 cal. BP. C/N ratios remain elevated at 20-24 between *c.* 3600 and 2600 cal. BP. At *c.* 2600-600 cal. BP, C/N

decreases to a value of about 18, followed by a moderate increase to a maximum of 24 at the top of the core.

Bulk organic $\delta^{13}C$ and $\delta^{15}N$ values in the Svartkälstjärn sediments are very stable during the Holocene (Figure 5-4). At the start of the record, $\delta^{13}C$ values are very high (–22‰) at *c.* 9500 cal. BP, followed by a substantial decrease to –30‰ by *c.* 8800 cal. BP. From *c.* 8800 to 7000 cal. BP, $\delta^{13}C$ increases slightly to –29‰, and afterwards, $\delta^{13}C$ values remain relatively constant with an average of –29‰ between *c.* 7000 and 100 cal. BP. There is a slight rise in $\delta^{13}C$ to –28‰ at the top of the core. In comparison, $\delta^{15}N$ is somewhat more variable than $\delta^{13}C$ at the start of the record. $\delta^{15}N$ values are very high with a maximum of +9.6‰ at 9600 cal. BP, but quickly decrease to –1.2‰ by *c.* 9150 cal. BP. At *c.* 9150-7000 cal. BP, $\delta^{15}N$ values show high variability, but generally increase to +2.4‰ by *c.* 7000 cal. BP. During the period of *c.* 7000 to 100 cal. BP, $\delta^{15}N$ values are fairly consistent within the range of +0.5 to +1.9‰, but with slight fluctuations at *c.* 3600-2600 cal. BP. From 100 cal. BP to the present, $\delta^{15}N$ values rise to +2.8‰.

Magnetic susceptibility values are high (0.14 $\mu m^3 kg^{-1}$) at the start of the record, and gradually decline to minimum values by *c.* 7000 cal. BP (Figure 5-4). Low values in the range of 0-0.08 $\mu m^3 kg^{-1}$ persist between *c.* 7000 and 200 cal. BP, with another minimum occurring at *c.* 2800 cal. BP. From 200 cal. BP to the present, magnetic susceptibility increases to a maximum value of 0.17 $\mu m^3 kg^{-1}$ at the top of the core.

5.4.4 Lake Keitjoru

There is considerable variation in the organic carbon and nitrogen content and stable-isotope compositions for Lake Keitjoru (Figure 5-5). Following a rise to TOC values of 14% by *c.* 8000 cal. BP, TOC content remains elevated with values in the range of 14-17 % between *c.* 8000 and 4500 cal. BP. After *c.* 4500 cal. BP, there is a shift to lower TOC values that fluctuate in the range of about 11-15 % until *c.* 100 cal. BP. However, superimposed on the low TOC trend are three sharp peaks having TOC content of 13, 19 and 15 % occurring at *c.* 3050, 2500 and 1500 cal. BP, respectively. From *c.* 100 cal. BP to the present, the TOC content rises sharply to values as high as 17 %. TN values positively correlate with TOC variations, with elevated TN values that vary in the range of 1.0-1.3 % between *c.* 8000-4500

cal. BP. A sharp decline in TN values occurs at *c.* 3400 cal. BP, followed by a slow steady rise to the present, with minor variations between 0.7-1.0 %. C/N values have been relatively stable (11-16) throughout the Holocene, except during the periods at *c.* 3700-2500 and 100 cal. BP to the present where C/N values reach as high as 16-22.

Bulk organic $\delta^{13}C$ values decrease to –29‰ by *c.* 8000 cal. BP, followed by an increase to values varying between –29 and –27‰ at *c.* 8000-5200 cal. BP (Figure 5-5). Starting at *c.* 5200 cal. BP, $\delta^{13}C$ values decrease to a minimum of –30‰ by *c.* 4300 cal. BP, followed by an increase to –27‰ by *c.* 3250 cal. BP. From *c.* 3250 cal. BP to the present, $\delta^{13}C$ values remain relatively stable within the range of –28 to –27‰, but with a slight increase to –26‰ in recent sediments. Bulk organic $\delta^{15}N$ values generally range between –1.5 and –0.3‰ prior to *c.* 4300 cal. BP, followed by an increase to values varying mainly between –0.5 and +0.6‰ during the latter half of the Holocene.

Magnetic susceptibility displays very low values (0.21 $\mu m^3 kg^{-1}$) before *c.* 3000 cal. BP, followed by a general rise throughout the rest of the core, reaching a maximum value of 1.47 $\mu m^3 kg^{-1}$ at the top of the record (Figure 5-5).

5.4.5 Oikojärvi

The elemental and isotope composition of carbon and nitrogen in the Oikojärvi sediments show differing trends and less variability than those of Lake Keitjoru (Figure 5-6). TOC values rise to a peak of 10 % at *c.* 8800 cal. BP, after which values remain relatively low during *c.* 8800-6100 cal. BP, reaching a minimum value of 7 % at *c.* 7200 cal. BP. At *c.* 6100-4000 cal. BP, TOC values increase slightly to within the range of 10-12 %. During the period of *c.* 4000 to 0 cal. BP, there is a gradual decline in TOC content to *c.* 8 %, followed by an abrupt rise to 10 % at the top of the core. TON positively correlates with trends in TOC, with generally low and consistent values ranging from 0.6 to 1.0 % between *c.* 9000 cal. BP to the present. C/N ratios at the start of the record reach a maximum value of 16 at *c.* 9800 cal. BP, and this coincides with low TOC, low TON, and high magnetic susceptibility. At *c.* 9000-2000 cal. BP, C/N ratios remain relatively stable with values averaging around 13. After 2000 cal. BP, C/N ratios show a slight decline reaching a value of *c.* 12 at present.

Bulk organic $\delta^{13}C$ values are low (–30.5‰) at *c.* 9400 cal. BP, followed by an enrichment to –28.0‰ by *c.* 8000 cal. BP (Figure 5-6). For the period of *c.* 8000-6400 cal. BP, $\delta^{13}C$ values remained slightly elevated in the range of –28.5 to –28.0‰. A shift towards more depleted $\delta^{13}C$ values of –28.9 to –28.2‰ occurs at *c.* 6400-4000 cal. BP, followed by a period of enriched values narrowly fluctuating between –28.4 and –27.4‰ until the present. Bulk organic $\delta^{15}N$ shows a moderate enrichment to a value of +2.1‰ by *c.* 8000 cal. BP, and remains elevated with values fluctuating within the range of +1.6 to +2.3‰ between *c.* 8000 and 5000 cal. BP. After *c.* 5000 cal BP, $\delta^{15}N$ values show a distinct depletion to a minimum value of +1.5‰, followed by relatively steady fluctuations between +1.4 and +1.9‰ to *c.* 2000 cal. BP. From *c.* 2000 cal. BP to the present, $\delta^{15}N$ values increase to a maximum of 2.3‰ at the top of the core.

At the base of the record, magnetic susceptibility values reach high values with a maximum of 0.63 $\mu m^3 kg^{-1}$, followed by a steep decrease to values ranging between 0 and 0.06 $\mu m^3 kg^{-1}$ at 9000 cal. BP to the present (Figure 5-6). A slight rise to a value of 0.08 $\mu m^3 kg^{-1}$ in magnetic susceptibility occurs at the top of the core.

5.4.6 Arbovatten

Trends in the carbon and nitrogen content in the Arbovatten record are rather invariant during the Holocene (Figure 5-7). The Arbovatten record also contains the highest organic matter content of all sites in this study. TOC rises from 10 % at the start of the record to 28 % at *c.* 10,000 cal. BP. Between *c.* 10,000 and 9000 cal. BP, TOC remains at 28 %, followed by a gradual steady increase to 51 % by 4600 cal. BP. From *c.* 4600 to 1000 cal. BP, TOC values slowly decreases to 44 %, followed by a greater decrease to 32 % at present. TON content follows parallel trends with TOC with an initial rise to 1.1 % by *c.* 10,000 cal. BP, where TON remains low until *c.* 9000 cal. BP. At *c.* 9000-4600 cal. BP, TON increases to a maximum value of 2.0 %, followed by a gradual decrease to 1.8 % by *c.* 1000 cal. BP. From *c.* 1000 cal. BP to the present, TON sharply decreases to a minimum of 0.8 %, before increasing slightly to 1.3 % at the top of the core. At *c.* 10,200-8100 cal. BP, C/N ratios remain relatively steady with values ranging between 23-27, followed by slightly lower values (22-25) at *c.* 8100-6000 cal. BP. Between *c.* 6000 and 2700 cal. BP, C/N ratios

gradually increase to a maximum value of 31. At *c.* 2700-200 cal. BP, C/N ratios gradually decline having fluctuations in the range of 24-30, followed by an abrupt increase to a maximum of 40 at the top of the core.

Bulk organic $\delta^{13}C$ and $\delta^{15}N$ values in Arbovatten sediments reveal trends that are relatively stable for much of the Holocene (Figure 5-7). $\delta^{13}C$ values decrease from –26‰ at the start of the record to –29‰ by *c.* 10,000-9200 cal. BP, but remain constant at an average of –30‰ between *c.* 9200 and 6000 cal. BP. Following a gradual increase to –29‰ by *c.* 4000 cal. BP, $\delta^{13}C$ values remain fairly constant at 4000-1000 cal. BP. There is a subtle rise in $\delta^{13}C$ to –28‰ by *c.* 100 cal. BP, followed by a sharp decrease to –29‰ at the top of the core. $\delta^{15}N$ decreases from +2.1‰ at the start of the record to +0.3‰ by *c.* 9900 cal. BP. Between *c.* 9900 to 3700 cal. BP, $\delta^{15}N$ values gradually decrease to –0.4‰, followed by a slight increase, reaching a value of +0.04‰ by *c.* 2000 cal. BP. From *c.* 2000 cal. BP to the present, $\delta^{15}N$ moderately increases from –0.6‰ to +0.6‰.

Magnetic susceptibility values are generally high (0.69 $\mu m^3 kg^{-1}$) between *c.* 10,500 and 9400 cal. BP, and then drastically decline to 0.04 $\mu m^3 kg^{-1}$ by *c.* 9000 cal. BP (Figure 5-7). Minimum values (0-0.04 $\mu m^3 kg^{-1}$) persist for most of the record until about 200 cal. BP. At *c.* 200 cal. BP, there is a subtle rise to a value of 0.12 $\mu m^3 kg^{-1}$ occurring at the top of the core.

5.5 Discussion

5.5.1 Origin of organic matter

5.5.1.1 Lake Spåime

Magnetic susceptibility shows parallel trends with TOC and TN content in Spåime sediments (Figure 5-3). The elevated magnetic susceptibility values before *c.* 3700 cal. BP are likely not related to catchment erosion, transportation and deposition of mineral matter. As illustrated in Figure 5-8a, a positive linear relationship between TOC content and magnetic susceptibility indicates that the fine-grained ferromagnetic minerals are associated with organic matter produced *in situ* by magnetotactic bacteria in the lake (Snowball *et al.*, 2002;

Hammarlund *et al.*, 2004). After 3700 cal. BP, both magnetic susceptibility and TOC values decline and become less variable, which is likely related to low inputs of detrital ferromagnetic minerals originating from the surrounding catchment. In addition, fluctuations to lower magnetic susceptibility (and lower TOC and TN) during this stage are generally reflecting lower aquatic productivity (Hammarlund *et al.*, 2004). Modern soil samples, which have been corrected for minor inorganic nitrogen, have C/N ratios ranging between 36-39 and $\delta^{15}N$ values of –4 to –2‰, whereas the plant material has C/N ratios ranging between 51-114 and $\delta^{15}N$ values of –4 to 0.4‰ (Figure 5-8b; Hammarlund *et al.*, 2004). This illustrates that the lake sediment C/N and $\delta^{15}N$ values are not the result of increased in-wash of organic detritus matter, since soil and vegetation samples exhibit C/N and $\delta^{15}N$ values considerably outside the range of those from the lake sediments, similar to results of Hammarlund *et al.* (2004).

5.5.1.2 Svartkälstjärn

C/N ratios (average 20) are relatively high in the Svartkälstjärn sediments (Figure 5-4), and this may be a reflection of nitrogen limitation in a highly productive lake rather than an indication of terrestrial contamination (*cf.* Hecky *et al.*, 1993; Talbot and Lærdal, 2000; Brahney *et al.*, 2006). The low magnetic susceptibility throughout much of the profile also lends support to reduced in-wash of terrestrial organic matter, especially at *c.* 7000 when lake productivity was at its maximum (Barnekow *et al.*, 2008). For the sediments after *c.* 200 cal. BP, high C/N ratios coincide with low TOC, low TON and high magnetic susceptibility, which likely indicate an increase in minerogenic material corresponding to the timing of logging in the region (Barnekow *et al.*, 2008). Figure 5-9 illustrates how the uppermost sediments trend towards an elemental and isotopic composition characteristic of mineral soil (Table 5-1). Because of the potential for contamination due to an increase in minerogenic material, the uppermost cellulose-inferred $\delta^{18}O$ value may be questionable (Figure 5-4; Chapter 3). The trend of data points represented at *c.* 9700-8700 cal. BP in Figure 5-9 also reflects a period of increased input of mineral matter from the catchment to the lake sediments soon after deglaciation. The rest of the elemental and isotopic data of the sediment profile is distinctly separate from that of the soil samples. In addition, the positive linear trend observed in the lake sediment data in the TON versus $\delta^{15}N$ crossplot suggests that only

in-lake processes are preserved. For instance, when TON content is low, the $\delta^{15}N$ approach values close to 0‰, a value that is characteristic of specialized phytoplankton (i.e., cyanobacteria) that is capable of assimilating atmospheric N_2 and can flourish under limiting nitrogen conditions in a lake (Talbot, 2001). On the other hand, when TON content is higher (maximum 1.6%), $\delta^{15}N$ approach values of around 2‰, possibly indicating a change in nitrogen assimilation favouring dissolved nitrate or ammonium.

5.5.1.3 Lake Keitjoru

Most of the Lake Keitjoru sediments have C/N ratios less than 15 (Figure 5-5), indicating that the organic matter content originates from in-lake processes (*cf.* Meyers and Lallier-Vergès, 1999). As verification, the elemental content and isotopic composition of soil samples collected in Lake Keitjoru catchment (Table 5-1) are compared with the lake sediments. Before *c.* 4400 cal. BP, lake sediments have a much lower average C/N ratio of 13 and more depleted $\delta^{15}N$ (average –1.0‰) than organic soils (Table 5-1). Lake sediments after *c.* 4400 cal. BP have low TOC and low TN contents and have $\delta^{15}N$ values that are substantially lower than that of mineral soil (Table 5-1). There are exceptionally high C/N ratios in the range of 16-22 that occur at *c.* 3050-2500, 1500 and 140 cal. BP to present. These C/N peaks also coincide with spikes in TOC, strongly suggesting that terrestrial material from the catchment was introduced into the lake at these intervals. Therefore, as a precautionary measure, the cellulose $\delta^{18}O$ samples at *c.* 2700, 2500 and 1500 cal. BP were excluded from subsequent interpretations (Figure 5-5; Chapter 2), as these were characteristically high and may have recorded a terrestrial signal (i.e., evaporative enrichment in leaf waters).

5.5.1.4 Oikojärvi

Fairly low C/N ratios averaging 13 occur between *c.* 9300 cal. BP to the present, supporting an aquatic origin for the Oikojärvi organic sediments (Figure 5-6; *cf.* Meyers and Lallier-Vergès, 1999). This lake is moderately deeper and the surface area is larger than the other lakes in this study, thus reducing the potential for the delivery of terrestrial organic matter into the lake sediments. For sediments deposited before *c.* 9300 cal. BP, C/N ratios reach up to 16 and coincide with substantially low TOC, low TON and high magnetic susceptibility,

and compare closely with that of the soil sample collected in the catchment (Table 5-1). Thus, the high C/N ratio at the start of the record is likely to represent a greater flux of detrital material during the early stages of lake and catchment soil development, coinciding with low lake productivity.

5.5.1.5 Arbovatten

The Arbovatten organic sediments that are shown in Figure 5-7 display very high C/N ratios (average 25) suggesting a terrestrial origin. However, similar to Svartkälstjärn organic sediments, the TON content is very low (less than 2.1 %). Thus, it is likely that high lake productivity, as indicated by coherent trends in TOC and TON and inversely with C/N, is taking place under nitrogen limiting conditions (*cf.* Hecky *et al.*, 1993; Talbot and Lærdal, 2000; Brahney *et al.*, 2006). As further emphasis, the magnetic susceptibility is extremely low for most of the profile, supporting the interpretation that most of the Arbovatten sediments are likely aquatic in origin. In comparison, the top and bottom intervals of the organic sediments illustrate markedly high C/N ratios (>40), which correspond with decreased values of TOC and TON content, and elevated magnetic susceptibility. These trends in the organic content observed at the top of the sediments are more likely related to allochthonous inputs due to recent liming. An increase in detrital material due to unstable soils in the catchment soon after deglaciation likely explains the trends observed in the organic matter at the base of the core.

5.5.2 Nutrient cycling during the Holocene

The relationship between $\delta^{13}C$ and $\delta^{15}N$ and organic matter content at a regional scale is demonstrated in Figure 5-10. The data points shown in Figure 5-10a show a separation between forested lakes (Arbovatten and Svartkälstjärn) and subarctic to subalpine lakes (Oikojärvi, Keitjoru, and Spåime). In the C/N versus $\delta^{15}N$ plot there appears to be a shift only in the C/N ratio between these two lake groupings. This indicates that the nitrogen isotope signature reflects variability in the nitrogen cycling within the lake and changes in the pathway for DIN sources, regardless of vegetation density in the catchment. In the C/N versus $\delta^{13}C$ plot, the forested lakes have higher C/N ratios and more depleted $\delta^{13}C$ signatures

than the subarctic to subalpine lakes. This trend suggests that soil respiration in forested organic matter has a strong impact in defining the signature of the DIC in lakes.

The data points shown in Figure 5-10b are divided into two time periods: pre- and post-4000 cal. BP. The time of 4000 cal. BP is chosen because it marks a drastic change in climate across Fennoscandia, generally from warm and dry conditions to cooler and wetter conditions (Hammarlund *et al.*, 2003; Snowball *et al.*, 2004). This time is also marked by significant changes in vegetation, such as the deforestation at Lake Spåime, in central Scandes Mountains (Hammarlund *et al.*, 2004), the spruce establishment at Svartkälstjärn, east-central Sweden (Barnekow *et al.*, 2008), the retreat of the pine tree-line in northern Fennoscandia (Seppä and Birch, 2001; Bjune *et al.*, 2004), and the decline of *Corylus* and *Quercus* in southern Sweden (Seppä *et al.*, 2005).

In Figure 5-10b, a shift in $\delta^{15}N$ and $\delta^{13}C$ at 4000 cal. BP is readily apparent at all sites. For $\delta^{15}N$, shifts to lower values occur in both forested (i.e., Arbovatten, Svartkälstjärn) and subalpine (i.e., Oikojärvi) lakes, and positive $\delta^{15}N$ shifts occur in Lake Spåime and Lake Keitjoru. This pattern demonstrates that there is no correlation between sites of differing vegetation density and the nature of nitrogen cycling in these lakes. Rather, the nitrogen isotope signatures may be reflecting a greater dependence on the hydrological regime, especially since the magnitude of $\delta^{15}N$ change in these lakes is small (±3‰). For example, a negative $\delta^{15}N$ shift could reflect conditions where ^{15}N-enriched DIN from soil decomposition and productivity-driven ^{15}N enrichment from preferential uptake of ^{14}N by phytoplankton changes to conditions of nitrogen limitation and algal fixation of atmospheric N_2. Similar conclusions for decreasing $\delta^{15}N$ have been drawn in other studies, for example, at the forest-tundra transition at Middendorf Lake, Russia (Wolfe *et al.*, 1999) and at Lake Victoria, Africa (Talbot and Lærdal, 2000). In comparison, a positive $\delta^{15}N$ shift may represent a change where high lake productivity takes place in an abundant nitrogen supply and rapid hydrological flushing, which maintains ^{15}N abundance at low concentrations in the lake, to conditions of nitrogen limitation and subsequent ^{15}N enrichment. This pattern of $\delta^{15}N$ change has been documented in Lake Yarnyshnoe-3 on the Kola Peninsula, Russia during the transition from moist to dry conditions at 4500 ^{14}C BP (5150 cal. BP; Wolfe *et al.*, 2003).

One common characteristic for lakes that show a negative shift in $\delta^{15}N$ at 4000 cal. BP is a longer residence time of water (>44 days), as compared to the lakes showing a positive shift in $\delta^{15}N$, having a residence time of <15 days. During the period before 4000 cal. BP, a significant proportion of rainfall, as shown by cellulose-inferred lake water $\delta^{18}O$ at Lake Spåime (Figure 5-3) and Lake Keitjoru (Figure 5-5), is likely to have kept soils moist throughout the summer months, allowing for decomposition of organically bound nitrogen to produce an abundant supply of ^{15}N-enriched DIN. Subsequent flushing of this DIN in Lake Spåime and Lake Keitjoru may have been rapid, since these lakes have short residence times and have their hydrological regime strongly influenced by changes in the seasonal distribution of precipitation. For the other lakes with longer residence times, the DIN from the catchment remains in the water column for longer periods, building up the ^{15}N concentration during lake productivity. After 4000 cal. BP, increased snow-rich winters and a higher frequency of summer droughts, likely reduced the nitrogen availability to each lake, leading to a gradual decline in lake productivity and ^{15}N-enrichment, and a possible switch to N-fixation as a source of nitrogen. The results show important connections between the response of lakes and the timing of nitrogen release from soils during spring snowmelt (Grogan and Jonasson, 2003), which can be a significant means of nitrogen loss in a lake system, and thus have an impact on lake productivity.

In Figure 5-10b, the C/N ratio versus $\delta^{13}C$ trend observed in the data points at 4000 cal. BP for all lakes show a shift to higher $\delta^{13}C$ values. In all cases, the ^{13}C-enrichment in the sediments is likely reflecting a reduction in soil-derived nutrients and a change to atmospheric CO_2 as the source of carbon to the lake, as postulated to be the case elsewhere (Wolfe *et al.*, 1996, 1999, 2003; Hammarlund *et al.*, 2004).

The following discussion considers nutrient cycling specific to each lake, detailing the key changes, as described above, in the context of changing catchment vegetation and climate during the Holocene.

5.5.2.1 Lake Spåime

The carbon and nitrogen elemental and isotopic composition of sediments from Lake Spåime have been previously presented by Hammarlund *et al.* (2004). The increased resolution of

the profiles in this study provides an opportunity to compare changes related to the timing of altitudinal tree-limit retreat in the catchment and variability in the cellulose-inferred lake water $\delta^{18}O$ profile. In Figure 5-3, high TOC and TN content and low C/N ratios at *c.* 9400-3700 cal. BP indicate high lake productivity. This is the time when the stands of *Betula pubescens* and *Pinus sylvestris* grew at the site, based on pollen frequencies obtained from the same core and macrofossils found in the area (Hammarlund *et al.*, 2004). Low $\delta^{13}C$ values during this stage reflect an increase of ^{13}C-depleted DIC from soil respiration when the catchment was forested. However, the shift to significantly lower $\delta^{13}C$ at *c.* 7800-7400 cal. BP may also reflect pronounced respiration within the water column and bottom sediments at this time. Interestingly, this shift to low $\delta^{13}C$ at *c.* 7800-7400 cal. BP coincides with a shift to low $\delta^{18}O$, which is likely associated with an increase of snow contributions. Overall, the low $\delta^{13}C$ values (–27.8‰ average) in sediments during the first half of the Holocene coincides with high $\delta^{18}O$, indicating an enhanced influx of ^{13}C-depleted DIC during warm, wet summers. In comparison, low $\delta^{15}N$ values (+0.4‰ average) characterize the first half of the Holocene and may have been maintained by rapid hydrological flushing through the lake. This conclusion is similar to mid-Holocene $\delta^{15}N$ results from Lake Yarnyshnoe-3 on the Kola Peninsula, Russia, in response to wetter conditions (Wolfe *et al.*, 2003).

The stratigraphic shift to low TOC, low TN and high C/N ratios occurring roughly at *c.* 3700 cal. BP (Figure 5-3) likely indicates a decline in lake productivity (Hammarlund *et al.*, 2004). A corresponding subtle shift to high $\delta^{13}C$ (–27.1‰ average) and high $\delta^{15}N$ (+0.7‰ average) values occur after 3700 cal. BP, reflecting a decrease in the availability of nutrient supply from the catchment. This stratigraphic change in the carbon and nitrogen elemental and isotopic composition corresponds to the local retreat of continuous forest at Lake Spåime, based on pollen and plant macrofossil analyses (Hammarlund *et al.*, 2004). Thus, after the forest retreat at *c.* 3700 cal. BP, the decline in lake productivity and an increased demand for nitrogen likely caused a slight overall enrichment in both $\delta^{13}C$ and $\delta^{15}N$ values. The positive shift in $\delta^{15}N$ starting at *c.* 4000 cal. BP coincides closely with the negative shift in $\delta^{18}O$ values. This may be an indication that the timing of the forest retreat, reduction of

nutrient delivery to the lake, and decline in lake productivity were responses to climate change that may have initiated around 4000 cal. BP. The deforestation was possibly in response to reduced growth season and extended snow cover in spring, as evidently shown by the low $\delta^{18}O$ values, since mean July air temperature, reconstructed from chironomid head capsules, was still increasing during this time (Hammarlund *et al.*, 2004).

5.5.2.2 Svartkälstjärn

Variability in the organic matter content in Svartkälstjärn sediments have been shown to coincide with vegetational changes during the Holocene as inferred from a pollen record obtained from the same core (Barnekow *et al.*, 2008). In Figure 5-4, the large variations in C/N ratio, $\delta^{13}C$ and $\delta^{15}N$ values in Svartkälstjärn sediments at *c.* 10000-8600 cal. BP likely reflect a period of soil development, variability in the nutrient supply to the lake, and episodes of erosion in the catchment soon after deglaciation in the area (see Figure 5-9).

Between *c.* 8600 and 7000 cal. BP, the establishment of a dense forest, mainly consisting of *Betula pubescens*, *Pinus sylvestris* and *Alnus* coincided with a rise in lake productivity, as indicated by high TOC and TON contents, and a slight decrease in C/N ratios (Figure 5-4; Barnekow *et al.*, 2008). The lower magnetic susceptibility during this interval reflects stabilization of soils in the catchment, such that sedimentation in the lake is the result of increased lake productivity. At *c.* 8600-7800 cal. BP, values of $\delta^{13}C$ in the sediments are low, probably reflecting enhanced influx of ^{13}C-depleted DIC derived from decomposing soil organic matter in the catchment and/or recycling of nutrients within the water column and lake bottom. A gradual increase in $\delta^{13}C$ by 7000 cal. BP coincides with the increase in lake productivity. Similarly, $\delta^{15}N$ values also show a general increase at *c.* 8600-7000 cal. BP in concert with increasing $\delta^{13}C$. Productivity-driven enrichment of both ^{13}C and ^{15}N in the DIC and DIN pools, respectively, appear to occur. This interpretation is supported by the lowered magnetic susceptibility, implying a decreased flux of soil-derived nutrients. The decreasing trend in cellulose-inferred lake water $\delta^{18}O$, shown in Figure 5-4, reflects a change from summer rainfall-dominated precipitation to snow-rich winters, such that summers are likely becoming increasingly dry (Chapter 3). By *c.* 7000 cal. BP, the peak in $\delta^{15}N$ correlates well with a minimum in magnetic susceptibility and a peak in $\delta^{18}O$ that is likely associated with a

combination of reduced winter precipitation and summer evaporative enrichment. A limited presence of charcoal particles in Svartkälstjärn sediments has been noted at *c.* 7000 cal. BP (Barnekow *et al.*, 2008), supporting dry summers occurring at this time. In addition, the occurrence of pollen of broad-leaved thermophilous trees, such as *Ulmus*, *Quercus* and *Tilia* (Barnekow *et al.*, 2008), coincides with the Holocene thermal optimum in northern Fennoscandia at *c.* 8000-6500 cal. BP. (Seppä and Birks, 2001, 2002). The effect of warm, dry summers is likely to have promoted high rates of lake productivity under limiting supply of catchment nutrients.

Between *c.* 7000 and 3200 cal. BP, the decreasing trend in both TOC and TON content corresponds with a subtle rise in C/N ratios, reflecting a very slow decline in lake productivity (Figure 5-4). During this interval, a dense forest cover of *Betula* and *Pinus* was established, based on the pollen record from Svartkälstjärn (Barnekow *et al.*, 2008). The constant presence of vegetation around the lake is reflected in the relatively constant values of $\delta^{13}C$ in the sediments throughout this interval, and indicates very stable soil conditions and a constant nutrient supply in the catchment. This interpretation is supported by elevated and steady values of magnetic susceptibility beginning around 6000 cal. BP, suggesting limited catchment disturbance (Barnekow *et al.*, 2008). In addition, lower cellulose-inferred lake water $\delta^{18}O$ values also occur during this period, signifying cool, humid summer conditions (Chapter 3).

In contrast to the $\delta^{13}C$ profile, the $\delta^{15}N$ record follows a decreasing trend from *c.* 7000 to 3200 cal. BP (Figure 5-4). Considering the decline in the organic matter content, the $\delta^{15}N$ values in the Svartkälstjärn sediments may be interpreted in two ways. One possibility is that decreasing $\delta^{15}N$ values may be reflecting a reduced rate of nitrogen uptake as compared to conditions at *c.* 7000 cal. BP when productivity was high. Secondly, the lower $\delta^{15}N$ values may be due to an increasing importance of N-fixing cyanobacteria in the lake while the supply of nitrogen from the catchment is limited. There is a consistent presence of dense vegetation and stable soil conditions, as noted previously, and so the $\delta^{15}N$ values are not likely related to changes in source isotopic composition of DIN from the catchment. Therefore, the variability in $\delta^{15}N$ must be related to a change in the phytoplankton flora. The

rate of supply of dissolved nitrate from the catchment is probably limited, thus increasing the importance of atmospheric N_2 as a source of nitrogen in the lake. Water column stability is likely to dominate during this period reflecting minimal vertical mixing usually in humid climate conditions (Talbot and Johannessen, 1992; Talbot, 2001), as portrayed by lower $\delta^{18}O$ values.

At around 3400-2800 cal. BP, there are considerable increases in both TOC and TON contents and high C/N ratios, reflecting fluctuations in the soil stability in response to changing vegetational makeup in the catchment (Figure 5-4). For instance, by *c.* 3200 cal. BP, *Picea abies* was established as a major forest component in the catchment (Barnekow *et al.*, 2008). This vegetation change is also accompanied by an increased frequency of *Sphagnum* spores, indicating an expansion of peat deposits around the lake in association with cooler and wetter climatic conditions (Barnekow *et al.*, 2008). At *c.* 3400-3200 cal. BP, this change coincides with increased $\delta^{15}N$ values and very subtle variations in the $\delta^{13}C$ profile (Figure 5-4). Notably, the timing of high $\delta^{15}N$ parallels with high $\delta^{18}O$ values and elevated magnetic susceptibility, possibly in response to increased contributions of summer rain (Chapter 3). An increased flux of ^{15}N-enriched soil-derived nutrients may have directed a switch from nitrogen fixation to nitrate assimilation, but a limited supply of nitrogen may have also led to ^{15}N-enrichment, similar to conditions at *c.* 7000 cal. BP. The shift to low $\delta^{15}N$ values at *c.* 3200-2200 cal. BP coincides with low $\delta^{18}O$ values, possibly reflecting a return to nitrogen fixation of atmospheric N_2 as a source of nitrogen in the lake while summer rain contributions are considerably reduced. After *c.* 2200 cal. BP, $\delta^{15}N$ shifts to positive values in concert with increased $\delta^{18}O$ values and elevated magnetic susceptibility, possibly reflecting reduced lake productivity under limited nutrient supply from the catchment. Fairly stable TOC and TON contents and a corresponding decline in C/N ratios between *c.* 2800 and 200 cal. BP probably reflect a general decrease in lake productivity as the nitrogen consumption in relation to the supply is reduced (Barnekow *et al.*, 2008). This assumption is also supported by the gradual enrichment in $\delta^{13}C$ values.

After *c.* 200 cal. BP, significant decreases in the organic content in the sediments occurred in response to increased contributions of minerogenic matter, as indicated by a substantial increase in magnetic susceptibility, and enhanced in-wash of terrestrial organic detritus as inferred from high C/N ratios and high $\delta^{15}N$ values. All of these modifications in the upper part of the carbon and nitrogen records are related to anthropogenic activities involving extensive logging and ditching in the area (Barnekow *et al.*, 2008).

5.5.2.3 Lake Keitjoru

As shown in Figure 5-5, the carbon and nitrogen elemental and isotopic records obtained from Lake Keitjoru display notable variability, which is comparable to the magnitude of change observed in the Lake Spåime records. The similarities between these two lakes may be a characteristic feature of lakes with short water residence times. The variability is assumed to reflect changes in aquatic productivity and nutrient cycling in the lake in response to changes in catchment vegetation and climate. The vegetation in Lake Keitjoru catchment during the Holocene is likely to have maintained a composition of mixed *Betula pubescens* and *Pinus sylvestris* that is typical of the subalpine ecotone since *c.* 9350 cal. BP to the present (Olsson, unpublished data; Seppä and Weckström, 1999; Seppä and Birks, 2002; Bjune *et al.*, 2004). From *c.* 9350 to 8000 cal. BP, there is a gradual rise in both TOC and TN coinciding with stable C/N ratios, a pronounced decrease in $\delta^{13}C$ and a moderate decrease in $\delta^{15}N$ (Figure 5-5). During this time, soon after deglaciation, the area was dominantly *Betula* and *Salix*, both of which favour moist summer conditions (Olsson, unpublished data; Seppä and Weckström, 1999). This trend is accompanied by high annual precipitation, as inferred from pollen reconstructions from a record obtained at nearby Lake Tsuolbmajavri (Seppä and Birks, 2001). In addition, the annual precipitation is likely to have changed from snow-rich winters to rainy summers as suggested by the trend in the cellulose-inferred lake water $\delta^{18}O$. The decrease in $\delta^{13}C$ values may be the result of enhanced in-wash of ^{13}C-depleted DIC from the catchment under moist conditions and increased soil development. The low $\delta^{13}C$ values, especially at *c.* 8500-8000 cal. BP may also be due to enhanced respiration of organic matter within the water column and bottom sediments, which recycles ^{13}C-depleted nutrients back into the epilimnion DIC pool. Both processes that account for the decrease in $\delta^{13}C$ are likely to occur while the lake deepens in response to

increased annual precipitation (Figure 5-5). In-lake recycling of DIC likely ceased by *c.* 8000 cal. BP, as indicated by a return to higher $\delta^{13}C$ values.

From *c.* 8000 to 5500 cal. BP, both TOC and TN content reach the highest levels observed in the record while the C/N ratios remain unchanged (Figure 5-5). In addition, magnetic susceptibility is low during this period, thus reflecting stable soils in the catchment. High lake productivity coincides with a period of dense forest development based on pollen accumulation rates at Lake Tsuolbmajavri (Seppä and Birks, 2001). A gradual increase in *Pinus sylvestris* and a parallel decline in *Betula pubescens* in the area (Olsson, unpublished data; Seppä and Weckström, 1999; Seppä and Birks, 2002; Bjune *et al.*, 2004) suggest that summer conditions were warm, as shown by the maximum mean July temperatures of 1.7–1.6°C higher than present (Figure 5-5; Seppä and Birks, 2001). An increase in $\delta^{13}C$ values at *c.* 8000-5500 cal. BP is likely due to enrichment in ^{13}C of lake DIC because of increased lake productivity. In comparison, $\delta^{15}N$ values show a gradual decline since the start of the record, reaching values of less than –1‰ at *c.* 8000-5500 cal. BP (Figure 5-5). An adequate supply of ^{15}N-depleted DIN must have been available to the phytoplankton for assimilation during high lake productivity in order to explain the low $\delta^{15}N$ values. Similar to $\delta^{15}N$ at Lake Spåime, the low $\delta^{15}N$ at Lake Keitjoru may be the result of rapid hydrological throughflow during the summer that dilutes the ^{15}N concentration in the lake's DIN pool. This conclusion is supported by elevated $\delta^{18}O$ values during *c.* 8000-5500 cal. BP, signifying that an increased proportion of rain makes up the total annual precipitation (Chapter 2).

At *c.* 5500-4200 cal. BP, there is a gradual decrease in TOC and TN content, and a slight rise in C/N ratios, marking a decline in lake productivity (Figure 5-5). The decline in lake productivity coincides with an increase in *Betula*, which gradually replaced *Pinus* starting at *c.* 5500-4000 cal. BP, probably in response to lower summer temperatures (Seppä and Weckström, 1999; Seppä and Birks, 2001; Seppä *et al.*, 2002; Bjune *et al.*, 2004). The magnitude of change in $\delta^{13}C$ shows a return to values similar to that which occurred at *c.* 8500-8000 cal. BP, suggesting similar conditions governing DIC cycling. The decrease in $\delta^{13}C$ coincides with an increase in the pollen-inferred annual precipitation and high $\delta^{18}O$ values, suggesting rainy summers. An increase in lake levels likely resulted in water column

mixing and recycling of ^{13}C-depleted nutrients through respiration of organic matter. This interpretation is supported by the notable dip in C/N ratios at *c.* 4200 cal. BP, suggesting that the carbon content is degraded as dissolved CO_2 and CH_4 are produced during respiration (Meyers and Lallier-Vergès, 1999). Since lake productivity decreases during this period, the uptake of ^{13}C-depleted DIC nutrients from the catchment is likely to decline, which further amplifies the lowering of $\delta^{13}C$. The small, gradual increase in $\delta^{15}N$ at *c.* 5500-4200 cal. BP may correspond to productivity-driven enrichment of ^{15}N in the lake's DIN pool under limiting nitrogen supply, which may have induced the decline in lake productivity at this time.

From *c.* 4200 cal. BP to the present, there are stratigraphic shifts to low TOC, low TN, high C/N, high $\delta^{13}C$ and high $\delta^{15}N$ (Figure 5-5), which is similar to the trend observed in the Lake Spåime record during the forest/tundra transition at around 3700 cal. BP (Figure 5-3). Some changes in catchment vegetation dynamics also took place at Lake Keitjoru likely in response to cooler summers and higher effective humidity, which synchronously caused a shift to lower lake productivity. Beginning at *c.* 4500 cal. BP, there is an increase in *Sphagnum* spores, reflecting increased distribution of peatlands in northern Fennoscandia (Seppä 1996; Seppä and Birks, 2001). In addition, the rise in *Picea abies*, which is adaptable to cold winters and moist, acidic soils, occurs at *c.* 3550 cal. BP (Seppä and Birks, 2001). In general, the total pollen accumulation rate for records in the region decreased after *c.* 4000 (Seppä and Weckström, 1999; Seppä *et al.*, 2002; Bjune *et al.*, 2004), which is an indication that CO_2 production from soil decomposition may have declined, similar to other sites during the late Holocene (Wolfe *et al.*, 1999; Hammarlund *et al.*, 2004). At the same time, influx of ^{13}C-depleted DIC from the catchment may also have been limited because of frequent dry spells during the summer. This interpretation is supported by inferred low annual precipitation at *c.* 4200-1500 cal. BP and substantially low $\delta^{18}O$ values at *c.* 4200-1500 and 800 cal. BP to present, indicating that a major proportion of the total annual precipitation is snow (Figure 5-5). A decline in ^{13}C-depleted DIC runoff likely enhanced the gradual enrichment in $\delta^{13}C$ observed in the lake sediments, and perhaps an increasing importance of atmospheric CO_2 as a source of carbon. Notably, a small shift to low $\delta^{13}C$ values occurs at *c.* 1500-800 cal. BP (Figure 5-5), suggesting a minor increase in catchment-derived ^{13}C-

depleted DIC entering the lake's DIC pool, and possibly recycling of respired ^{13}C-depleted CO_2 from organic matter in the water column. As further support, the low $\delta^{13}C$ values at *c.* 1500-800 cal. BP correspond with rain-dominated precipitation, as inferred from high $\delta^{18}O$ values at this time.

Lake Keitjoru $\delta^{15}N$ values gradually increase from *c.* 4200 cal. BP to the present, which may reflect ^{15}N-enrichment of the lake's DIN pool due to a limited nutrient supply (Figure 5-5). In particular, the trend towards high $\delta^{15}N$ is in concert with low $\delta^{18}O$ values, signifying increased snow component in the total annual precipitation. The increase in snow contribution at *c.* 4200-1500 and 800 cal. BP to the present may have enhanced the loss of nitrogen via flushing of DIN sources through the lake system during spring snowmelt (Grogan and Jonasson, 2003). The general rise in magnetic susceptibility up-core also supports the idea of an increase in the minerogenic matter in response to increase snowmelt (Snowball *et al.*, 2002). Since the $\delta^{15}N$ values fluctuate around 0‰, this may reflect an increased importance of atmospheric N_2 as a nitrogen source during growth of phytoplankton.

5.5.2.4 Oikojärvi

In Figure 5-6, the carbon and nitrogen organic content and isotopic composition in the Oikojärvi sediments show a narrower range of values and slightly different trends than in Lake Keitjoru sediments. This difference reflects a much longer water residence time in Oikojärvi and less sensitivity to changes in soil and terrestrial vegetation. In comparison, Lake Keitjoru's hydrology responds rapidly to changes in the seasonal distribution of precipitation, which is reflected as fluctuations in nutrient cycling. Oikojärvi is situated in the same region as Lake Keitjoru, and thus experiences the same climate conditions and has similar vegetation. The proximity of the two lakes allows for an interesting comparison of nutrient cycling within each lake system at a local scale.

Between *c.* 10,200 and 9100 cal. BP, the very low TOC and low TON content, high C/N ratios and high magnetic susceptibility at Oikojärvi suggest a period of catchment soil development and concurrent lake ecosystem stabilization (Figure 5-6). Likewise, the very low $\delta^{13}C$ values at *c.* 9400 cal. BP may represent lake bottom respiration as the lake deepens,

similar to in-lake processes that occurred at Lake Keitjoru during the early Holocene. At *c.* 9100-7200 cal. BP, TOC and TON content and C/N ratios are fairly stable, indicating very little change in lake productivity. This period coincides with a gradual warming, reaching maximum mean July temperatures by *c.* 7200 cal. BP, as inferred from the pollen-based reconstruction at Lake Tsuolbmajavri (Seppä and Birks, 2001). The cellulose-inferred lake water $\delta^{18}O$ displays a gradual increase, reaching highest values at *c.* 7200 cal. BP, suggesting evaporative enrichment of the lake water. The elevated annual precipitation from pollen-based reconstruction at Lake Tsuolbmajavri (Seppä and Birks, 2001) during this period likely had a greater snow component, based on Lake Keitjoru $\delta^{18}O$. The trend towards warm and dry summers perhaps reflects a period of reduced runoff of nutrients into Oikojärvi. Thus, moderately high $\delta^{13}C$ and high $\delta^{15}N$ values may be reflecting ^{13}C and ^{15}N enrichment in the DIC and DIN pools during this period of nutrient limitation.

At *c.* 7200-4000 cal. BP, TOC and TON contents synchronously increase slightly and reach highest values by *c.* 5000 cal. BP (Figure 5-6). The C/N ratios show a modest decline since the previous interval, indicating a small rise in aquatic productivity. The timing of maximum level of lake productivity occurs about 1000 years later than Lake Keitjoru. Since both catchments were likely characterized by forest dominantly comprising *Pinus sylvestris* and *Betula pubescens* (Seppä and Weckström, 1999; Seppä and Birks, 2002; Bjune *et al.*, 2004), the change in aquatic productivity in Oikojärvi likely relates to a change in water balance, whereas in Lake Keitjoru, aquatic productivity responded to changes mainly in the seasonal distribution of precipitation. At Oikojärvi, the trend towards lower cellulose-inferred lake water $\delta^{18}O$ values and decreasing mean July temperature at *c.* 7200-5500 cal. BP suggests a decline in evaporative enrichment in response to an increase in the effective humidity (Figure 5-6; Chapter 2). The abrupt increase in Oikojärvi $\delta^{18}O$ values at *c.* 5500 cal. BP corresponds to the increase in the pollen-inferred mean annual precipitation and higher summer rain contributions, as inferred from Lake Keitjoru $\delta^{18}O$ values (Figure 5-5), consistent with a transition from warm, dry summers to cool, wet summers.

The $\delta^{13}C$ values at Oikojärvi shows a shift to slightly more negative values at *c.* 6400-4000 cal. BP, suggesting an increased influx of ^{13}C-depleted DIC from the catchment (Figure 5-6). The period of low $\delta^{13}C$ values corresponds with the period of high pollen frequencies of *Pinus sylvestris* at Lake Toskaljavri (Seppä and Birks, 2002), a site that is *c.* 30 km north of Oikojärvi. This correspondence suggests that soil catchment respiration, which likely provided a source of ^{13}C-depleted nutrients, may have been significant during this time. There is a small peak in $\delta^{13}C$ at *c.* 5000 cal. BP that may be related to a reduction in the production of ^{13}C-depleted soil nutrients when *Pinus* pollen percentages declined for a short period, followed by another increase in *Pinus* at *c.* 4500-4000 cal. BP (Seppä and Birks, 2002). The low $\delta^{13}C$ values during this interval may also be due to recycling of ^{13}C-depleted DIC through respiration within the water column and lake bottom sediments, although this process may have been minor based on the small magnitude of $\delta^{13}C$ change during this interval compared to the pronounced decrease that occurred at *c.* 9400 cal. BP and the low $\delta^{13}C$ values at Lake Keitjoru during *c.* 5500-4200 cal. BP (Figure 5-5). The subsequent increase in $\delta^{13}C$ with values ranging between –28 and –27‰ and a decline in lake productivity at *c.* 4000 cal. BP to the present, suggest a reduction in soil-derived DIC, perhaps replaced by an increased exchange with atmospheric CO_2 as a source of carbon to the lake (Figure 5-6).

In comparison, the trend in $\delta^{15}N$ values in Oikojärvi sediments differs from the $\delta^{13}C$ profile (Figure 5-6). After a slight shift to low $\delta^{15}N$ values at *c.* 7200 cal. BP, a gradual rise occurs until *c.* 5000 cal. BP. The high $\delta^{15}N$ values may be the result of enhanced influx of ^{15}N-enriched DIN from the catchment, similar to processes related to the carbon nutrient cycling in the lake. However, C/N ratios show a parallel increase with TOC and TON at *c.* 6000-5400 cal. BP, while $\delta^{15}N$ values are high. This trend suggests that weak denitrification of the organic matter occurred at *c.* 6000-5400 cal. BP. A shift to lower $\delta^{15}N$ values by as much as 0.8‰ at *c.* 5000 cal. BP coincides with a subtle decrease in C/N ratios, while no change is apparent in the TOC and TON content. Summer climate conditions at *c.* 5000 cal. BP may have been moderately warm and dry, in support of fluctuations observed in the *Pinus* pollen frequencies in the area, as well as a small increase in pollen-inferred mean July temperature

(Figure 5-6; Seppä and Birks, 2001, 2002). Additionally, this shift to low $\delta^{15}N$ values may correspond to a modest decline in rain contributions, as shown by a decrease in Lake Keitjoru $\delta^{18}O$ values (Figure 5-5). A possible interpretation for this shift at *c.* 7200 cal. BP and after *c.* 5000 cal. BP is a change in the nitrogen source involving a reduction in soil-derived DIN from the catchment and an increase in N-fixation, making atmospheric N_2 available while the rate of lake productivity remained constant (Figure 5-6).

The changes in both $\delta^{13}C$ and $\delta^{15}N$ observed in Oikojärvi at around 4000 cal. BP reflect a change in nutrient cycling from a catchment-derived nutrient supply to an atmospherically-derived source, similar to the isotopic patterns observed in organic matter from Middendorf Lake, Russia, representing the transition from forest to tundra conditions in the catchment (Wolfe *et al.*, 1999). This change correlates with the reduction in pollen-inferred annual precipitation at Lake Tsuolbmajavri (Seppä and Birks, 2001) and an increase in snow contribution, as inferred from Lake Keitjoru $\delta^{18}O$ record. The small fluctuations in $\delta^{13}C$ and $\delta^{15}N$ observed in Oikojärvi sediments from *c.* 4000 cal. BP to the present suggest that the nutrient sources to the lake may have been moderately variable and dependent on summer moisture conditions (Figure 5-6). For example, as observed in Lake Keitjoru sediments, Oikojärvi $\delta^{13}C$ values also decrease slightly at *c.* 1500-800 cal. BP in response to moist summers and increased rain contribution, as indicated by low $\delta^{18}O$ values in Oikojärvi and Lake Keitjoru cellulose records (Chapter 2). The decreasing trend observed in the C/N ratios for the last 2000 years may reflect diagenesis related to the degradation of the nitrogen component in the lake organic matter content. A loss of TOC content of about 2.5% in the upper 14 cm, with very little change in TON content, is evident in Figure 5-6, and likely reflects the remineralization of carbon under anaerobic conditions while ammonium is absorbed by clay minerals (Meyers and Lallier-Vergès, 1999).

5.5.2.5 Arbovatten

For the period during *c.* 10,500-10,000 cal. BP, low TOC and TON content, high C/N ratios, high $\delta^{13}C$, and high $\delta^{15}N$ coincide with high magnetic susceptibility, possibly reflecting the early stages of soil development and lake ecosystem stabilization at Arbovatten (Figure 5-7). The nutrient supply and influx of minerogenic material likely varied in response to glacio-

isostatic rebound in the region, shortly after the Fennoscandian ice sheet retreated from the Swedish west coast (Björck and Digerfeldt, 1986; Schoning, 2002). The cellulose inferred lake water $\delta^{18}O$ reflects the input water composition (precipitation, groundwater) associated with open-drainage hydrology of the basin. The small magnitude of variability in the $\delta^{18}O$ record matches closely with the GRIP ice core $\delta^{18}O$ record (Chapter 4), which supports that Arbovatten $\delta^{18}O$ reflects input waters, without any effects of evaporative enrichment during dry periods. This means that the nutrient pools of DIC and DIN in the lake will strongly depend on soil conditions in the catchment, which in turn reflects changing vegetation. For most of the Holocene, the trends in the carbon and nitrogen elemental and isotopic composition are fairly stable and magnetic susceptibility very low, which signify a consistent forest presence and developed soils in the catchment. Vegetation dynamics in the region have been linked to changes in climate, with cool and moist conditions occurring at 10,000-8000 cal. BP, followed by a shift to predominantly dry and warm at *c.* 8000-4300 cal. BP, and then a return to cool, moist conditions at *c.* 4300 cal. BP to the present (Seppä *et al.*, 2005).

There is a small parallel shift in both TOC and TON contents from low to slightly higher values occurring at *c.* 9200 cal. BP (Figure 5-7). The C/N ratios show a very subtle decrease, indicating that aquatic productivity may still be low or slightly increasing during *c.* 10,000-8000 cal. BP in response to lengthening growing season and climatic warming (Seppä *et al.*, 2005). A dramatic drop in magnetic susceptibility to low values support that sedimentation after *c.* 9200 cal. BP is possibly derived solely from aquatic productivity as influx of mineral matter decreased. At *c.* 9000, soil stabilization in the catchment is likely to have occurred while a mixed forest of *Betula*, *Pinus*, *Alnus*, *Corylus* and *Ulmus* became established in southern Sweden (Digerfeldt, 1988; Seppä *et al.*, 2005). Correspondingly, a shift from high to low $\delta^{13}C$ values at *c.* 9000 cal. BP is likely reflecting enhanced influx of ^{13}C-depleted DIC generated from decomposing soil organic matter in the catchment. This process may be occurring in combination with rapid throughflow of water, which would counteract the effects of lake productivity-driven ^{13}C-enrichment on the DIC (e.g., Wolfe *et al.*, 1999; Hammarlund *et al.*, 2004).

From *c.* 8000 to 4300 cal. BP, TOC and TON contents continue to rise while magnetic susceptibility remains consistently low during this interval (Figure 5-7). C/N ratios remain consistently until *c.* 6000 cal. BP, followed by an increasing trend to *c.* 4300 cal. BP. The low $\delta^{13}C$ likely reflects a continuing supply of ^{13}C-depleted DIC from the catchment until 6000 cal. BP, followed by a gradual increase by *c.* 4300 cal. BP. The change in the organic content and $\delta^{13}C$ at *c.* 6000 cal. BP coincides with a decrease in the pollen abundance of *Corylus* and *Ulmus* at Lake Flarken, located 80 km northeast of Arbovatten, probably in response to a shift to slightly cooler temperatures and a more continental climate (Seppä *et al.*, 2005). Increasing C/N ratios, high organic matter content and increasing $\delta^{13}C$ values suggest that lake productivity occurred while the availability of nutrients from the catchment decreased. This decline in soil-derived nutrient supply is consistent with a period of dry conditions in southern Sweden *c.* 8000-4300 cal. BP, based on studies of lake-level reconstruction (Digerfeldt, 1988) and carbonate-inferred lake water $\delta^{18}O$ (Hammarlund *et al.*, 2003). A gradual decline in lake productivity is inferred at *c.* 4300-200 cal. BP, based on parallel decreases in TOC and TON content and an increase in C/N ratios, corresponding to a transition to a cool and moist climate (Hammarlund *et al.*, 2003). $\delta^{13}C$ values remain consistently elevated during this period, which is likely related to ^{13}C-enrichment of lake water DIC under limiting nutrient conditions.

The gradual decline in $\delta^{15}N$ values beginning at *c.* 10,000 to 4300 cal. BP may reflect a trend towards increased importance of atmospheric N_2 as a source of nitrogen to the lake (Figure 5-7). At *c.* 10,000-4300 cal. BP, higher $\delta^{15}N$ values correspond with high lake productivity, as indicated by elevated TOC and TON contents. High $\delta^{15}N$ values are likely the result of productivity-driven ^{15}N-enrichment of the DIN pool and/or increased influx of ^{15}N-enriched DIN from the catchment soils. The latter is consistent with the process leading to low $\delta^{13}C$ values as a result of rapid flushing of nutrients leached from the catchment. Likewise, remineralization during soil decomposition can supply ^{15}N-enriched nitrate to the lake.

As suggested by elevated $\delta^{13}C$ values at *c.* 4300-200 cal. BP, the supply of ^{15}N-enriched DIN from the catchment becomes limited. In contrast, there is a corresponding decrease in

$\delta^{15}N$ to values close to the atmospheric isotopic composition. The elevated C/N ratio (average 25) in the Arbovatten record may be an indicator that nitrogen is a limiting nutrient in the lake (*cf.* Brahney *et al.*, 2006). Thus, during times of limited soil-derived nutrient availability from the catchment, atmospheric-derived nitrogen becomes an important source to the lake. As an example in Middendorf Lake, Russia, gradual trends toward positive $\delta^{13}C$ and negative $\delta^{15}N$ values in lake sediments occurred from mid- to late Holocene, reflecting decreased soil organic matter decomposition, reduced leaching of catchment derived nutrients, and a relative increase in the importance of atmospheric-derived nitrogen (Wolfe *et al.*, 1999).

At *c.* 200 cal. BP, there is a significant rise in $\delta^{13}C$ and $\delta^{15}N$ values that accompanies an increase in magnetic susceptibility and a subtle decline in organic matter that is analogous to the changes observed before *c.* 9200 cal. BP (Figure 5-7). These trends may be indicating catchment erosion related to logging and farming in the region (Björkman, 1997). Signs of human activities were evident in the vicinity of the lake. In the field, remains of an old stone wall, perhaps belonging to a farm, was found in the forested area north of the lake, and a small patch of freshly cut trees were observed southwest of the lake. Catchment disturbance of vegetation and subsequent soil erosion may explain the tendency for the cellulose-inferred lake water $\delta^{18}O$ to obtain much lower values at *c.* 9200 cal. BP and after *c.* 200 cal. BP, thus adding to the uncertainty in lake water $\delta^{18}O$ reconstruction at these intervals (Figure 5-7). Additional lake disturbance is marked by substantial shifts in the organic matter content, high C/N ratios, low $\delta^{13}C$ and high $\delta^{15}N$ in the upper sediments, due to liming in Arbovatten that begin in the late 1980s as part of a plan to remediate lake acidification due to acid rain pollution (Renberg and Hultberg, 1992).

5.6 Summary

The elemental and isotopic composition of nitrogen and carbon in organic matter was analyzed in five open-drainage lakes that span across different latitudes and elevations in Sweden. The interpretations were supported by magnetic susceptibility and cellulose-inferred water $\delta^{18}O$ from each lake, as well as documented changes in vegetation dynamics. The results show that the carbon nutrient balance was strongly governed by soil

decomposition and vegetation density, whereas the nitrogen nutrient balance appeared to be influenced by hydrology. A transition in climate from warm and dry to cool and moist conditions occurred at *c.* 4000 cal. BP in Fennoscandia resulting in major changes in vegetation, including tree limit descent in the Scandes Mountains (Hammarlund *et al.*, 2004; Kullman and Kjällgren, 2006), latitudinal *Pinus* retreat in northern Fennoscandia (Seppä and Birks, 2001, 2002), and compositional changes in east-central and southern Sweden (Seppä *et al.*, 2005; Barnekow *et al.*, 2008). A change from high to low organic matter content also occurred at *c.* 4000 cal. BP, marking a significant decline in lake productivity in response to changes in terrestrial vegetation in the catchment. The residence time of water in the lakes may be key to understanding the rates and magnitude of change observed in nitrogen isotopes in lake sediments. Three main results from this study are summarized below:

1) Variability in $\delta^{13}C$ in lake sediments of this study reflect changes in the DIC supply generated from the decomposition of soil organic matter in the catchment. During the early to mid-Holocene, high lake productivity occurred in response to ample supply of ^{13}C-depleted DIC produced in catchment soils when the catchment was densely forested. After climate deterioration at *c.* 4000 cal. BP, vegetation density declined, leading to a reduction in the supply of ^{13}C-depleted nutrients from the catchment. As a result, lake productivity declined and subsequent ^{13}C-enrichment of the DIC pool occurred in the lakes.

2) Trends in $\delta^{15}N$ in the lake sediments also reflect changes in the DIN supply generated from the decomposition of soil organic matter in the catchment. However, the patterns in $\delta^{15}N$ differ from $\delta^{13}C$, reflecting additional processes affecting the nitrogen cycle. The release of nitrogen from the soils occurs in the spring (Grogan and Jonasson, 2003). Therefore, periods of greater snowmelt would promote greater losses of nitrogen from the lake system. In early to mid-Holocene, the precipitation distribution was dominantly rain, contributing to increased moisture in soils, and enhancing the supply of ^{15}N-enriched DIN to the lakes. The period after *c.* 4000 cal. BP was characterized by snow-rich winters, shorter growing season, and frequent summer droughts, which may have contributed to a reduction of ^{15}N-enriched DIN supply to the lakes.

3) The response to changes in nitrogen supply is reflected in the water residence time of the lakes. Lakes with a short residence time (e.g., Lake Keitjoru and Lake Spåime with residence time of <15 days) have their hydrological regime strongly mediated by the seasonality of precipitation. Before *c.* 4000 cal. BP, increased rain contributions enhanced the supply of DIN to the lake. Enhanced flushing of this DIN from the catchment led to low concentrations of ^{15}N in the lake. After *c.* 4000 cal. BP, the DIN supply from the catchment may have been lost during spring snowmelt, leading to productivity-driven ^{15}N enrichment in these lakes. In comparison, lakes with a long residence time of water (>44 days), such as in Oikojärvi, Svartkälstjärn and Arbovatten, reveal opposite trends in $\delta^{15}N$ than the lakes with shorter residence times. The early to mid-Holocene trend reflects ^{15}N enrichment during high lake productivity, as an in-flux of DIN from the catchment is maintained within the water column over a longer period of time. After *c.* 4000 cal. BP, the reduction in catchment-derived DIN may have led to increased importance of atmospheric-derived nitrogen, resulting in lower $\delta^{15}N$ values in these lakes.

Table 5-1. Carbon and nitrogen elemental content and stable isotope composition of bulk soil samples collected in each lake catchment.

Lake	Bulk soil analyzed	TOC (%)	TN (%)	$\delta^{13}C$	$\delta^{15}N$	C/N
Svartkälstjärn:						
	organic	47.4	1.4	–28.5	-3.4	32.9
	mineral	1.0	0.1	–26.5	6.4	17.4
L. Keitjoru:						
	organic	39.2	2.2	–28.9	–0.2	17.6
	mineral	1.3	0.1	–26.8	4.1	13.6
	mineral	2.9	0.2	–25.9	4.8	17.2
Oikojärvi:						
	mineral	3.6	0.3	–27.0	4.1	13.2
Arbovatten:						
	mineral	7.0	0.4	–28.4	3.3	16.3

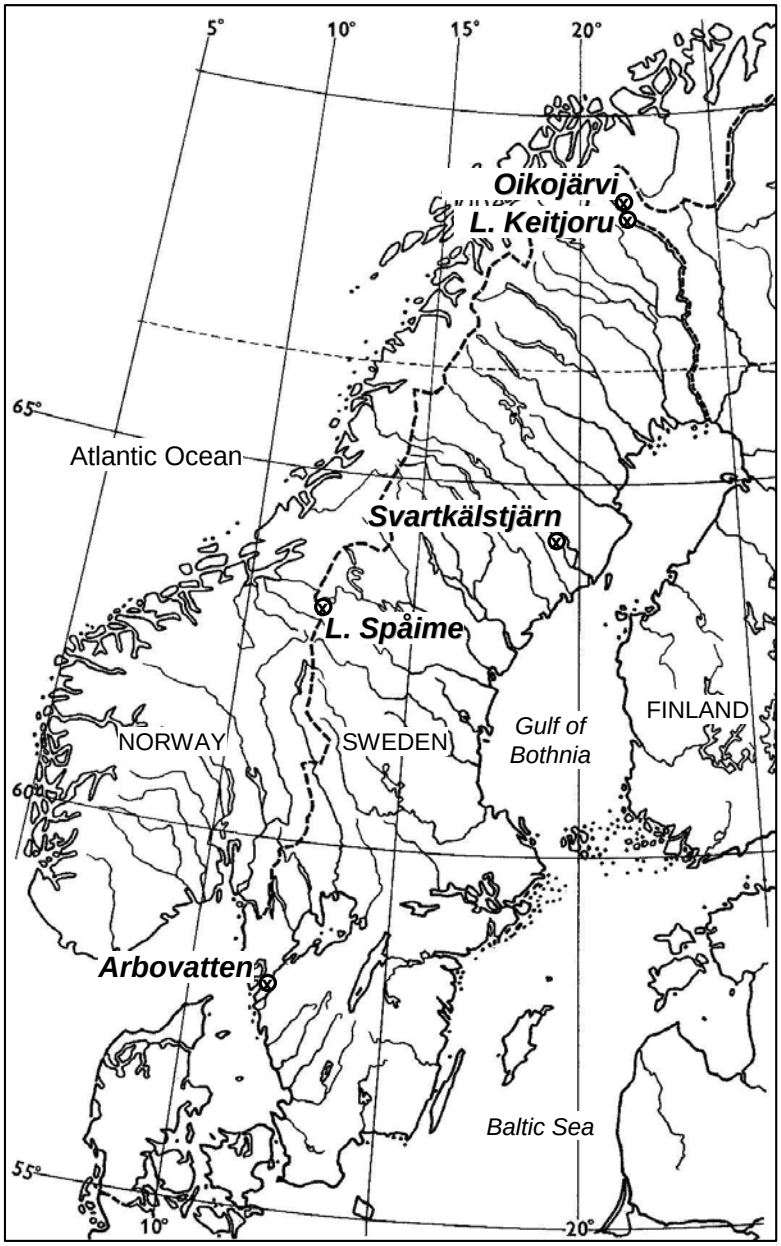

Figure 5-1. Map of Fennoscandia showing the location of study sites.

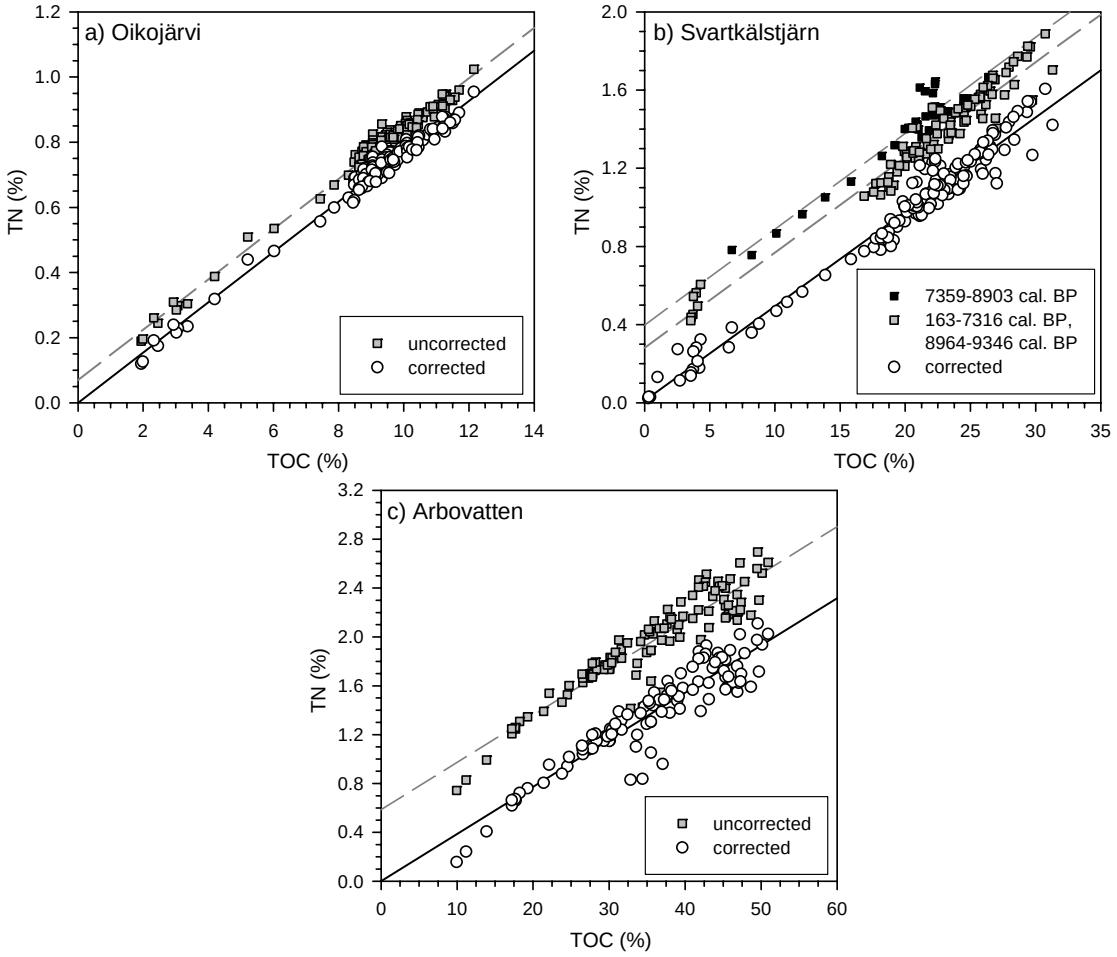

Figure 5-2. TN-TOC regression plots to correct for inorganic nitrogen (see Talbot, 2001). a) For Oikojärvi sediments, a correction of *c.* 0.1% was made to the TN content. b) For Svartkälstjärn sediments, a correction of *c.* 0.4 % was adjusted to the sequence between 4.71 and 5.15 m (7359-8903 cal. BP), as indicated by black squares. A correction of *c.* 0.3 % was made to the TN content at 5.16-5.22 m (8964-9346 cal. BP) and 4.69-3.24 m (163-7316 cal. BP), shown by the grey squares. No correction was needed for the remaining data, which are shown together with corrected values as open circles. c) For Arbovatten sediments, a correction of *c.* 0.6 % was made to the TN content.

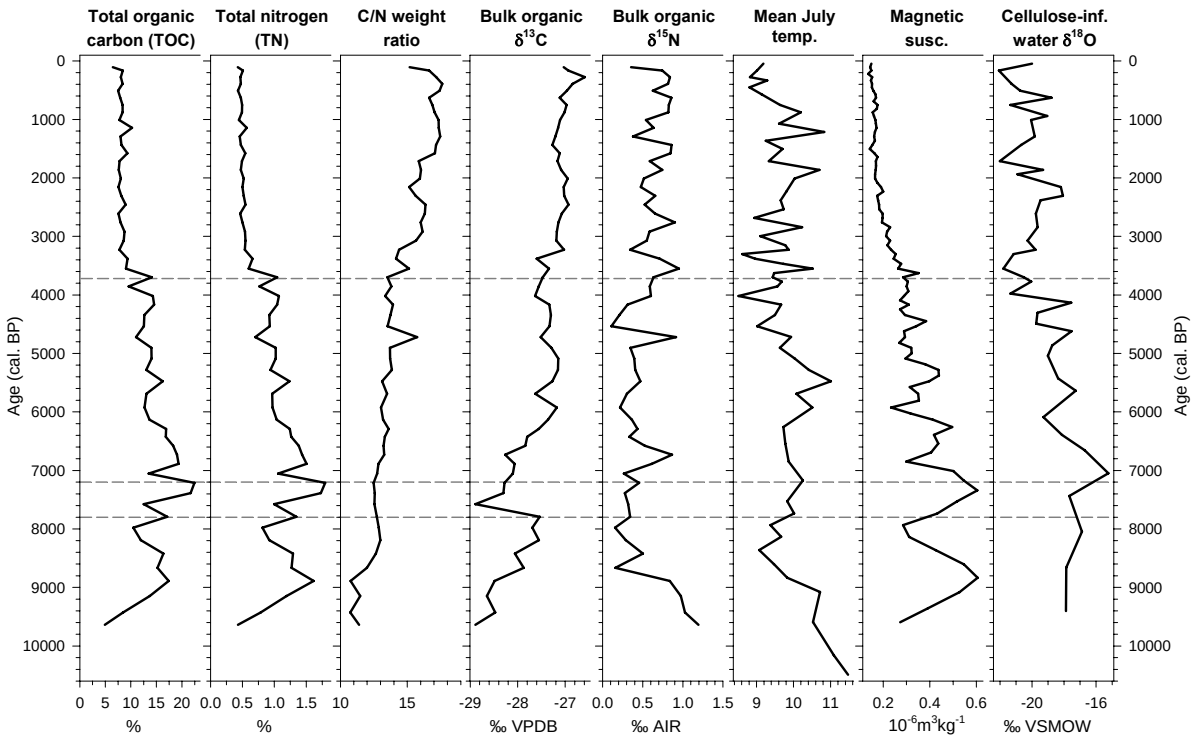

Figure 5-3. Lake Spåime records of total organic carbon content (TOC), total nitrogen content (TN), C/N weight ratio, $\delta^{13}C$ and $\delta^{15}N$ of bulk organic material, magnetic susceptibility and cellulose-inferred lake water $\delta^{18}O$. The mean July temperature record is reconstructed from chironomid head capsules obtained from the same core (Hammarlund *et al.*, 2004, Velle *et al.*, 2005). Grey horizontal lines highlight key changes in lake productivity inferred from the organic matter content. The horizon marked at *c.* 3700 cal. BP denotes timing of tree-limit descent.

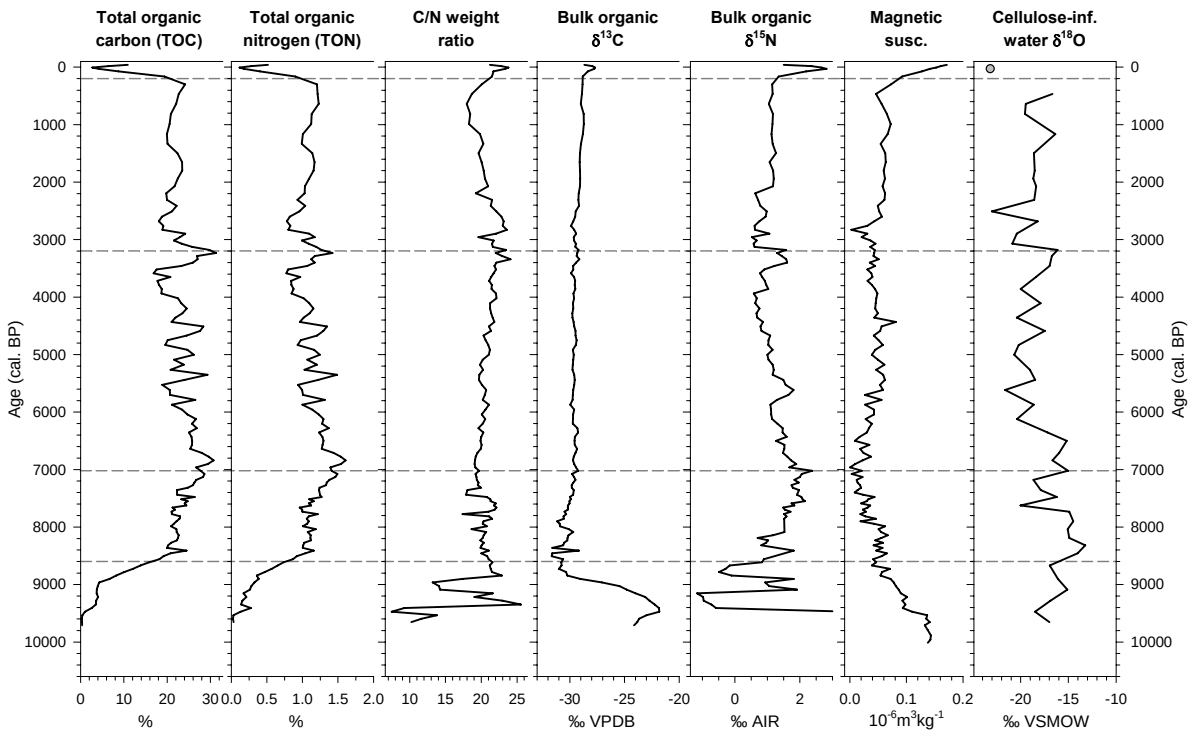

Figure 5-4. Svartkälstjärn records of total organic carbon content (TOC), total organic nitrogen content (TON), C/N weight ratio, $\delta^{13}C$ and $\delta^{15}N$ of bulk organic material, magnetic susceptibility, and cellulose-inferred lake water $\delta^{18}O$. The grey-filled circle represents a possible outlier in the cellulose $\delta^{18}O$ data due to terrestrial contaminants. Lake sediment TON and C/N ratios have been corrected for inorganic N content (Figure 5-2b). Grey horizontal lines mark changes in lake productivity based on organic matter content and changes in catchment vegetation.

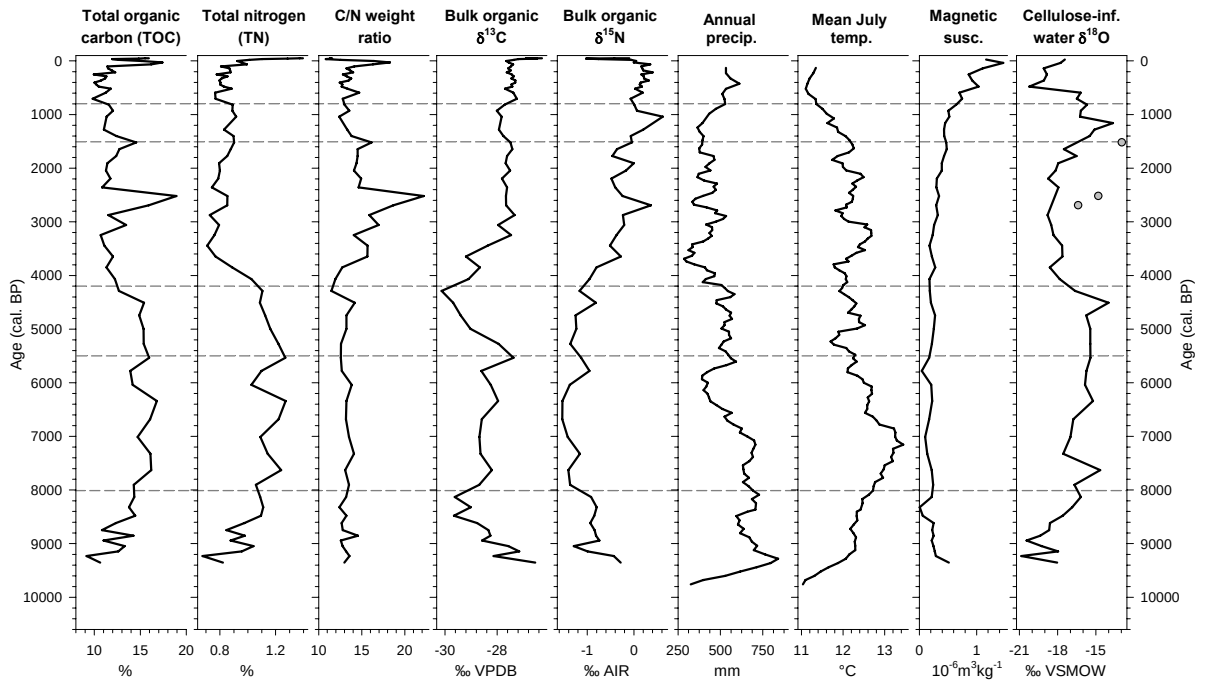

Figure 5-5. Lake Keitjoru records of total organic carbon content (TOC), total nitrogen content (TN), C/N weight ratio, $\delta^{13}C$ and $\delta^{15}N$ of bulk organic material, magnetic susceptibility, and cellulose-inferred lake water $\delta^{18}O$. Grey-filled circles represent likely outliers in the cellulose $\delta^{18}O$ data possibly due to terrestrial contaminants. The 5-point running average of annual precipitation and mean July temperature records are based on pollen reconstructions from Lake Tsuolbmajavri, Finland (Seppä and Birks, 2001). Grey horizontal lines mark changes in lake productivity inferred from the organic matter content and changes in nutrient cycling based on the $\delta^{13}C$ profile.

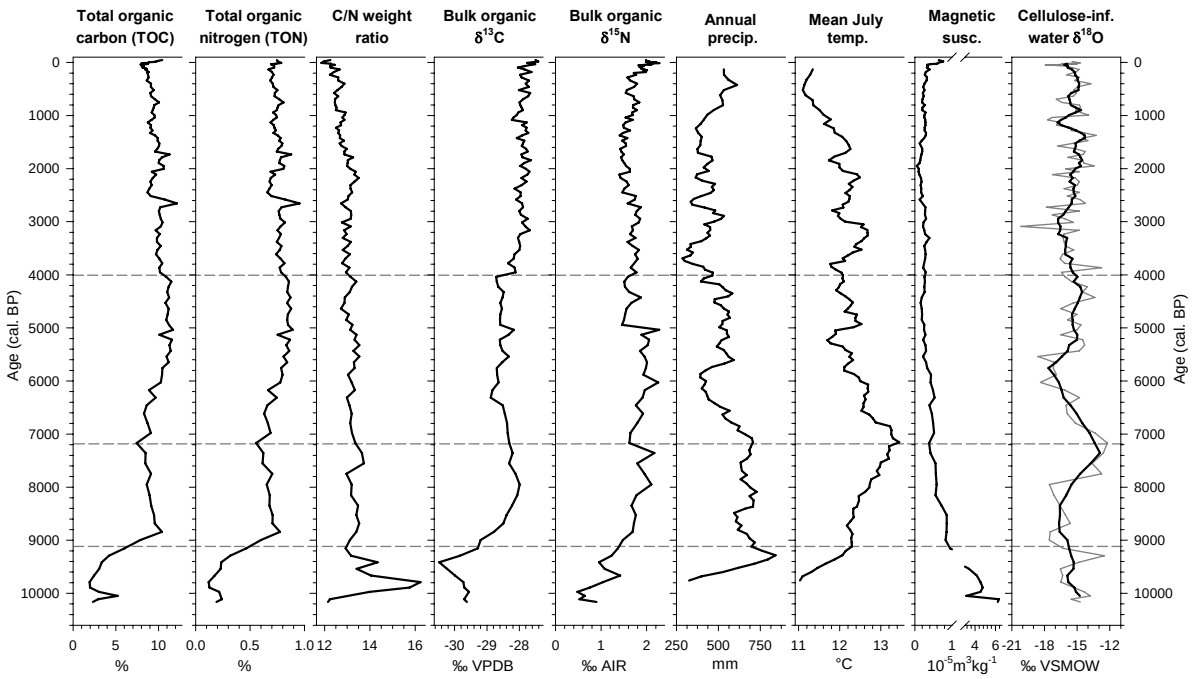

Figure 5-6. Oikojärvi records of total organic carbon content (TOC), total organic nitrogen content (TON), C/N weight ratio, $\delta^{13}C$ and $\delta^{15}N$ of bulk organic material, magnetic susceptibility, and cellulose-inferred lake water $\delta^{18}O$. The 5-point running average of annual precipitation and mean July temperature records are based on pollen reconstructions from Lake Tsuolbmajavri, Finland (Seppä and Birks, 2001). The thick line in $\delta^{18}O$ profile is the 5-point running average through the data. Lake sediment TON and C/N ratios have been corrected for inorganic N content (Figure 5-2a). For visual purposes, the lower half of the scale for magnetic susceptibility has been exaggerated. Grey horizontal lines mark changes in lake productivity inferred from changes in the organic matter content and C/N ratios.

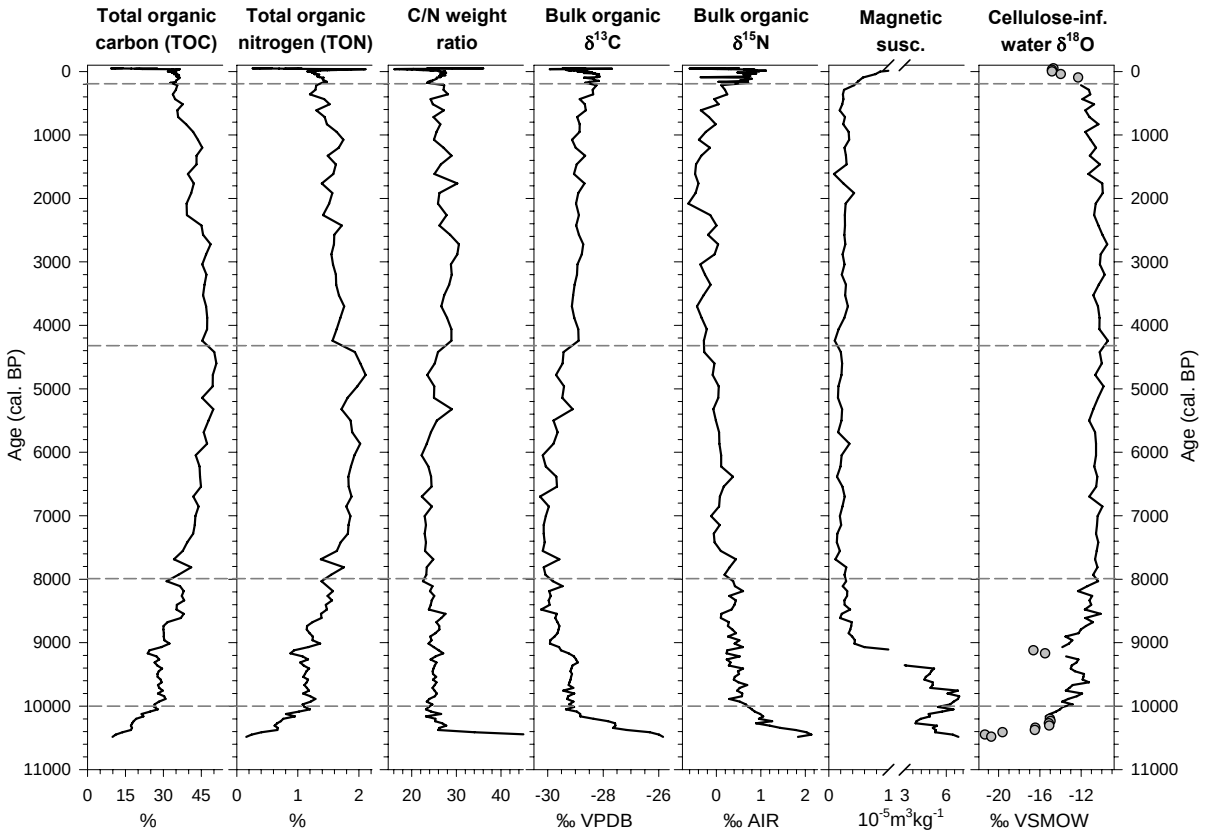

Figure 5-7. Arbovatten records of total organic carbon content (TOC), total organic nitrogen content (TON), elemental C/N ratio, $\delta^{13}C$ and $\delta^{15}N$ of bulk organic material, magnetic susceptibility, and cellulose-inferred lake water $\delta^{18}O$. Grey-filled circles represent suspect cellulose $\delta^{18}O$ data possibly due to unknown contaminants. Lake sediment TON and C/N ratios have been corrected for inorganic N content (Figure 5-2c). For visual purposes, the lower half of the scale for magnetic susceptibility has been exaggerated. Grey horizontal lines mark changes in lake productivity as inferred from the organic matter content.

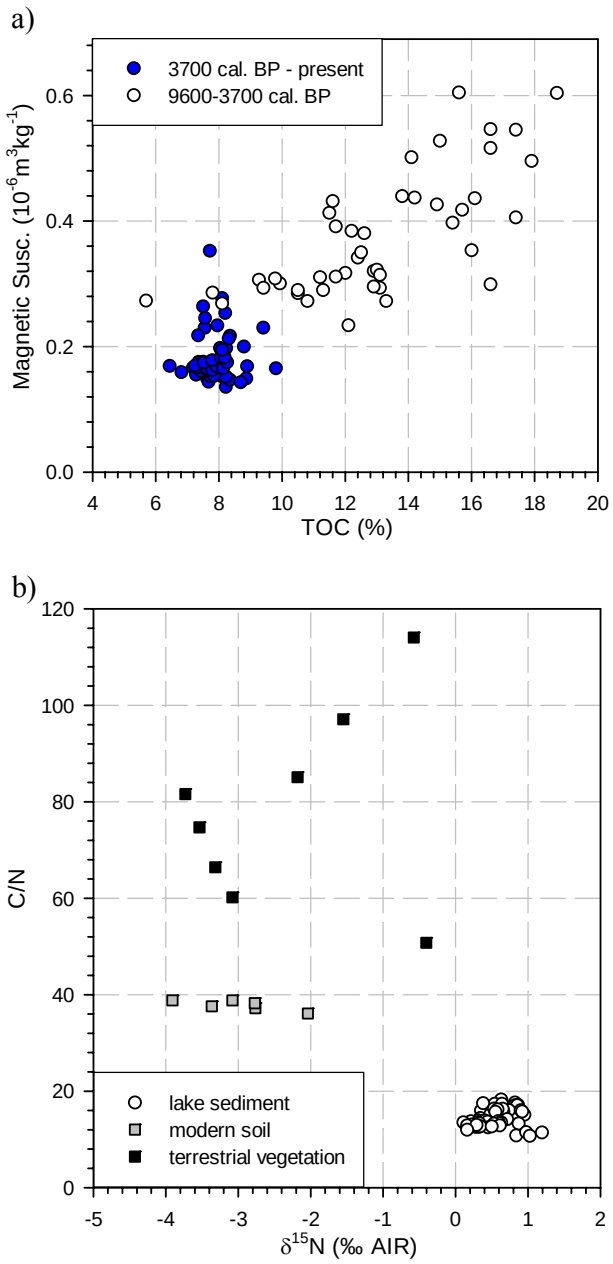

Figure 5-8. Lake Spåime geochemical and mineral magnetic relationships shown in crossplots of a) magnetic susceptibility versus the total organic carbon (TOC) content, displaying a positive linear relationship for sediments during the early to-mid-Holocene, indicating an autochthonous origin for the magnetic material (Snowball *et al.*, 2002), and a non-linear relationship in sediments deposited during the late Holocene, and b) C/N versus bulk organic $\delta^{15}N$ for samples of lake sediments, modern soil and terrestrial vegetation. Catchment-derived organic matter is likely not a contributing factor in lake sediments, since the lake sediment has a much lower C/N and higher $\delta^{15}N$ than the modern soil and vegetation (Hammarlund *et al.*, 2004).

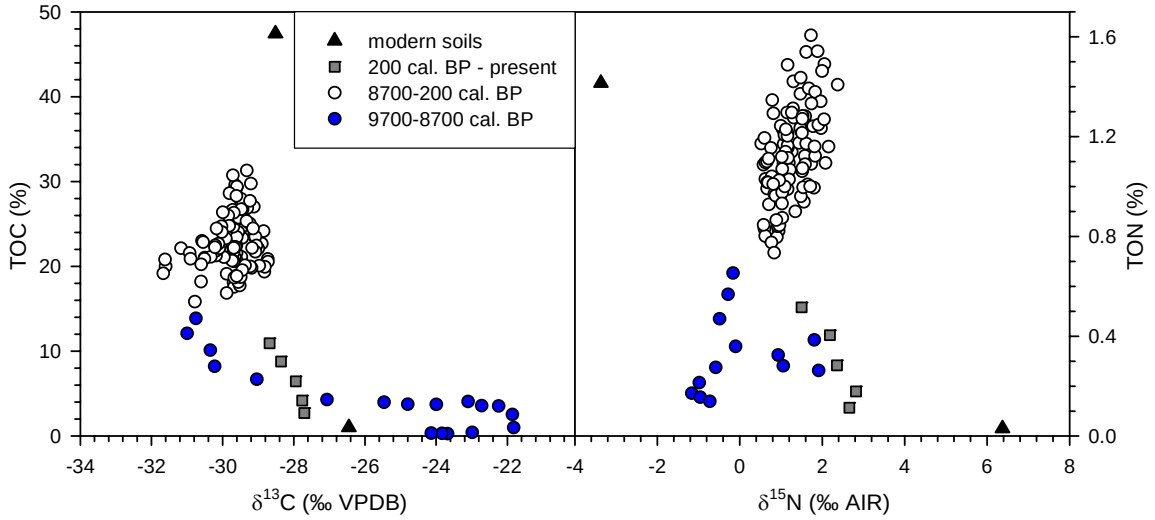

Figure 5-9. Crossplots of elemental and isotopic data from Svartkälstjärn sediments and modern soils collected in the catchment. Both plots show a separation between sediments (8700-200 cal. BP) and modern soils, whereas the early Holocene and after 200 cal. BP, sediments show a trend towards the elemental and isotopic compositions characteristic of mineral soil (see Table 5-1).

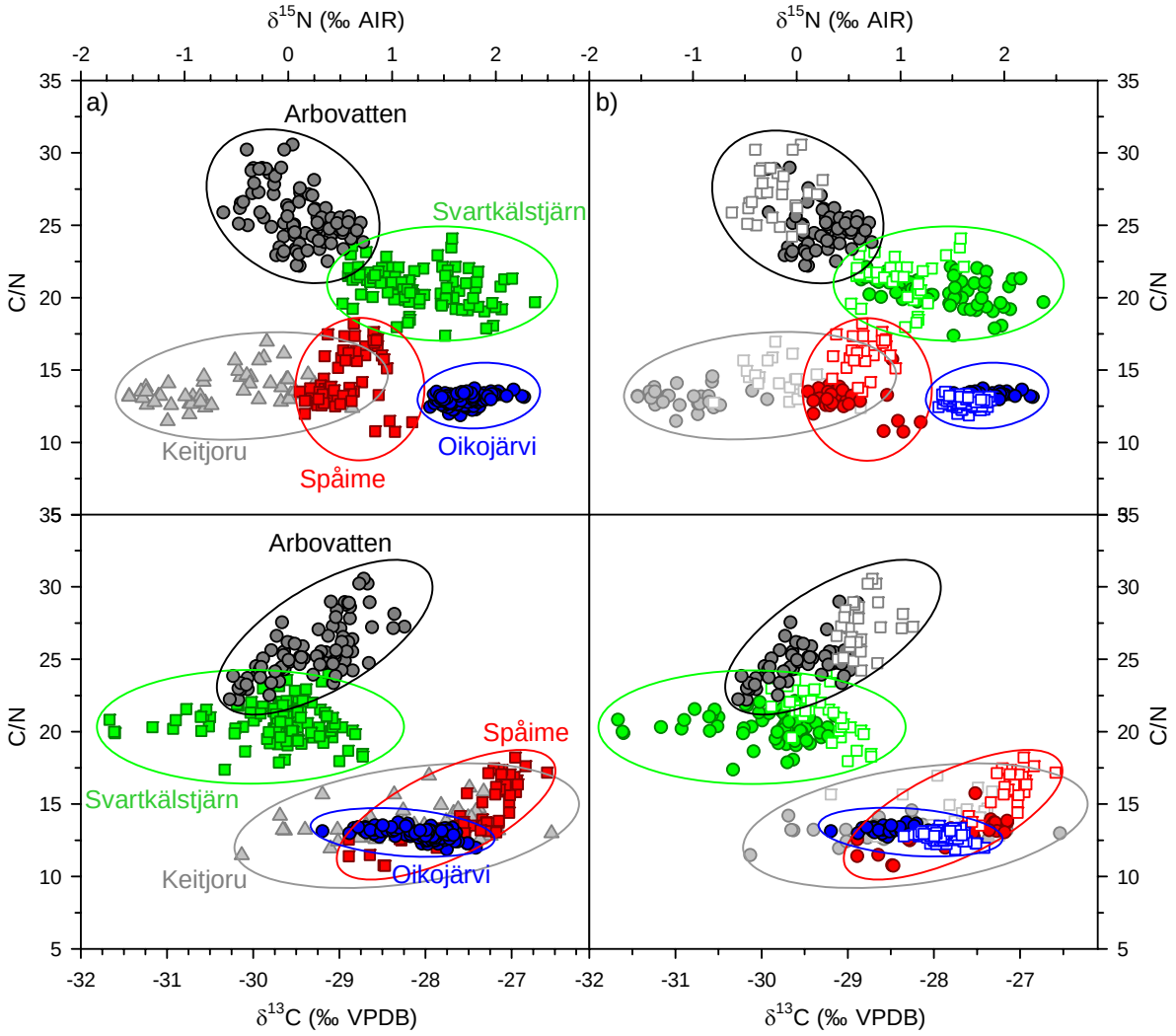

Figure 5-10. a) Comparison between the bulk organic $\delta^{13}C$ and $\delta^{15}N$ with C/N ratios in lake sediments from Lake Spåime, Lake Keitjoru, Arbovatten, Oikojärvi, and Svartkälstjärn throughout the Holocene. b) The same data points as in a), but with solid circles corresponding to values before 4000 cal. BP and open squares refer to the period after 4000 cal. BP to reflect the timing of significant changes in vegetation and climate in Fennoscandia.

Chapter 6
Summary and Synthesis

6.1 Summary of significant results

Chapters 2, 3, and 4 of this dissertation have focused on investigations of Holocene atmospheric circulation in Fennoscandia using oxygen–isotope records of lake sediment cellulose, combined with independent multi-proxy data. Chapter 5 focused on carbon and nitrogen elemental and isotopic records obtained from organic lake sediments, revealing changes in the nutrient cycling within the lakes under study in response to changes in atmospheric circulation. The results contribute to the multidisciplinary research programme HYDRO-ISO-CLIM (Hydrological and Meteorological Analysis of Precipitation Isotopic Composition as a Key to Present and Past Climates) funded by the Swedish Research Council.

In Chapter 2, two throughflow lakes with differing residence times, situated within the same climate region in northern Fennoscandia, provide contrasting records of lake water $\delta^{18}O$. The sediment cellulose-inferred $\delta^{18}O$ record from Lake Keitjoru provided information on changes in the seasonal distribution of precipitation type allowing winter precipitation to be quantitatively reconstructed by comparison with an independent record of pollen-inferred annual precipitation from Lake Tsuolbmajavri (Seppä and Birks, 2001). The Oikojärvi cellulose-inferred lake water $\delta^{18}O$ record reflects changes in water balance, such that the separation between Oikojärvi $\delta^{18}O$ and Lake Tibetanus $\delta^{18}O$ (Hammarlund *et al.*, 2002) provides a first-order approximation of evaporative enrichment in summer. Integration of the two reconstructions revealed changes in atmospheric circulation modes (zonal versus meridional) for winter and summer. In Chapter 3, two throughflow lakes were compared along a west-east gradient across central Sweden. The $\delta^{18}O$ record from Lake Spåime, located in the Scandes Mountains, is believed to reflect variations in the seasonal distribution of precipitation, which is directly governed by influences of air masses from the North Atlantic. In contrast, the $\delta^{18}O$ record from Svartkälstjärn, situated closer to the east coast of Sweden, reflects a more continental setting with strong influences from air masses traversing

the Baltic Sea. In Chapter 4, the Arbovatten cellulose-inferred lake water $\delta^{18}O$ record from southern Sweden is compared with corresponding reconstructions based on the Lake Spåime cellulose $\delta^{18}O$ record and the Lake Tibetanus carbonate $\delta^{18}O$ record, both situated in the Scandes Mountains. Changes in the offset from the modern Dansgaard (1964) $\delta^{18}O$-temperature relation during the Holocene are reconstructed with the use of independent proxy-inferred temperature records from the respective sites. In addition, the separation between the Lake Igelsjön carbonate $\delta^{18}O$ record (Hammarlund et al., 2003) and the Arbovatten cellulose $\delta^{18}O$ record provided a first-order approximation of evaporative enrichment in ^{18}O of lake water at Lake Igelsjön.

This research probes the possible existence of non-temperature-dependent variability during the Holocene in $\delta^{18}O$ of precipitation inferred from a lacustrine carbonate $\delta^{18}O$ record from Lake Tibetanus, northernmost Sweden by Hammarlund *et al.* (2002). These authors suggested that atmospheric circulation during the early Holocene was characterized by strong westerlies, which efficiently transported moisture across the Scandes Mountains, thus reducing the isotopic distillation of precipitation. High summer insolation, warmer sea surface temperatures and reduced sea ice extent at this time (Koç *et al.*, 1993) were suggested to be the primary drivers of the inferred atmospheric circulation patterns during the early Holocene. The subsequent gradual decline in precipitation $\delta^{18}O$ and the approach towards a modern temporal $\delta^{18}O$-temperature relation at Lake Tibetanus in the mid-Holocene was attributed to the attenuation of westerlies, resulting in increased continentality and greater isotopic distillation of precipitation. Together with studies showing similar long-term decreasing trends in precipitation $\delta^{18}O$ in northern Fennoscandia during the Holocene (e.g. Lauritzen and Lundberg, 1999; Shemesh et al., 2001; Hammarlund and Edwards, 2008) these data provide evidence of regionally coherent changes in $\delta^{18}O$ of precipitation that appear strongly linked to millennial-scale atmospheric circulation dynamics across the North Atlantic. Intriguingly, both positive (Lake Spåime) and negative (Arbovatten) offsets from the modern $\delta^{18}O$-temperature relation have been detected during the early Holocene, attributable to circulation-dependent effects, with both approaching the modern relation by the mid-Holocene. In addition, the cellulose-inferred lake water $\delta^{18}O$ records from the

northern (Lake Keitjoru, Oikojärvi) and central (Lake Spåime, Svartkälstjärn) sites in Fennoscandia reveal higher-frequency variability in atmospheric circulation that are also attributable to changes in the dominant modes of flow (zonal and meridional) in winter and summer during the Holocene.

In Chapter 5, the carbon and nitrogen elemental and isotopic records obtained on lake-sediment organic matter from each site (lakes Spåime, Oikojärvi, Keitjoru, Svartkälstjärn and Arbovatten) were examined in the light of accompanying records of magnetic susceptibility and cellulose $\delta^{18}O$. Site-specific variations in carbon and nitrogen nutrient cycling in the lakes are believed to be primarily controlled by lake productivity, vegetational composition in the catchment, water residence time, and delivery of nutrients into the lakes, all of which vary in response to climate forcing. Carbon and nitrogen nutrient balance changed in concert with significant declines in the altitudinal and latitudinal tree-limits and the spread of *Picea abies* and wetlands after *c.* 4000 cal. BP, probably in response to changes in atmospheric circulation. Specifically, nutrient balances were likely affected by increases in snow contributions and higher-frequency variability between wet and dry summers. At about this time there was also a general decline in lake productivity due to gradual cooling and shortening of the growing season. At present, Fennoscandian climate is characterized by relatively mild and wet winters (Lindström and Alexandersson, 2004), but if on-going warming at high latitudes persists, then reduction in snow contributions and lengthening growing season are likely to result in increased lake productivity, increased catchment vegetation and soil development, and enhanced influx of catchment-derived nutrients. This may lead to increased organic matter accumulation in lake sediments.

6.2 Synthesis

6.2.1 Atmospheric circulation and teleconnections

The cellulose records from Lake Spåime, Svartkälstjärn, and Oikojärvi in this study and the carbonate record from Lake Tibetanus (Hammarlund *et al.*, 2002) provide evidence of elevated $\delta^{18}O$ values of precipitation in relation to temperature during the early Holocene (10,000-6000 cal. BP), and similar signals have been found in central Canada during the same time frame (Edwards *et al.*, 1996). A common feature in both northern Fennoscandia

and central Canada is that air masses from the North Atlantic and the Pacific, respectively, must traverse across a topographic barrier (i.e., the Scandes and the Cordillera), hence affecting the transport efficiency and isotopic distillation of moisture that contributes to precipitation. Analogous effects are also seen in paleo isotope-climate relations in western Canada over the past millennium (Edwards *et al.*, 2008), as well as in modern precipitation (Birks, 2003), reflecting circulation-dependent effects on the precipitation and isotope shadows in the lee of the Cordillera. The elevated $\delta^{18}O$-temperature relations during the early Holocene in both northern Fennoscandia and central Canada likely reflect hemispheric teleconnections patterns in climate variability analogous to the Northern Hemisphere Annular Mode (Thompson and Wallace, 2001).

The results of the Arbovatten record are particularly intriguing because it shows low $\delta^{18}O$ values in relation to temperature in the early Holocene. The lack of a topographic barrier upwind of the site suggests that these isotope-climate signals are being directly transferred from the North Atlantic. This is supported by the similarity with the GRIP $\delta^{18}O$ ice core record, including the "8.2 kyr cold event" (Alley *et al.*, 1997), which has also been recorded in various proxies in the northern Europe (von Grafenstein *et al.*, 1998, 1999; McDermott *et al.*, 2001; Nesje *et al.*, 2001; Snowball *et al.*, 2002; Veski *et al.*, 2004; Hammarlund *et al.*, 2005; Seppä *et al.*, 2005). This event is attributed to the final draining of Lake Agassiz, resulting in weakening or temporary shutdown of the thermohaline circulation in the North Atlantic and an increase in sea-ice cover in the Nordic Seas (Barber *et al.*, 1999; Renssen *et al.*, 2002; Fisher *et al.*, 2002). Judging by the oxygen-isotope evidence in Arbovatten, this cold event had a profound influence in southern Sweden, likely because of a sudden weakening of the zonal atmospheric flow pattern and its replacement by dominantly anticyclonic circulation during the winter (Veski *et al.*, 2004). Evidence of such a circulation shift is also suggested, albeit less strongly, by the winter precipitation reconstruction from Lake Keitjoru in northern Fennoscandia.

The variability in winter atmospheric circulation inferred from the Lake Keitjoru $\delta^{18}O$ record and the high-frequency variability illustrated in the crossplot of Lake Spåime $\delta^{18}O$ versus Svartkälstjärn $\delta^{18}O$ appear to coincide with intervals of rapid climate change events defined by Mayewski *et al.* (2004) at 9000-8000, 6000-5000, 4200-3800, 3500-2500, 1200-

1000, and 600-150 cal. BP. These intervals are characterized by polar cooling and major atmospheric circulation changes that seem to recur at approximately 2500 and 1500-year intervals (Denton and Karlén, 1973; O'Brien *et al.*, 1995; Bond *et al.*, 1997, 2001; Mayewski *et al.*, 2004). It is suggested that Holocene climate varied in response to solar variability superimposed on long-term changes in insolation (Denton and Karlén, 1973; Bond *et al.*, 2001). The climate change events at 6000-5000, 3500-2500 and 600-150 cal. BP, evident in the cellulose $\delta^{18}O$ records, are associated with winter meridional circulation patterns as inferred from high concentrations of sea salt and terrestrial dust in the GISP2 ice core (O'Brien *et al.*, 1995), and coincide with periods of increased ice-rafting (Bond *et al.*, 1997) and low solar irradiance (Mayewski *et al.*, 2004). The climatic development at 4200-3800 cal. BP is accompanied by major changes in the carbon and nitrogen elemental and isotope records from the lakes in this study, as well as by a decline in $\delta^{18}O$ of precipitation at lakes Keitjoru and Spåime, and decreased evaporative enrichment at lakes Oikojärvi and Igelsjön. There is no evidence of solar forcing during this interval (Mayewski *et al.*, 2004). A peak in ice-rafted debris at about 4200 cal. BP (Bond et al., 1997), which reflects a period of surface ocean cooling, may indicate a tight coupling between ocean and atmosphere circulation dynamics at this time.

6.2.2 Oxygen isotopes in lake sediment cellulose

A common feature of the lakes studied in this research is the systematically lower cellulose-inferred water $\delta^{18}O$ values obtained from core-top sediments than actual measured lake water $\delta^{18}O$ values (Figure 6-1). As shown in Figure 6-1, the average cellulose-inferred lake water $\delta^{18}O$ values for core-top sediments are as much as 5‰ more depleted than the average isotopic composition of waters sampled in the lakes, whereas sediment samples may represent up to several hundred years of deposition. This is in contrast to other studies of lakes having higher rates of sedimentation, where there is less potential for a temporal mismatch between the time of cellulose production and the lake water sampling (Wolfe *et al.*, 2005, 2007, 2008). Although the isotope hydrological monitoring of the lakes has provided essential insight for interpreting the paleorecords, proper field-testing of the cellulose-water fractionation factor would require much more detailed field sediment sampling. On the other

hand, the abundant analyses of sediment from numerous lakes in North America (e.g., Edwards and McAndrews, 1989; MacDonald *et al.*, 1993; Wolfe *et al.*, 1996; Sauer *et al.*, 2001; Birks *et al.*, 2007) and elsewhere (e.g., Wolfe *et al.*, 2000, 2001b, 2003; Klisch *et al.*, 2007), as well as recent culture studies (Yi, 2008), support the continued use of the constant cellulose-water fractionation factor of 1.028.

The difference between the cellulose-inferred lake water $\delta^{18}O$ from the core-top sediments and measured lake water $\delta^{18}O$ may be attributable to rapidly changing hydrological conditions over the recent past (Figure 6-1). For example, lakes Keitjoru and Oikojärvi $\delta^{18}O$ core-top cellulose samples reflects lake water isotopic composition in the 1970s, whereas modern lake water samples represent the period of 2002-2006. This span of time encompasses considerable change in climate in the North Atlantic region since the 1980s in response to a more persistent positive index phase of the North Atlantic Oscillation in winter, as deduced from long instrumental records (Hurrell, 1995).

In addition, the cellulose $\delta^{18}O$ records from the five sites may be incorporating effects of ^{18}O-depleted lake waters in spring. To illustrate this effect, the respective minimum lake water $\delta^{18}O$ values during the spring are compared with the cellulose $\delta^{18}O$ values (Figure 6-1), revealing a better fit than for average water $\delta^{18}O$ values. Indeed, lakes with short water residence times (i.e., lakes Keitjoru and Spåime) show the largest shift between the average and spring lake water $\delta^{18}O$ compared to lakes with longer residence times (i.e., lakes Oikojärvi, Arbovatten, and Svartkälstjärn). Oikojärvi, in particular, is a large lake with a relatively large catchment that naturally damps much of the seasonal variability in precipitation $\delta^{18}O$ and hence is unlikely to record a strongly ^{18}O-depleted snowmelt signal in cellulose $\delta^{18}O$.

6.3 Recommendations for future research

This research demonstrates the usefulness and significance of applying a multiproxy approach to reconstructing past climate, especially in combining proxies that reflect varying aspects of the climate system at seasonal to millennial scales. An opportunity exists to develop records at higher frequency over the past millennium to assess rates of change occurring at human timescales, and for predicting future climate change. This includes

sediment gravity cores from lakes Keitjoru, Oikojärvi and Arbovatten that can still be analyzed for cellulose $\delta^{18}O$ and other proxies. Additional gravity cores could also be collected at various sites in Fennoscandia, for which interpretations of atmospheric circulation can be compared and further constrained with meteorological records (e.g., Bergström and Moberg, 2002; Moberg *et al.*, 2002) and paleoarchives (e.g., speleothems – Lauritzen and Lundberg, 1999; tree-rings records – Linderholm and Gunnarson, 2005; lake sediments – Rosqvist *et al.*, 2007; etc.).

During future fieldwork to obtain sediment cores, it would also be of value to conduct detailed process studies of the links between cellulose $\delta^{18}O$ and lake water $\delta^{18}O$. For example, artificial substrates, which are made of plastic or other materials that can be substituted for the natural lake bottom (Johan Wiklund, personal communication), could be used as a follow-up to aquarium culture experiments (e.g., Yakir and DeNiro, 1990; Sauer *et al.*, 2001; Yi, 2008).

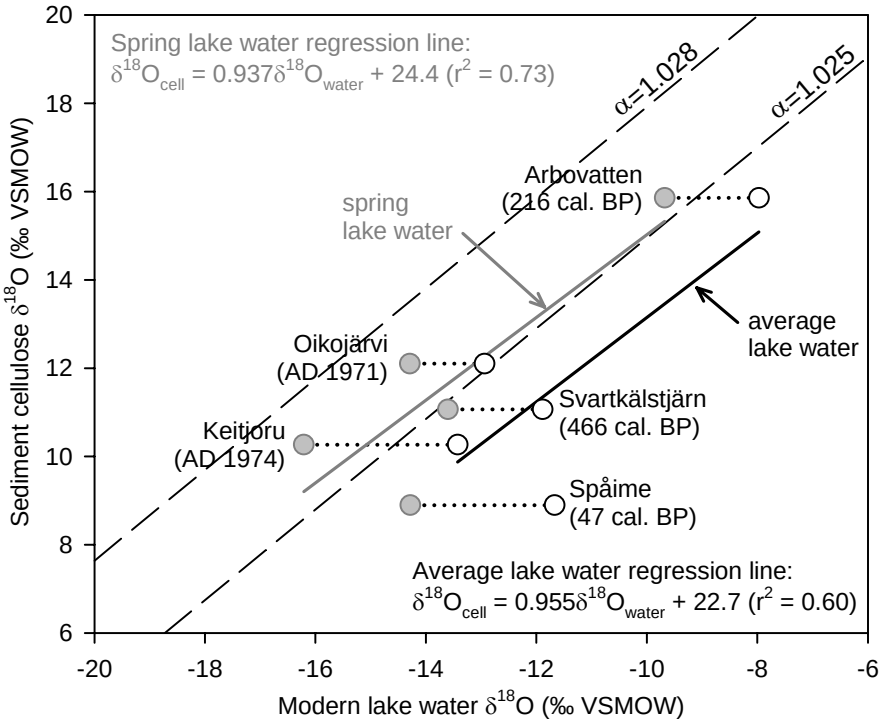

Figure 6-1. Comparison between the topmost sediment cellulose $\delta^{18}O$ and modern lake water $\delta^{18}O$ using measured average (open circles) and minimum spring (grey-filled circles) values for each lake. For reference, constant cellulose-water fractionation lines are shown for factors of 1.028 and 1.025. The middle age value for the topmost sediment cellulose $\delta^{18}O$ data are given in parentheses. The offset between inferred and measured lake water composition probably reflects ongoing decreases in the proportion of snowmelt related to recent climate change.

Appendix A – Modern Isotope Hydrology Data

Samples of lake water are taken at the surface, except for those stated otherwise.

Lake Keitjoru, Northern Sweden (68º40'N, 21º30'E)

Date	Sample Type	$\delta^{18}O$	$\delta^{2}H$
Aug. 21, 2002	Lake, east shore	-13.44	-96.8
Aug. 23, 2002	Lake, centre	-13.45	-96.9
Aug. 23, 2002	Lake, northeast shore	-13.32	-95.9
Sep. 02, 2002	Lake	-12.89	-94.3
Oct. 04, 2002	Lake	-13.28	-95.6
Nov. 01, 2002	Lake	-13.25	-95.0
Jan. 04, 2003	Lake	-13.00	-94.4
May. 15, 2003	Lake, depth 0.8m	-15.55	-109.2
May. 15, 2003	Lake, depth 1.5m	-14.93	-104.2
Jun. 07, 2003	Lake	-12.36	-92.0
Jul. 04, 2003	Lake	-12.27	-92.0
Aug. 01, 2003	Lake	-12.30	-91.7
Sep. 07, 2003	Lake	-13.05	-95.6
Oct. 04, 2003	Lake	-13.17	-94.3
Nov. 07, 2003	Lake	-13.35	-96.1
Jan. 02, 2004	Lake	-13.18	-94.6
Mar. 01, 2004	Lake	-13.29	-94.4
Apr. 07, 2004	Lake	-13.23	-94.5
May. 05, 2004	Lake	-16.21	-116.9
Jun. 04, 2004	Lake	-14.82	-106.8
Jul. 03, 2004	Lake	-14.45	-102.7
Aug. 05, 2004	Lake	-13.04	-93.6
Sep. 02, 2004	Lake	-12.63	-90.1
Oct. 03, 2004	Lake	-12.89	-90.4
Nov. 05, 2004	Lake	-13.07	-91.4
Jan. 07, 2005	Lake	-13.26	-93.1
Mar. 08, 2005	Lake	-13.10	-92.4
Apr. 10, 2005	Lake	-13.05	-91.8

May. 06, 2005	Lake	-13.22	-94.5
Jun. 01, 2005	Lake	-14.73	-106.8
Aug. 08, 2005	Lake	-13.98	-103.1
Jul. 13, 2006	Lake	-14.01	-100.5
Jul. 14, 2006	Lake	-13.84	-99.7
Aug. 23, 2002	Outlet	-13.49	-96.9
May. 14, 2003	Outlet	-15.64	-111.2
Aug. 21, 2002	Inlet	-13.54	-96.1
May. 14, 2003	Inlet	-16.12	-118.9
May. 14, 2003	Inlet	-15.75	-111.9
Jul. 14, 2006	Inlet	-13.25	-95.6
Aug. 23, 2002	Groundwater	-13.93	-99.7
May. 14, 2003	Groundwater	-15.77	-116.1
May. 14, 2003	Snowpack	-19.56	-137.6
Aug. 21, 2002	Closed basin lake, 600m SW of Naimakka	-8.41	-74.3

Oikojärvi, Northern Finland (68°50’N, 21°10’E)

Date	Sample Type	$\delta^{18}O$	$\delta^{2}H$
Aug. 22, 2002	Lake	-12.27	-93.5
Aug. 22, 2002	Lake	-12.29	-93.9
Aug. 22, 2002	Lake, depth 2.5m	-12.35	-94.1
Aug. 22, 2002	Lake, depth 7m	-12.43	-94.2
Sep. 02, 2002	Lake	-11.97	-92.9
Oct. 04, 2002	Lake	-11.97	-93.1
Nov. 03, 2002	Lake	-12.33	-94.2
Jan. 04, 2003	Lake	-12.78	-97.6
Mar. 03, 2003	Lake	-12.89	-97.9
May. 16, 2003	Lake, depth 1.0m	-13.13	-98.1
May. 16, 2003	Lake, depth 3.0m	-12.87	-96.6
May. 16, 2003	Lake, depth 7.5m	-13.02	-96.5
Jun. 06, 2003	Lake	-13.25	-99.2
Jul. 04, 2003	Lake	-12.05	-93.3
Aug. 01, 2003	Lake	-12.15	-92.1
Sep. 07, 2003	Lake	-11.80	-91.9

Oct. 07, 2003	Lake	-11.95	-91.0
Nov. 07, 2003	Lake	-12.56	-94.8
Jan. 02, 2004	Lake	-12.64	-95.7
Mar. 01, 2004	Lake	-12.56	-95.5
Apr. 07, 2004	Lake	-12.63	-95.9
May. 06, 2004	Lake	-13.70	-102.1
Jun. 04, 2004	Lake	-14.01	-103.9
Jul. 03, 2004	Lake	-13.18	-98.1
Aug. 05, 2004	Lake	-12.68	-92.9
Sep. 02, 2004	Lake	-12.50	-92.0
Oct. 03, 2004	Lake	-12.65	-91.8
Nov. 05, 2004	Lake	-13.51	-97.3
Jan. 07, 2005	Lake	-13.56	-97.4
Mar. 08, 2005	Lake	-13.54	-98.0
Apr. 10, 2005	Lake	-13.34	-98.9
May. 06, 2005	Lake	-14.29	-103.8
Jun. 12, 2005	Lake	-13.50	-103.1
Aug. 06, 2005	Lake	-13.68	-103.4
Jul. 05, 2006	Lake	-13.61	-100.8
Jul. 05, 2006	Lake, depth 3m	-13.63	-100.7
Jul. 05, 2006	Lake, depth 7m	-13.70	-101.8
Jul. 13, 2006	Lake	-13.49	-99.7
Aug. 23, 2006	Lake	-12.52	-94.8
Aug. 23, 2006	Lake, depth 4m	-12.55	-95.2
Aug. 23, 2006	Lake, depth 8m	-13.03	-98.5
May. 16, 2003	Outlet	-12.71	-95.5
May. 16, 2003	Snowpack	-14.44	-104.9

Könkämäälven at Naimmakka, Northern Sweden

Date	Sample Type	$\delta^{18}O$	$\delta^{2}H$
Aug. 21, 2002	River	-12.81	-94.4
Sep. 02, 2002	River	-12.52	-90.0
Oct. 04, 2002	River	-12.84	-94.9
Nov. 01, 2002	River	-13.19	-97.3

Jan. 04, 2003	River	-13.91	-101.3
Mar. 02, 2003	River	-14.47	-105.5
May. 15, 2003	River	-14.61	-105.6
Jun. 07, 2003	River	-12.59	-91.8
Jul. 04, 2003	River	-12.54	-91.5
Aug. 01, 2003	River	-12.65	-91.4
Sep. 07, 2003	River	-12.46	-91.9
Oct. 04, 2003	River	-12.89	-94.1
Nov. 07, 2003	River	-13.14	-96.4
Jan. 02, 2004	River	-13.41	-97.6
Mar. 01, 2004	River	-13.65	-98.7
Apr. 07, 2004	River	-13.67	-100.0
May. 05, 2004	River	-15.51	-113.1
Jun. 04, 2004	River	-14.11	-102.4
Jul. 03, 2004	River	-13.60	-96.7
Aug. 05, 2004	River	-12.93	-93.1
Sep. 02, 2004	River	-12.79	-92.2
Oct. 03, 2004	River	-12.99	-93.0
Nov. 05, 2004	River	-13.40	-95.1
Mar. 08, 2005	River	-13.91	-98.4
Apr. 10, 2005	River	-13.89	-100.5
May. 06, 2005	River	-13.97	-100.4
Jun. 01, 2005	River	-15.60	-111.4
Aug. 08, 2005	River	-13.34	-97.3
Jul. 05, 2006	River	-13.99	-101.8
Jul. 13, 2006	River	-13.11	-96.3
Jul. 13, 2006	River	-13.05	-94.7
Aug. 23, 2006	River	-12.84	-97.0

Lake Spåime, West-Central Sweden (63°07’N, 12°19’E)

Date	Sample Type	$\delta^{18}O$	$\delta^{2}H$
Apr. 15, 1999	Lake	-14.29	-102.6
Jul. 12, 2001	Lake	-10.54	-74.8
Dec. 08, 2001	Lake	-11.85	-84.3

Feb. 27, 2002	Lake	-11.94	-85.7
Feb. 27, 2002	Lake	-11.91	-85.8
Feb. 28, 2002	Lake	-12.03	-86.3
Apr. 11, 2006	Lake	-11.68	-81.3
Apr. 12, 2006	Lake	-11.75	-82.0
Aug. 05, 2000	Outlet	-10.99	-77.7
Aug. 09, 2000	Outlet	-11.08	-78.0
Jun. 15, 2003	Outlet	-11.65	-81.1
Aug. 05, 2000	Inlet	-11.17	-76.0
Jun. 15, 2003	Inlet	-11.65	-81.1
Aug. 05, 2000	Groundwater	-10.98	
Aug. 05, 2000	Groundwater	-11.77	
Jul. 12, 2001	Groundwater	-10.72	-77.5
Jul. 12, 2001	Groundwater	-13.25	-92.7
Feb. 27, 2002	Groundwater	-11.92	-85.7
Aug. 06, 2000	Precipitation	-11.57	
Aug. 06, 2000	Precipitation	-13.36	
Aug. 07, 2000	Precipitation	-11.88	
Aug. 07, 2000	Precipitation	-10.11	
Aug. 08, 2000	Precipitation	-8.83	
Apr. 12, 1999	Precipitation	-12.29	-89.8
Apr. 12, 1999	Snowpack	-14.73	-107.0
Feb. 27, 2002	Snowpack	-17.22	-122.9
Aug. 05, 2000	Nearby River, Storulvån	-10.98	
Aug. 05, 2000	Nearby River, Lillulvån	-10.88	
Aug. 06, 2000	Nearby River, NW inflow to L. Pojktjärn	-11.46	
Aug. 06, 2000	Nearby River, SE inflow to L. Pojktjärn	-11.62	
Aug. 07, 2000	Nearby River, Sylälven	-11.93	
Aug. 07, 2000	Nearby River, Storulvån	-11.37	
Jul. 11, 2001	Nearby River, Handölan	-11.39	-80.4
Jul. 12, 2001	Nearby River, inflow to L. Stentjärn	-10.14	-74.6
Jul. 12, 2001	Nearby River, Storulvån	-11.06	-79.1
Feb. 25, 2002	Nearby River, Handölan	-12.44	-89.4
Feb. 27, 2002	Nearby River, Storulvån	-12.20	-86.1
Jun. 15, 2003	Nearby River, Storulvån	-11.22	-77.4

Jul. 12, 2001	Nearby lake, N of Enkälssjön	-10.48	-76.2
Jul. 12, 2001	Nearby lake, Enkälssjön	-10.91	-79.1
Jul. 12, 2001	Nearby lake, NW of Enkälssjön	-9.74	-72.7
Jul. 12, 2001	Nearby lake, SE of Mieskentjakke	-9.04	-71.3
Jul. 12, 2001	Nearby lake, SE of Mieskentjakke	-11.21	-81.4

Svartkälstjärn, East-Central Sweden (64°16′N; 19°33′E)

Date	Sample Type	$\delta^{18}O$	$\delta^{2}H$
Feb. 21, 2002	Lake	-12.72	-91.6
Feb. 21, 2002	Lake, depth 3m	-12.55	-91.0
Mar. 19, 2002	Lake	-12.62	-89.4
Apr. 17, 2002	Lake	-13.47	-96.1
Jun. 04, 2002	Lake	-11.70	-88.1
Jun. 18, 2002	Lake	-10.85	-84.2
Aug. 05, 2002	Lake	-9.82	-78.5
Aug. 26, 2002	Lake	-8.50	-73.9
Sep. 24, 2002	Lake	-9.33	-76.7
Oct. 17, 2002	Lake	-9.58	-77.7
Dec. 02, 2002	Lake	-10.89	-84.4
Jan. 09, 2003	Lake	-10.99	-85.9
Feb. 18, 2003	Lake	-11.43	-87.3
Apr. 10, 2003	Lake	-12.73	-93.4
May. 23, 2003	Lake	-12.72	-93.4
Jun. 19, 2003	Lake	-11.86	-89.2
Jul. 14, 2003	Lake	-10.67	-83.1
Aug. 21, 2003	Lake	-10.43	-79.5
Sep. 19, 2003	Lake	-10.90	-80.5
Oct. 16, 2003	Lake	-11.35	-81.1
Nov. 17, 2003	Lake	-12.42	-86.8
Dec. 14, 2003	Lake	-12.55	-87.3
Jan. 16, 2004	Lake	-12.42	-87.3
Feb. 17, 2004	Lake	-12.15	-85.2
Mar. 17, 2004	Lake	-12.31	-86.0
Apr. 16, 2004	Lake	-12.81	-89.9

May. 18, 2004	Lake	-12.89	-91.1
Jun. 16, 2004	Lake	-11.98	-86.8
Jul. 15, 2004	Lake	-11.97	-85.1
Aug. 20, 2004	Lake	-11.24	-82.5
Sep. 21, 2004	Lake	-11.45	-83.2
Oct. 21, 2004	Lake	-11.93	-85.3
Nov. 18, 2004	Lake	-12.50	-88.8
Dec. 15, 2004	Lake	-12.48	-89.3
Jan. 20, 2005	Lake	-13.05	-92.9
Feb. 17, 2005	Lake	-13.09	-93.0
Mar. 17, 2005	Lake	-12.62	-90.0
Apr. 15, 2005	Lake	-13.60	-97.2
May. 22, 2005	Lake	-13.00	-93.4
Jun. 14, 2005	Lake	-12.11	-89.8
Jul. 20, 2005	Lake	-10.26	-79.8
Aug. 19, 2005	Lake	-11.21	-79.7
Sep. 19, 2005	Lake	-11.53	-82.3
Oct. 28, 2005	Lake	-11.72	-83.1
Feb. 22, 2002	Outlet	-12.70	-91.2
Sep. 19, 2003	Inlet	-12.70	-91.0
Sep. 19, 2003	Inlet	-12.31	-88.1
Sep. 20, 2003	Inlet	-12.78	-92.5
Sep. 20, 2003	Groundwater	-13.05	-94.2
Feb. 22, 2002	Snowpack	-14.95	-99.1
Feb. 23, 2002	Snowpack	-16.74	-122.1

Vindelälven at Åmsele, East-Central Sweden

Date	Sample Type	$\delta^{18}O$	$\delta^{2}H$
Apr. 15, 2002	River	-13.78	-101.4
Jun. 04, 2002	River	-13.64	-99.0
Jun. 17, 2002	River	-13.66	-98.7
Aug. 05, 2002	River	-12.30	-92.6
Aug. 19, 2002	River	-12.50	-93.0
Sep. 16, 2002	River	-12.25	-90.9

Oct. 14, 2002	River	-12.56	-92.4
Nov. 18, 2002	River	-12.70	-95.3
Dec. 16, 2002	River	-12.73	-95.5
Jan. 13, 2003	River	-12.95	-95.3
Feb. 17, 2003	River	-12.94	-96.5
Mar. 17, 2003	River	-13.58	-99.0
Apr. 14, 2003	River	-12.98	-97.0
May. 19, 2003	River	-13.52	-99.8
Jun. 16, 2003	River	-13.16	-96.5
Jul. 14, 2003	River	-13.20	-96.4
Aug. 18, 2003	River	-12.55	-93.1
Sep. 15, 2003	River	-12.45	-92.9
Oct. 13, 2003	River	-12.49	-90.6
Nov. 17, 2003	River	-12.77	-92.9
Dec. 14, 2003	River	-13.07	-94.7
Jan. 19, 2004	River	-13.06	-94.5
Feb. 16, 2004	River	-12.86	-94.4
Mar. 15, 2004	River	-13.29	-96.3
May. 17, 2004	River	-13.74	-98.4
Jun. 14, 2004	River	-13.61	-97.3
Jul. 13, 2004	River	-13.37	-95.2
Aug. 16, 2004	River	-12.83	-92.2
Sep. 13, 2004	River	-12.56	-91.3
Oct. 21, 2004	River	-12.82	-91.3
Nov. 15, 2004	River	-13.10	-95.2
Dec. 13, 2004	River	-13.40	-97.2
Jan. 18, 2005	River	-13.27	-96.5
Feb. 14, 2005	River	-13.28	-97.0
Mar. 14, 2005	River	-13.32	-97.2
Apr. 18, 2005	River	-13.58	-99.7
May. 16, 2005	River	-14.00	-103.0
Jun. 13, 2005	River	-13.70	-100.3
Jul. 18, 2005	River	-13.51	-98.7
Aug. 19, 2005	River	-12.46	-91.5
Sep. 19, 2005	River	-12.82	-92.4

Oct. 17, 2005	River	-12.80	-92.9

Arbovatten, Southern Sweden (58º04'N, 12º04'E)

Date	Sample Type	$\delta^{18}O$	$\delta^{2}H$
Sep. 23, 2002	Lake	-6.82	-53.0
Sep. 23, 2002	Lake, depth 5.5m	-8.62	-60.6
Sep. 24, 2002	Lake, depth 5.3m	-8.95	-62.6
Sep. 12, 2004	Lake	-7.19	-54.5
Sep. 12, 2004	Lake, depth 2.7m	-8.84	-63.6
Sep. 12, 2004	Lake, depth 4.7m	-8.86	-62.9
Oct. 10, 2004	Lake	-7.67	-50.5
Nov. 14, 2004	Lake	-7.84	-51.4
Dec. 12, 2004	Lake	-8.20	-54.5
Jan. 09, 2005	Lake	-7.84	-49.8
Feb. 13, 2005	Lake	-8.32	-53.6
Mar. 13, 2005	Lake	-8.60	-59.1
Apr. 10, 2005	Lake	-8.38	-56.5
May. 15, 2005	Lake	-7.53	-53.6
Jun. 12, 2005	Lake	-7.32	-52.6
Jul. 10, 2005	Lake	-5.97	-48.0
Aug. 14, 2005	Lake	-7.16	-51.5
Sep. 11, 2005	Lake	-7.22	-57.5
Oct. 15, 2005	Lake	-7.36	-51.6
Nov. 15, 2005	Lake	-7.77	-51.2
Dec. 11, 2005	Lake	-8.25	-53.4
Jan. 15, 2006	Lake	-9.68	-66.5
Feb. 12, 2006	Lake	-9.30	-63.1
Mar. 15, 2006	Lake	-9.25	-62.4
Apr. 15, 2006	Lake	-9.46	-64.1
May. 16, 2006	Lake	-8.50	-61.0
Jun. 15, 2006	Lake	-7.86	-57.9
Jul. 16, 2006	Lake	-7.07	-51.9
Aug. 13, 2006	Lake	-6.21	-47.8
Sep. 16, 2006	Lake	-7.79	-55.0

Oct. 15, 2006	Lake	-7.77	-53.9
Sep. 24, 2002	Outlet	-7.55	-56.5
Sep. 12, 2004	Outlet	-7.06	-52.3
Sep. 24, 2002	Inlet	-9.01	-63.4
Sep. 12, 2004	Inlet	-8.67	-59.3
Sep. 12, 2004	Inlet	-9.01	-64.3

Gårdsjön, Southern Sweden

Date	Sample Type	$\delta^{18}O$	$\delta^{2}H$
Sep. 24, 2002	Lake	-5.98	-48.1
Sep. 24, 2002	Inlet	-8.64	-60.0
Sep. 24, 2002	Inlet	-8.50	-59.1

Appendix B – Carbon and Nitrogen Elemental, Stable Isotope, and Mineral Magnetic Records (Long Cores)

Depth values in the tables below are in reference to the top of the water surface. Represented in the tables are the repeated analyses and corresponding averages for the total organic carbon and total nitrogen contents and isotope compositions. Raw cellulose $\delta^{18}O$ values are given as well as the average cellulose-inferred water $\delta^{18}O$ values using a cellulose-water isotopic fractionation factor of 1.028. Age intervals represent the final age chronology as described in the thesis. Mineral magnetic records are also included.

Lake Keitjoru, Northern Sweden (68º40'N, 21º30'E)

Depth Interval (m)	Age Interval (cal. BP)	TOC (%)			TN (%)			$\delta^{13}C_{org}$ (‰ PDB)			$\delta^{15}N$ (‰ AIR)		
		(1)	(2)	(3)	(1)	(2)	(3)	(1)	(2)	(3)	(1)	(2)	(3)
1.89 1.92	-43 -10	15.72			0.94			-27.83			0.00		
1.92 1.95	-10 84	19.10	19.15		0.99	0.94		-27.69	-27.83		0.17	-0.37	
1.95 1.98	84 195	15.40	15.57		0.94	0.94		-27.66	-27.67		-0.02	0.08	
1.98 2.01	195 307	11.93			0.83			-27.41			-0.02		
2.01 2.04	307 422	12.36			0.88			-27.56			0.25		
2.04 2.07	422 536	11.79			0.88			-27.70			0.02		
2.07 2.10	536 650	11.25			0.77			-27.38			0.19		
2.10 2.13	650 761	9.83			0.77			-27.24			-0.07		
2.13 2.16	761 872	11.58	11.58		0.88	0.90		-27.68	-27.74		0.00	0.02	
2.16 2.19	872 983	12.05			0.89			-28.01			0.07		
2.19 2.22	983 1100	11.34			0.92			-27.83			0.62		
2.22 2.25	1100 1220	15.10			1.31			-28.47			1.44		
2.25 2.28	1220 1340	11.04			0.83			-27.93			0.20		
2.28 2.31	1340 1460	12.39			0.90			-27.76			-0.07		
2.31 2.34	1460 1580	14.54	14.56		0.90	0.91		-27.49	-27.49		0.01	-0.09	
2.34 2.37	1580 1708	12.74			0.88			-27.42			-0.36		
2.37 2.40	1708 1840	12.39			0.85			-27.62			-0.46		
2.40 2.43	1840 1972	11.42			0.79			-27.67			0.00		
2.43 2.46	1972 2114	11.27			0.80			-27.51			-0.17		
2.46 2.49	2114 2276	11.77			0.79			-27.82			-0.48		
2.49 2.52	2276 2438	10.75	10.95		0.74	0.75		-27.62	-27.62		-0.43	-0.37	
2.52 2.55	2438 2600	18.66	19.10	19.00	0.88	0.84	0.84	-27.61	-27.68	-27.70	0.33	-0.55	-0.50

2.55 2.58	2600 2783	15.92	0.85	-27.66	0.36
2.58 2.61	2783 2966	11.53	0.73	-27.33	-0.24
2.61 2.64	2966 3149	13.47	0.79	-27.96	-0.21
2.64 2.67	3149 3344	10.71	0.76	-27.47	-0.37
2.67 2.70	3344 3545	11.26 10.96	0.71 0.71	-28.42 -28.31	-0.52 -0.50
2.70 2.73	3545 3746	12.04	0.77	-29.20	-0.28
2.73 2.76	3746 3954	11.33	0.89	-28.66	-0.80
2.76 2.79	3954 4176	12.25	1.03	-29.10	-0.95
2.79 2.82	4176 4398	12.68	1.11	-30.13	-1.16
2.82 2.85	4398 4620	15.42	1.09	-29.69	-0.82
2.85 2.88	4620 4866	14.97 14.80	1.12 1.13	-29.37 -29.42	-1.22 -1.29
2.88 2.91	4866 5128	15.36	1.16	-29.02	-1.23
2.91 2.94	5128 5422	15.37	1.22	-27.94	-1.36
2.94 2.96	5422 5650	15.97	1.27	-27.37	-1.13
2.96 2.98	5650 5910	13.93	1.10	-28.61	-0.95
2.98 3.00	5910 6170	14.18	1.03	-28.24	-1.37
3.00 3.02	6170 6510	16.74 16.86	1.27 1.28	-27.95 -27.98	-1.54 -1.53
3.02 3.04	6510 6850	16.07	1.22	-28.59	-1.53
3.04 3.06	6850 7172	14.73	1.09	-28.68	-1.42
3.06 3.08	7172 7476	16.11	1.14	-28.64	-1.16
3.08 3.10	7476 7780	16.21	1.24	-28.20	-1.40
3.10 3.12	7780 8027	14.30	1.06	-28.69	-1.37
3.12 3.14	8027 8235	14.32 14.37	1.09 1.08	-29.63 -29.64	-0.94 -0.90
3.14 3.16	8235 8405	13.78	1.11	-29.01	-0.80
3.16 3.18	8405 8554	14.45	1.09	-29.65	-0.85
3.18 3.20	8554 8682	12.35	0.98	-28.77	-0.94
3.20 3.22	8682 8810	10.84	0.85	-28.34	-0.84
3.22 3.24	8810 8898	14.27 14.25	0.98 0.98	-28.27 -28.25	-0.80 -0.82
3.24 3.26	8898 8986	11.02	0.88	-28.58	-0.74
3.26 3.28	8986 9106	13.31	1.04	-27.57	-1.29
3.28 3.30	9106 9182	12.61	0.96	-27.16	-0.99
3.30 3.32	9182 9277	9.16	0.68	-28.13	-0.43
3.32 3.35	9277 9430	10.65	0.82	-26.54	-0.28

Lake Keitjoru, Northern Sweden (68º40'N, 21º30'E)

Depth Interval (m)	Age Interval (cal. BP)	Average: TOC (%)	TN (%)	$\delta^{13}C_{org}$ (‰)	$\delta^{15}N$ (‰)	Cellulose $\delta^{18}O$ (‰ VSMOW) (1)	(2)	(3)	(4)	Average cellulose-inf. water $\delta^{18}O$ (‰)	Magnetic Susc. ($10^{-6}m^3kg^{-1}$)
1.89 1.92	-43 -10	15.72	0.94	-27.83	0.00	10.27				-17.44	1.165
1.92 1.95	-10 84	19.13	0.97	-27.76	-0.10	11.39	8.45			-17.77	1.467
1.95 1.98	84 195	15.49	0.94	-27.66	0.03	9.49	7.66			-19.09	1.108
1.98 2.01	195 307	11.93	0.83	-27.41	-0.02	8.85	8.80			-18.84	0.862
2.01 2.04	307 422	12.36	0.88	-27.56	0.25	8.21	8.95			-19.08	0.925
2.04 2.07	422 536	11.79	0.88	-27.70	0.02	7.40				-20.23	1.036
2.07 2.10	536 650	11.25	0.77	-27.38	0.19	11.46	11.65			-16.19	0.699
2.10 2.13	650 761	9.83	0.77	-27.24	-0.07	10.95	11.54			-16.49	0.746
2.13 2.16	761 872	11.58	0.89	-27.71	0.01	11.90	12.25			-15.68	0.644
2.16 2.19	872 983	12.05	0.89	-28.01	0.07	11.10	12.02			-16.18	0.507
2.19 2.22	983 1100	11.34	0.92	-27.83	0.62	11.16	11.84			-16.24	0.523
2.22 2.25	1100 1220	15.10	1.31	-28.47	1.44	14.23	14.10			-13.65	0.451
2.25 2.28	1220 1340	11.04	0.83	-27.93	0.20	12.46	12.87			-15.11	0.431
2.28 2.31	1340 1460	12.39	0.90	-27.76	-0.07	11.86	12.69			-15.49	0.435
2.31 2.34	1460 1580	14.55	0.90	-27.49	-0.04	14.31	15.44			-12.96	0.471
2.34 2.37	1580 1708	12.74	0.88	-27.42	-0.36	8.79	11.59			-17.52	0.480
2.37 2.40	1708 1840	12.39	0.85	-27.62	-0.46	10.94	11.50			-16.52	0.431
2.40 2.43	1840 1972	11.42	0.79	-27.67	0.00	9.33	10.16			-17.95	0.395
2.43 2.46	1972 2114	11.27	0.80	-27.51	-0.17	8.60	10.45			-18.17	0.394
2.46 2.49	2114 2276	11.77	0.79	-27.82	-0.48	7.58	10.27			-18.75	0.307
2.49 2.52	2276 2438	10.85	0.74	-27.62	-0.40	9.49	10.03			-17.93	0.299
2.52 2.55	2438 2600	18.92	0.85	-27.66	-0.24	12.77	13.19			-14.81	0.345
2.55 2.58	2600 2783	15.92	0.85	-27.66	0.36	11.43	11.25			-16.40	0.296
2.58 2.61	2783 2966	11.53	0.73	-27.33	-0.24	7.94	9.80			-18.80	0.321
2.61 2.64	2966 3149	13.47	0.79	-27.96	-0.21	10.75	7.61			-18.50	0.259
2.64 2.67	3149 3344	10.71	0.76	-27.47	-0.37	8.87	9.86			-18.32	0.234
2.67 2.70	3344 3545	11.11	0.71	-28.36	-0.51	8.65	11.47			-17.64	0.180
2.70 2.73	3545 3746	12.04	0.77	-29.20	-0.28	9.92	10.23			-17.63	0.219
2.73 2.76	3746 3954	11.33	0.89	-28.66	-0.80	8.67	9.44			-18.62	0.278
2.76 2.79	3954 4176	12.25	1.03	-29.10	-0.95	9.71	10.01			-17.84	0.176
2.79 2.82	4176 4398	12.68	1.11	-30.13	-1.16	11.40	10.80			-16.63	0.185
2.82 2.85	4398 4620	15.42	1.09	-29.69	-0.82	13.62	13.98			-14.01	0.204
2.85 2.88	4620 4866	14.88	1.13	-29.40	-1.25	11.45	12.57			-15.75	0.274
2.88 2.91	4866 5128	15.36	1.16	-29.02	-1.23	12.56	12.09			-15.44	0.254

2.91	2.94	5128	5422	15.37	1.22	-27.94	-1.36	12.68	11.98			-15.44	0.221
2.94	2.96	5422	5650	15.97	1.27	-27.37	-1.13	12.56	12.11			-15.43	0.172
2.96	2.98	5650	5910	13.93	1.10	-28.61	-0.95	12.09	11.93			-15.75	0.043
2.98	3.00	5910	6170	14.18	1.03	-28.24	-1.37	11.60	12.19			-15.86	0.208
3.00	3.02	6170	6510	16.80	1.27	-27.97	-1.53	12.10	13.00			-15.22	0.226
3.02	3.04	6510	6850	16.07	1.22	-28.59	-1.53	11.12	10.80			-16.77	0.173
3.04	3.06	6850	7172	14.73	1.09	-28.68	-1.42	11.47	9.96			-17.01	0.103
3.06	3.08	7172	7476	16.11	1.14	-28.64	-1.16	10.09	10.22			-17.55	0.138
3.08	3.10	7476	7780	16.21	1.24	-28.20	-1.40	12.01	14.26			-14.65	0.219
3.10	3.12	7780	8027	14.30	1.06	-28.69	-1.37	10.87	11.22			-16.69	0.242
3.12	3.14	8027	8235	14.35	1.09	-29.63	-0.92	11.20	11.95			-16.17	0.219
3.14	3.16	8235	8405	13.78	1.11	-29.01	-0.80	10.63	11.12			-16.85	0.008
3.16	3.18	8405	8554	14.45	1.09	-29.65	-0.85	11.00	9.21			-17.60	0.061
3.18	3.20	8554	8682	12.35	0.98	-28.77	-0.94	8.79	9.36			-18.60	0.249
3.20	3.22	8682	8810	10.84	0.85	-28.34	-0.84	9.41	8.98	8.46	9.18	-18.67	0.227
3.22	3.24	8810	8898	14.26	0.98	-28.26	-0.81	8.26	7.69	8.90		-19.37	0.250
3.24	3.26	8898	8986	11.02	0.88	-28.58	-0.74	6.70	7.10	7.76		-20.44	0.216
3.26	3.28	8986	9106	13.31	1.04	-27.57	-1.29	8.35	8.56	8.05	8.64	-19.26	0.247
3.28	3.30	9106	9182	12.61	0.96	-27.16	-0.99	9.73				-17.96	0.270
3.30	3.32	9182	9277	9.16	0.68	-28.13	-0.43	8.85	6.59	5.99	5.64	-20.84	0.291
3.32	3.35	9277	9430	10.65	0.82	-26.54	-0.28	9.65				-18.04	0.516

Oikojärvi, Northern Finland (68°50'N, 21°10'E)

Depth Interval (m)		Age Interval (cal. BP)		TOC (%)		TN (%)		$\delta^{13}C_{org}$ (‰ PDB)		$\delta^{15}N$ (‰ AIR)		Average:			
				(1)	(2)	(1)	(2)	(1)	(2)	(1)	(2)	TOC (%)	TN (%)	$\delta^{13}C_{org}$ (‰)	$\delta^{15}N$ (‰)
8.00	8.03	-53	-33	9.16		0.82		-27.50		1.57		9.16	0.82	-27.50	1.57
8.03	8.06	-33	-7	9.05		0.83		-27.42		1.55		9.05	0.83	-27.42	1.55
8.06	8.09	-7	15	9.24	9.41	0.84	0.88	-27.77	-27.74	1.63	1.68	9.33	0.86	-27.75	1.66
8.09	8.12	15	28	9.05		0.81		-27.52		1.81		9.05	0.81	-27.52	1.81
8.12	8.15	28	39	8.51		0.76		-27.51		1.76		8.51	0.76	-27.51	1.76
8.15	8.18	39	57	8.76		0.77		-27.64		1.37		8.76	0.77	-27.64	1.37
8.18	8.21	57	82	8.84		0.79		-27.85		1.60		8.84	0.79	-27.85	1.60
8.21	8.24	82	114	8.84		0.79		-28.04		1.59		8.84	0.79	-28.04	1.59
8.24	8.27	114	156	8.43	8.53	0.73	0.75	-27.84	-27.83	1.68	1.57	8.48	0.74	-27.84	1.62
8.27	8.30	156	205	8.72		0.77		-27.62		1.72		8.72	0.77	-27.62	1.72
8.30	8.33	205	257	8.77		0.79		-27.97		1.77		8.77	0.79	-27.97	1.77

8.33	8.36	257	311	8.84		0.77		-27.93		1.58		8.84	0.77	-27.93	1.58
8.36	8.39	311	370	8.63		0.75		-27.70		1.64		8.63	0.75	-27.70	1.64
8.39	8.42	370	430	9.13		0.78		-27.80		1.79		9.13	0.78	-27.80	1.79
8.42	8.45	430	489	9.10	9.12	0.78	0.79	-27.69	-27.72	1.69	1.76	9.11	0.78	-27.71	1.72
8.45	8.48	489	548	9.44		0.78		-28.01		1.56		9.44	0.82	-28.01	1.56
8.48	8.51	548	606	9.04		0.78		-27.66		1.54		9.04	0.80	-27.66	1.54
8.51	8.54	606	664	9.13		0.78		-27.73		1.71		9.13	0.79	-27.73	1.71
8.54	8.57	664	722	9.58		0.78		-27.89		1.73		9.58	0.84	-27.89	1.73
8.57	8.60	722	777	10.07		0.78		-28.00		1.84		10.07	0.88	-28.00	1.84
8.60	8.63	777	826	9.53	9.46	0.78	0.83	-27.99	-27.95	1.77	1.64	9.49	0.83	-27.97	1.70
8.63	8.66	826	873	9.44		0.78		-27.93		1.70		9.44	0.82	-27.93	1.70
8.66	8.69	873	919	9.33		0.78		-27.89		1.79		9.33	0.82	-27.89	1.79
8.69	8.72	919	966	9.20		0.78		-28.04		1.68		9.20	0.78	-28.04	1.68
8.72	8.75	966	1012	9.53		0.78		-28.08		1.69		9.53	0.81	-28.08	1.69
8.75	8.78	1012	1059	9.54		0.78		-28.18		1.54		9.54	0.82	-28.18	1.54
8.78	8.81	1059	1107	9.22	9.15	0.78	0.78	-28.25	-28.22	1.66	1.73	9.18	0.78	-28.23	1.69
8.81	8.84	1107	1155	8.76		0.78		-27.77		1.54		8.76	0.76	-27.77	1.54
8.84	8.87	1155	1204	9.13		0.78		-27.91		1.49		9.13	0.79	-27.91	1.49
8.87	8.90	1204	1253	9.05		0.78		-27.78		1.50		9.05	0.79	-27.78	1.50
8.90	8.93	1253	1302	9.31		0.78		-27.81		1.63		9.31	0.81	-27.81	1.63
8.93	8.96	1302	1351	9.02		0.78		-27.72		1.48		9.02	0.79	-27.72	1.48
8.96	8.99	1351	1400	9.63	9.53	0.78	0.82	-27.91	-27.91	1.57	1.25	9.58	0.82	-27.91	1.41
8.99	9.02	1400	1449	9.90		0.78		-28.08		1.58		9.90	0.85	-28.08	1.58
9.02	9.05	1449	1498	9.88		0.78		-27.85		1.47		9.88	0.84	-27.85	1.47
9.05	9.08	1498	1548	10.10		0.78		-27.89		1.54		10.10	0.87	-27.89	1.54
9.08	9.11	1548	1599	10.05		0.78		-27.93		1.55		10.05	0.86	-27.93	1.55
9.11	9.14	1599	1652	9.85		0.78		-27.79		1.42		9.85	0.83	-27.79	1.42
9.14	9.17	1652	1706	9.42	9.76	0.78	0.82	-27.77	-27.72	1.44	1.45	9.59	0.82	-27.74	1.44
9.17	9.20	1706	1760	11.30		0.78		-27.93		1.50		11.30	0.95	-27.93	1.50
9.20	9.23	1760	1814	10.42		0.78		-27.90		1.44		10.42	0.86	-27.90	1.44
9.23	9.26	1814	1868	10.08		0.78		-27.65		1.47		10.08	0.84	-27.65	1.47
9.26	9.29	1868	1922	10.02		0.78		-27.85		1.51		10.02	0.84	-27.85	1.51
9.29	9.32	1922	1976	10.59		0.78		-27.97		1.55		10.59	0.89	-27.97	1.55
9.32	9.35	1976	2030	10.24	10.94	0.78	0.91	-27.80	-27.79	1.57	1.69	10.59	0.88	-27.79	1.63
9.35	9.38	2030	2085	9.20		0.78		-27.69		1.63		9.20	0.76	-27.69	1.63
9.38	9.41	2085	2145	9.73		0.78		-27.75		1.40		9.73	0.80	-27.75	1.40
9.41	9.44	2145	2210	9.33		0.78		-27.94		1.43		9.33	0.76	-27.94	1.43
9.44	9.47	2210	2277	9.04		0.78		-27.78		1.56		9.04	0.75	-27.78	1.56

9.47	9.50	2277	2345	9.19		0.78		-27.93		1.60		9.19	0.77	-27.93	1.60
9.50	9.53	2345	2412	8.91	8.91	0.78	0.74	-28.16	-28.13	1.63	1.39	8.91	0.75	-28.15	1.51
9.53	9.56	2412	2480	8.72		0.78		-27.96		1.47		8.72	0.73	-27.96	1.47
9.56	9.59	2480	2548	9.09		0.78		-27.96		1.76		9.09	0.77	-27.96	1.76
9.59	9.62	2548	2618	10.72		0.78		-28.10		1.74		10.72	0.89	-28.10	1.74
9.62	9.65	2618	2690	12.15		0.78		-27.91		1.58		12.15	1.02	-27.91	1.58
9.65	9.68	2690	2762	10.20		0.78		-27.88		1.87		10.20	0.86	-27.88	1.87
9.68	9.71	2762	2834	10.04	10.04	0.78	0.83	-28.02	-27.99	1.82	1.75	10.04	0.83	-28.01	1.78
9.71	9.74	2834	2906	10.13		0.78		-27.95		1.75		10.13	0.84	-27.95	1.75
9.74	9.77	2906	2978	10.25		0.78		-27.74		1.86		10.25	0.85	-27.74	1.86
9.77	9.80	2978	3050	10.47		0.78		-27.91		1.82		10.47	0.89	-27.91	1.82
9.80	9.83	3050	3123	10.26		0.78		-27.81		1.68		10.26	0.85	-27.81	1.68
9.83	9.86	3123	3197	9.68		0.78		-27.68		1.70		9.68	0.82	-27.68	1.70
9.86	9.89	3197	3270	10.14	10.18	0.78	0.86	-27.93	-28.01	1.67	1.60	10.16	0.85	-27.97	1.63
9.89	9.92	3270	3344	9.81		0.78		-28.05		1.76		9.81	0.84	-28.05	1.76
9.92	9.95	3344	3417	9.81		0.78		-28.01		1.58		9.81	0.82	-28.01	1.58
9.95	9.98	3417	3492	10.26		0.78		-27.97		1.69		10.26	0.86	-27.97	1.69
9.98	10.01	3492	3571	9.87		0.78		-28.00		1.83		9.87	0.84	-28.00	1.83
10.01	10.04	3571	3654	9.70		0.78		-28.15		1.75		9.70	0.81	-28.15	1.75
10.04	10.07	3654	3740	10.14	10.05	0.78	0.84	-28.16	-28.20	1.86	1.75	10.10	0.85	-28.18	1.81
10.07	10.10	3740	3825	10.44		0.78		-28.35		1.73		10.44	0.89	-28.35	1.73
10.10	10.13	3825	3911	10.11		0.78		-28.15		1.65		10.11	0.84	-28.15	1.65
10.13	10.16	3911	3996	10.16		0.78		-28.12		1.78		10.16	0.86	-28.12	1.78
10.16	10.19	3996	4084	10.91		0.78		-28.72		1.59		10.91	0.90	-28.72	1.59
10.19	10.22	4084	4177	11.50		0.78		-28.70		1.51		11.50	0.93	-28.70	1.51
10.22	10.25	4177	4275	11.24	11.15	0.78	0.92	-28.66	-28.65	1.46	1.59	11.19	0.92	-28.66	1.52
10.25	10.28	4275	4375	11.02		0.78		-28.48		1.62		11.02	0.91	-28.48	1.62
10.28	10.31	4375	4478	11.25		0.78		-28.52		1.88		11.25	0.94	-28.52	1.88
10.31	10.34	4478	4584	10.81		0.78		-28.59		1.66		10.81	0.91	-28.59	1.66
10.34	10.37	4584	4692	11.18		0.78		-28.54		1.56		11.18	0.95	-28.54	1.56
10.37	10.40	4692	4797	11.06		0.78		-28.59		1.53		11.06	0.92	-28.59	1.53
10.40	10.42	4797	4894	10.88	10.90	0.78	0.91	-28.64	-28.56	1.47	1.53	10.89	0.91	-28.60	1.50
10.42	10.44	4894	4988	11.21		0.78		-28.59		1.46		11.21	0.92	-28.59	1.46
10.44	10.46	4988	5082	11.70		0.78		-28.17		2.27		11.70	0.96	-28.17	2.27
10.46	10.48	5082	5176	10.10		0.78		-28.33		1.89		10.10	0.82	-28.33	1.89
10.48	10.50	5176	5274	11.57		0.78		-28.60		2.05		11.57	0.94	-28.60	2.05
10.50	10.52	5274	5378	11.27		0.78		-28.59		2.02		11.27	0.90	-28.59	2.02
10.52	10.54	5378	5486	11.43	11.41	0.78	0.92	-28.49	-28.54	1.80	1.91	11.42	0.93	-28.52	1.85

10.54	10.56	5486	5594	10.94		0.78		-28.33		1.95		10.94	0.88	-28.33	1.95
10.56	10.58	5594	5702	11.19		0.78		-28.53		2.01		11.19	0.91	-28.53	2.01
10.58	10.60	5702	5819	10.45		0.78		-28.70		1.98		10.45	0.85	-28.70	1.98
10.60	10.62	5819	5954	10.42		0.78		-28.69		1.93		10.42	0.87	-28.69	1.93
10.62	10.64	5954	6098	10.26		0.78		-28.64		2.25		10.26	0.85	-28.64	2.25
10.64	10.66	6098	6242	9.77	7.97	0.78	0.66	-28.81	-28.85	1.98	1.94	8.87	0.73	-28.83	1.96
10.66	10.68	6242	6386	9.68		0.78		-28.88		1.91		9.68	0.82	-28.88	1.91
10.68	10.70	6386	6536	8.62		0.78		-28.51		1.76		8.62	0.73	-28.51	1.76
10.70	10.72	6536	6703	8.31		0.78		-28.45		1.92		8.31	0.70	-28.45	1.92
10.72	10.74	6703	6886	8.71		0.78		-28.38		1.79		8.71	0.73	-28.38	1.79
10.74	10.76	6886	7074	9.11		0.78		-28.36		1.65		9.11	0.76	-28.36	1.65
10.76	10.78	7074	7262	7.85	7.02	0.78	0.57	-28.33	-28.29	1.76	1.49	7.43	0.63	-28.31	1.62
10.78	10.80	7262	7453	8.48		0.78		-28.20		2.17		8.48	0.69	-28.20	2.17
10.80	10.82	7453	7650	8.44		0.78		-28.32		1.79		8.44	0.68	-28.32	1.79
10.82	10.84	7650	7850	9.13		0.78		-28.12		1.95		9.13	0.77	-28.12	1.95
10.84	10.86	7850	8050	8.62		0.78		-27.99		2.10		8.62	0.72	-27.99	2.10
10.86	10.88	8050	8250	8.96		0.78		-28.06		1.78		8.96	0.75	-28.06	1.78
10.88	10.90	8250	8439	9.14	9.14	0.78	0.75	-28.21	-28.25	1.68	1.66	9.14	0.75	-28.23	1.67
10.90	10.92	8439	8606	9.48		0.78		-28.40		1.76		9.48	0.78	-28.40	1.76
10.92	10.94	8606	8762	9.55		0.78		-28.50		1.72		9.55	0.78	-28.50	1.72
10.94	10.96	8762	8918	10.39		0.78		-28.78		1.69		10.39	0.85	-28.78	1.69
10.96	10.98	8918	9074	7.86		0.78		-29.20		1.48		7.86	0.67	-29.20	1.48
10.98	11.00	9074	9222	6.02		0.78		-29.29		1.37		6.02	0.54	-29.29	1.37
11.00	11.02	9222	9354	4.17	4.21	0.78	0.38	-29.77	-29.89	1.52	0.93	4.19	0.39	-29.83	1.23
11.02	11.04	9354	9478	3.36		0.78		-30.48		0.96		3.36	0.30	-30.48	0.96
11.04	11.06	9478	9602	3.07		0.78		-30.23		1.08		3.07	0.30	-30.23	1.08
11.06	11.08	9602	9726	2.45		0.78		-29.99		1.42		2.45	0.24	-29.99	1.42
11.08	11.10	9726	9840	1.94		0.78		-29.73		1.04		1.94	0.19	-29.73	1.04
11.10	11.12	9840	9932	1.99		0.78		-29.70		0.75		1.99	0.20	-29.70	0.75
11.12	11.14	9932	10011	3.03	3.01	0.78	0.29	-29.54	-29.57	0.42	0.54	3.02	0.29	-29.56	0.48
11.14	11.16	10011	10079	5.21		0.78		-29.36		0.64		5.21	0.51	-29.36	0.64
11.16	11.18	10079	10136	2.93		0.78		-29.70		0.53		2.93	0.31	-29.70	0.53
11.18	11.20	10136	10190	2.33		0.78		-29.62		0.90		2.33	0.26	-29.62	0.90

Oikojärvi, Northern Finland (68°50'N, 21°10'E)

Depth Interval (m)		Age Interval (cal. BP)		Cellulose $\delta^{18}O$ (‰ VSMOW) (1)	(2)	Average cellulose-inf. water $\delta^{18}O$ (‰)	Magnetic Susc. ($10^{-6}m^3kg^{-1}$)
8.00	8.03	-53	-33				0.645
8.03	8.06	-33	-7	11.59	12.61	-15.47	0.764
8.06	8.09	-7	15	12.73	13.00	-14.72	0.624
8.09	8.12	15	28	11.02	11.21	-16.43	0.606
8.12	8.15	28	39	11.60	13.54	-15.01	0.405
8.15	8.18	39	57	9.52	9.63	-17.92	0.327
8.18	8.21	57	82	11.67	11.48	-15.98	0.350
8.21	8.24	82	114	12.08	12.04	-15.51	0.326
8.24	8.27	114	156	14.00	11.57	-14.80	0.396
8.27	8.30	156	205	13.03	11.90	-15.11	0.291
8.30	8.33	205	257	11.47	11.72	-15.96	0.268
8.33	8.36	257	311	11.78	13.82	-14.79	0.327
8.36	8.39	311	370	12.19	12.48	-15.24	0.315
8.39	8.42	370	430	13.65	14.11	-13.74	0.258
8.42	8.45	430	489	12.44	12.76	-14.98	0.224
8.45	8.48	489	548	12.24	12.28	-15.31	0.258
8.48	8.51	548	606	12.62	12.41	-15.06	0.216
8.51	8.54	606	664	11.91	12.53	-15.35	0.237
8.54	8.57	664	722	10.70	10.53	-16.91	0.205
8.57	8.60	722	777	11.24	11.03	-16.41	0.194
8.60	8.63	777	826	12.72	12.90	-14.78	0.269
8.63	8.66	826	873	12.90		-14.69	0.209
8.66	8.69	873	919	12.85	12.07	-15.12	0.199
8.69	8.72	919	966	12.60	13.23	-14.67	0.289
8.72	8.75	966	1012	13.91	13.43	-13.94	0.258
8.75	8.78	1012	1059	10.53	9.90	-17.30	0.255
8.78	8.81	1059	1107	9.73	9.90	-17.69	0.280
8.81	8.84	1107	1155	11.43	10.49	-16.57	0.284
8.84	8.87	1155	1204	11.89	9.38	-16.89	0.282
8.87	8.90	1204	1253	12.64	11.50	-15.49	0.262
8.90	8.93	1253	1302	12.06	11.98	-15.54	0.265
8.93	8.96	1302	1351	13.66	12.91	-14.31	0.304
8.96	8.99	1351	1400	15.44	13.33	-13.24	0.294
8.99	9.02	1400	1449	12.73	13.48	-14.49	0.250

9.02	9.05	1449	1498	13.20	13.98	-14.02	0.184
9.05	9.08	1498	1548	12.83	11.50	-15.40	0.126
9.08	9.11	1548	1599	10.88	10.65	-16.77	0.165
9.11	9.14	1599	1652	12.86	12.02	-15.14	0.199
9.14	9.17	1652	1706	13.59	13.11	-14.25	0.200
9.17	9.20	1706	1760	13.89	12.39	-14.46	0.176
9.20	9.23	1760	1814	11.34	12.09	-15.84	0.159
9.23	9.26	1814	1868	13.70	12.45	-14.52	0.150
9.26	9.29	1868	1922	14.41	12.00	-14.39	0.125
9.29	9.32	1922	1976	14.19	14.17	-13.44	0.049
9.32	9.35	1976	2030	11.18	11.82	-16.05	0.109
9.35	9.38	2030	2085	12.88	12.67	-14.81	0.096
9.38	9.41	2085	2145	10.24	10.25	-17.27	0.122
9.41	9.44	2145	2210	11.50	13.28	-15.19	0.163
9.44	9.47	2210	2277	12.61	12.93	-14.82	0.181
9.47	9.50	2277	2345	12.42	12.80	-14.97	0.154
9.50	9.53	2345	2412	12.02	10.70	-16.18	0.172
9.53	9.56	2412	2480	12.55	13.06	-14.78	0.168
9.56	9.59	2480	2548	11.38	11.91	-15.91	0.214
9.59	9.62	2548	2618	12.86		-14.73	0.130
9.62	9.65	2618	2690	12.97	13.77	-14.23	0.208
9.65	9.68	2690	2762	8.99	10.39	-17.81	0.286
9.68	9.71	2762	2834	12.71	12.87	-14.80	0.274
9.71	9.74	2834	2906	9.97	10.51	-17.27	0.271
9.74	9.77	2906	2978	11.77	11.06	-16.13	0.305
9.77	9.80	2978	3050	11.95	12.51	-15.34	0.232
9.80	9.83	3050	3123	7.63	6.87	-20.19	0.220
9.83	9.86	3123	3197	13.87	11.69	-14.80	0.257
9.86	9.89	3197	3270	11.14	11.56	-16.20	0.273
9.89	9.92	3270	3344	11.27	11.25	-16.28	0.391
9.92	9.95	3344	3417	11.35	11.37	-16.19	0.313
9.95	9.98	3417	3492	11.72	11.21	-16.08	0.253
9.98	10.01	3492	3571	12.61	11.92	-15.31	0.274
10.01	10.04	3571	3654	10.87	11.56	-16.33	0.289
10.04	10.07	3654	3740	11.16	10.79	-16.56	0.277
10.07	10.10	3740	3825	10.53	12.22	-16.17	0.251
10.10	10.13	3825	3911	14.98	14.80	-12.75	0.224
10.13	10.16	3911	3996	11.47	10.73	-16.44	0.295

10.16 10.19	3996	4084	11.39	11.50	-16.10	0.260
10.19 10.22	4084	4177	12.31	11.82	-15.50	0.272
10.22 10.25	4177	4275	14.21	12.86	-14.07	0.254
10.25 10.28	4275	4375	13.17	13.05	-14.49	0.265
10.28 10.31	4375	4478	14.17	14.34	-13.37	0.187
10.31 10.34	4478	4584	11.12	13.33	-15.34	0.155
10.34 10.37	4584	4692	11.66	10.41	-16.50	0.185
10.37 10.40	4692	4797	13.25	11.86	-15.02	0.196
10.40 10.42	4797	4894	12.07	11.32	-15.86	0.187
10.42 10.44	4894	4988	13.18	12.71	-14.64	0.255
10.44 10.46	4988	5082	12.29	12.87	-15.00	0.244
10.46 10.48	5082	5176	11.40	10.69	-16.49	0.284
10.48 10.50	5176	5274	14.04	12.17	-14.49	0.223
10.50 10.52	5274	5378	13.26	13.33	-14.31	0.285
10.52 10.54	5378	5486	12.80	12.76	-14.81	0.304
10.54 10.56	5486	5594	8.86	8.90	-18.60	0.219
10.56 10.58	5594	5702	9.67	11.19	-17.09	0.305
10.58 10.60	5702	5819	10.66	9.98	-17.20	0.331
10.60 10.62	5819	5954	10.62	10.64	-16.90	0.436
10.62 10.64	5954	6098	9.50	8.76	-18.36	0.425
10.64 10.66	6098	6242	11.34	11.51	-16.13	0.488
10.66 10.68	6242	6386	12.38	13.24	-14.78	0.532
10.68 10.70	6386	6536	10.53	12.53	-16.02	0.394
10.70 10.72	6536	6703	11.81	11.47	-15.91	0.459
10.72 10.74	6703	6886	11.82	12.99	-15.17	0.494
10.74 10.76	6886	7074	12.66	15.88	-13.36	0.515
10.76 10.78	7074	7262	15.25	15.61	-12.23	0.386
10.78 10.80	7262	7453	15.33	14.79	-12.59	0.421
10.80 10.82	7453	7650	13.73	14.25	-13.63	0.555
10.82 10.84	7650	7850	15.10	14.71	-12.74	0.569
10.84 10.86	7850	8050	10.44	9.49	-17.54	0.588
10.86 10.88	8050	8250	10.23	10.54	-17.13	0.556
10.88 10.90	8250	8439	10.95	11.01	-16.55	0.724
10.90 10.92	8439	8606	11.57	11.40	-16.06	0.860
10.92 10.94	8606	8762	11.80	12.05	-15.64	0.856
10.94 10.96	8762	8918	10.07	10.01	-17.47	0.856
10.96 10.98	8918	9074	9.81	10.08	-17.56	0.827
10.98 11.00	9074	9222	10.54	11.97	-16.29	0.949

11.00	11.02	9222	9354	14.50	15.77	-12.51	1.321
11.02	11.04	9354	9478	13.35	12.14	-14.84	2.300
11.04	11.06	9478	9602	11.01	10.98	-16.54	3.403
11.06	11.08	9602	9726	10.91	11.53	-16.32	4.164
11.08	11.10	9726	9840	11.04	11.05	-16.49	4.526
11.10	11.12	9840	9932	11.68	12.88	-15.29	4.750
11.12	11.14	9932	10011	13.27	13.22	-14.35	4.537
11.14	11.16	10011	10079	13.64	14.00	-13.80	3.140
11.16	11.18	10079	10136	11.75	12.28	-15.55	6.337
11.18	11.20	10136	10190	13.36	12.38	-14.72	6.235

Lake Spåime, West-Central Sweden (63°07'N, 12°19'E)

Depth Interval (m)		Age Interval (cal. BP)		TOC (%)		TN (%)		$\delta^{13}C_{org}$ (‰ PDB)		$\delta^{15}N$ (‰ AIR)		Average:			
				(1)	(2)	(1)	(2)	(1)	(2)	(1)	(2)	TOC (%)	TN (%)	$\delta^{13}C_{org}$ (‰)	$\delta^{15}N$ (‰)
3.43	3.46	79	137	6.48		0.43		-27.03		0.35		6.48	0.43	-27.03	0.35
3.46	3.49	137	193	8.42		0.51		-26.94		0.74		8.42	0.51	-26.94	0.74
3.53	3.56	251	305	8.08	7.99	0.47	0.46	-26.61	-26.57	0.81	0.87	8.04	0.47	-26.59	0.84
3.59	3.62	364	419	8.39		0.48		-26.84		0.82		8.39	0.48	-26.84	0.82
3.65	3.68	481	539	7.51		0.43		-26.96		0.63		7.51	0.43	-26.96	0.63
3.71	3.74	601	660	7.92		0.48		-27.12		0.86		7.92	0.48	-27.12	0.86
3.77	3.81	720	788	8.37		0.50		-26.97		0.83		8.37	0.50	-26.97	0.83
3.84	3.86	850	906	8.37		0.49		-27.02		0.82		8.37	0.49	-27.02	0.82
3.90	3.93	976	1041	7.71	7.78	0.45	0.45	-27.10	-27.12	0.48	0.60	7.74	0.45	-27.11	0.54
3.96	3.99	1107	1178	10.24		0.59		-27.15		0.64		10.24	0.59	-27.15	0.64
4.02	4.06	1252	1331	7.98		0.46		-27.21		0.38		7.98	0.46	-27.21	0.38
4.09	4.12	1401	1470	8.16		0.48		-27.27		0.86		8.16	0.48	-27.27	0.86
4.15	4.18	1541	1616	9.32		0.55		-27.12		0.85		9.32	0.55	-27.12	0.85
4.20	4.24	1669	1755	7.79		0.49		-27.16		0.59		7.79	0.49	-27.16	0.59
4.27	4.30	1828	1901	7.43	7.83	0.46	0.49	-27.08	-27.09	0.67	0.81	7.63	0.48	-27.09	0.74
4.33	4.36	1974	2048	8.02		0.50		-26.95		0.51		8.02	0.50	-26.95	0.51
4.38	4.42	2115	2196	7.57		0.50		-27.03		0.48		7.57	0.50	-27.03	0.48
4.45	4.48	2271	2345	8.13		0.52		-27.02		0.66		8.13	0.52	-27.02	0.66
4.51	4.54	2420	2494	8.98		0.55		-26.93		0.53		8.98	0.55	-26.93	0.53
4.57	4.60	2574	2649	7.57		0.46		-27.07		0.65		7.57	0.46	-27.07	0.65
4.63	4.66	2718	2805	7.99		0.50		-27.14		0.90		7.99	0.50	-27.14	0.90
4.69	4.72	2880	2959	8.73	8.75	0.54	0.54	-27.18	-27.17	0.53	0.64	8.74	0.54	-27.18	0.58

4.75 4.79	3033 3114	8.60		0.55		-27.19		0.55		8.60	0.55	-27.19	0.55
4.82 4.85	3188 3266	7.73		0.54		-27.03		0.34		7.73	0.54	-27.03	0.34
4.88 4.91	3334 3425	9.34		0.66		-27.60		0.71		9.34	0.66	-27.60	0.71
4.95 4.98	3509 3589	9.04		0.60		-27.34		0.95		9.04	0.60	-27.34	0.95
5.01 5.04	3662 3734	14.12		1.04		-27.47		0.63		14.12	1.04	-27.47	0.63
5.07 5.11	3811 3896	9.55		0.69		-27.56		0.59		9.55	0.69	-27.56	0.59
5.14 5.18	3976 4060	14.19	14.41	1.07	1.08	-27.62	-27.65	0.61	0.59	14.30	1.07	-27.63	0.60
5.20 5.24	4126 4206	14.55		1.04		-27.34		0.31		14.55	1.04	-27.34	0.31
5.27 5.32	4285 4404	12.66		0.92		-27.30		0.21		12.66	0.92	-27.30	0.21
5.35 5.39	4492 4582	12.55		0.93		-27.33		0.11		12.55	0.93	-27.33	0.11
5.42 5.46	4660 4779	11.02		0.70		-27.52		0.92		11.02	0.70	-27.52	0.92
5.49 5.52	4860 4948	14.02		1.02		-27.29		0.35		14.02	1.02	-27.29	0.35
5.54 5.59	5042 5136	15.17	12.88	1.11	0.94	-27.11	-27.19	0.44	0.35	14.03	1.02	-27.15	0.39
5.62 5.65	5235 5328	13.02		0.94		-27.15		0.41		13.02	0.94	-27.15	0.41
5.68 5.71	5431 5523	16.25		1.24		-27.27		0.47		16.25	1.24	-27.27	0.47
5.74 5.78	5626 5751	13.05		0.97		-27.63		0.30		13.05	0.97	-27.63	0.30
5.81 5.84	5863 5987	12.66		0.97		-27.18		0.22		12.66	0.97	-27.18	0.22
5.86 5.89	6068 6193	13.66		1.04		-27.36		0.37		13.66	1.04	-27.36	0.37
5.98 5.92	6258 6324	16.58	17.26	1.22	1.27	-27.58	-27.53	0.44	0.43	16.92	1.24	-27.56	0.44
5.98 5.95	6392 6460	16.83		1.26		-27.80		0.33		16.83	1.26	-27.80	0.33
5.96 5.98	6539 6618	18.28		1.38		-27.84		0.53		18.28	1.38	-27.84	0.53
6.00 6.01	6694 6769	19.05		1.44		-28.26		0.87		19.05	1.44	-28.26	0.87
6.03 6.04	6848 6928	19.35		1.51		-28.07		0.61		19.35	1.51	-28.07	0.61
6.06 6.07	7011 7094	13.49		1.06		-28.10		0.27		13.49	1.06	-28.10	0.27
6.08 6.10	7172 7250	22.35	22.51	1.78	1.81	-28.27	-28.28	0.48	0.43	22.43	1.80	-28.28	0.45
6.11 6.13	7342 7433	21.71		1.73		-28.30		0.28		21.71	1.73	-28.30	0.28
6.14 6.16	7529 7625	12.51		1.00		-28.89		0.32		12.51	1.00	-28.89	0.32
6.17 6.19	7736 7847	17.12		1.35		-27.54		0.34		17.12	1.35	-27.54	0.34
6.20 6.22	7936 8024	10.46		0.81		-27.69		0.16		10.46	0.81	-27.69	0.16
6.23 6.25	8136 8247	11.96		0.92		-27.55		0.29		11.96	0.92	-27.55	0.29
6.26 6.28	8364 8481	16.60	16.10	1.31	1.28	-28.07	-28.05	0.48	0.52	16.35	1.29	-28.06	0.50
6.29 6.31	8604 8728	15.21		1.27		-27.87		0.16		15.21	1.27	-27.87	0.16
6.32 6.33	8835 8943	17.40		1.62		-28.49		0.84		17.40	1.62	-28.49	0.84
6.35 6.36	9078 9214	13.70		1.19		-28.65		0.98		13.70	1.19	-28.65	0.98
6.38 6.39	9356 9499	8.45		0.79		-28.47		1.03		8.45	0.79	-28.47	1.03
6.40 6.41	9593 9687	4.95	4.85	0.43	0.43	-28.92	-28.86	1.17	1.22	4.90	0.43	-28.89	1.19

Lake Spåime, West-Central Sweden (63°07'N, 12°19'E)

Depth Interval (m)	Age Interval (cal. BP)	Cellulose $\delta^{18}O$ (‰ VSMOW)							Average cellulose-inf. water $\delta^{18}O$ (‰)
		(1)	(2)	(3)	(4)	(5)	(6)	(7)	
3.39 3.43	14 79	-20.00							-20.00
3.46 3.49	137 193	-21.28	-22.85						-22.07
3.59 3.62	364 419	-21.32	-21.23						-21.27
3.65 3.68	481 539	-21.07	-20.41						-20.74
3.71 3.74	601 660	-18.78							-18.78
3.77 3.81	720 788	-21.52	-21.17						-21.35
3.86 3.90	906 976	-18.54	-18.10	-20.51					-19.05
3.90 3.93	976 1041	-19.74	-20.38						-20.06
4.02 4.06	1252 1331	-20.65	-19.01						-19.83
4.09 4.12	1401 1470	-21.43	-21.96	-18.35	-20.36	-21.16	-21.92	-19.57	-20.68
4.20 4.24	1669 1755	-21.69	-22.33						-22.01
4.27 4.30	1828 1901	-19.24	-19.39						-19.31
4.30 4.33	1901 1974	-20.09	-18.07	-21.50	-22.59	-20.93	-21.46	-21.67	-20.90
4.38 4.42	2115 2196	-18.19							-18.19
4.45 4.48	2271 2345	-18.07							-18.07
4.48 4.51	2345 2420	-19.11	-18.74	-20.53					-19.46
4.57 4.60	2574 2649	-19.50	-20.01						-19.76
4.66 4.69	2805 2880	-18.73	-16.49	-21.93	-21.45				-19.65
4.75 4.79	3033 3114	-20.88	-19.67						-20.27
4.82 4.85	3188 3266	-19.70	-19.85						-19.78
4.85 4.88	3266 3334	-20.68	-19.97	-21.83	-22.14				-21.15
4.95 4.98	3509 3589	-21.88	-21.70						-21.79
5.01 5.04	3662 3734	-20.75	-20.26						-20.51
5.04 5.07	3734 3811	-20.30	-19.18	-20.91	-19.81				-20.05
5.11 5.18	3896 3976	-21.35							-21.35
5.18 5.24	4060 4206	-18.58	-17.23	-16.85					-17.56
5.24 5.32	4206 4404	-19.65							-19.65
5.32 5.39	4404 4582	-19.74							-19.74
5.39 5.42	4582 4660	-17.54							-17.54
5.46 5.52	4779 4948	-18.74							-18.74
5.52 5.59	4948 5136	-19.60	-18.44						-19.02
5.65 5.71	5328 5523	-18.37							-18.37
5.71 5.78	5523 5626	-18.31	-18.09	-15.95	-17.60	-17.04	-16.66		-17.28
5.84 5.89	5987 6193	-20.09	-20.70	-19.68	-19.03	-17.78	-18.46		-19.29

5.92	5.95	6324	6460	-19.20	-17.07			-18.13
5.96	6.01	6539	6769	-16.72				-16.72
6.04	6.08	6928	7172	-15.26	-15.22			-15.24
6.10	6.14	7250	7625	-20.30	-15.05			-17.67
6.19	6.25	7847	8247	-16.73	-17.83	-16.09		-16.88
6.28	6.32	8481	8835	-18.75	-17.71	-17.14		-17.86
6.36	6.40	9214	9593	-17.89				-17.89

Lake Spåime, West-Central Sweden (63°07'N, 12°19'E)

Depth Interval (m)		Age Interval (cal. BP)		Magnetic Susc. ($10^{-6}m^3kg^{-1}$)
3.39	3.43	14	79	0.150
3.43	3.46	79	137	0.144
3.46	3.49	137	193	0.149
3.49	3.53	193	251	0.136
3.53	3.56	251	305	0.153
3.56	3.59	305	364	0.147
3.59	3.62	364	419	0.152
3.62	3.65	419	481	0.152
3.65	3.68	481	539	0.158
3.68	3.71	539	601	0.166
3.71	3.74	601	660	0.169
3.74	3.77	660	720	0.159
3.77	3.81	720	788	0.176
3.81	3.84	788	850	0.173
3.84	3.86	850	906	0.155
3.86	3.90	906	976	0.161
3.90	3.93	976	1041	0.167
3.93	3.96	1041	1107	0.168
3.96	3.99	1107	1178	0.171
3.99	4.02	1178	1252	0.164
4.02	4.06	1252	1331	0.161
4.06	4.09	1331	1401	0.165
4.09	4.12	1401	1470	0.153
4.12	4.15	1470	1541	0.143
4.15	4.18	1541	1616	0.162
4.18	4.20	1616	1669	0.176

4.20	4.24	1669	1755	0.169
4.24	4.27	1755	1828	0.169
4.27	4.30	1828	1901	0.168
4.30	4.33	1901	1974	0.165
4.33	4.36	1974	2048	0.165
4.36	4.38	2048	2115	0.175
4.38	4.42	2115	2196	0.191
4.42	4.45	2196	2271	0.200
4.45	4.48	2271	2345	0.174
4.48	4.51	2345	2420	0.178
4.51	4.54	2420	2494	0.182
4.54	4.57	2494	2574	0.183
4.57	4.60	2574	2649	0.197
4.60	4.63	2649	2718	0.198
4.63	4.66	2718	2805	0.195
4.66	4.69	2805	2880	0.230
4.69	4.72	2880	2959	0.217
4.72	4.75	2959	3033	0.213
4.75	4.79	3033	3114	0.230
4.79	4.82	3114	3188	0.218
4.82	4.85	3188	3266	0.234
4.85	4.88	3266	3334	0.253
4.88	4.91	3334	3425	0.245
4.91	4.95	3425	3509	0.277
4.95	4.98	3509	3589	0.264
4.98	5.01	3589	3662	0.352
5.01	5.04	3662	3734	0.285
5.04	5.07	3734	3811	0.306
5.07	5.11	3811	3896	0.300
5.11	5.14	3896	3976	0.308
5.14	5.18	3976	4060	0.290
5.18	5.20	4060	4126	0.272
5.20	5.24	4126	4206	0.310
5.24	5.27	4206	4285	0.272
5.27	5.32	4285	4404	0.293
5.32	5.35	4404	4492	0.384
5.35	5.39	4492	4582	0.342
5.39	5.42	4582	4660	0.290

5.42	5.46	4660	4779	0.293
5.46	5.49	4779	4860	0.269
5.49	5.52	4860	4948	0.320
5.52	5.54	4948	5042	0.323
5.54	5.59	5042	5136	0.295
5.59	5.62	5136	5235	0.380
5.62	5.65	5235	5328	0.437
5.65	5.68	5328	5431	0.440
5.68	5.71	5431	5523	0.397
5.71	5.74	5523	5626	0.314
5.74	5.78	5626	5751	0.350
5.78	5.81	5751	5863	0.353
5.81	5.84	5863	5987	0.234
5.84	5.86	5987	6068	0.317
5.86	5.89	6068	6193	0.413
5.89	5.92	6193	6324	0.496
5.92	5.95	6324	6460	0.418
5.95	5.98	6460	6618	0.436
5.98	6.01	6618	6769	0.406
6.01	6.04	6769	6928	0.299
6.04	6.07	6928	7094	0.501
6.07	6.10	7094	7250	0.545
6.10	6.13	7250	7433	0.604
6.13	6.16	7433	7625	0.516
6.16	6.19	7625	7847	0.432
6.19	6.22	7847	8024	0.286
6.22	6.25	8024	8247	0.311
6.25	6.28	8247	8481	0.426
6.28	6.31	8481	8728	0.546
6.31	6.33	8728	8943	0.605
6.33	6.36	8943	9214	0.528
6.36	6.39	9214	9499	0.391
6.39	6.41	9499	9687	0.273

Svartkälstjärn, East-Central Sweden (64°16′N; 19°33′E)

Depth Interval (m)	Age Interval (cal. BP)	TOC (%)			TN (%)			$\delta^{13}C_{org}$ (‰ PDB)			$\delta^{15}N$ (‰ AIR)		
		(1)	(2)	(3)	(1)	(2)	(3)	(1)	(2)	(3)	(1)	(2)	(3)
3.13 3.15	-52 -29	10.41	11.45		0.49	0.54		-28.26	-29.10		1.64	1.36	
3.15 3.17	-29 -6	6.65	6.25		0.27	0.30		-28.00	-27.89		2.69	2.03	
3.17 3.19	-6 17	3.02	2.38		0.11	0.12		-27.65	-27.76		2.64	2.68	
3.19 3.21	17 40	4.55	3.81		0.17	0.19		-27.76	-27.77		2.80	2.85	
3.21 3.23	40 110	8.77			0.40			-28.36			2.19		
3.23 3.25	110 216	19.37			1.18			-28.83			1.35		
3.25 3.27	216 381	23.93	24.37		1.48	1.49		-28.90	-28.79		1.17	1.11	
3.27 3.29	381 552	22.67			1.50			-28.90			1.16		
3.29 3.31	552 727	22.08			1.51			-29.00			1.05		
3.31 3.33	727 904	20.86			1.41			-28.73			1.17		
3.33 3.35	904 1079	20.54			1.41			-28.73			1.15		
3.35 3.37	1079 1250	19.93			1.29			-28.81			1.12		
3.37 3.39	1250 1416	20.08			1.27			-28.97			1.16		
3.39 3.41	1416 1576	22.35			1.42			-29.08			1.26		
3.41 3.43	1576 1728	23.54	23.36		1.46	1.44		-29.19	-29.01		0.94	1.19	
3.43 3.45	1728 1872	23.48			1.44			-29.08			1.17		
3.45 3.47	1872 2008	22.44			1.38			-29.05			1.19		
3.47 3.49	2008 2135	21.71			1.32			-29.08			1.17		
3.49 3.51	2135 2253	19.81			1.31			-29.19			0.62		
3.51 3.53	2253 2362	19.97			1.21			-29.22			0.71		
3.53 3.55	2362 2463	22.18			1.32			-29.17			0.78		
3.55 3.57	2463 2557	21.11			1.24			-29.48			0.98		
3.57 3.59	2557 2643	18.71	18.81		1.10	1.11		-29.53	-29.50		0.87	1.01	
3.59 3.61	2643 2722	18.11			1.06			-29.70			0.75		
3.61 3.63	2722 2795	19.11			1.11			-29.88			0.60		
3.63 3.65	2795 2864	18.89			1.08			-29.61			0.62		
3.65 3.67	2864 2927	24.19			1.38			-29.41			1.06		
3.67 3.69	2927 2987	22.96			1.45			-29.65			0.52		
3.69 3.71	2987 3044	21.56			1.27			-29.61			0.67		
3.71 3.73	3044 3099	23.36			1.37			-29.45			0.58		
3.73 3.75	3099 3153	25.84	25.77		1.48	1.47		-29.51	-29.49		0.58	0.62	
3.75 3.77	3153 3206	29.74			1.55			-29.21			1.57		
3.77 3.79	3206 3260	31.29			1.70			-29.32			1.30		
3.79 3.81	3260 3314	26.92			1.46			-29.39			1.44		

3.81	3.83	3314	3370	27.02		1.40		-29.13		1.58	
3.83	3.85	3370	3428	25.95		1.45		-29.43		1.61	
3.85	3.87	3428	3488	23.31		1.35		-29.70		1.21	
3.87	3.89	3488	3552	17.57		1.08		-29.68		0.90	
3.89	3.91	3552	3619	16.72	16.98	1.06	1.06	-29.84	-29.94	0.73	0.82
3.91	3.93	3619	3682	20.75		1.25		-29.61		0.84	
3.93	3.95	3682	3749	17.73		1.12		-29.52		0.92	
3.95	3.97	3749	3821	18.13		1.13		-29.56		0.96	
3.97	3.99	3821	3897	18.73		1.16		-29.49		1.03	
3.99	4.01	3897	3978	18.67		1.13		-29.67		0.58	
4.01	4.03	3978	4063	22.50		1.30		-29.61		0.67	
4.03	4.05	4063	4153	23.28		1.38		-29.71		0.62	
4.05	4.07	4153	4247	24.51	24.49	1.44	1.43	-29.64	-29.72	0.71	0.80
4.07	4.09	4247	4320	23.53		1.38		-29.76		0.66	
4.09	4.10	4320	4396	21.95		1.30		-29.76		0.69	
4.10	4.12	4396	4471	21.02		1.25		-29.66		0.87	
4.12	4.13	4471	4548	28.37		1.63		-29.61		0.79	
4.13	4.15	4548	4627	27.62		1.58		-29.48		0.82	
4.15	4.16	4627	4708	24.51		1.49		-29.48		1.08	
4.16	4.18	4708	4790	20.11		1.26		-29.37		1.03	
4.18	4.19	4790	4874	19.51	19.58	1.21	1.22	-29.50	-29.40	1.03	1.02
4.19	4.21	4874	4959	24.66		1.45		-29.74		1.16	
4.21	4.22	4959	5045	26.18		1.53		-29.65		1.00	
4.22	4.24	5045	5131	21.61		1.35		-29.69		1.03	
4.24	4.25	5131	5219	23.86		1.49		-29.72		1.16	
4.25	4.27	5219	5307	20.81		1.31		-29.76		1.20	
4.27	4.28	5307	5395	29.33		1.77		-29.60		1.16	
4.28	4.30	5395	5483	24.04		1.50		-29.56		1.49	
4.30	4.31	5483	5570	18.64	19.08	1.21	1.23	-29.62	-29.59	1.58	1.53
4.31	4.32	5570	5658	20.59		1.28		-29.69		1.80	
4.32	4.34	5658	5745	20.65		1.29		-29.73		1.65	
4.34	4.35	5745	5831	26.51		1.60		-29.75		1.29	
4.35	4.37	5831	5915	21.08		1.28		-29.97		1.09	
4.37	4.38	5915	5999	23.45		1.42		-29.61		1.11	
4.38	4.40	5999	6081	24.65		1.51		-29.70		1.12	
4.40	4.41	6081	6162	26.67		1.58		-29.72		1.15	
4.41	4.43	6162	6241	25.83	25.68	1.56	1.55	-29.66	-29.80	1.27	1.35
4.43	4.44	6241	6318	26.87		1.65		-29.31		1.47	

4.44	4.46	6318	6393	25.03			1.52			-29.24			1.47				
4.46	4.47	6393	6466	25.61			1.56			-29.54			1.59				
4.47	4.49	6466	6537	25.78			1.58			-29.57			1.26				
4.49	4.50	6537	6605	25.57	25.89		1.56	1.57		-29.55	-29.55		1.44	1.61			
4.50	4.52	6605	6674	25.33			1.55			-29.33			1.52				
4.52	4.53	6674	6743	27.96			1.72			-29.48			1.48				
4.53	4.55	6743	6809	29.59			1.82			-29.65			1.61				
4.55	4.56	6809	6872	30.73			1.89			-29.71			1.73				
4.56	4.58	6872	6934	29.39			1.82			-29.60			1.89				
4.58	4.59	6934	6992	26.70			1.68			-29.44			1.67				
4.59	4.61	6992	7048	27.73			1.69			-29.23			2.38				
4.61	4.62	7048	7102	28.62			1.77			-29.81			2.06				
4.62	4.64	7102	7153	28.42	28.17		1.75	1.74		-29.83	-29.40		1.76	2.23			
4.64	4.65	7153	7203	26.72			1.66			-29.48			1.83				
4.65	4.67	7203	7250	26.32			1.62			-29.69			1.96				
4.67	4.68	7250	7295	25.98			1.61			-29.84			1.74				
4.68	4.70	7295	7338	24.78			1.52			-29.82			1.78				
4.70	4.71	7338	7379	21.41	23.16		1.66	1.60		-29.62	-29.65		1.94	2.01			
4.71	4.73	7379	7419	21.11	21.57	21.82	1.62	1.57	1.59	-31.84	-31.92	-31.75	4.54	4.53	4.55		
4.73	4.74	7419	7458	21.17	23.42		1.65	1.64		-29.69	-29.71		1.93	1.88			
4.74	4.76	7458	7496	26.37			1.67			-29.99			2.05				
4.76	4.77	7496	7533	23.13	23.40		1.48	1.50		-29.81	-30.02		1.92	2.25			
4.77	4.79	7533	7570	24.71			1.56			-30.03			2.16				
4.79	4.80	7570	7606	24.03			1.49			-30.02			1.74				
4.80	4.82	7606	7643	24.45			1.52			-30.17			1.83				
4.82	4.83	7643	7679	21.26			1.36			-30.18			1.48				
4.83	4.85	7679	7716	21.81			1.39			-30.19			1.53				
4.85	4.86	7716	7755	21.01			1.40			-30.50			1.71				
4.86	4.88	7755	7794	23.17	20.06	20.12	1.51	1.66	1.67	-30.49	-30.23	-30.27	1.48	1.59	1.46		
4.88	4.89	7794	7835	22.66	23.33		1.44	1.53		-30.56	-30.60		1.80	1.38			
4.89	4.91	7835	7878	22.85			1.46			-30.55			1.51				
4.91	4.92	7878	7920	22.13			1.49			-31.17			4.73				
4.92	4.94	7920	7965	20.91	22.21		1.40	1.53		-30.91	-30.94		5.02	4.51			
4.94	4.95	7965	8012	20.88			1.40			-30.90			5.22				
4.95	4.97	8012	8062	22.12			1.59			-30.09			5.03				
4.97	4.98	8062	8115	22.18			1.47			-29.68			1.53				
4.98	5.00	8115	8172	22.67			1.51			-30.12			1.17				
5.00	5.01	8172	8211	22.47			1.51			-30.21			0.70				

5.01	5.02	8211	8252	22.24			1.52			-30.22			1.02		
5.02	5.03	8252	8295	20.88			1.42			-30.51			0.96		
5.03	5.04	8295	8339	20.23			1.41			-30.60			0.81		
5.04	5.05	8339	8386	19.96			1.40			-31.60			5.24		
5.05	5.06	8386	8433	24.58	24.34		1.57	1.54		-28.91	-29.38		1.64	1.99	
5.06	5.07	8433	8483	20.80			1.44			-31.61			4.80		
5.07	5.08	8483	8534	19.17			1.32			-31.67			4.60		
5.08	5.09	8534	8586	18.20			1.26			-30.61			0.89		
5.09	5.10	8586	8641	15.83			1.13			-30.78			0.84		
5.10	5.11	8641	8696	13.85			1.05			-30.75			-0.16		
5.11	5.12	8696	8754	12.10			0.97			-31.00			-0.28		
5.12	5.13	8754	8812	10.10			0.87			-30.35			-0.49		
5.13	5.14	8812	8872	8.21			0.76			-30.23			-0.10		
5.14	5.15	8872	8933	6.74	6.64		0.79	0.78		-28.93	-29.15		1.80	1.82	
5.15	5.16	8933	8995	4.29			0.61			-27.07			0.93		
5.16	5.17	8995	9058	3.98	3.95		0.57	0.56		-25.55	-25.39		1.20	0.91	
5.17	5.18	9058	9122	3.74			0.54			-24.80			1.91		
5.18	5.19	9122	9186	3.71			0.45			-24.00			-1.16		
5.19	5.20	9186	9250	4.06			0.50			-23.10			-0.98		
5.20	5.21	9250	9314	3.56			0.44			-22.72			-0.96		
5.21	5.22	9314	9378	3.53			0.42			-22.24			-0.72		
5.22	5.23	9378	9442	2.01	2.52	3.08	0.23	0.27	0.32	-21.99	-21.77	-21.81	-0.59	-0.60	-0.55
5.23	5.24	9442	9505	1.09	0.88		0.15	0.12		-21.76	-21.88		3.62	3.68	
5.24	5.25	9505	9566	0.26	0.57		0.03			-23.51	-22.46		7.35		
5.25	5.26	9566	9626	0.17	0.36		0.02			-24.44	-22.91		9.60		
5.26	5.27	9626	9684	0.29	0.34		0.03			-23.81	-23.86		4.81		
5.27	5.28	9684	9739	0.33						-24.14					

Svartkälstjärn, East-Central Sweden (64°16′N; 19°33′E)

Depth Interval (m)		Age Interval (cal. BP)		Average: TOC (%)	TN (%)	$\delta^{13}C_{org}$ (‰)	$\delta^{15}N$ (‰)	Cellulose $\delta^{18}O$ (‰ VSMOW) (1)	(2)	Average cellulose-inf. water $\delta^{18}O$ (‰)	Magnetic Susc. ($10^{-6}m^3kg^{-1}$)
3.13	3.15	-52	-29	10.93	0.52	-28.68	1.50	4.35			1.716
3.15	3.17	-29	-6	6.45	0.28	-27.94	2.36				1.606
3.17	3.19	-6	17	2.70	0.11	-27.70	2.66				1.526
3.19	3.21	17	40	4.18	0.18	-27.77	2.82			-23.19	1.415
3.21	3.23	40	110	8.77	0.40	-28.36	2.19	11.90	10.24		1.272

3.23	3.25	110	216	19.37	1.18	-28.83	1.35	8.66	7.72		0.925
3.25	3.27	216	381	24.15	1.49	-28.85	1.14	7.60	8.61		0.729
3.27	3.29	381	552	22.67	1.50	-28.90	1.16			-16.66	0.462
3.29	3.31	552	727	22.08	1.51	-29.00	1.05	11.38		-19.46	0.560
3.31	3.33	727	904	20.86	1.41	-28.73	1.17			-19.54	0.656
3.33	3.35	904	1079	20.54	1.41	-28.73	1.15	9.17	8.95		0.725
3.35	3.37	1079	1250	19.93	1.29	-28.81	1.12			-16.36	0.668
3.37	3.39	1250	1416	20.08	1.27	-28.97	1.16	9.23	9.09		0.546
3.39	3.41	1416	1576	22.35	1.42	-29.08	1.26	8.86	9.11	-18.61	0.626
3.41	3.43	1576	1728	23.45	1.45	-29.10	1.07	8.88	9.72		0.636
3.43	3.45	1728	1872	23.48	1.44	-29.08	1.17			-18.52	0.599
3.45	3.47	1872	2008	22.44	1.38	-29.05	1.19	8.38	9.82	-18.68	0.619
3.47	3.49	2008	2135	21.71	1.32	-29.08	1.17			-18.38	0.578
3.49	3.51	2135	2253	19.81	1.31	-29.19	0.62	4.72	4.32		0.624
3.51	3.53	2253	2362	19.97	1.21	-29.22	0.71			-18.58	0.614
3.53	3.55	2362	2463	22.18	1.32	-29.17	0.78	9.48	5.00		0.496
3.55	3.57	2463	2557	21.11	1.24	-29.48	0.98			-23.03	0.518
3.57	3.59	2557	2643	18.76	1.10	-29.52	0.94				0.567
3.59	3.61	2643	2722	18.11	1.06	-29.70	0.75	6.51	7.90	-18.21	0.432
3.61	3.63	2722	2795	19.11	1.11	-29.88	0.60				0.309
3.63	3.65	2795	2864	18.89	1.08	-29.61	0.62				0.028
3.65	3.67	2864	2927	24.19	1.38	-29.41	1.06	6.27	7.20	-20.42	0.309
3.67	3.69	2927	2987	22.96	1.45	-29.65	0.52				0.209
3.69	3.71	2987	3044	21.56	1.27	-29.61	0.67	11.04	12.17		0.367
3.71	3.73	3044	3099	23.36	1.37	-29.45	0.58			-20.87	0.454
3.73	3.75	3099	3153	25.81	1.48	-29.50	0.60	11.83	10.16		0.361
3.75	3.77	3153	3206	29.74	1.55	-29.21	1.57			-16.14	0.442
3.77	3.79	3206	3260	31.29	1.70	-29.32	1.30				0.430
3.79	3.81	3260	3314	26.92	1.46	-29.39	1.44	9.81	11.68	-16.73	0.419
3.81	3.83	3314	3370	27.02	1.40	-29.13	1.58				0.512
3.83	3.85	3370	3428	25.95	1.45	-29.43	1.61				0.353
3.85	3.87	3428	3488	23.31	1.35	-29.70	1.21	9.45	9.12	-16.97	0.449
3.87	3.89	3488	3552	17.57	1.08	-29.68	0.90				0.309
3.89	3.91	3552	3619	16.85	1.06	-29.89	0.77				0.381
3.91	3.93	3619	3682	20.75	1.25	-29.61	0.84	6.17	9.09	-18.40	0.400
3.93	3.95	3682	3749	17.73	1.12	-29.52	0.92				0.311
3.95	3.97	3749	3821	18.13	1.13	-29.56	0.96				0.389
3.97	3.99	3821	3897	18.73	1.16	-29.49	1.03	9.46	10.08	-20.00	0.446

3.99	4.01	3897	3978	18.67	1.13	-29.67	0.58			0.488
4.01	4.03	3978	4063	22.50	1.30	-29.61	0.67			0.469
4.03	4.05	4063	4153	23.28	1.38	-29.71	0.62	7.38	7.06	-17.92	0.456
4.05	4.07	4153	4247	24.50	1.44	-29.68	0.76			0.450
4.07	4.09	4247	4320	23.53	1.38	-29.76	0.66			0.497
4.09	4.10	4320	4396	21.95	1.30	-29.76	0.69	9.65	10.81	-20.40	0.433
4.10	4.12	4396	4471	21.02	1.25	-29.66	0.87			0.814
4.12	4.13	4471	4548	28.37	1.63	-29.61	0.79			0.563
4.13	4.15	4548	4627	27.62	1.58	-29.48	0.82	7.32	7.54	-17.48	0.536
4.15	4.16	4627	4708	24.51	1.49	-29.48	1.08			0.421
4.16	4.18	4708	4790	20.11	1.26	-29.37	1.03	7.42	6.46	0.510
4.18	4.19	4790	4874	19.55	1.21	-29.45	1.02			-20.20	0.584
4.19	4.21	4874	4959	24.66	1.45	-29.74	1.16			0.453
4.21	4.22	4959	5045	26.18	1.53	-29.65	1.00	9.82	7.46	-20.68	0.389
4.22	4.24	5045	5131	21.61	1.35	-29.69	1.03			0.497
4.24	4.25	5131	5219	23.86	1.49	-29.72	1.16	8.57	9.85	0.613
4.25	4.27	5219	5307	20.81	1.31	-29.76	1.20			-19.03	0.467
4.27	4.28	5307	5395	29.33	1.77	-29.60	1.16	6.59	5.33	0.591
4.28	4.30	5395	5483	24.04	1.50	-29.56	1.49			-18.47	0.619
4.30	4.31	5483	5570	18.86	1.22	-29.61	1.56			0.533
4.31	4.32	5570	5658	20.59	1.28	-29.69	1.80	8.54	9.52	-21.63	0.585
4.32	4.34	5658	5745	20.65	1.29	-29.73	1.65			0.267
4.34	4.35	5745	5831	26.51	1.60	-29.75	1.29			0.562
4.35	4.37	5831	5915	21.08	1.28	-29.97	1.09	6.92	7.54	-18.64	0.272
4.37	4.38	5915	5999	23.45	1.42	-29.61	1.11			0.427
4.38	4.40	5999	6081	24.65	1.51	-29.70	1.12			0.428
4.40	4.41	6081	6162	26.67	1.58	-29.72	1.15	10.75	10.35	-20.39	0.279
4.41	4.43	6162	6241	25.75	1.56	-29.73	1.31			0.390
4.43	4.44	6241	6318	26.87	1.65	-29.31	1.47	11.74	13.44	0.340
4.44	4.46	6318	6393	25.03	1.52	-29.24	1.47			-17.17	0.302
4.46	4.47	6393	6466	25.61	1.56	-29.54	1.59			0.175
4.47	4.49	6466	6537	25.78	1.58	-29.57	1.26	11.79		-15.18	0.088
4.49	4.50	6537	6605	25.73	1.57	-29.55	1.53			0.348
4.50	4.52	6605	6674	25.33	1.55	-29.33	1.52	10.39	11.74	0.184
4.52	4.53	6674	6743	27.96	1.72	-29.48	1.48			-15.96	0.239
4.53	4.55	6743	6809	29.59	1.82	-29.65	1.61			0.375
4.55	4.56	6809	6872	30.73	1.89	-29.71	1.73	13.12	12.36	-16.67	0.226
4.56	4.58	6872	6934	29.39	1.82	-29.60	1.89			0.095

4.58	4.59	6934	6992	26.70	1.68	-29.44	1.67			0.006
4.59	4.61	6992	7048	27.73	1.69	-29.23	2.38	9.75	8.28	-15.03	0.212
4.61	4.62	7048	7102	28.62	1.77	-29.81	2.06			0.033
4.62	4.64	7102	7153	28.29	1.74	-29.61	2.00			0.225
4.64	4.65	7153	7203	26.72	1.66	-29.48	1.83			-18.66	0.120
4.65	4.67	7203	7250	26.32	1.62	-29.69	1.96	9.80			0.137
4.67	4.68	7250	7295	25.98	1.61	-29.84	1.74				0.179
4.68	4.70	7295	7338	24.78	1.52	-29.82	1.78				0.201
4.70	4.71	7338	7379	22.28	1.63	-29.63	1.97	9.85	13.20	-17.89	0.137
4.71	4.73	7379	7419	21.50	1.59	-31.84	4.54			0.087
4.73	4.74	7419	7458	22.30	1.65	-29.70	1.91			0.238
4.74	4.76	7458	7496	26.37	1.67	-29.99	2.05			-16.21	0.437
4.76	4.77	7496	7533	23.27	1.49	-29.91	2.08	7.03	8.20		0.327
4.77	4.79	7533	7570	24.71	1.56	-30.03	2.16				0.300
4.79	4.80	7570	7606	24.03	1.49	-30.02	1.74				0.200
4.80	4.82	7606	7643	24.45	1.52	-30.17	1.83	12.27	13.45	-20.02	0.361
4.82	4.83	7643	7679	21.26	1.36	-30.18	1.48			0.316
4.83	4.85	7679	7716	21.81	1.39	-30.19	1.53			0.231
4.85	4.86	7716	7755	21.01	1.40	-30.50	1.71			-14.92	0.287
4.86	4.88	7755	7794	21.12	1.61	-30.33	1.51	13.41	13.20		0.186
4.88	4.89	7794	7835	22.99	1.49	-30.58	1.59				0.272
4.89	4.91	7835	7878	22.85	1.46	-30.55	1.51				0.463
4.91	4.92	7878	7920	22.13	1.49	-31.17	4.73	11.68	13.70	-14.48	0.189
4.92	4.94	7920	7965	21.56	1.47	-30.93	4.77				0.425
4.94	4.95	7965	8012	20.88	1.40	-30.90	5.22				0.624
4.95	4.97	8012	8062	22.12	1.59	-30.09	5.03	13.32	12.43	-15.08	0.509
4.97	4.98	8062	8115	22.18	1.47	-29.68	1.53				0.551
4.98	5.00	8115	8172	22.67	1.51	-30.12	1.17				0.673
5.00	5.01	8172	8211	22.47	1.51	-30.21	0.70	14.72	14.47	-14.91	0.558
5.01	5.02	8211	8252	22.24	1.52	-30.22	1.02				0.448
5.02	5.03	8252	8295	20.88	1.42	-30.51	0.96				0.585
5.03	5.04	8295	8339	20.23	1.41	-30.60	0.81	13.76		-13.23	0.421
5.04	5.05	8339	8386	19.96	1.40	-31.60	5.24				0.577
5.05	5.06	8386	8433	24.46	1.56	-29.15	1.82				0.465
5.06	5.07	8433	8483	20.80	1.44	-31.61	4.80			-14.04	0.654
5.07	5.08	8483	8534	19.17	1.32	-31.67	4.60	10.60	10.95		0.560
5.08	5.09	8534	8586	18.20	1.26	-30.61	0.89				0.412
5.09	5.10	8586	8641	15.83	1.13	-30.78	0.84				0.465

5.10	5.11	8641	8696	13.85	1.05	-30.75	-0.16			-16.94	0.388
5.11	5.12	8696	8754	12.10	0.97	-31.00	-0.28	11.52	11.77		0.712
5.12	5.13	8754	8812	10.10	0.87	-30.35	-0.49				0.569
5.13	5.14	8812	8872	8.21	0.76	-30.23	-0.10				0.541
5.14	5.15	8872	8933	6.69	0.78	-29.04	1.81	12.69	12.65	-16.10	0.720
5.15	5.16	8933	8995	4.29	0.61	-27.07	0.93				0.778
5.16	5.17	8995	9058	3.96	0.56	-25.47	1.06				0.813
5.17	5.18	9058	9122	3.74	0.54	-24.80	1.91	10.86		-15.10	0.864
5.18	5.19	9122	9186	3.71	0.45	-24.00	-1.16				0.900
5.19	5.20	9186	9250	4.06	0.50	-23.10	-0.98				1.013
5.20	5.21	9250	9314	3.56	0.44	-22.72	-0.96	9.43	8.94	-16.87	0.928
5.21	5.22	9314	9378	3.53	0.42	-22.24	-0.72				0.982
5.22	5.23	9378	9442	2.54	0.27	-21.86	-0.58				0.935
5.23	5.24	9442	9505	0.98	0.13	-21.82	3.65	10.73		-18.49	1.103
5.24	5.25	9505	9566	0.41	0.03	-22.98	7.35				1.368
5.25	5.26	9566	9626	0.27	0.02	-23.68	9.60				1.352
5.26	5.27	9626	9684	0.32	0.03	-23.83	4.81			-16.99	1.411
5.27	5.28	9684	9739	0.33		-24.14					1.327
5.28	5.30	9739	9841								1.377
5.30	5.32	9841	9926								1.434
5.32	5.34	9926	9990								1.424
5.34	5.37	9990	10036								1.381

Arbovatten, Southern Sweden (58º04'N, 12º04'E)

Depth Interval (m)		Age Interval (cal. BP)		TOC (%)			TN (%)			$\delta^{13}C_{org}$ (‰ PDB)			$\delta^{15}N$ (‰ AIR)		
				(1)	(2)	(3)	(1)	(2)	(3)	(1)	(2)	(3)	(1)	(2)	(3)
5.20	5.25	-54	-38	31.60			1.90			-29.49			0.38		
5.25	5.30	-38	-14	33.53			1.69			-28.94			0.57		
5.30	5.35	-14	16	32.79	32.84		1.42	1.41		-28.52	-28.51		0.17	0.06	
5.35	5.40	16	69	34.39			1.42			-28.25			0.13		
5.40	5.45	69	124	37.05			1.55			-28.16			0.15		
5.45	5.50	124	180	35.50			1.64			-28.27			-0.03		
5.50	5.55	180	253	35.48			1.89			-28.24			0.11		
5.55	5.60	253	325	34.93			1.87			-28.37			0.20		
5.60	5.65	325	398	33.65	33.73		1.78	1.79		-28.38	-28.35		0.27	0.23	
5.65	5.70	398	470	34.64			2.02			-28.85			-0.05		
5.70	5.75	470	565	37.60			2.11			-28.66			0.05		

5.75	5.80	565	660	35.51			1.89			-28.62			-0.35		
5.80	5.85	660	775	35.81			2.03			-28.94			-0.16		
5.85	5.90	775	890	38.95			2.06			-28.85			-0.01		
5.90	5.95	890	1015	41.75	41.74		2.22	2.22		-28.83	-28.87		-0.27	-0.21	
5.95	6.00	1015	1140	43.65			2.33			-29.12			-0.39		
6.00	6.05	1140	1265	45.31			2.26			-28.99			-0.14		
6.05	6.10	1265	1390	43.12			2.08			-28.65			-0.34		
6.10	6.15	1390	1540	43.09			2.21			-28.96			-0.46		
6.15	6.20	1540	1690	39.70			2.17			-29.05			-0.48		
6.20	6.25	1690	1840	41.91	42.19		1.99	1.97		-28.71	-28.63		-0.47	-0.33	
6.25	6.30	1840	1990	41.00			2.15			-28.90			-0.47		
6.30	6.35	1990	2173	39.16			2.10			-28.98			-0.63		
6.35	6.40	2173	2355	39.28			2.00			-28.88			-0.14		
6.40	6.44	2355	2501	45.09			2.31			-28.97			0.00		
6.44	6.48	2501	2647	45.68			2.18			-28.88			-0.19		
6.48	6.52	2647	2800	48.70	48.58		2.18	2.18		-28.71	-28.73		0.13	-0.05	
6.52	6.56	2800	2960	46.87			2.14			-28.77			-0.04		
6.56	6.60	2960	3120	45.40			2.16			-28.92			-0.36		
6.60	6.64	3120	3280	47.03			2.21			-28.94			-0.25		
6.64	6.68	3280	3440	46.24			2.22			-29.03			-0.13		
6.68	6.72	3440	3610	45.68			2.26			-29.08			-0.29		
6.72	6.76	3610	3790	46.80	46.90		2.35	2.34		-29.14	-29.12		-0.41	-0.46	
6.76	6.80	3790	3970	47.36			2.28			-29.04			-0.33		
6.80	6.84	3970	4150	47.28			2.22			-28.90			-0.21		
6.84	6.88	4150	4330	45.32			2.16			-28.89			-0.28		
6.88	6.92	4330	4510	50.13			2.52			-29.43			-0.27		
6.92	6.96	4510	4690	50.91			2.61			-29.46			-0.04		
6.96	7.00	4690	4870	49.61	49.45		2.69	2.70		-29.75	-29.64		-0.03	-0.14	
7.00	7.04	4870	5050	49.46			2.56			-29.41			0.06		
7.04	7.08	5050	5230	45.30			2.40			-29.47			0.04		
7.08	7.12	5230	5411	48.81	50.62		2.23	2.37		-29.10	-29.09		-0.02	-0.12	
7.12	7.16	5411	5593	47.28	47.29	48.87	2.40	2.45	2.50	-29.82	-29.93	-29.62	0.05	0.10	-0.18
7.16	7.20	5593	5775	45.93			2.48			-29.64			0.06		
7.20	7.24	5775	5957	47.22			2.61			-29.79			0.07		
7.24	7.28	5957	6139	42.80			2.51			-30.18			0.11		
7.28	7.32	6139	6308	44.31			2.46			-30.07			0.11		
7.33	7.37	6308	6464	44.48			2.41			-29.69			0.38		
7.37	7.41	6464	6620	44.64	45.06		2.40	2.44		-29.66	-29.66		0.15	0.18	

7.41	7.45	6620	6776	41.79			2.47			-30.27			0.08		
7.45	7.49	6776	6932	43.95			2.38			-29.96			0.06		
7.49	7.53	6932	7078	42.67			2.45			-30.06			-0.12		
7.53	7.57	7078	7214	42.42			2.42			-30.14			0.08		
7.57	7.61	7214	7350	41.76			2.41			-30.14			-0.05		
7.61	7.65	7350	7486	39.22	39.65		2.30	2.28		-30.12	-30.10		-0.01	-0.07	
7.65	7.69	7486	7622	37.69			2.23			-30.17			0.10		
7.69	7.73	7622	7750	34.16			1.96			-29.57			0.44		
7.73	7.77	7750	7870	40.98			2.34			-30.15			0.30		
7.77	7.80	7870	7990	35.92			2.13			-30.08			0.18		
7.80	7.83	7990	8068	31.27			1.98			-29.81			0.38		
7.83	7.86	8068	8146	36.68	36.47		2.08	2.06		-29.47	-29.45		0.43	0.41	
7.86	7.89	8146	8224	37.99			2.16			-29.95			0.60		
7.89	7.92	8224	8298	37.23			2.07			-29.89			0.29		
7.92	7.95	8298	8370	38.20			2.15			-29.97			0.44		
7.95	7.98	8370	8442	35.35			2.04			-29.92			0.41		
7.98	8.01	8442	8512	35.20			2.06			-30.23			0.34		
8.01	8.04	8512	8578	37.85	38.12		1.98	1.95		-29.70	-29.63		0.03	0.19	
8.04	8.07	8578	8644	36.91			1.97			-29.73			0.10		
8.07	8.10	8644	8710	31.64			1.83			-29.64			0.28		
8.10	8.13	8710	8766	30.09			1.74			-29.58			0.26		
8.13	8.16	8766	8821	30.04			1.73			-29.60			0.36		
8.16	8.19	8821	8877	30.16			1.78			-29.65			0.44		
8.19	8.22	8877	8932	29.84	30.43		1.83	1.84		-29.78	-29.71		0.30	0.23	
8.22	8.25	8932	8988	30.38			1.83			-29.91			0.52		
8.25	8.28	8988	9043	32.42			1.95			-29.92			0.41		
8.28	8.31	9043	9096	29.17			1.76			-29.59			0.60		
8.31	8.34	9096	9144	24.50			1.53			-29.52			0.25		
8.34	8.37	9144	9192	23.74	23.87		1.47	1.46		-29.24	-29.25		0.25	0.21	
8.37	8.40	9192	9240	27.31			1.66			-29.06			0.53		
8.40	8.43	9240	9288	28.31			1.75			-28.97			0.23		
8.43	8.46	9288	9336	26.55			1.63			-28.91			0.32		
8.46	8.49	9336	9384	27.57			1.68			-29.10			0.28		
8.49	8.52	9384	9429	29.46			1.77			-29.15			0.60		
8.52	8.55	9429	9473	28.12	28.18		1.73	1.72		-29.20	-29.15		0.37	0.60	
8.55	8.58	9473	9516	27.66			1.70			-29.12			0.51		
8.58	8.61	9516	9560	27.73			1.67			-29.15			0.41		
8.61	8.64	9560	9603	28.92			1.75			-29.17			0.39		

8.64	8.67	9603	9647	29.32			1.73			-29.21			0.50		
8.67	8.70	9647	9690	27.86			1.69			-29.24			0.70		
8.70	8.73	9690	9734	28.42	28.31		1.74	1.74		-29.04	-29.10		0.75	0.30	
8.73	8.76	9734	9777	29.76			1.77			-29.44			0.47		
8.76	8.79	9777	9821	27.82			1.67			-29.04			0.59		
8.79	8.82	9821	9864	30.33			1.79			-29.26			0.58		
8.82	8.85	9864	9908	30.82			1.87			-29.30			0.29		
8.85	8.88	9908	9951	28.20			1.79			-29.07			0.53		
8.88	8.91	9951	9993	26.46	26.59		1.66	1.67		-29.26	-29.19		0.73	0.59	
8.91	8.94	9993	10030	26.43			1.70			-29.04			0.72		
8.94	8.97	10030	10068	27.78			1.78			-29.34			0.80		
8.97	9.00	10068	10105	24.73			1.60			-28.95			0.87		
9.00	9.03	10105	10143	21.40			1.39			-28.83			0.99		
9.03	9.06	10143	10180	22.11			1.54			-28.82			1.05		
9.06	9.09	10180	10218	19.18	19.36		1.33	1.37		-28.36	-28.32		0.71	1.21	
9.09	9.12	10218	10253	18.23			1.31			-27.83			1.26		
9.12	9.15	10253	10289	17.71			1.25			-27.57			0.89		
9.15	9.18	10289	10324	17.21			1.21			-27.56			1.20		
9.18	9.21	10324	10359	17.65			1.26			-27.65			1.44		
9.21	9.24	10359	10394	17.19			1.25			-27.14			1.78		
9.24	9.27	10394	10430	13.86	13.88		1.00	0.99		-26.32	-26.33		1.96	2.09	
9.27	9.30	10430	10465	11.19			0.83			-25.99			2.14		
9.30	9.33	10465	10500	9.94			0.74			-25.84			1.83		

Arbovatten, Southern Sweden (58º04'N, 12º04'E)

Depth Interval (m)		Age Interval (cal. BP)		Average: TOC (%)	TN (%)	$\delta^{13}C_{org}$ (‰)	$\delta^{15}N$ (‰)	Cellulose $\delta^{18}O$ (‰ VSMOW) (1)	(2)	Average cellulose-inf. water $\delta^{18}O$ (‰)	Magnetic Susc. ($10^{-6}m^3kg^{-1}$)
5.20	5.25	-54	-38	31.60	1.90	-29.49	0.38	12.97	13.21	-14.70	1.243
5.25	5.30	-38	-14	33.53	1.69	-28.94	0.57	13.10	12.82	-14.82	1.185
5.30	5.35	-14	16	32.82	1.42	-28.51	0.11	13.41	12.51	-14.82	0.862
5.35	5.40	16	69	34.39	1.42	-28.25	0.13	14.06	13.62	-13.97	0.782
5.40	5.45	69	124	37.05	1.55	-28.16	0.15	15.55	15.59	-12.29	0.574
5.45	5.50	124	180	35.50	1.64	-28.27	-0.03				0.495
5.50	5.55	180	253	35.48	1.89	-28.24	0.11	15.54	16.17	-12.01	0.424
5.55	5.60	253	325	34.93	1.87	-28.37	0.20	16.36	16.90	-11.25	0.255
5.60	5.65	325	398	33.69	1.78	-28.36	0.25	16.60	16.95	-11.11	0.238

5.65	5.70	398	470	34.64	2.02	-28.85	-0.05	16.07	15.91	-11.88	0.243
5.70	5.75	470	565	37.60	2.11	-28.66	0.05	17.25	17.06	-10.74	0.224
5.75	5.80	565	660	35.51	1.89	-28.62	-0.35	16.25	16.33	-11.59	0.184
5.80	5.85	660	775	35.81	2.03	-28.94	-0.16	16.13	17.27	-11.18	0.272
5.85	5.90	775	890	38.95	2.06	-28.85	-0.01	17.91	17.27	-10.32	0.242
5.90	5.95	890	1015	41.75	2.22	-28.85	-0.24	16.12	16.46	-11.59	0.334
5.95	6.00	1015	1140	43.65	2.33	-29.12	-0.39	16.76	16.85	-11.08	0.341
6.00	6.05	1140	1265	45.31	2.26	-28.99	-0.14	17.09	17.61	-10.55	0.265
6.05	6.10	1265	1390	43.12	2.08	-28.65	-0.34	16.64	16.83	-11.15	0.287
6.10	6.15	1390	1540	43.09	2.21	-28.96	-0.46	17.54	17.93	-10.18	0.300
6.15	6.20	1540	1690	39.70	2.17	-29.05	-0.48	16.74	16.40	-11.31	0.088
6.20	6.25	1690	1840	42.05	1.98	-28.67	-0.40	18.06	17.89	-9.94	0.247
6.25	6.30	1840	1990	41.00	2.15	-28.90	-0.47	17.81	18.23	-9.90	0.423
6.30	6.35	1990	2173	39.16	2.10	-28.98	-0.63	17.47	17.17	-10.58	0.282
6.35	6.40	2173	2355	39.28	2.00	-28.88	-0.14	17.56	16.78	-10.73	0.270
6.40	6.44	2355	2501	45.09	2.31	-28.97	0.00	17.65	17.52	-10.32	0.272
6.44	6.48	2501	2647	45.68	2.18	-28.88	-0.19	17.96	18.02	-9.93	0.263
6.48	6.52	2647	2800	48.64	2.18	-28.72	0.04	18.63	18.30	-9.47	0.277
6.52	6.56	2800	2960	46.87	2.14	-28.77	-0.04	17.89	17.73	-10.10	0.232
6.56	6.60	2960	3120	45.40	2.16	-28.92	-0.36	17.59	17.86	-10.19	0.265
6.60	6.64	3120	3280	47.03	2.21	-28.94	-0.25	18.30	18.11	-9.72	0.218
6.64	6.68	3280	3440	46.24	2.22	-29.03	-0.13	17.81	17.42	-10.30	0.288
6.68	6.72	3440	3610	45.68	2.26	-29.08	-0.29	17.39	16.79	-10.81	0.273
6.72	6.76	3610	3790	46.85	2.35	-29.13	-0.44	17.61	17.46	-10.37	0.320
6.76	6.80	3790	3970	47.36	2.28	-29.04	-0.33	17.82	17.58	-10.21	0.262
6.80	6.84	3970	4150	47.28	2.22	-28.90	-0.21	17.43	17.96	-10.22	0.165
6.84	6.88	4150	4330	45.32	2.16	-28.89	-0.28	18.94	18.13	-9.40	0.102
6.88	6.92	4330	4510	50.13	2.52	-29.43	-0.27	17.82	17.59	-10.20	0.202
6.92	6.96	4510	4690	50.91	2.61	-29.46	-0.04	17.96	17.90	-9.99	0.224
6.96	7.00	4690	4870	49.53	2.70	-29.70	-0.08	17.03	17.53	-10.62	0.211
7.00	7.04	4870	5050	49.46	2.56	-29.41	0.06	18.04	18.14	-9.83	0.163
7.04	7.08	5050	5230	45.30	2.40	-29.47	0.04	17.61	17.48	-10.36	0.154
7.08	7.12	5230	5411	49.72	2.30	-29.10	-0.07	17.43	16.72	-10.82	0.223
7.12	7.16	5411	5593	47.81	2.45	-29.79	-0.01	16.53	16.78	-11.23	0.212
7.16	7.20	5593	5775	45.93	2.48	-29.64	0.06	17.35	17.14	-10.66	0.156
7.20	7.24	5775	5957	47.22	2.61	-29.79	0.07	17.21	17.48	-10.55	0.348
7.24	7.28	5957	6139	42.80	2.51	-30.18	0.11	17.01	17.69	-10.55	0.216
7.28	7.32	6139	6308	44.31	2.46	-30.07	0.11	17.31	17.06	-10.71	0.194

7.33	7.37	6308	6464	44.48	2.41	-29.69	0.38	17.39	17.57	-10.43	0.137
7.37	7.41	6464	6620	44.85	2.42	-29.66	0.17	17.49	17.23	-10.54	0.229
7.41	7.45	6620	6776	41.79	2.47	-30.27	0.08	16.99	16.37	-11.21	0.267
7.45	7.49	6776	6932	43.95	2.38	-29.96	0.06	17.90	18.08	-9.93	0.230
7.49	7.53	6932	7078	42.67	2.45	-30.06	-0.12	17.84	17.19	-10.39	0.187
7.53	7.57	7078	7214	42.42	2.42	-30.14	0.08	17.33	17.55	-10.46	0.207
7.57	7.61	7214	7350	41.76	2.41	-30.14	-0.05	17.48	17.20	-10.56	0.143
7.61	7.65	7350	7486	39.44	2.29	-30.11	-0.04	17.63	17.53	-10.33	0.136
7.65	7.69	7486	7622	37.69	2.23	-30.17	0.10	17.41	17.41	-10.49	0.185
7.69	7.73	7622	7750	34.16	1.96	-29.57	0.44	17.26	17.23	-10.65	0.110
7.73	7.77	7750	7870	40.98	2.34	-30.15	0.30	17.32	17.66	-10.41	0.293
7.77	7.80	7870	7990	35.92	2.13	-30.08	0.18	16.99	17.16	-10.82	0.264
7.80	7.83	7990	8068	31.27	1.98	-29.81	0.38	17.18	17.96	-10.34	0.291
7.83	7.86	8068	8146	36.58	2.07	-29.46	0.42	16.32	16.68	-11.38	0.235
7.86	7.89	8146	8224	37.99	2.16	-29.95	0.60	15.38	15.71	-12.31	0.309
7.89	7.92	8224	8298	37.23	2.07	-29.89	0.29	16.71	17.22	-10.93	0.307
7.92	7.95	8298	8370	38.20	2.15	-29.97	0.44	16.80	16.61	-11.18	0.260
7.95	7.98	8370	8442	35.35	2.04	-29.92	0.41	17.06	16.68	-11.02	0.266
7.98	8.01	8442	8512	35.20	2.06	-30.23	0.34	16.40	16.08	-11.63	0.357
8.01	8.04	8512	8578	37.99	1.96	-29.67	0.11	17.50	18.11	-10.11	0.217
8.04	8.07	8578	8644	36.91	1.97	-29.73	0.10	16.18	16.38	-11.59	0.187
8.07	8.10	8644	8710	31.64	1.83	-29.64	0.28	16.81	17.27	-10.85	0.385
8.10	8.13	8710	8766	30.09	1.74	-29.58	0.26		16.35	-11.53	0.375
8.13	8.16	8766	8821	30.04	1.73	-29.60	0.36	15.81	15.88	-12.02	0.362
8.16	8.19	8821	8877	30.16	1.78	-29.65	0.44	15.74	15.47	-12.25	0.334
8.19	8.22	8877	8932	30.13	1.83	-29.74	0.26	14.35	14.26	-13.52	0.392
8.22	8.25	8932	8988	30.38	1.83	-29.91	0.52	14.21	15.76	-12.86	0.439
8.25	8.28	8988	9043	32.42	1.95	-29.92	0.41	15.79	13.54	-13.17	0.431
8.28	8.31	9043	9096	29.17	1.76	-29.59	0.60	14.94	13.03	-13.82	0.597
8.31	8.34	9096	9144	24.50	1.53	-29.52	0.25	10.91	11.32	-16.62	1.120
8.34	8.37	9144	9192	23.80	1.47	-29.24	0.23	12.06	12.47	-15.49	1.415
8.37	8.40	9192	9240	27.31	1.66	-29.06	0.53	14.16	14.58	-13.45	1.401
8.40	8.43	9240	9288	28.31	1.75	-28.97	0.23	15.33	15.85	-12.26	1.538
8.43	8.46	9288	9336	26.55	1.63	-28.91	0.32	15.38	15.41	-12.46	2.047
8.46	8.49	9336	9384	27.57	1.68	-29.10	0.28	15.17	14.66	-12.92	3.105
8.49	8.52	9384	9429	29.46	1.77	-29.15	0.60	14.98	14.70	-12.99	5.128
8.52	8.55	9429	9473	28.15	1.73	-29.18	0.49	15.43	15.07	-12.60	4.925
8.55	8.58	9473	9516	27.66	1.70	-29.12	0.51	16.11	16.19	-11.72	4.800

8.58	8.61	9516	9560	27.73	1.67	-29.15	0.41	16.26	15.89	-11.79	4.530
8.61	8.64	9560	9603	28.92	1.75	-29.17	0.39	16.09	15.93	-11.86	4.422
8.64	8.67	9603	9647	29.32	1.73	-29.21	0.50	16.17	17.12	-11.23	5.016
8.67	8.70	9647	9690	27.86	1.69	-29.24	0.70	15.28	14.78	-12.81	5.020
8.70	8.73	9690	9734	28.36	1.74	-29.07	0.53	15.00	14.41	-13.13	4.864
8.73	8.76	9734	9777	29.76	1.77	-29.44	0.47	14.68	14.01	-13.47	6.838
8.76	8.79	9777	9821	27.82	1.67	-29.04	0.59	15.81	16.12	-11.90	6.093
8.79	8.82	9821	9864	30.33	1.79	-29.26	0.58	15.39	15.50	-12.41	6.932
8.82	8.85	9864	9908	30.82	1.87	-29.30	0.29	14.74	14.41	-13.25	6.839
8.85	8.88	9908	9951	28.20	1.79	-29.07	0.53	13.70	14.23	-13.84	6.521
8.88	8.91	9951	9993	26.53	1.66	-29.22	0.66	15.07	14.99	-12.81	6.278
8.91	8.94	9993	10030	26.43	1.70	-29.04	0.72	14.14	13.89	-13.79	5.403
8.94	8.97	10030	10068	27.78	1.78	-29.34	0.80	14.08	13.46	-14.03	6.516
8.97	9.00	10068	10105	24.73	1.60	-28.95	0.87	13.48	13.26	-14.43	5.700
9.00	9.03	10105	10143	21.40	1.39	-28.83	0.99	12.61	12.91	-15.02	4.735
9.03	9.06	10143	10180	22.11	1.54	-28.82	1.05	12.11	12.54	-15.44	4.825
9.06	9.09	10180	10218	19.27	1.35	-28.34	0.96	13.31	12.20	-15.02	4.169
9.09	9.12	10218	10253	18.23	1.31	-27.83	1.26	13.25	12.38	-14.96	3.853
9.12	9.15	10253	10289	17.71	1.25	-27.57	0.89	13.17	12.11	-15.14	3.800
9.15	9.18	10289	10324	17.21	1.21	-27.56	1.20	13.01	12.34	-15.10	5.327
9.18	9.21	10324	10359	17.65	1.26	-27.65	1.44	11.76	10.83	-16.44	5.035
9.21	9.24	10359	10394	17.19	1.25	-27.14	1.78	11.95	10.52	-16.50	5.243
9.24	9.27	10394	10430	13.87	0.99	-26.32	2.03	8.41	7.62	-19.63	5.201
9.27	9.30	10430	10465	11.19	0.83	-25.99	2.14	5.61	6.93	-21.33	6.478
9.30	9.33	10465	10500	9.94	0.74	-25.84	1.83	6.31	7.47	-20.72	6.871

Appendix C – Carbon and Nitrogen Elemental and Stable Isotope Records (Short Cores)

Depth values in the tables below are in reference to the top of the sediment.

Lake Keitjoru, Northern Sweden (68º40'N, 21º30'E)

Depth Interval (cm)		TOC (%)		TN (%)		$\delta^{13}C_{org}$ (‰ PDB)		$\delta^{15}N$ (‰ AIR)		Average:			
		(1)	(2)	(1)	(2)	(1)	(2)	(1)	(2)	TOC (%)	TN (%)	$\delta^{13}C_{org}$ (‰)	$\delta^{15}N$ (‰)
0.0	2.0	16.65	15.21	1.45	1.34	-25.74	-26.83	0.14	-0.34	15.93	1.40	-26.28	-0.10
2.0	4.0	15.53		1.37		-26.90		-0.42		15.53	1.37	-26.90	-0.42
4.0	6.0	14.85		1.29		-26.47		-1.03		14.85	1.29	-26.47	-1.03
6.0	7.0	11.95		1.10		-27.18		-0.76		11.95	1.10	-27.18	-0.76
7.0	8.0	12.68		1.01		-27.35		-0.06		12.68	1.01	-27.35	-0.06
8.0	9.0	15.18		0.93		-27.65		0.05		15.18	0.93	-27.65	0.05
9.0	10.0	17.42		0.95		-27.56		0.00		17.42	0.95	-27.56	0.00
10.0	11.0	16.20		0.99		-27.39		0.35		16.20	0.99	-27.39	0.35
11.0	12.0	11.42		0.81		-27.47		0.16		11.42	0.81	-27.47	0.16
12.0	13.0	11.42	11.57	0.86	0.88	-27.57	-27.59	0.21	0.15	11.50	0.87	-27.58	0.18
13.0	14.0	11.91		0.87		-27.48		0.20		11.91	0.87	-27.48	0.20
14.0	15.0	12.28		0.88		-27.63		0.40		12.28	0.88	-27.63	0.40
15.0	16.0	9.95		0.78		-27.44		0.16		9.95	0.78	-27.44	0.16
16.0	17.0	11.32		0.85		-27.36		0.22		11.32	0.85	-27.36	0.22
17.0	18.0	11.17		0.81		-27.45		0.22		11.17	0.81	-27.45	0.22
18.0	19.0	10.73		0.80		-27.30		0.32		10.73	0.80	-27.30	0.32
19.0	20.0	10.01		0.80		-27.31		0.15		10.01	0.80	-27.31	0.15
20.0	21.0	10.33	10.12	0.80	0.80	-27.52	-27.38	0.09	0.16	10.23	0.80	-27.45	0.12
21.0	22.0	10.50		0.83		-27.42		0.17		10.50	0.83	-27.42	0.17

Oikojärvi, Northern Finland (68°50'N, 21°10'E)

Depth Interval (cm)		TOC (%)		TN (%)		$\delta^{13}C_{org}$ (‰ PDB)		$\delta^{15}N$ (‰ AIR)		Average:			
		(1)	(2)	(1)	(2)	(1)	(2)	(1)	(2)	TOC (%)	TN (%)	$\delta^{13}C_{org}$ (‰)	$\delta^{15}N$ (‰)
0.0	2.0	10.34	10.54	1.22	1.24	-29.32	-29.41	1.95	2.01	10.44	1.23	-29.37	1.98
2.0	4.0	9.96		1.13		-28.74		1.99		9.96	1.13	-28.74	1.99
4.0	5.0	9.74		1.07		-28.31		2.06		9.74	1.07	-28.31	2.06
5.0	6.0	9.42		1.02		-28.00		1.98		9.42	1.02	-28.00	1.98

6.0	7.0	8.88		0.97		-27.97		2.21		8.88	0.97	-27.97	2.21
7.0	8.0	8.76		0.95		-27.99		2.09		8.76	0.95	-27.99	2.09
8.0	9.0	8.03		0.86		-27.81		2.28		8.03	0.86	-27.81	2.28
9.0	10.0	8.29		0.88		-27.71		2.03		8.29	0.88	-27.71	2.03
10.0	11.0	8.67	8.57	0.93	0.92	-27.78	-27.73	2.09	2.14	8.62	0.93	-27.75	2.12
11.0	12.0	8.77		0.91		-27.99		2.13		8.77	0.91	-27.99	2.13
12.0	13.0	8.58		0.89		-27.81		2.08		8.58	0.89	-27.81	2.08
13.0	14.0	8.42		0.88		-27.69		2.07		8.42	0.88	-27.69	2.07
14.0	15.0	7.92		0.82		-27.78		2.10		7.92	0.82	-27.78	2.10
15.0	16.0	8.20		0.84		-27.92		2.05		8.20	0.84	-27.92	2.05
16.0	17.0	8.18		0.84		-28.09		1.97		8.18	0.84	-28.09	1.97
17.0	18.0	7.99		0.83		-28.23		1.82		7.99	0.83	-28.23	1.82
18.0	19.0	8.14	8.12	0.85	0.84	-27.94	-27.80	1.87	2.02	8.13	0.85	-27.87	1.94
19.0	20.0	8.30		0.85		-27.97		1.94		8.30	0.85	-27.97	1.94
20.0	21.0	8.29		0.84		-28.11		1.84		8.29	0.84	-28.11	1.84
21.0	22.0	8.20		0.83		-27.96		1.88		8.20	0.83	-27.96	1.88
22.0	23.0	8.13		0.81		-27.78		1.89		8.13	0.81	-27.78	1.89
23.0	24.0	8.40		0.84		-27.92		1.87		8.40	0.84	-27.92	1.87
24.0	25.0	8.61		0.86		-27.93		1.89		8.61	0.86	-27.93	1.89
25.0	26.0	8.44		0.85		-28.10		1.95		8.44	0.85	-28.10	1.95
26.0	27.0	8.67		0.87		-27.98		2.01		8.67	0.87	-27.98	2.01
27.0	28.0	8.66	8.63	0.86	0.86	-27.99	-27.97	1.97	1.88	8.64	0.86	-27.98	1.93
28.0	29.0	8.85		0.89		-28.29		1.98		8.85	0.89	-28.29	1.98

Arbovatten, Southern Sweden (58º04'N, 12º04'E)

Depth Interval (cm)		TOC (%)		TN (%)		$\delta^{13}C_{org}$ (‰ PDB)		$\delta^{15}N$ (‰ AIR)		Average:			
		(1)	(2)	(1)	(2)	(1)	(2)	(1)	(2)	TOC (%)	TN (%)	$\delta^{13}C_{org}$ (‰)	$\delta^{15}N$ (‰)
0.0	1.0	13.86		0.90		-29.40		0.51		13.86	0.90	-29.40	0.51
1.0	1.5	10.96		0.71		-29.46		-0.27		10.96	0.71	-29.46	-0.27
1.5	2.0	9.40		0.59		-29.10		-0.43		9.40	0.59	-29.10	-0.43
2.0	2.5	17.27	17.35	1.02	1.02	-28.67	-28.61	-0.60	-0.60	17.31	1.02	-28.64	-0.60
2.5	3.0	18.71		1.13		-29.12		-0.40		18.71	1.13	-29.12	-0.40
3.0	3.5	19.36		1.15		-29.09		-0.09		19.36	1.15	-29.09	-0.09
3.5	4.0	27.58		1.39		-27.69		0.19		27.58	1.39	-27.69	0.19
4.0	4.5	19.13		1.11		-28.98		0.07		19.13	1.11	-28.98	0.07
4.5	5.0	20.40		1.33		-29.16		-0.13		20.40	1.33	-29.16	-0.13

5.0	5.5	21.83		1.66		-29.89		0.03		21.83	1.66	-29.89	0.03
5.5	6.0	33.64		2.41		-29.92		0.28		33.64	2.41	-29.92	0.28
6.0	6.5	36.34	36.52	2.44	2.43	-29.33	-29.34	0.33	0.33	36.43	2.44	-29.33	0.33
6.5	7.0	35.67		2.20		-29.08		0.61		35.67	2.20	-29.08	0.61
7.0	7.5	36.14		2.14		-29.34		0.86		36.14	2.14	-29.34	0.86
7.5	8.0	35.20		2.00		-28.92		0.63		35.20	2.00	-28.92	0.63
8.0	8.5	35.44		1.97		-29.32		0.89		35.44	1.97	-29.32	0.89
8.5	9.0	34.30		1.85		-29.27		0.90		34.30	1.85	-29.27	0.90
9.0	9.5	34.69		1.81		-29.17		0.88		34.69	1.81	-29.17	0.88
9.5	10.0	33.04		1.70		-29.22		0.88		33.04	1.70	-29.22	0.88
10.0	10.5	32.83	32.52	1.67	1.66	-29.17	-29.18	0.72	1.00	32.67	1.66	-29.18	0.86
10.5	11.0	32.26		1.63		-29.04		1.12		32.26	1.63	-29.04	1.12
11.0	11.5	31.82		1.55		-28.68		0.80		31.82	1.55	-28.68	0.80
11.5	12.0	31.81		1.54		-28.59		0.80		31.81	1.54	-28.59	0.80
12.0	12.5	33.16		1.60		-28.58		0.97		33.16	1.60	-28.58	0.97
12.5	13.0	31.76		1.48		-28.68		0.73		31.76	1.48	-28.68	0.73
13.0	13.5	35.07		1.61		-28.92		0.89		35.07	1.61	-28.92	0.89
13.5	14.0	32.43		1.51		-28.53		0.77		32.43	1.51	-28.53	0.77
14.0	14.5	34.44	33.90	1.59	1.59	-28.50	-28.51	0.69	0.72	34.17	1.59	-28.50	0.70
14.5	15.0	34.99		1.61		-28.43		0.74		34.99	1.61	-28.43	0.74
15.0	15.5	34.45		1.61		-28.39		0.48		34.45	1.61	-28.39	0.48
15.5	16.0	33.40		1.56		-28.60		0.49		33.40	1.56	-28.60	0.49
16.0	16.5	35.09		1.60		-28.69		0.73		35.09	1.60	-28.69	0.73
16.5	17.0	34.13		1.60		-28.28		0.90		34.13	1.60	-28.28	0.90
17.0	17.5	34.52		1.63		-28.35		0.73		34.52	1.63	-28.35	0.73
17.5	18.0	34.17		1.60		-28.15		0.66		34.17	1.60	-28.15	0.66
18.0	18.5	35.69		1.68		-28.22		0.61		35.69	1.68	-28.22	0.61
18.5	19.0	36.13	36.25	1.65	1.64	-28.20	-28.12	0.72	0.61	36.19	1.64	-28.16	0.67
19.0	19.5	35.15		1.67		-28.23		0.76		35.15	1.67	-28.23	0.76
19.5	20.0	35.16		1.65		-28.12		0.69		35.16	1.65	-28.12	0.69
20.0	20.5	35.67		1.68		-28.22		-0.35		35.67	1.68	-28.22	-0.35
20.5	21.0	36.45		1.75		-28.69		0.68		36.45	1.75	-28.69	0.68
21.0	21.5	35.92		1.73		-28.36		0.79		35.92	1.73	-28.36	0.79
21.5	22.0	35.08		1.75		-28.27		0.53		35.08	1.75	-28.27	0.53
22.0	22.5	35.01		1.77		-28.15		0.70		35.01	1.77	-28.15	0.70
22.5	23.0	35.03	34.88	1.80	1.81	-28.59	-28.39	0.57	-0.47	34.96	1.81	-28.49	0.05
23.0	23.5	32.80		1.73		-28.65		0.72		32.80	1.73	-28.65	0.72

Appendix D – Radioisotope Measurements and CRS Model ^{210}Pb Dates (Short Cores)

Depth values in the tables below are in reference to the top of the sediment.

Lake Keitjoru, Northern Sweden (68º40'N, 21º30'E)

Depth Interval (cm)		Dry Mass (g/cm^2)	^{210}Pb (Bq/kg)	1 std.dev.	^{214}Bi (Bq/kg)	1 std.dev.	^{137}Cs (Bq/kg)	1 std.dev.	CRS Date (year AD)
0.0	2.0	0.023	385.523	15.192	40.349	3.059	1.420	0.318	2003.0
2.0	4.0	0.030	297.581	12.837	0.976	0.113	4.020	0.711	1997.6
4.0	6.0	0.040	303.712	13.229	-5.768	0.745	3.332	0.630	1991.0
6.0	7.0	0.059	214.494	10.400	21.549	1.912	4.811	0.780	1979.2
7.0	8.0	0.078	104.406	6.899	7.147	0.745	8.554	1.095	1958.9
8.0	9.0	0.086	59.897	4.988	-0.266	0.031	-1.934	1.934	1932.7
9.0	10.0	0.133	9.630	1.509	21.603	1.794	-1.776	0.000	1881.8
10.0	11.0	0.092	61.915	5.099	-4.547	0.587	2.455	0.472	
11.0	12.0	0.079	-4.453	1.686	13.737	1.298	-0.416	0.131	
12.0	13.0	0.090	-2.583	0.758	7.622	0.795	-0.282	0.085	
13.0	14.0	0.098	-8.792	5.767	12.723	1.219	-2.584	1.492	
14.0	15.0	0.086							
15.0	16.0	0.081							
16.0	17.0	0.061							
17.0	18.0	0.059							
18.0	19.0	0.064							
19.0	20.0	0.079							
20.0	21.0	0.067							
21.0	22.0	0.031							

Oikojärvi, Northern Finland (68°50'N, 21°10'E)

Depth Interval (cm)		Dry Mass (g/cm^2)	^{210}Pb (Bq/kg)	1 std.dev.	^{214}Bi (Bq/kg)	1 std.dev.	^{137}Cs (Bq/kg)	1 std.dev.	CRS Date (year AD)
0.0	2.0	0.069	579.594	10.400	16.247	1.010	107.980	2.603	2003.0
2.0	4.0	0.080	344.553	7.236	26.367	1.449	124.528	2.821	1987.3
4.0	5.0	0.056	205.159	5.138	7.281	0.520	75.812	2.107	1969.1
5.0	6.0	0.046	109.014	3.418	10.023	0.682	21.442	1.098	1957.2
6.0	7.0	0.071	70.421	2.522	9.654	0.666	11.702	0.800	1950.5

7.0	8.0	0.060	57.014	3.028	18.736	1.584	17.073	1.376	1942.5
8.0	9.0	0.081	41.606	2.389	12.604	1.186	6.714	0.826	1935.8
9.0	10.0	0.081	43.976	2.486	11.098	1.063	9.543	1.006	1928.3
10.0	11.0	0.092	28.547	1.727	15.219	1.356	4.685	0.644	1917.6
11.0	12.0	0.095	32.455	1.957	14.887	1.365	0.655	0.146	1908.4
12.0	13.0	0.090	17.728	1.144	0.068	0.008	-0.418	0.121	1891.6
13.0	14.0	0.103	20.650	1.317	0.353	0.043	0.369	0.087	1883.1
14.0	15.0	0.103	17.757	1.151	5.500	0.590	0.237	0.058	1862.4
15.0	16.0	0.118	3.604	0.254	-10.372	1.834	2.721	0.460	1826.8
16.0	17.0	0.100	32.315	1.939	5.405	0.579	-1.233	0.504	
17.0	18.0	0.104							
18.0	19.0	0.097							
19.0	20.0	0.106							
20.0	21.0	0.107							
21.0	22.0	0.112							
22.0	23.0	0.108							
23.0	24.0	0.113							
24.0	25.0	0.124							
25.0	26.0	0.145							
26.0	27.0	0.116							
27.0	28.0	0.118							
28.0	29.0	0.104							

Arbovatten, Southern Sweden (58º04'N, 12º04'E)

Depth Interval (cm)		Dry Mass (g/cm^2)	^{210}Pb		^{214}Bi		^{137}Cs		CRS Date (year AD)	Liming Events	
			(Bq/kg)	1 std. dev.	(Bq/kg)	1 std. dev.	(Bq/kg)	1 std. dev.		Mid-Depth (cm)	Date (year AD)
0.0	1.0	0.187	56.282	2.473	6.565	0.567	20.977	0.930		0.5	2004.0
1.0	1.5	0.173	48.093	2.141	5.479	0.492	21.088	0.919		1.7	1998.0
1.5	2.0	0.181	32.378	1.627	6.424	0.551	25.743	1.009		3.0	1993.0
2.0	2.5	0.098	81.234	3.137	3.564	0.362	28.313	1.155		6.0	1987.0
2.5	3.0	0.085	109.681	3.980	2.820	0.304	56.398	1.775			
3.0	3.5	0.081	116.961	4.208	-0.149	0.019	63.480	1.931			
3.5	4.0	0.063	127.944	4.619	8.212	0.750	61.419	2.003			
4.0	4.5	0.095	89.491	3.503	3.655	0.379	66.904	1.929			
4.5	5.0	0.076	97.749	3.700	13.954	1.049	72.511	2.010			
5.0	5.5	0.110	67.742	2.966	6.466	0.606	34.184	1.396			

5.5	6.0	0.036	179.674	6.426	25.211	1.844	54.011	2.218			
6.0	6.5	0.034	212.797	7.473	21.601	1.729	52.561	2.334	1986.0		
6.5	7.0	0.034	185.574	7.250	16.352	1.468	45.961	2.333	1982.6		
7.0	7.5	0.037	145.421	6.128	32.394	2.356	19.177	1.433	1979.4		
7.5	8.0	0.037	131.164	5.649	21.875	1.780	19.551	1.430	1976.4		
8.0	8.5	0.034	107.086	4.855	25.887	1.963	15.050	1.201	1973.4		
8.5	9.0	0.036	110.334	5.119	30.980	2.290	13.658	1.189	1971.1		
9.0	9.5	0.033	89.113	4.496	10.506	1.045	10.874	1.077	1968.3		
9.5	10.0	0.038	78.013	4.078	14.088	1.314	10.613	1.051	1966.2		
10.0	10.5	0.041	66.430	3.603	21.732	1.805	14.306	1.236	1963.8		
10.5	11.0	0.043	67.702	3.605	26.656	2.050	13.100	1.149	1961.6		
11.0	11.5	0.039	68.783	3.680	18.210	1.579	8.985	0.937	1958.9		
11.5	12.0	0.042	68.325	3.722	24.800	2.005	7.205	0.838	1956.3		
12.0	12.5	0.046	57.788	3.333	36.494	2.669	13.399	1.244	1953.3		
12.5	13.0	0.043	56.296	3.247	35.509	2.597	13.037	1.210	1950.3		
13.0	13.5	0.043	52.593	3.034	33.064	2.418	12.139	1.127	1947.4		
13.5	14.0	0.046	40.795	2.504	22.012	1.847	4.723	0.643	1944.3		
14.0	14.5	0.045	44.907	2.728	21.044	1.811	11.993	1.165	1941.8		
14.5	15.0	0.049	51.189	3.001	40.205	2.794	4.333	0.607	1938.7		
15.0	15.5	0.048	46.709	2.803	15.475	1.431	5.396	0.708	1934.2		
15.5	16.0	0.051	44.429	2.717	21.596	1.852	5.690	0.741	1929.7		
16.0	16.5	0.045	45.705	2.795	22.244	1.907	5.860	0.763	1924.6		
16.5	17.0	0.046	30.915	2.000	18.392	1.632	5.551	0.723	1918.9		
17.0	17.5	0.056	37.623	2.380	13.240	1.280	-0.472	0.126	1914.9		
17.5	18.0	0.054	25.414	1.704	36.642	2.665	1.291	0.248	1907.3		
18.0	18.5	0.058	36.196	2.264	15.498	1.415	1.337	0.253	1902.2		
18.5	19.0	0.052	16.617	1.169	8.896	0.918	-2.051	1.450			
19.0	19.5	0.046	16.473	1.168	16.320	1.509	2.462	0.416			
19.5	20.0	0.043	17.374	1.228	30.449	2.400	5.977	0.778			
20.0	20.5	0.046	35.910	2.308	13.983	1.352	4.661	0.666			
20.5	21.0	0.046	17.854	1.263	-1.064	0.137	3.533	0.559			
21.0	21.5	0.041	17.286	1.227	13.048	1.286	4.933	0.698			
21.5	22.0	0.041	15.582	1.120	48.048	3.372	-0.220	0.055			
22.0	22.5	0.043	28.650	1.945	-5.122	0.732	1.438	0.282			
22.5	23.0	0.043	28.641	1.920	23.026	1.997	-2.188	1.263			
23.0	23.5	0.048	1.176	0.092	11.766	1.177	0.387	0.086			

References

Alexandersson H., Karlström C., Larsson-McCann S. 1991. Temperature and precipitation in Sweden, 1961-90. Reference normals. Swedish Meteorological and Hydrological Institute, Norrköping, Sweden, Meteorologi 81.

Alexandersson H. and Andersson, T. 1995. Precipitation and Thunderstorms. In: Raab B., Vedin H. (eds) Climate, Lakes and Rivers, National Atlas of Sweden, Stockholm: 76-90.

Alley R.B., Mayewski P.A., Sowers T., Stuiver M., Taylor K.C., Clark P.U. 1997. Holocene climatic instability: A prominent, widespread event 8200 yr ago. *Geology* 25: 483-486.

Almquist-Jacobson H. 1995. Lake-level fluctuations at Ljustjärnen, central Sweden and their implications for the Holocene climate of Fennoscandia. *Palaeogeography, Palaeoclimatology, Palaeoecology* 118: 269-290.

Amundson R.G., Chadwick O.A., Kendall C., Wang Y., DeNiro M.J. 1996. Isotopic evidence for shifts in atmospheric circulation patterns during the late Quaternary in mid-North America. *Geology* 24: 23-26.

Anderson L., Abbott M.B., Finney B.P. 2001. Holocene climate inferred from oxygen isotope ratios in lake sediments, central Brooks Range, Alaska. *Quaternary Research* 55: 313-321.

Andersson F., Olsson B. 1985. Lake Gårdsjon: an acid forest lake and its catchment. *Ecological Bulletins* 37: 1-336.

Antonsson K., Chen D., Seppä H. 2008. Anticyclonic atmospheric circulation as an analogue for the warm and dry mid-Holocene summer climate in central Scandinavia. *Climate of the Past* 4: 215-224.

Bakke J, Dahl SO, Paasche Ø, Løvlie R, Nesje A. 2005. Glacier fluctuations, equilibrium-line altitudes and palaeoclimate in Lyngen, northern Norway, during the Lateglacial and Holocene. *The Holocene* 15: 518-540.

Barber D.C., Dyke A., Hillaire-Marcel C., Jennings A.E., Andrews J.T., Kerwin M.W., Bilodeau G., McNeely R., Southon J., Morehead M.D., Gagnon J.M. 1999. Forcing of the cold event of 8,200 years ago by catastrophic drainage of Laurentide lakes. *Nature* 400: 344-348.

Barnekow L. 1999. Holocene tree-line dynamics and inferred climatic changes in the Abisko area, northern Sweden, based on macrofossil and pollen records. *The Holocene* 9: 253-265.

Barnekow L. 2000. Holocene regional and local vegetation history and lake-level changes in the Tornetrask area, northern Sweden. *Journal of Paleolimnology* 23: 399-420.

Barnekow L., Sandgren P. 2001. Palaeoclimate and tree-line changes during the Holocene based on pollen and plant macrofossil records from six lakes at different altitudes in northern Sweden. *Review of Palaeobotany and Palynology* 117: 109-118.

Barnekow L., Bragée P., Hammarlund D., St.Amour N. 2008. Boreal forest dynamics in north-eastern Sweden during the last 10,000 years based on pollen analysis. *Vegetation History and Archaeobotany* 17: 687-700.

Bergström H., Moberg A. 2002. Daily air temperature and pressure series for Uppsala (1722-1998). *Climatic Change* 53: 213-252.

Beuning K.R.M., Kelts K., Russell J., Wolfe B.B. 2002. Reassessment of Lake Victoria-upper Nile River paleohydrology from oxygen isotope records of lake-sediment cellulose. *Geology* 30: 559-562.

Birks C.J.A., Koç N. 2002. A high-resolution diatom record of late-Quaternary sea-surface temperatures and oceanographic conditions from the eastern Norwegian Sea. *Boreas* 31: 323-344.

Birks S.J. 2003. Water isotope partitioning in aquitards and precipitation on the Northern Great Plains. PhD Thesis, University of Waterloo: 203pp.

Birks S.J., Edwards T.W.D., Remenda V.H. 2007. Isotopic evolution of Glacial Lake Agassiz: New insights from cellulose and porewater isotopic archives. *Palaegeography, Palaeoclimatology, Palaeoecology* 246: 8-22.

Björck S., Digerfeldt G. 1986. Late Weichselian-Early Holocene shore displacement west of Mt. Billingen, within the Middle Swedish end-moraine zone. *Boreas* 15: 1-18.

Björkman L. 1997. The history of Fagus forest in southwestern Sweden during the last 1500 years. *The Holocene* 7: 419-432.

Bjune A.E., Birks H.J.B., Seppä H. 2004. Holocene vegetation and climate history on a continental-ocean transect in northern Fennoscandia based on pollen and plant macrofossils. *Boreas* 33: 211-223.

Blundell A., Barber K. 2005. A 2800-year palaeoclimatic record from Tore Hill Moss, Strathspey, Scotland: the need for a multi-proxy approach to peat-based climate reconstructions. *Quaternary Science Reviews* 24: 1261-1277.

Bond G., Showers W.J., Cheseby M., Lotti R., Almasi P., deMenocal P., Priore P., Cullen H., Hajdas I., Bonani G. 1997. A pervasive millennial-scale cycle in North Atlantic Holocene and glacial climates. *Science* 278: 1257-1266.

Bond G., Kromer B., Beer J., Muscheler R., Evans M.N., Showers W., Hoffmann S., Lotti-Bond R., Hajdas I., Bonani G. 2001. Persistent solar influence on North Atlantic climate during the Holocene. *Science* 294: 2130-2136.

Borgmark A. 2005. Holocene climate variability and periodicities in south-central Sweden, as interpreted from peat humification analysis. *The Holocene* 15: 387-395.

Brahney J., Bos D.G., Pellatt M.G., Edwards T.W.D., Routledge R. 2006. The influence of nitrogen limitation on $\delta^{15}N$ and carbon : nitrogen ratios in sediments from sockeye salmon nursery lakes in British Columbia, Canada. *Limnology and Oceanography* 51: 2333-2340.

Bringfelt B., Forsman A 1995: Humidity and evaporation. In: Raab B., Vedin H. (eds) Climate, Lakes and Rivers, National Atlas of Sweden, Stockholm: 66-69.

Brunel J.P., Simpson H.J., Herczeg A.L., Whitehead R., Walker G.R. 1992. Stable Isotope Composition of Water Vapor as an Indicator of Transpiration Fluxes from Rice Crops. *Water Resources Research* 28: 1407-1416.

Burgman J.O., Calles B., Westman F. 1987. Conclusions from a ten year study of oxygen-18 in precipitation and runoff in Sweden. In: Proceedings of an International Symposium on the use of Isotope Techniques in Water Resources Development, International Atomic Energy Agency, Vienna: 579-590.

Busuioc A., Chen D., Hellström C. 2001. Temporal and spatial variability of precipitation in Sweden and its link with the large-scale atmospheric circulation. *Tellus* 53A: 348-367.

Calvo E., Grimalt J., Jansen E. 2002. High resolution $U^{37}K$ sea surface temperature reconstruction in the Norwegian Sea during the Holocene. *Quaternary Science Reviews* 21: 1385-1394.

Calles B., Westman F. 1989. Oxygen-18 and deuterium in precipitation in Sweden. University of Uppsala, Uppsala, Sweden, Report Series A 47: 20pp.

Charles C.D., Rind D., Jouzel J., Koster R.D., Fairbanks R.G. 1994. Glacial-interglacial changes in moisture sources for Greenland; influences on the ice core record of climate. *Science* 263: 508-511.

Cook E.R. 2003. Multi-proxy reconstructions of the North Atlantic Oscillation (NAO) index; a critical review and a new well-verified winter NOA index reconstruction back to AD 1400. In: Hurrell J.W., Kushnir Y., Ottersen G., Visbeck M. (eds), The North Atlantic Oscillation: climatic significance and environmental impact. *AGU Geophysical Monograph* 134: 63-79.

Coplen T.B. 1996. New guidelines for reporting stable hydrogen, carbon, and oxygen isotope-ratio data. *Geochimica et Cosmochimica Acta* 60: 3359-3360.

Craig H. 1961. Isotopic variations in meteoric waters. *Science* 133: 1702-1703.

Craig H., Gordon L.I. 1965. Deuterium and oxygen-18 variations in the ocean and marine atmosphere. In: Tongiorgi E. (ed), Stable Isotopes in Oceanographic Studies and Paleotemperatures, Spoleto, Consiglio Nazionale Delle Ricerche Laboratorio Di Geologi Nucleare:: 9-130.

Dahl S.O., Nesje A. 1996. A new approach to calculating Holocene winter precipitation by combining glacier equilibrium-line altitudes and pine-trees limits: a case study from Hardangerjøkulen, central southern Norway. *The Holocene* 6: 381-398.

Dansgaard W. 1964. Stable isotopes in precipitation. *Tellus* 16: 436-468.

Dansgaard W., Johnsen S.J., Reeh N., Gundestrup N., Clausen H.B., Hammer C.U. 1975. Climatic changes, Norsemen and modern man. *Nature* 255: 24-28.

Dansgaard W., Johnsen S.J., Clausen H.B., Dahl-Jensen D., Gundestrup N.S., Hammer C.U., Hvidberg C.S., Steffensen J.P., Sveinbjornsdottir A.E., Jouzel J., Bond G. 1993. Evidence for general instability of past climate from a 250-kyr ice-core record. *Nature* 364: 218-220.

De Jong R., Björck S., Björkman L., Clemmensen L.B. 2006. Storminess variation during the last 6500 years as reconstructed from an ombrotrophic peat bog in Halland, southwest Sweden. *Journal of Quaternary Science* 21: 905-919.

DeNiro M.J., Epstein S.A. 1981. Isotopic composition of cellulose from aquatic organisms. *Geochimica et Cosmochimica Acta* 45: 1885-1894.

Denton G.H., Karlén W. 1973. Holocene climatic variations: Their pattern and possible cause. *Quaternary Research* 3: 155-205.

Digerfeldt G. 1988. Reconstruction and regional correlation of Holocene lake-level fluctuations in Lake Bysjön, South Sweden. *Boreas* 17: 165-182.

Digerfeldt G. 1997. Reconstruction of Holocene lake-level changes in Lake Kalvsjön, southern Sweden, with a contribution to the local palaeohydrology at the Elm Decline. *Vegetation History and Archaeobotany* 6: 9-14.

Edwards T.W.D., Aravena R.O., Fritz P., Morgan A.V. 1985. Interpreting paleoclimate from ^{18}O and ^{2}H in plant cellulose: comparison with evidence from fossil insects and relict permafrost in southwestern Ontario. *Canadian Journal of Earth Sciences* 22: 1720-1726.

Edwards T.W.D., McAndrews J.H. 1989. Paleohydrology of a Canadian Shield inferred from ^{18}O in sediment cellulose. *Canadian Journal of Earth Sciences* 26: 1850-1859.

Edwards T.W.D. 1993. Interpreting past climate from stable isotopes in continental organic matter. In: Swart P.K., Lohmann K.*C*., McKenzie J.A., Savin S. (eds), *Climate Change in Continental Isotopic Records*. AGU Geophysical Monograph 78: 333-341.

Edwards T.W.D., Wolfe B.B., MacDonald G.M. 1996. Influence of changing atmospheric circulation on precipitation $\delta^{18}O$-temperature relations in Canada during the Holocene. *Quaternary Research* 46: 211-218.

Edwards T.W.D., Birks S.J., Gibson J.J. 2002. Isotope tracers in global water and climate studies of the past and present. In: Proceedings, Study of Environmental Change Using Isotope Techniques, Vienna, April 2001, IAEA-CN-80/66, 187-194.

Edwards T.W.D., Wolfe B.B., Gibson J.J., Hammarlund D. 2004. Use of water isotope tracers in high-latitude hydrology and paleohydrology. In: Pienitz R., Douglas M.S.V., Smol J.P. (eds), Long-Term Environmental Change in Arctic and Antarctic Lakes, Springer, Dordrecht, The Netherlands: 187-207.

Edwards T.W.D., Birks S.J., Luckman, B.H., MacDonald, G.M. 2008. Climatic and hydrologic variability during the past millennium in the eastern Rock Mountains and northern Great Plains of western Canada. *Quaternary Research* 70: 188-197.

Epstein S., Thompson P., Yapp C.J. 1977. Oxygen and hydrogen isotopic ratios in plant cellulose. *Science* 198: 1209-1215.

Eronen M., Hyvärinen H., Zetterberg P. 1999. Holocene humidity changes in northern Finnish Lapland inferred from lake sediments and submerged Scots pines dated by tree-rings. *The Holocene* 9: 569-580.

Fisher T.G., Smith D.G., Andrews, J.T. 2002. Preboreal oscillation caused by a glacial Lake Agassiz flood. *Quaternary Science Reviews* 21: 873-978.

Fricke H.C., O'Neil J.R. 1999. The correlation between $^{18}O/^{16}O$ ratios of meteoric water and surface temperature: its use in investigating terrestrial climate change over geologic time. *Earth and Planetary Science Letters* 170: 181-196.

Gat J.R. 1981. Lakes. In: Gat J.R., Gonfiantini R. (eds), Stable Isotope Hydrology: Deuterium and Oxygen-18 in the Water Cycle, International Atomic Energy Agency, Technical Reports Series 210: 203-221.

Gat J.R., Bowser C.J., Kendall C. 1994. The contribution of evaporation from the Great Lakes to the continental atmosphere: Estimate based on stable isotope data. *Geophysical Research Letters* 21: 557-560.

Gat J.R. 1996. Oxygen and hydrogen isotopes in the hydrologic cycle. *Annual Review of Earth and Planetary Sciences* 24: 225-262.

Gibson J.J., Edwards T.W.D. 2002. Regional water balance trends and evaporation-transpiration partitioning from a stable isotope survey of lakes in northern Canada. *Global Biogeochemical Cycles* 16: doi:10.1029/2001GB001839.

Gibson J.J., Birks S.J., Edwards T.W.D. 2008. Global prediction of δ_A and δ^2H-$\delta^{18}O$ evaporation slopes for lakes and soil water accounting for seasonality. Global Biogeochemical Cycles 22: doi:10.1029/2007GB002997.

Giesecke T. 2005. Holocene dynamics of the southern boreal forest in Sweden. *The Holocene* 15: 858-872.

Giesecke T., Bjune A.E., Chiverrell R.C., Seppä H., Ojala A.E.K., Birks H.J.B. 2008. Exploring Holocene continentality changes in Fennoscandia using present and past tree distributions. *Quaternary Science Reviews* 27: 1296-1308.

Gonfiantini R. 1986. Environmental isotopes in lake studies. In: Fritz P., Fontes J.Ch. (eds), Handbook of Environmental Isotope Geochemistry, Vol. 2: The Terrestrial Environment, Elsevier, New York: 113-168.

Grogan P., Jonasson S. 2003. Controls on annual nitrogen cycling in the understory of a subarctic birch forest. *Ecology* 84: 202-218.

Grudd H. 2008. Torneträsk tree-ring width and density AD 500-2004: a test of climatic sensitivity and a new 1500-year reconstruction of north Fennoscandian summers. *Climate Dynamics* 31: 843-857.

Gunnarson B.E., Borgmark A., Wastegård S. 2003. Holocene humidity fluctuations in Sweden inferred from dendrochronology and peat stratigraphy. *Boreas* 32: 347-360.

Håkansson S. 1985. A review of various factors influencing the stable carbon isotope ratio of organic lake sediments by the change from glacial to post-glacial environmental conditions. *Quaternary Science Reviews* 4: 135-146.

Hammarlund D., Barnekow L., Birks H.J.B., Buchardt B., Edwards T.W.D. 2002. Holocene changes in atmospheric circulation recorded in the oxygen-isotope stratigraphy of lacustrine carbonates from northern Sweden. *The Holocene* 12: 339-351.

Hammarlund D., Björck S.J., Buchardt B., Israelson C., Thomsen C.T. 2003. Rapid hydrological changes during the Holocene revealed by stable isotope records of lacustrine carbonates from Lake Igelsjon, southern Sweden. *Quaternary Science Reviews* 22: 353-370.

Hammarlund D., Velle G., Wolfe B.B., Edwards T.W.D., Barnekow L., Bergman J., Holmgren S., Lamme S., Snowball I.F., Wohlfarth B., Possnert G. 2004. Palaeolimnological and sedimentary responses to Holocene forest retreat in the Scandes Mountains, west-central Sweden. *The Holocene* 14: 862-876.

Hammarlund D., Björck S., Buchardt B., Thomsen C.T. 2005. Limnic responses to increased effective humidity during the 8200 cal. yr BP cooling event in southern Sweden. *Journal of Paleolimnology* 34: 471-480.

Hammarlund D., Edwards T.W.D. 2008. Stable isotope variations in stalagmites from northwestern Sweden document changes in temperature and vegetation during the early Holocene: a comment on Sundqvist *et al.* 2007a. *The Holocene* 18: 1007-1010.

Heikkilä M., Seppä H. 2003. A 11,000 yr palaeotemperature reconstruction from the southern boreal zone in Finland. *Quaternary Science Reviews* 22: 541-554.

Hecky R.E., Campbell P., Hendzel L.L. 1993. The stoichiometry of carbon, nitrogen, and phosphorus in particulate matter of lakes and oceans. *Limnology and Oceanography* 38: 709-724.

Hoffmann G., Jouzel J., Masson V. 2000. Stable water isotopes in atmospheric general circulation models. *Hydrological Processes* 14: 1385-1406.

Hollander D.J., Mckenzie J.A. 1991. CO_2 control on carbon-isotope fractionation during aqueous photosynthesis: A paleo-pCO_2 barometer. *Geology* 19: 929-932.

Horita J., Wesolowski D.J. 1994. Liquid-vapor fractionation of oxygen and hydrogen isotopes of water from the freezing to the critical temperature. *Geochimica et Cosmochimica Acta* 58: 3425-3437.

Hultberg H, Grennfelt P. 1986. Gårdsjön Project: Lake acidification, chemistry in catchment runoff, lake liming and microcatchment manipulations. *Water, Air, and Soil Pollution* 30: 31-46.

Hurrell J.W. 1995. Decadal trends in the North Atlantic Oscillation: regional temperatures and precipitation. *Science* 269: 676-679.

Hurrell J.W., Kushnir Y., Ottersen G., Visbeck M. 2003. An overview of the North Atlantic Oscillation. In: Hurrell J.W., Kushnir Y., Ottersen G., Visbeck M. (eds), The North Atlantic Oscillation: climatic significance and environmental impact. *AGU Geophysical Monograph* 134: 1-35.

Hyvärinen H., Alhonen P. 1994. Holocene lake-level changes in the Fennoscandian tree-line region, western Finnish Lapland: diatom and cladoceran evidence. *The Holocene* 4: 251-258.

Ingraham N.L. 1998. Isotopic variations in precipitation. In: Kendall C., McDonnell J.J. (eds), Isotope Tracers in Catchment Hydrology, Elsevier, Amsterdam: 87-118.

IPCC. 2007. Climate Change 2007: Climate Change Impacts, Adaptation and Vulnerability. Working Group II Contribution to the Intergovernmental Panel on Climate Change Fourth Assessment Report: 23pp.

Jacobeit J., Jönsson P., Bärring L., Beck C., Ekstrom M. 2001. Zonal indices for Europe 1780-1995 and running correlations with temperature. *Climatic Change* 48: 219-241.

Jacobeit J., Wanner H., Luterbacher J., Beck C., Philipp A., Sturm K. 2003. Atmospheric circulation variability in the North-Atlantic--European area since the mid-seventeenth century. *Climate Dynamics* 20: 341-352.

Johannessen T.W. 1970. The climate of Scandinavia. In: Wallén (ed), Climates of Northern and Western Europe. World Survey of Climatology Volume 5, Elsevier Publishing Company, Amsterdam: 23-79.

Johnsen S.J., Dansgaard W., White J.W.C. 1989. The origin of Arctic precipitation under present and glacial conditions. *Tellus* 41B: 452-468.

Johnsen S.J., Dahl-Jensen D., Gundestrup N.S., Steffensen J.P., Clausen H.B., Miller H., Masson-Delmotte V., Sveinbjornsdottir A.E., White J.W.C. 2001. Oxygen isotope and palaeotemperature records from six Greenland ice-core stations; Camp Century, Dye-3, GRIP, GISP2, Renland and NorthGRIP. *Journal of Quaternary Science* 16: 299-307.

Jouzel J., Koster R., Joussaume S. 1996. Climate reconstruction from water isotopes: What do we learn from isotopic models? In: Jones P.D., Bradley R.S., Jouzel J. (eds), *Climatic Variations and Forcing Mechanisms of the Last 2000 Years,* Springer-Verlag, Berlin: 213-241.

Jouzel J., Koster R.D., Hoffmann G., Armengaud A. 1998. Model evaluations of the water isotope-climate relationships used in reconstructing palaeotemperatures. In: Proceedings of an International Symposium on Isotope Techniques in the Study of Past and Current Environmental Changes in the Hydrosphere and the Atmosphere. International Atomic Energy Agency, Vienna: 485-502.

Karlén W. 1976. Lacustrine sediments and tree-limit variations as indicators of Holocene climatic fluctuations in Lappland, northern Sweden. *Geografiska Annaler* 58A: 1-34.

Karlén W. 1988. Fennoscandian glacial and climatic fluctuations during the Holocene. *Quaternary Science Reviews* 7: 199-209.

Kauppinen J. 2003. Worst water shortage since the 1940s [with English summary]. *Suomen Luonto* 6: 16-19.

Klisch M., Rozanski K., Goslar T., Edwards T.W.D., Shemesh A. 2007. $\delta^{18}O$ of cellulose organic fraction combined with $\delta^{18}O$ of calcite and $\delta^{18}O$ of diatoms in lake sediments: a new tool for palaeoclimate reconstructions on continents? European Society for Isotope Research, IX Workshop, Cluj-Napoca, Romania, June 2007: 3pp.

Koç N., Jansen E., Haflidason H. 1993. Paleoceanographic reconstructions of surface ocean conditions in the Greenland, Iceland and Norwegian seas through the last 14 ka based on diatoms. *Quaternary Science Reviews* 12: 115-140.

Korhola A., Olander H., Blom T. 2000. Cladoceran and chironomid assemblages as qualitative indicators of water depth in subarctic Fennoscandian lakes. *Journal of Paleolimnology* 24: 43-54.

Korhola A., Tikkanen M., Weckström J. 2005. Quantification of Holocene lake-level changes in Finnish Lapland using a cladocera-lake depth transfer model. *Journal of Paleolimnology* 34: 175-190.

Krabbenhoft D.P., Bowser C.J., Anderson M.P., Valley J.W. 1990. Estimating Groundwater Exchange with Lakes: 1. The Stable Isotope Mass Balance Method. *Water Resources Research* 26: 2445-2453.

Kreutz K.J., Mayewski P.A., Meeker L.D., Twickler M.S., Whitlow S.I., Pittalwala I.I. 1997. Bipolar changes in atmospheric circulation during the Little Ice Age. *Science* 277: 1294-1296.

Kullman L. 1988. Holocene history of the forest-alpine tundra ecotone in the Scandes Mountains (central Sweden). *New Phytologist* 108: 101-110.

Kullman L. 1989. Tree-limit history during the Holocene in the Scandes Mountains, Sweden, inferred from subfossil wood. *Review of Palaeobotany and Palynology* 58: 163-171.

Kullman L. 1992. Orbital forcing and tree-limit history: hypothesis and preliminary interpretation of evidence from Swedish Lappland. *The Holocene* 2: 131-137.

Kullman L. 1995. Holocene tree-limit and climate history from the Scandes Mountains, Sweden. *Ecology* 76: 2490-2502.

Kullman L. 1999. Early Holocene tree growth at a high elevation site in the northernmost Scandes of Sweden (Lapland); a palaeobiogeographical case study based on megafossil evidence. *Geografiska Annaler* 81: 63-74.

Kullman L., Kjällgren L. 2006. Holocene pine tree-line evolution in the Swedish Scandes: Recent tree-line rise and climate change in a long-term perspective. *Boreas* 35: 159-168.

Lamb H.H. 1977. Climate, Present, Past and Future. Climatic History and the Future, vol. 2. Methuen, London, 835pp.

Lauritzen S.E., Lundberg J. 1999. Calibration of the speleothem delta function; an absolute temperature record for the Holocene in Northern Norway. *The Holocene* 9: 659-669.

Lee X., Feng Z., Guo L., Wang L., Jin L., Huang D., Jiang W., Jiang Q., Cheng H. 2005. Carbon isotope of bulk organic matter: A proxy for precipitation in the arid and semiarid central East Asia. *Global Biogeochemical Cycles* 19: doi:10:1029/2004GB002303.

Lindström G., Alexandersson H. 2004. Recent mild and wet years in relation to long observation records and future climate change in Sweden. *Ambio* 33: 183-186.

Lundqvist J. 1998: Glacials and interglacials. In: Fredén, C. (ed.) Geology, 2nd Edition, National Atlas of Sweden, Stockholm: 120-135.

Lundqvist J., Wohlfarth B. 2001. Timing and east-west correlation of south Swedish ice marginal lines during the Late Weichselian. *Quaternary Science Reviews* 20: 1127-1148.

MacDonald G.M., Edwards T.W.D., Moser K.A., Pienitz R., Smol J.P. 1993. Rapid response of treeline vegetation and lakes to past climate warming. *Nature* 361: 243-246.

Magny M., Begeot C., Guiot J., Peyron O. 2003. Contrasting patterns of hydrological changes in Europe in response to Holocene climate cooling phases. *Quaternary Science Reviews* 22: 1589-1596.

Mayewski P.A., Meeker L.D., Twickler M.S., Whitlow S., Yang Q., Lyons W.B., Prentice M. 1997. Major features and forcing of high-latitude northern hemisphere atmospheric circulation using a 110,000-year-long glaciochemical series. *Journal of Geophysical Research* 102: 26345-26366.

Mayewski P.A., Rohling E.E., Stager J.C., Karlén W., Maasch K.A., Meeker L.D., Meyerson E.A., Gasse F., van Kreveld S., Holmgren K., Lee-Thorp J., Rosqvist G., Rack F., Staubwasser M., Schneider R.R., Steig E.J. 2004. Holocene climate variability. *Quaternary Research* 62: 243-255.

McDermott F., Mattey D.P., Hawkesworth C. 2001. Centennial-scale Holocene climate variability revealed by a high-resolution speleothem $\delta^{18}O$ record from SW Ireland. *Science* 294: 1328-1331.

McKenzie J.A. and Hollander D.J. 1993. Oxygen-isotope record in recent carbonate sediments from Lake Greifen, Switzerland (1750-1986): Application of continental isotopic indicator for evaluation of changes in climate and atmospheric circulation patterns. In: Swart P.K., Lohmann K.*C*., McKenzie J.A., Savin S. (eds), Climate Change in Continental Isotopic Records. *AGU Geophysical Monograph* 78: 374.

Meeker L.D., Mayewski P.A. 2002. A 1400-year high-resolution record of atmospheric circulation over the North Atlantic and Asia. *The Holocene* 12: 257-266.

Meyers P.A., Lallier-Verges E. 1999. Lacustrine sedimentary organic matter records of Late Quaternary paleoclimates. *Journal of Paleolimnology* 21: 345-372.

Meyers P.A., Teranes J.L. 2001. Sediment organic matter. In: Last W.M., Smol J.P. (eds), Tracking Environmental Change Using Lake Sediments, Vol. 2: Physical and Geochemical Methods, Kluwer Academic Publishers, Dordrecht, The Netherlands: 239-269.

Moberg A., Bergström H., Krigsman J.R., Svanered O. 2002. Daily air temperature and pressure series for Stockholm (1756-1998). *Climatic Change* 53: 171-212.

Moldan F., Hultberg H., Andersson I. 1995. Covered catchment experiment at Gårdsjön: Changes in runoff chemistry after four years of experimentally reduced acid deposition. *Water, Air, and Soil Pollution* 85: 1599-1604.

Mysterud A., Stenseth N.*C.*, Yoccoz N.G., Ottersen G., Langvatn R. 2003. The response of terrestrial ecosystems to climate variability associated with the North Atlantic Oscillation. In: Hurrell J.W., Kushnir Y., Ottersen G., Visbeck M. (eds), The North Atlantic Oscillation: climatic significance and environmental impact. *AGU Geophysical Monograph* 134: 235-262.

Nesje, A., Dahl, S.O. 1991. Holocene glacier variations of Bláisen, Hardangerjøkulen, central southern Norway. *Quaternary Research* 35: 25-40.

Nesje A., Kvamme M. 1991. Holocene glacier and climate variations in western Norway; evidence for early Holocene glacier demise and multiple Neoglacial events. *Geology* 19: 610-612.

Nesje A., Matthews J.A., Dahl S.O., Berrisford M.S., Andersson C. 2001. Holocene glacier fluctuations of Flatebreen and winter-precipitation changes in the Jostedalsbreen region, western Norway; based on glaciolacustrine sediment records. *The Holocene* 11: 267-280.

Nesje A., Dahl S.O. 2003. The "Little Ice Age": only temperature? *The Holocene* 13: 139-145.

Nyberg L., Stähli M., Mellander P.E., Bishop K.H. 2001. Soil frost effects on soil water and runoff dynamics along a boreal forest transect: 1. Field investigations. *Hydrological Processes* 15: 909-926.

O'Brien S.R., Mayewski P.A., Meeker L.D., Meese D.A., Twickler M.S., Whitlow S.I. 1995. Complexity of Holocene climate as reconstructed from a Greenland ice core. *Science* 270: 1962-1964.

Oksanen, P.O. 2006. Holocene development of the Vaisjeäggi palsa mire, Finnish Lapland. *Boreas* 35: 81-95.

Oldfield F., Appleby P.G. 1984. Empirical testing of ^{210}Pb-dating models for lake sediments. In: Haworth E.Y., Lund J.W.G. (eds.), Lake Sediments and Environmental History. University of Minnesota Press, Minneapolis: 93-124.

Renberg I., Hultberg H. 1992. A paleolimnological assessment of acidification and liming effects on diatom assemblages in a Swedish lake. *Canadian Journal of Fisheries and Aquatic Sciences* 49: 65-72.

Renberg I., Bindler R., Braennvall M.L. 2001. Using the historical atmospheric lead-deposition record as a chronological marker in sediment deposits in Europe. *Holocene* 11: 511-516.

Rodhe A. 1987. The origin of streamwater traced by oxygen-18. Report Series A41, Uppsala University, Sweden: 260pp.

Rosqvist G.C., Leng M.J., Jonsson C. 2007. North Atlantic region atmospheric circulation dynamics inferred from a late-Holocene lacustrine carbonate isotope record, northern Swedish Lapland. *The Holocene* 17: 867-873.

Rozanski K., Araguás-Araguás L., Gonfiantini R. 1992. Relation-between long-term trends of oxygen-18 isotope composition of precipitation and climate. *Science* 258: 981-985.

Rozanski K., Araguás-Araguás L. and Gonfiantini R. 1993. Isotopic patterns in modern global precipitation. In: Swart P.K., Lohmann K.*C*., McKenzie J.A., Savin S. (eds), Climate Change in Continental Isotopic Records. *AGU Geophysical Monograph* 78: 1-36.

Renssen H., Goosse H., Fichefet T. 2002. Modeling the effect of freshwater pulses on the early Holocene climate: The influence of high-frequency climate variability. *Paleoceanography* 17: doi:10.1029/2001PA000649.

Sachse D., Radke J., Gleixner G. 2004. Hydrogen isotope ratios of recent lacustrine sedimentary n-alkanes record modern climate variability. *Geochimica et Cosmochimica Acta* 68: 4877-4889.

Sarmaja-Korjonen K., Hyvärinen H. 1999. Cladoceran and diatom stratigraphy of calcareous lake sediments from Kuusamo, NE Finland. Indications of Holocene lake-level changes. *Fennia* 177: 55-70.

Sarmaja-Korjonen K, Nyman M, Kultti S, Väliranta M. 2006. Palaeolimnological development of Lake Njargajavri, northern Finnish Lapland, in a changing Holocene climate and environment. *Journal of Paleolimnology* 35: 65-81.

Sauer P.E., Miller G.H., Overpeck J.T. 2001. Oxygen isotope ratios of organic matter in arctic lakes as a paleoclimate proxy: field and laboratory investigations. *Journal of Paleolimnology* 25: 43-64.

Schoning K. 2002. Palaeohydrography and marine conditions in the south-western part of the Vänern basin during the Younger Dryas and Early Preboreal. *GFF* 124: 1-10.

Schrag D.P., Hampt G., Murray D.W. 1996. Pore fluid constraints on the temperature and oxygen isotopic composition of the glacial ocean. *Science* 272: 1930-1932.

Seppä H, Weckström J. 1999. Holocene vegetational and limnological changes in the Fennoscandian tree-line area as documented by pollen and diatom records from Lake Tsuolbmajavri, Finland. *Ecoscience* 6: 621-635.

Seppä H., Hammarlund D. 2000. Pollen-stratigraphical evidence of Holocene hydrological change in northern Fennoscandia supported by independent isotopic data. *Journal of Paleolimnology* 24: 69-79.

Seppä H., Birks H.J.B. 2001. July mean temperature and annual precipitation trends during the Holocene in the Fennoscandian tree-line area; pollen-based climate reconstructions. *The Holocene* 11: 527-539.

Seppä H., Birks H.J.B. 2002. Holocene climate reconstructions from the Fennoscandian tree-line area based on pollen data from Toskaljavri. *Quaternary Research* 57: 191-199.

Seppä H., Nyman M., Korhola A., Weckström J. 2002. Changes of treelines and alpine vegetation in relation to post-glacial climate dynamics in northern Fennoscandia based on pollen and chironomid records. *Journal of Quaternary Science* 17: 287-301.

Seppä H., Hammarlund D., Antonsson K. 2005. Low- and high-frequency changes in temperature and effective humidity during the Holocene in south-central Sweden: implications for atmospheric and oceanic forcings of climate. *Climate Dynamics* 25: 285-297.

Shemesh A., Rosqvist G., Rietti-Shati M., Rubensdotter L., Bigler C., Yam R., Karlén W. 2001. Holocene climatic change in Swedish Lapland inferred from an oxygen-isotope record of lacustrine biogenic silica. *The Holocene* 11: 447-454.

Smith L.M., Andrews J.T., Castañeda I.S., Kristjánsdóttir G.B., Jennings A.E., Sveinbjörnsdóttir Á.E. 2005. Temperature reconstructions for SW and N Iceland waters over the last 10 cal ka based on $\delta^{18}O$ records from planktic and benthic Foraminifera. *Quaternary Science Reviews* 24: 1723-1740.

Snowball I.F., Sandgren P., Petterson G. 1999. The mineral magnetic properties of an annually laminated Holocene lake-sediment sequence in northern Sweden. *Holocene* 9: 353-362.

Snowball I.F., Zillén L., Gaillard M.-J. 2002. Rapid early-Holocene environmental changes in northern Sweden based on studies of two varved lake-sediment sequences. *The Holocene* 12: 7-16.

Snowball I., Korhola A., Briffa K.R., Koç N. 2004. Holocene climate dynamics in Fennoscandia and the North Atlantic. *Developments in Paleoenvironmental Research* 6: 465-494.

Sorensen P.L., Jonasson S., Michelsen A. 2006. Nitrogen fixation, denitrification, and ecosystem nitrogen pools in relation to vegetation development in the subarctic. *Arctic, Antarctic, and Alpine Research* 38: 263-272.

Straile D., Livingstone D.M., Weyhenmeyer G.A., George D.G. 2003. The response of freshwater ecosystems to climate variability associated with the North Atlantic Oscillation. In: Hurrell J.W., Kushnir Y., Ottersen G., Visbeck M. (eds), The North Atlantic Oscillation: climatic significance and environmental impact. *AGU Geophysical Monograph* 134: 263-279.

Sternberg L.d.S.L., DeNiro M.J. 1983. Biogeochemical implications of the isotopic equilibrium fractionation factor between the oxygen atoms of acetone and water. *Geochimica et Cosmochimica Acta* 47: 2271-2274.

Sturm K., Hoffmann G., Langmann B., Stichler W. 2005. Simulation of $\delta^{18}O$ in precipitation by the regional circulation model $REMO_{ISO}$. *Hydrological Processes* 19: 3425-3444.

Sundqvist H.S., Holmgren K., Lauritzen S.-E. 2007. Stable isotope variations in stalagmites from northwestern Sweden document climate and environmental changes during the early Holocene. *The Holocene* 17: 259-267.

Svedhage K. 1985. Shore displacement during Late Weichselian and early Holocene in the Risveden area, SW Sweden. Publication A 51, University of Göteborg: 111pp.

Talbot M.R., Johannessen T. 1992. A high resolution palaeoclimatic record for the last 27,500 years in tropical West Africa from the carbon and nitrogen isotopic composition of lacustrine organic matter. *Earth and Planetary Science Letters* 110: 23-37.

Talbot M.R., Laerdal T. 2000. The late Pleistocene-Holocene palaeolimnology of Lake Victoria, East Africa, based upon elemental and isotopic analyses of sedimentary organic matter. *Journal of Paleolimnology* 23: 141-164.

Talbot M.R. 2001. Nitrogen isotopes in palaeolimnology. In: Last W.M., Smol J.P. (eds). Tracking Environmental Change Using Lake Sediments, Vol. 2: Physical and Geochemical Methods. Kluwer Academic Publishers, Dordrecht, The Netherlands: 401-439.

Teranes J.L., McKenzie J.A. 2001. Lacustrine oxygen isotope record of 20^{th}-century climate change in Central Europe; evaluation of climatic controls on oxygen isotopes in precipitation. *Journal of Paleolimnology* 26: 131-146.

Thompson D.W.J., Wallace J.M. 2001. Regional climate impacts of the Northern Hemisphere annular mode. *Science* 293: 85-89.

Uvo C.B. 2003. Analysis and regionalization of northern European winter precipitation based on its relationship with the North Atlantic Oscillation. *International Journal of Climatology* 23: 1185-1194.

Velle G., Brooks S.J., Birks H.J.B., Willassen E. 2005. Chironomids as a tool for inferring Holocene climate: an assessment based on six sites in southern Fennoscandia. *Quaternary Science Reviews* 24: 1429-1462.

Verburg P. 2006. The need to correct for the Suess effect in the application of $\delta^{13}C$ in sediment of autotrophic Lake Tanganyika, as a productivity proxy in the Anthropocene. *Journal of Paleolimnology* 37: 591-602.

Veski S, Seppä H, Ojala AEK. 2004. Cold event at 8200 yr B.P. recorded in annually laminated lake sediments in eastern Europe. *Geology* 32: 681-684.

von Grafenstein U., Erlenkeuser H., Mueller J., Jouzel J., Johnsen S.J. 1998. The cold event 8200 years ago documented in oxygen isotope records of precipitation in Europe and Greenland. *Climate Dynamics* 14: 73-81.

von Grafenstein U., Erlenkeuser H. , Brauer A., Jouzel J., Johnsen S.J. 1999. A mid-European decadal isotope-climate record from 15,500 to 5000 years BP. *Science* 284: 1654-1657.

Wallén C.C. (ed) 1970. Climates of Northern and Western Europe. World Survey of Climatology Volume 5, Elsevier Publishing Company, Amsterdam, 1-21.

Watson E., Luckman B.H. 2004. Tree-ring-based mass-balance estimates for the past 300 years at Peyto Glacier, Alberta, Canada. *Quaternary Research* 62: 9-18.

Wolfe B.B., Edwards T.W.D., Aravena R.O., MacDonald G.M. 1996. Rapid Holocene hydrologic change along boreal treeline revealed by $\delta^{13}C$ and $\delta^{18}O$ in organic lake sediments, Northwest Territories, Canada. *Journal of Paleolimnology* 15: 171-181.

Wolfe B.B., Edwards T.W.D. 1997. Hydrologic control on the oxygen-isotope relation between sediment cellulose and lake water, western Taimyr Peninsula, Russia: Implications for the use of surface-sediment calibrations in paleolimnology. *Journal of Paleolimnology* 18: 283-291.

Wolfe B.B., Edwards T.W.D., Aravena R.O. 1999. Changes in carbon and nitrogen cycling during tree-line retreat recorded in the isotopic content of lacustrine organic matter, western Taimyr Peninsula, Russia. *The Holocene* 9: 215-222.

Wolfe B.B., Edwards T.W.D., Aravena R.O., Forman S.L., Warner B.G., Velichko A.A., MacDonald G.M. 2000. Holocene paleohydrology and paleoclimate at treeline, north-central Russia, inferred from oxygen isotope records in lake sediment cellulose. *Quaternary Research* 53: 319-329.

Wolfe B.B., Edwards T.W.D., Elgood R.J., Beuning K.R.M. 2001a. Carbon and oxygen isotope analysis of lake sediment cellulose: methods and applications. In: Last W.M., Smol J.P. (eds), Tracking Environmental Change Using Lake Sediments, Vol. 2: Physical and Geochemical Methods, Kluwer Academic Publishers, Dordrecht, The Netherlands: 373-400.

Wolfe B.B., Aravena R.O., Abbott M.B., Seltzer G.O., Gibson J.J. 2001b. Reconstruction of paleohydrology and paleohumidity from oxygen isotope records in the Bolivian Andes. *Palaeogeography, Palaeoclimatology, Palaeoecology* 176: 177-192.

Wolfe B.B., Edwards T.W.D., Jiang H.B., MacDonald G.M., Gervais B.R., Snyder J.A. 2003. Effect of varying oceanicity on early- to mid-Holocene palaeohydrology, Kola Peninsula, Russia: isotopic evidence from treeline lakes. *Holocene* 13: 153-160.

Wolfe B.B., Karst-Riddoch T.L., Vardy S.R., Falcone M.D., Hall R.I., Edwards T.W.D. 2005. Impacts of climate and river flooding on the hydro-ecology of a floodplain basin, Peace-Athabasca Delta, Canada since A.D. 1700. *Quaternary Research* 64: 147-162.

Wolfe B.B., Falcone M.D., Clogg-Wright K.P., Mongeon C.L., Yi Y., Brock B.E., St.Amour N.A., Mark W.M., Edwards T.W.D. 2007. Progress in isotope paleohydrology using lake sediment cellulose. *Journal of Paleolimnology* 37: 221-231.

Wolfe B.B., Hall R.I. Edwards T.W.D., Vardy S.R., Falcone M.D., Sjunneskog C., Sylvestre F., McGowan S., Leavitt P.R., van Driel P. 2008. Hydroecological responses of the Athabasca Delta, Canada, to changes in river flow and climate during the 20th century. *Ecohydrology* 1: 131-148.

Yakir D., DeNiro M.J. 1990. Oxygen and hydrogen isotope fractionation during cellulose metabolism in *Lemna gibba*. *Plant Physiology* 93: 325-332.

Yakir D. 1992. Variations in the natural abundance of O-18 and deuterium in plant carbohydrates. *Plant Cell and Environment* 15: 1005-1020.

Yi, Y. 2008. Developing and refining the use of water isotope tracers in hydrology and paleohydrology. PhD Thesis, University of Waterloo, 159pp. http://hdl.handle.net/10012/3903.

Yu G., Harrison S.P. 1995. Holocene changes in atmospheric circulation patterns as shown by lake status changes in Northern Europe. *Boreas* 24: 260-268.

Zuber A. 1983. On the environmental isotope method for determining the water balance components of some lakes. *Journal of Hydrology* 61: 409-427.